



CROSMOR; CROSS-SHORE MODELLING AND APPLICATIONS

- 1. Introduction**
- 2. Description of Crosmor-model**
 - 2.1 General**
 - 2.2 Basic model equations**
 - 2.3 Model settings**
 - 2.4 Model runs for testing of numerical and physical parameters**
 - 2.5 Example wave heights Payra channel Bangladesh**
- 3. Dune zone cases**
 - 3.1 Erosion of sand dune due to extreme storms; exposed Holland coast, The Netherlands**
 - 3.2 Erosion of high berm in front of hard dike; sheltered lake coast Markermeer, The Netherlands**
 - 3.3 Overwash over dune crest; Lagos coast, Nigeria**
 - 3.4 Beach-dune erosion of Test Dunes at site Sand Motor, The Netherlands**
 - 3.5 Beach-dune erosion at site De Haan, Belgium**
 - 3.6 Beach-dune erosion at the site HBZ Petten, Netherlands**
- 4. Beach and surf zone cases**
 - 4.1 Beach stability under daily waves; sheltered coast Lake Markermeer, The Netherlands**
 - 4.2 Beach stability under daily waves; sheltered south-east coast of Texel island, The Netherlands**
 - 4.3 Erosion of beach nourishment for annual wave climate; Holland coast, The Netherlands**
 - 4.4 Sediment sorting in beach and surf zone; Katwijk beach, The Netherlands**
 - 4.5 Sedimentation and erosion of mining pit for land reclamation; China**
 - 4.6 Onshore bar migration at beach; Duck beach , USA**
 - 4.7 Erosion of steep slope**
 - 4.8 Long term bed level changes Black Sea Coast of Romania**
 - 4.9 Effect of runup, sand particle size and gradation coefficient on beach erosion**
 - 4.10 Results of sensitivity tests**
- 5. Offshore zone cases**
 - 5.1 Shoreface nourishment; Holland coast**
- 6. Hard structures at sea bed**
 - 6.1 General**
 - 6.2 Model approach**
 - 6.3 Erosion downstream of submerged dam**
 - 6.4 Erosion of plane sloping beach with hard layer**
 - 6.5 Erosion in lee of hard submerged shore-parallel breakwater**
 - 6.6 Erosion of beach with emerged shore-parallel breakwater**
 - 6.7 Effect of submerged at artificial beach**
 - 6.8 Effect of structure**
- 7. Gravel beach erosion**
 - 7.1 General**
 - 7.2 Short and long term runs for beach of gravel ($d_{50}=40$ mm)**
 - 7.2.1 Validation of CROSMOR-model for gravel beaches**



7.2.2 Results of CROSMOR-runs for gravel beach of Benin/Togo, Case4 ($d_{50}=40$ mm)

- 7.3 Erosion of gravel barrier/dune due to extreme storms; exposed Pevensey Bay, UK**
- 7.4 Results of sensitivity tests**

1. Introduction

This document describes various applications of the CROSMOR-model, which can be used to compute the distribution of the bed level changes along a cross-shore coastal profile between the most landward dune zone and the most seaward offshore zone.

The CROSMOR-model is a numerical model (FORTRAN-code) which can compute the following parameters: wave height, wave asymmetry, undertow velocity, longshore current velocity, Longuet-Higgins streaming, bed load and suspended load transport and bed profile development over time along the cross-shore coastal profile in a situation with minor alongshore gradients (almost uniformity in alongshore direction).

Typical problems that can be solved using the CROMOR-model are:

1. Dune zone
 - storm erosion of dune front (exposed and sheltered sites);
 - erosion of high sand berms in front of hard structures (dikes);
 - storm erosion of gravel barriers;
 - overwash of dune crest;
2. Beach and surf zone
 - erosion of beach and surf zone nourishments;
 - sorting of beach sediment;
 - bar migration;
 - erosion and sedimentation of mining pits
 - toe scour near hard structures;
 - slope erosion of nearshore pit
3. Offshore zone
 - erosion of sand mounds;
 - erosion/deposition of sand mining pits.



2. Description of CROSMOR-model

2.1 General

The CROSMOR2013-model can be used to compute the cross-shore profile distribution of wave heights, peak orbital velocities, undertow velocity, longshore currents, bed and suspended load transport and the bed profile development as function of time.

The CROSMOR2013-model is an updated version of the CROSMOR2004-model (Van Rijn, 1997, 2006, 2007d). The model has been extensively validated by Van Rijn (2008) and Van Rijn et al. (2003). All relevant literature is given in References.

The CROSMOR2013-model is a morphodynamic model for the computation of bed level changes along a sandy profile normal to the coast line. The model includes submodels for waves, longshore and cross-shore currents, longshore and cross-shore sand transport.

The propagation and transformation of individual waves (wave by wave approach) along the cross-shore profile is described by a probabilistic model solving the wave energy equation for each individual wave. The individual waves shoal until an empirical criterion for breaking is satisfied. The maximum wave height is given by $H_{max} = \gamma_{br} h$ with γ_{br} = breaking coefficient and h = local water depth. The default wave breaking coefficient is represented as a function of local wave steepness and bottom slope. The default breaking coefficient varies between 0.4 for a horizontal bottom and 0.8 for a very steep sloping bottom. The model can also be run with a constant breaking coefficient (input value). Wave height decay after breaking is modelled by using an energy dissipation method. Wave-induced set-up and set-down and breaking-associated longshore currents are also modelled. Laboratory and field data have been used to calibrate and to verify the model. Generally, the measured $H_{1/3}$ -wave heights are reasonably well represented by the model in all zones from deep water to the shallow surf zone. The fraction of breaking waves is reasonably well represented by the model in the upsloping zones of the bottom profile. Verification of the model results with respect to wave-induced longshore current velocities has shown reasonably good results for barred and non-barred profiles.

A definition sketch of wave and current directions is given in **Figure 2.1**.

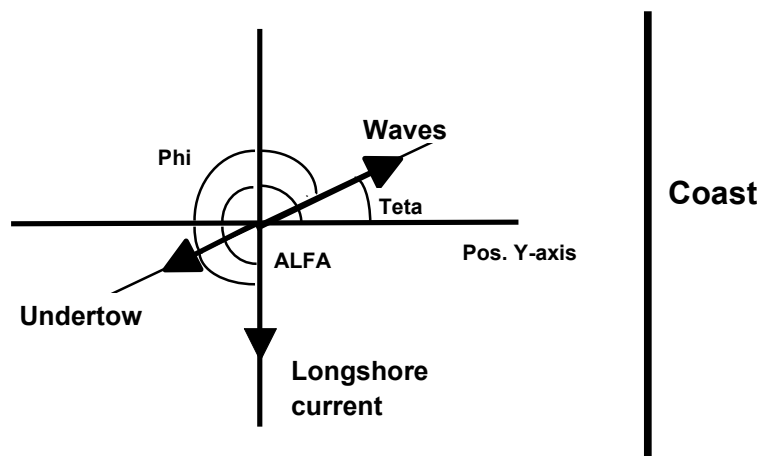


Figure 2.1 *Definition sketch*
Teta= angle between wave direction and positive y-axis



Phi= angle between wave and current direction
Alfa= angle between longshore current direction and positive y-axis
($v_{long} < 0$ m/s; $\alpha = 270^\circ$ and $v_{long} > 0$ m/s; $\alpha = 90^\circ$)

The complicated wave mechanics in the swash zone is not explicitly modeled, but taken into account in a schematized way. The limiting water depth of the last (process) grid point is set by the user of the model (input parameter; typical values of 0.1 to 0.2 m). Based on the input value, the model determines the last grid point by interpolation after each time step (variable number of grid points).

The cross-shore wave velocity asymmetry under shoaling and breaking waves is described by a semi-empirical method. Near-bed streaming effects are modelled by semi-empirical expressions. The velocity due to low-frequency waves in the swash zone is also taken into account by an empirical method.

The depth-averaged return current (u_r) under the wave trough of each individual wave (summation over wave classes) is derived from linear mass transport and the water depth (h_t) under the trough. The mass transport is given by $0.125 g H^2/C$ with $C = (g h)^{0.5} =$ phase velocity in shallow water. The contribution of the rollers of broken waves to the mass transport and to the generation of longshore currents is taken into account.

The sand transport of the CROSMOR2007-model is based on the TRANSPOR2004 sand transport formulations. The effect of the local cross-shore bed slope on the transport rate is taken into account.

The sand transport rate is determined for each wave (or wave class), based on the computed wave height, depth-averaged cross-shore and longshore velocities, orbital velocities, friction factors and sediment parameters. The net (averaged over the wave period) total sediment transport is obtained as the sum of the net bed load (q_b) and net suspended load (q_s) transport rates. The net bed-load transport rate is obtained by time-averaging (over the wave period) of the instantaneous transport rate using a formula-type of approach.

The net suspended load transport is obtained as the sum ($q_s = q_{s,c} + q_{s,w}$) of the current-related and the wave-related suspended transport components.

The current-related suspended load transport ($q_{s,c}$) is defined as the transport of sediment particles by the time-averaged (mean) current velocities (longshore currents, rip currents, undertow currents).

The wave-related suspended sediment transport ($q_{s,w}$) is defined as the transport of suspended sediment particles by the oscillating fluid components (cross-shore orbital motion). The oscillatory or wave-related suspended load transport ($q_{s,w}$) has been implemented in the model.

Computation of the wave-related and current-related suspended load transport components requires information of the time-averaged current velocity profile and sediment concentration profile. The convection-diffusion equation is applied to compute the time-averaged sediment concentration profile based on current-related and wave-related mixing. The bed-boundary condition is applied as a prescribed reference concentration based on the time-averaged bed-shear stress due to current and wave conditions. The sediment composition can also be taken into account.



2.2 Basic model equations

2.2.1 Wave heights, radiation stresses and longshore currents

Wave action balance

The wave action balance reads as (Van Rijn and Wijnberg, 1996):

$$d[(EC_{g,r} \cos\theta + u)/\omega_r]/dx + (D_{bf} + D_{br})/\omega_r = 0 \quad (1)$$

in which:

$E = \rho g H^2 / 8$ = wave energy per unit area;

$C_{g,r} = n C_r$ = relative wave group velocity;

$\omega_r = 2\pi / T_r$ = relative wave angular frequency;

$\theta = \arcsin[(C_r / C_{r,o}) \sin\theta_o]$ = angle of wave ray and x-axis normal to coast;

D_{bf} = energy dissipation per unit area by bottom friction;

D_{br} = energy dissipation per unit area by breaking;

H = wave height;

$T_r = T / [1 - (T / L) \cos\varphi]$ = relative wave period;

ρ = fluid density;

g = acceleration of gravity;

v = depth-averaged velocity vector;

u = depth-averaged current velocity component in cross-shore x-direction;

φ = angle between wave propagation direction and current direction;

$C_r = L / T_r$ = relative wave propagation velocity;

L = wave length;

T = absolute wave period;

$n = 0.5 [1 + 2kh / \sinh(2kh)]$ = coefficient;

$k = 2\pi / L$ = wave number;

x = coordinate normal to shore (positive in onshore direction).

The wave length is defined by the dispersion relation including the current refraction (Doppler shifting) effect:

$$[L/T - |v| \cos\varphi]^2 = g L / (2\pi) \tanh(2\pi h / L) \quad (2)$$

Energy dissipation by bottom friction is described by:

$$D_{bf} = \rho [f_w / (6\pi)] [\omega_r H / \sinh(2\pi h / L)]^3 \quad (3)$$

The friction coefficient (f_w) in the hydraulically rough regime can be expressed as:

$$f_w = \exp[-6 + 5.2(A/k_{s,w})^{-0.19}], f_{w,max} = 0.3 \quad (4)$$

in which:

A = peak value of orbital excursion;

$k_{s,w}$ = effective bed roughness height related to waves.



Wave breaking

Waves are assumed to break if the local wave height (H) found in the model is larger than the local maximum possible wave height (H_{\max}) associated with breaking.

The energy dissipation in a breaking wave can be described by an expression based on the analogy between dissipation of energy in a breaking wave and in a bore, yielding:

$$D_{br} = 0.25\alpha_2 \rho g [H^2 - H_{\max}^2] / T_r \quad \text{for } H > H_{\max} \quad (5)$$
$$H_{\max} = \text{minimum}[\gamma h, 0.14L \tanh(kh)]$$

with: α_2 = calibration coefficient.

Equation (5) implies that the H_{\max} -value is determined by wave breaking either on depth ($H_{\max} = \gamma h$) or on steepness ($H_{\max} = 0.14L \tanh(kh)$). The fraction of breaking waves at a certain location is obtained by summing the percentages of occurrence of the wave height classes that are breaking $H > H_{\max}$ at that location.

The α_2 -factor is found to be 1.5 by calibration using laboratory and field data. The breaking coefficient γ is assumed to depend on the ratio of the local bottom slope ($\tan\beta$) and the local wave steepness (H/L). The local bottom slope is taken to be the average bottom slope of the profile over a distance of α times the local wave length seaward of the local coordinate. In most computations: α -factor=0.5. A negative bottom slope on the landward side of a sand bar is set to a zero slope value.

In the CROSMOR-model the γ -factor varies between 0.45 and 1 depending on the ratio of $\tan\beta$ and H/L , as presented in **Figure 2.2.1**. This curve was obtained by calibration.

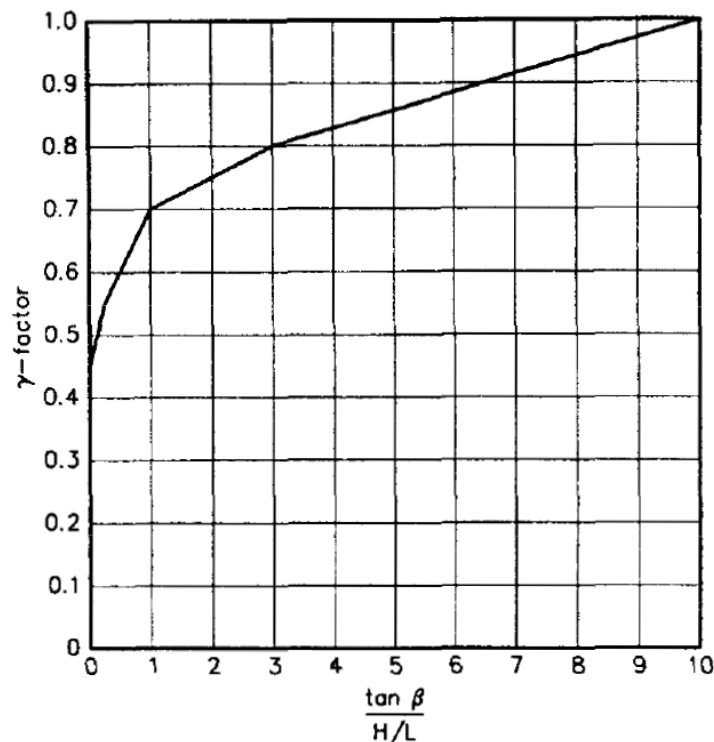


Figure 2.2.1 Breaking coefficient



Wave set-up

The wave-induced set-up and set-down are determined from the time-averaged momentum balance neglecting inertial effects and bed-shear stress, which reads as follows:

$$dS_{xx}/dx + \rho g(h+s) ds/dx - \tau_{sf}=0 \quad (6)$$

in which:

S_{xx} = onshore radiation force (herein the terminology force rather than stress is preferred because S_{xx} represents a force per unit length);

s = mean water level change (set-up/set-down);

$\tau_{sf} = \tau_{wind} + \tau_{sr}$ = shear stress at water surface to account for the wind effect and the breaking roller effect;

The wind-shear stress can be represented as $\tau_{wind} = \rho_a f_a w_{10} |w_{10,x}|$

with:

ρ_a = air density (1.25 kg/m³),

f_a = friction coefficient (0.001 to 0.002),

w_{10} = magnitude of the wind velocity vector at 10 m above the surface,

$w_{10,x}$ = wind velocity component in x-direction.

The breaker roller effect can also be represented by a shear stress acting at the wave trough level.

The τ_{sr} -parameter is herein modelled as: $\tau_{sr} = \alpha_{sr} \rho f_s C^2$

with:

$C^2 = g(h + s)$,

f_s = friction coefficient (= 0.001 to 0.005),

α_{sr} = efficiency coefficient (ratio of roller length and wave length; range =0.01 to 0.1).

The τ_{sr} -stress is applied for $H > H_{max}$ (breaking wave conditions).

The roller effect may be important in the swash bar zone where plunging breaking waves are present.

The radiation force component is described by:

$$S_{xx}=(n - 0.5 + n \cos^2\theta)E \quad (7)$$

Equation (6) is solved for each wave height class. Each s -value is multiplied by the percentage of occurrence of the corresponding wave height class and the final representative s -value is obtained by summation over all classes. It may be argued whether this approach is valid because the set-up/set-down effect may not respond on the scale of individual waves. Comparison of measured and computed results show however reasonably good agreement.

Equations (1) and (6) are re-arranged in to coupled set of differential equations, as follows:

$$dY/dz = -(Y/a_1) (da_1/dx - (a_2/a_1) Y^{1.5} - (a_3/a_1) (Y-Y_{max})) \quad (8)$$

$$ds/dx = - (a_4/(h+s)) dY/dx - (1/(h+s)) Y da_4/dx + \alpha_{sr} \quad (9)$$

which are solved simultaneously using a Runge Kutta method.

$Y=H^2$, $Y_{max}=H_{max}^2$, s = wave setup,



$a_1, a_2, a_3, a_4, \alpha_{sr}$ = wave-related parameters and coefficients.

Momentum balance for longshore current including wind

The depth-averaged longshore current related to breaking waves can be derived from the depth-averaged momentum equation for the longshore direction. Including wind-induced shear stress at the water surface and the (tide and wind-induced) longshore water surface gradient, the momentum equation reads, as:

$$dS_{xy}/dx + \rho(h+s) d(h+s)/dy - \tau_{s,y} + \tau_{b,y} - d(h\tau_{xy})/dx = 0 \quad (10)$$

in which:

S_{xy} = radiation force in longshore direction,

$\tau_{s,y}$ = shear stress at water surface due to longshore wind,

$\tau_{b,y}$ = shear stress at bottom due to longshore current,

τ_{xy} = depth-averaged shear stress at side plane of water column,

x = cross-shore coordinate (positive in onshore direction),

y = longshore coordinate (positive in northward direction).

The gradient of the radiation force can be modelled as:

$$d(S_{xy})/dx = -D_{br} \sin\theta/C \quad (11)$$

in which:

D_{br} = wave energy dissipation due to breaking,

C = wave propagation velocity,

θ = angle between wave propagation direction and shore normal.

Equation (11) represents a local approach, which means that the wave-induced longshore velocity is related to the local value of the wave energy dissipation. It may be argued whether this is a realistic representation of the physics involved. It may take some distance (say $0.5L$ to $1L$ with L = wave length) before the momentum of the breaking waves is fully transferred into momentum associated with the longshore current (through the roller mechanism), which can be seen as a relaxation or memory effect (transition zone). The relaxation effect of the roller mechanism in the transition zone on the computed longshore velocities will be studied in this paper.

The wind-induced shear stress is modelled, as: $\tau_{s,y} = \rho_a f_a w_{10} |w_{10,y}|$

with:

ρ_a = density of air (1.25 kg/m^3),

f_a = friction coefficient ($= 0.001$),

$w_{10,y}$ = wind velocity component in the y -direction.

The bed-shear stress is modelled as: $\tau_{b,y} = \rho f_c v |v|$

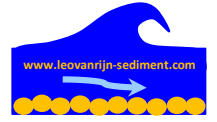
with:

$f_c = g/C_f^2$ = current-related friction coefficient,

$C_f = 18 \log(12h/k_a)$ = Chezy-coefficient,

k_a = apparent bed roughness height,

v = depth-averaged longshore current (in y -direction).



In this approach the effect of the near-bed wave motion on the near-bed current velocities is taken into account by use of the apparent bed roughness height (k_a) resulting in an increase of the physical current-related bed roughness (for example generated by the bed ripples). It has been shown that in a time-averaged approach the resulting bed-shear stress can be obtained by summation of the wave-related and the current-related bed-shear stresses, provided that the effect of the waves on the current velocity is taken into account.

The apparent bed roughness is modelled, as:

$$k_a = k_{s,c} \exp[\xi U/v], \quad k_{a,max} = 10k_{s,c}$$

with:

$$\xi = 0.8 + \varphi - 0.3 \varphi^2 \quad \varphi^2 = \text{coefficient};$$

φ = angle between current direction and wave propagation direction (in radians); $\varphi \leq \pi$, else $\varphi = 2\pi - \varphi$,

$k_{s,c}$ = physical current-related bed-roughness,

U = peak value of orbital velocity at edge of wave boundary layer based on $H_{1/3}$ and $T_{1/3}$,

v = depth-averaged longshore current velocity.

The longshore water surface gradient $d(h + s)/dy$ is incorporated in Equation (8) to represent the longshore water surface gradients related to two-dimensional flow systems (for example tide and wind-induced flow). The magnitude of the longshore surface gradient should be known a priori. Measured longshore depth-averaged velocities around peak tidal flow outside the surf zone (offshore boundary) may be used to estimate the longshore surface gradient based on the Chezy-law.

The last term of Eq. (8) representing the cross-shore exchange of momentum is modelled as a dispersion term, as follows:

$$d(h\tau_{xy})/dx = \rho(h+s) \varepsilon d^2v/dx^2 \tag{12}$$

with:

ε = large scale mixing coefficient (0.1 to 10 m²/s).

Equation (10) is solved iteratively by using wave distribution-averaged variables. The D_{br} -parameter is represented as $D_{br} = \sum p_i D_{br,i}$ with p_i = percentage of occurrence of wave height class i and $D_{br,i}$ = local wave energy dissipation for wave height class i . Similarly, $\theta = \sum p_i \theta_i$; and $C = \sum p_i C_i$.

2.2.2 Wave asymmetry

Three methods are given: 1) Modified Isobe-Horikawa, 2) Ruessink-Van Rijn and 3. Ruessink-Abreu

Modified method of Isobe-Horikawa

The orbital velocities of a skewed wave can be computed by using two sine-waves, as follows:

$$U_{w,on} = + \hat{U}_{w,on} \sin[\{2\pi/(2T_{on})\} t] \quad \text{for} \quad 0 < t < T_{on}$$

$$U_{w,off} = - \hat{U}_{w,off} \sin[\{2\pi/(2T_{off})\} (t - T_{on})] \quad \text{for} \quad T_{on} < t < T_{off}$$

The duration of onshore and offshore phases of wave cycle can be determined from:

$$\int_0^{T_{on}} U_{w,on} dt = T_{on} \int_{T_{on}}^{T_{off}} U_{w,off} dt \quad \text{and} \quad T_{on} + T_{off} = T$$

or

$$(2/\pi) T_{on} \hat{U}_{w,on} = (2/\pi) T_{off} \hat{U}_{w,off} \quad \text{or} \quad T_{on}/T_{off} = \hat{U}_{w,off} / \hat{U}_{w,on}$$



Thus: T_{on} = duration of onshore phase of wave cycle = $[\hat{U}_{w,off}/(\hat{U}_{w,on} + \hat{U}_{w,off})] T$
 T_{off} = duration of offshore phase of wave cycle = $[\hat{U}_{w,on}/(\hat{U}_{w,on} + \hat{U}_{w,off})] T$

As both the onshore and offshore wave cycles are represented by sinusoidal functions, the asymmetry effects (saw-tooth waves) cannot be represented.

The peak velocities are based on the modified method of Isobe and Horikawa (1982). The modifications are described in: "Breaker bar formation and migration" by Grasmeijer and Van Rijn, ICCE 1998, Copenhagen, Denmark

The high-frequency near-bed orbital velocities (low-frequency effects are neglected) are computed using a modification of the method of Isobe and Horikawa (1982). The method of Isobe and Horikawa method is a parameterisation of fifth-order Stokes wave theory and third-order cnoidal wave theory which can be used over a wide range of wave conditions. In the original formulation the near-bed value of \hat{u} (defined as: $u_{on} + u_{off}$) is derived from deep water wave conditions as follows:

$$\hat{u} = 2.r.u_{linear} \quad (13)$$

with:

$$r_3 = -27.3 \log_{10} \left(\frac{H_0}{L_0} \right) - 16.3 \quad (14)$$

$$r_2 = 1.28 \quad (15)$$

$$r_1 = 1 \quad (16)$$

$$r = r_1 - r_2 \exp \left\{ -r_3 \frac{h}{L_0} \right\} \quad (17)$$

u_{linear} = peak near-bed velocity computed using linear wave theory (m/s), H_0 = deep water wave height (m), L_0 = deep water wave length (m), h = local water depth (m).

The method has been modified by improving the r-factor using the local wave conditions (instead of the deep water wave height) to determine the near-bed value of \hat{u} . The r-factor was found by calibration using laboratory and field data with random waves (see Table C1). This resulted in:

$$r = 1 - 3.2 \left(\frac{H}{L} \right)^{0.65} \left(\frac{H}{L} \right)^{3.4 \frac{h}{L}} \quad (18)$$

with: H = local wave height (m), L = local wave length (m), u_{linear} = near-bed velocity computed using linear waves theory.

In 2001, Eq. (18) was revised into:

$$r = 0.75 - 0.1 \tanh(2.5(H/L) - 1.4) \quad (19)$$

The basic data are given in **Table 2.2.1**.



Description	Testnumber	h (m)	H _{m0} (m)	T _p (s)
Field: Terschelling, The Netherlands	Fop05330	9.0	1.89	8.0
	Fop17352	9.4	0.37	17.1
	Fop17576	10.5	4.20	10.2
	Fra05330	5.6	1.87	8.0
	Fra17576	7.7	3.42	9.7
	Fre05330	4.1	1.70	8.1
	Fre17352	5.4	0.37	16.5
Field: Egmond aan Zee, The Netherlands	1B_04430	1.9	0.76	6.1
Lab: small scale flume Delft Univ. of Techn.	TUDB2_01	0.60	0.18	2.2
	TUDB2_05	0.31	0.17	2.2
	TUDB2_07	0.51	0.15	2.2
Field: Muriwai, New Zealand	Muriwai2	1.83	0.92	19.7
Field: Skallingen, Denmark	Sk304_08	1.8	0.80	11.0
	Sk310_01	2.6	1.49	8.8
Lab: Delta Flume Lip11D WL Delft Hydraulics	1A0203_02	2.31	0.92	5.0
	1A0203_07	0.91	0.62	5.0
	1B0213_02	2.30	1.19	5.0
	1B0213_07	0.89	0.57	5.0
	1C0204_02	2.25	0.63	8.0
	1C0204_03	1.77	0.63	8.0
	1C0204_05	1.16	0.63	8.0
	1C0204_11	1.59	0.63	8.0

Table 2.2.1 Basic data of measurements used in calibration of *r*-factor.

Measured signals of surface elevation and horizontal orbital velocity near the bed were analysed using spectral analysis. High- and low-frequency oscillations were separated (by filtering) at a period of 2 times the wave spectrum peak period, T_p . The high-frequency signals were separated into shorter time series each containing 10-15 individual waves. Each of the short time series was defined as one single wave class with one representative wave height, wave period, crest velocity near the bed, and trough velocity near the bed. The mean values were chosen to represent the wave class. A comparison between measured and computed values of \hat{u} is presented in Figure C1. The broken lines indicate a 20% error band.

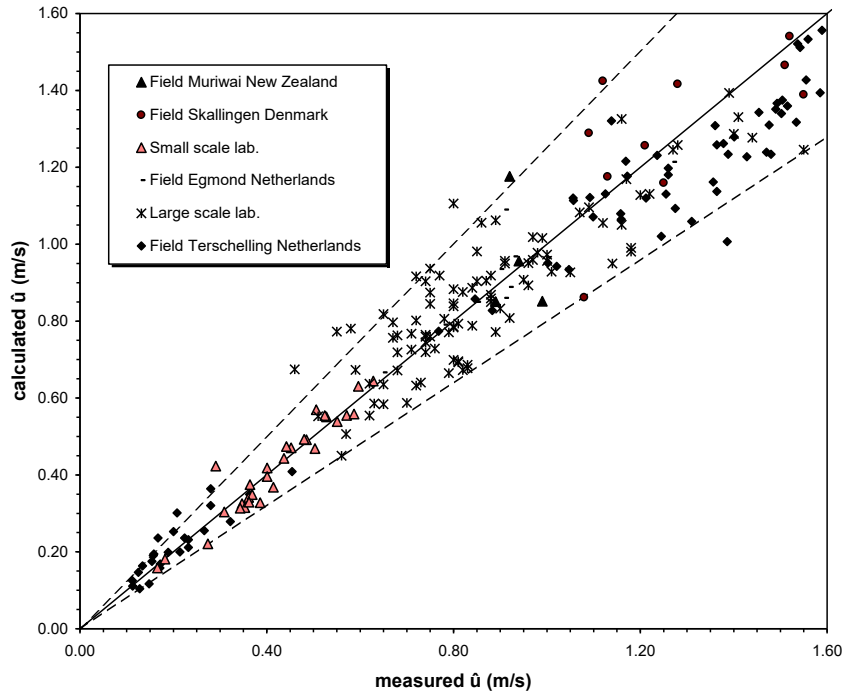


Figure 2.2.2. Comparison between measured and computed values of near-bed orbital velocity \hat{u} defined as $u_{on} + u_{off}$.

The following formulae, Eq.(20)-Eq.(27), were derived to account for the asymmetry of the velocity profile (Isobe and Horikawa, 1982). Eq.(20)-Eq.(25) is a parameterisation of fifth-order Stokes wave theory and third-order cnoidal wave theory. Eq.(C26) and Eq.(27) were introduced to take into account the deformation of the velocity profile due to bottom slope.

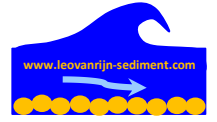
$$\left(\frac{u_{on}}{\hat{u}} \right)_a = \lambda_1 + \lambda_2 \left(\frac{\hat{u}}{\sqrt{gh}} \right) + \lambda_3 \exp \left(-\lambda_4 \left(\frac{\hat{u}}{\sqrt{gh}} \right) \right) \quad (20)$$

with:

$$\lambda_1 = 0.5 - \lambda_3 \quad (21)$$

$$\lambda_2 = \lambda_3 \lambda_4 + \lambda_5 \quad (22)$$

$$\lambda_3 = \frac{(0.5 - \lambda_5)}{\lambda_4 - 1 + \exp(-\lambda_4)} \quad (23)$$



$$\lambda_4 = \begin{cases} -15 + 1.35 \left(T \sqrt{\frac{g}{h}} \right), & T \sqrt{\frac{g}{h}} \leq 15 \\ -2.7 + 0.53 \left(T \sqrt{\frac{g}{h}} \right), & T \sqrt{\frac{g}{h}} > 15 \end{cases} \quad (24)$$

$$\lambda_5 = \begin{cases} 0.0032 \left(T \sqrt{\frac{g}{h}} \right)^2 + 0.000080 \left(T \sqrt{\frac{g}{h}} \right)^3, & T \sqrt{\frac{g}{h}} \leq 30 \\ 0.0056 \left(T \sqrt{\frac{g}{h}} \right)^2 - 0.000040 \left(T \sqrt{\frac{g}{h}} \right)^3, & T \sqrt{\frac{g}{h}} > 30 \end{cases} \quad (25)$$

$$\left(\frac{u_{on}}{\hat{u}} \right)_{modified} = 0.5 + \left(\left(\frac{u_{on}}{\hat{u}} \right)_{max} - 0.5 \right) \tanh \left(\frac{\left(\frac{u_{on}}{\hat{u}} \right)_a - 0.5}{\left(\frac{u_{on}}{\hat{u}} \right)_{max} - 0.5} \right) \quad (26)$$

with:

$$\left(\frac{u_{on}}{\hat{u}} \right)_{max} = 0.62 + \frac{0.003}{\text{bed slope}} \quad (27)$$

A comparison between preliminary computations using the present model and laboratory tests showed that the influence of the bed slope might be less pronounced. The following relation gave more realistic results:

$$\left(\frac{u_{on}}{\hat{u}} \right)_{max} = 0.62 + \frac{0.001}{\text{bed slope}} \quad (28)$$

In 2001, Eq. (28) was revised into:

$$(u_{on}/\hat{u})_{max} = -2.5(h/L) + 0.85 \quad (29)$$

with:

$$(u_{on}/\hat{u})_a = (u_{on}/\hat{u})_{max} \quad \text{if } (u_{on}/\hat{u})_a > (u_{on}/\hat{u})_{max}$$

$$(u_{on}/\hat{u})_{max} = 0.75 \quad \text{if } (u_{on}/\hat{u})_a > 0.75$$

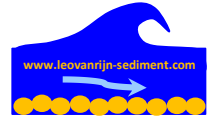
$$(u_{on}/\hat{u})_{max} = 0.62 \quad \text{if } (u_{on}/\hat{u})_a < 0.62$$

The offshore-directed peak orbital velocity follows from: $u_{off} = \hat{u} - u_{on}$

The asymmetry of the peak orbital velocity is reduced in the nearshore zone ($3h_{grens} < h_x < h_{grens}$), as follows:

if $(u_{on} < 0.62 \hat{u}$ and $3h_{grens} < h_x < h_{grens}$), then $u_{on} = 0.62 \hat{u}$ and $u_{off} = 0.38 \hat{u}$

The present model includes a sinusoidal distribution of the instantaneous velocities during the forward and backward phase of the wave cycle. The duration period of each phase is corrected to obtain zero net flow over the full cycle (in contrast to the original approach of Isobe and Horikawa).



Method of Ruessink and Van Rijn (2008)

According to Ruessink and Van Rijn, the skewness and asymmetry of the near-bed velocity in the inner surf and swash zone can to certain extent be represented by:

$$\tilde{U} = \hat{U}_1 \cos(\omega t) + \hat{U}_2 \cos(2\omega t - \beta) \quad (30)$$

with: \hat{U}_1 = amplitude of first harmonic, \hat{U}_2 = amplitude of second harmonic, β = phase difference.

The skewness of this wave signal (velocity as a function of time) represents the wave asymmetry with respect to the onshore and offshore velocities (high and narrow peaks; wide and shallow troughs) and is defined as:

$$S_k = \langle U^3 \rangle / (\sigma_U)^3 \text{ with } (\sigma_U)^2 = \langle U^2 \rangle = 0.5[(\hat{U}_1)^2 + (\hat{U}_2)^2] \text{ and } \langle \dots \rangle = \text{time-averaging.}$$

The asymmetry with respect to time within the wave cycle (forward leaning waves) is defined as the Hilbert transform of the velocity signal which can also be defined as the skewness of the derivative of the velocity signal:

$$A_s = -\langle (\omega \, d\tilde{U}/dt)^3 \rangle / (\sigma_U)^3.$$

Symmetric waves (in time) yield a value of $A_s = 0$.

Using these definitions, it follows that:

$$S_k = \frac{0.75 (\hat{U}_1)^2 (\hat{U}_2) \cos(\beta)}{(\sigma_U)^3} \quad \text{and} \quad A_s = - \frac{0.75 (\hat{U}_1)^2 (\hat{U}_2) \sin(\beta)}{(\sigma_U)^3} \quad (31)$$

$$\tan(\beta) = -A_s/S_k \text{ or } \beta = -\text{atan}(A_s/S_k) \quad (32)$$

$$(\hat{U}_2)^3 - 2(\sigma_U)^2 \hat{U}_2 + (4/3) (\sigma_U)^3 S_k / \cos(\beta) = 0 \quad (33)$$

$$(\hat{U}_1)^2 + (\hat{U}_2)^2 = 2(\sigma_U)^2 \quad (34)$$

Equation (C19) can be solved analytically using a complex function approach, yielding:

$$\hat{U}_2 = 2(P)^{0.5} \cos(\varphi) \quad (35)$$

with:

$$P = 2(\sigma_U)^2/3,$$

$$Q = (4/3) (\sigma_U)^3 S_k / \cos(\beta) \text{ and}$$

$$\varphi = 1/3[\arccos(-0.5Q P^{-1.5}) + n(2\pi)];$$

$n = 0, 1, 2$ yields three roots; the smallest positive root is the solution.

\hat{U}_1 follows from Equation (34).

Using linear wave theory, the standard deviation of the velocity is defined as:

$$\sigma_U = \pi H_{rms} / (1.41 T \sinh(kh)).$$



Based on the analysis of a large field data set of measured velocity time series, the parameters S_k , A_s and β are found to be:

$$\begin{aligned}
 S_k &= B \cos(\beta), \\
 A_s &= B \sin(\beta), \\
 \beta &= -90 + 90 \tanh(0.6373/U_r^{0.5995}), \\
 B &= 0.7939 [1 + \exp(K)]^{-1}, \\
 K &= 2.8256[-0.6065 - {}^{10}\log(U_r)], \\
 U_r &= 0.75(0.5H_{M0}) k (kh)^{-3}, \\
 k &= (2\pi/L) = \text{wave number, } h = \text{water depth, } H_{M0} = 1.41 H_{rms}.
 \end{aligned}$$

Almost perfect sinusoidal waves are present for Ursell numbers smaller than $U_r < 0.01$.

Skewed waves are present for $0.01 < U_r < 0.1$.

Skewed and asymmetric waves (bore type waves) are present for $U_r > 0.1$. The phase angle β (in degrees) increases to -90 degrees

Figure 2.2.3 shows the saw-tooth near-bed velocity time signal for $h = 0.3$ m, $H_{rms} = 0.3$ m, $T = 7$ s. The peak landward and seaward velocities are almost the same. The duration of the forward phase is about 3 s and that of the backward phase is 4 s. The peak landward velocity occurs at about 1.3 s after $t = 0$ and the peak seaward velocity at about 1.3 s before t_{end} .

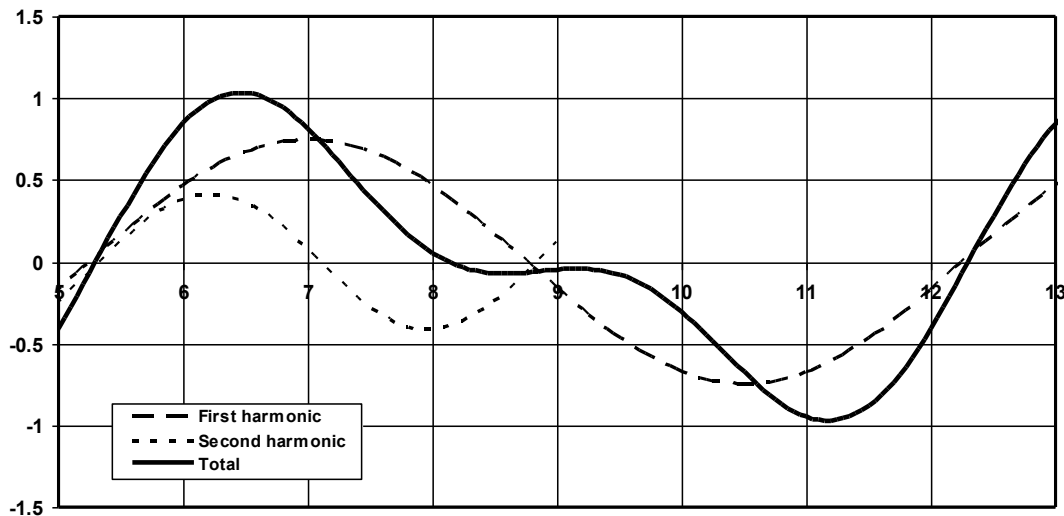


Figure 2.2.3 Velocity time series for $H_{rms} = 0.3$ m, $T = 7$ s, $h = 0.3$ m, $L = 11.9$ m



Method of Abreu-Ruessink (2010)

Abreu et al. (2010) have proposed another method for asymmetric waves. The orbital velocities near the bottom are described by:

$$U_t = \hat{U}_w f \frac{\sin(\omega t) + \{r(1+f)^{-1}\} \sin \varphi}{1 - r \cos(\omega t + \varphi)} \quad (36)$$

with: $r =$ coefficient, $f = (1 - r^2)^{0.5}$, $\varphi =$ phase angle, $\hat{U}_w = 0.5 [|\hat{U}_{on}| + |\hat{U}_{off}|]$

The r -coefficient varies in the range $-1 < r < 1$.

The φ -value varies in the range $-90^\circ < \varphi < 0^\circ$ for realistic asymmetric with larger onshore velocities.

A sinusoidal wave (linear wave) is obtained for $r = 0$ and $\varphi = 0$, see **Figure 2.2.4**.

Using $\varphi = 0^\circ$, Equation (36) yields:

$$U_t = \hat{U}_w f \frac{\sin(\omega t)}{1 - r \cos(\omega t)} \quad (37)$$

This represents an asymmetric velocity signal with a peak onshore velocity equal to the peak offshore velocity (bore-type wave).

Figure 2.2.4 shows computed velocities for $\varphi = 0$, $\varphi = -45^\circ$ and $\varphi = -90^\circ$ and $r = 0, 0.25, 0.5$ and 0.75 . The wave period is set to $T = 8$ s. The \hat{U}_w -value is set to 1 m/s.

Asymmetric velocity signals are obtained for $\varphi = 0$ and $\varphi = -45^\circ$ with $r = 0.25, 0.50$ and 0.75 (increasing asymmetry for increasing r -value). The peak onshore and offshore velocity are equal for $\varphi = 0$ and unequal for $\varphi = -45^\circ$ (larger peak onshore than peak offshore velocity).

Saw-tooth waves are obtained for $\varphi = 0$ and $r = 0.75$.

Skewed velocity signals are obtained for $\varphi = -90^\circ$ with $r = 0.25, 0.50$ and 0.75 (increasing peak onshore velocity for increasing r -value). The peak onshore and offshore velocity are equal for $r = 0$.

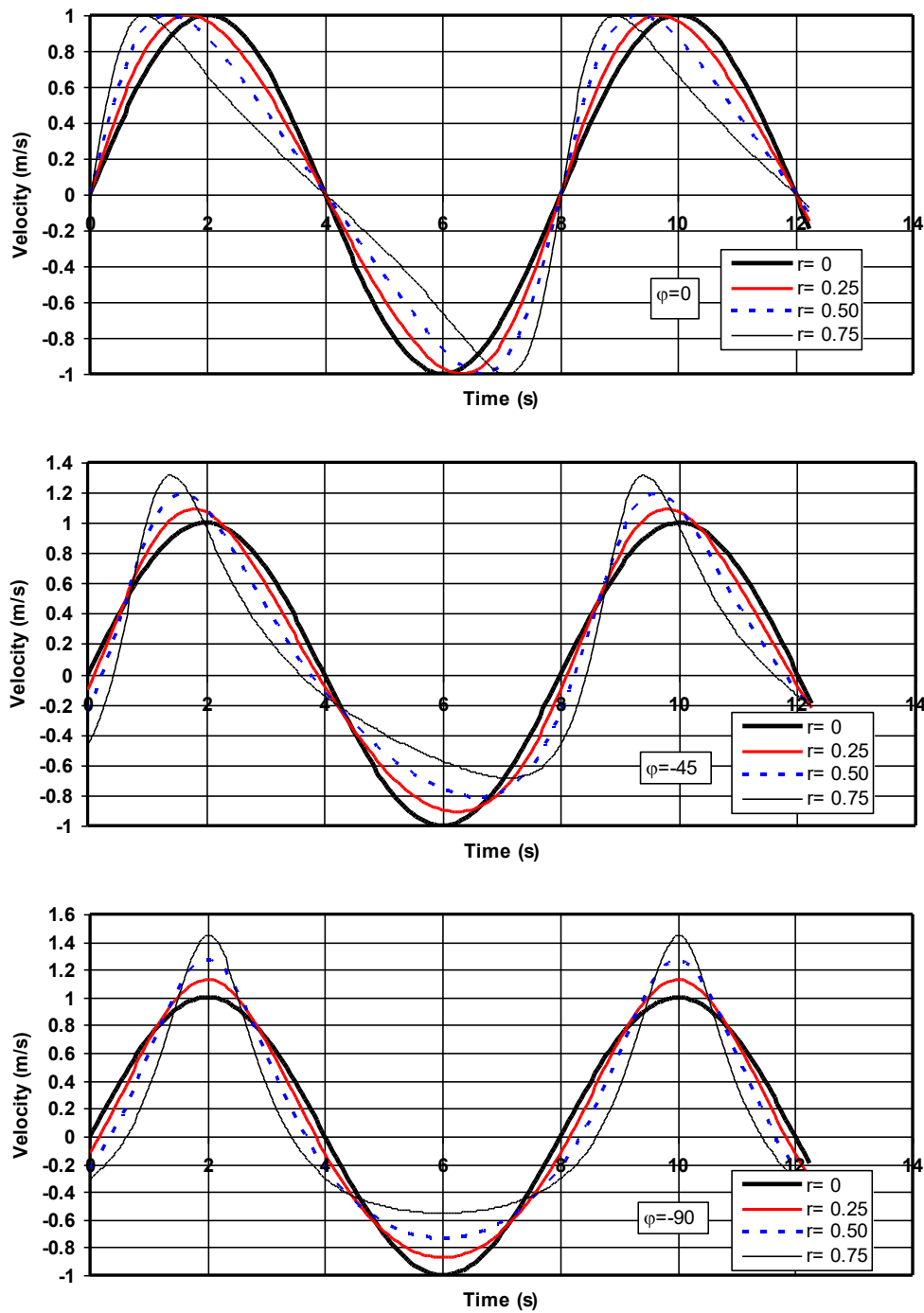


Figure 2.2.4 Velocity as function of time for various values of ϕ and r
(based on Abreu et al., 2010)



Based on measured field data of near-bed velocities, Ruessink et al. (2011) has proposed expressions for the r , φ and \hat{U}_w parameters as function of the Ursell number (UR), as follows:

$$r = \tanh[0.9305\{0.8507/(1+\exp(-1.586-3.367\log(\text{UR})))\}] \quad (38)$$

$$\varphi = - (90^\circ/360^\circ) 2\pi \tanh[0.815/(\text{UR}^{0.672})] \text{ in radians} \quad (39)$$

$$\varphi = -90^\circ \tanh[0.815/(\text{UR}^{0.672})] \text{ in degrees} \quad (40)$$

$$\hat{U}_w = \pi H_{1/3}/\{T \sinh(kh)\} \quad (41)$$

with:

$$\text{UR} = 0.75(0.5H_{M0}) k (kh)^{-3} = 0.375 H_{M0} k (kh)^{-3} \quad (42)$$

H_{M0} = wave height based on wave spectrum, $H_{M0} = 1.41 H_{rms}$, $H_{M0} \cong H_{1/3}$,

$k = 2\pi/L$ = wave number,

h = water depth.

The \hat{U}_w -parameter can be computed by using H_{rms} or $H_{1/3}$. If H_{rms} is used, the rms value of peak orbital velocities of all individual waves of the wave train are considered. If $H_{1/3}$ is used, the mean of the highest 33% of the waves are considered only.

Figure 2.2.5 shows the r , f and φ as functions of the Ursell number (UR).

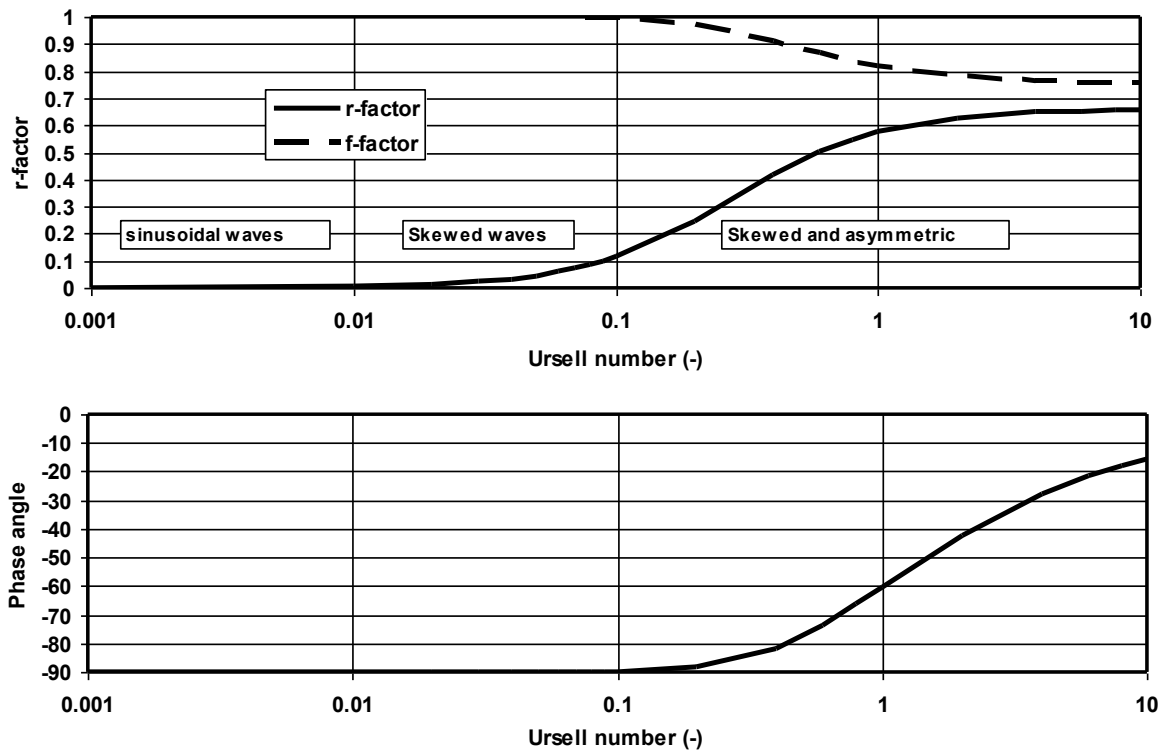


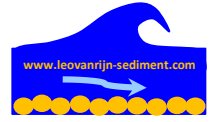
Figure 2.2.5 r , f (upper) and φ (lower) parameters as function of Ursell number

Almost perfect sinusoidal waves are present for Ursell numbers smaller than $U_r < 0.01$.

Skewed waves are present for $0.01 < U_r < 0.1$.

Skewed and asymmetric waves (bore type waves) are present for $U_r > 0.1$.

The phase angle φ is -90° for sinusoidal waves and goes to about -15° for very asymmetric waves.



2.2.3 Undertow velocities over the water depth

The undertow velocity profile is schematized into the following three layers.

Near-bed layer ($z_0 < z \leq \delta_m$)

$$\text{Velocity profile: } u_{r,z} = \alpha_r [u_{r,\delta} / \ln(\delta_m/z_0)] \ln(z/z_0) \quad (43)$$

with:

$z_0 = k_{s,c} / 30$	= zero-velocity level,
$\delta_m = 0.216 A_\delta (A_\delta / k_{s,w})^{0.25}$	= thickness of mixing layer near bed
$u_{r,\delta} = [u_r / (-1 + \ln(30h/k_a))] \ln(30\delta_m/k_a)$	= velocity at $z = \delta_m$
A_δ	= amplitude of near-bed orbital excursion
k_a	= apparent bed roughness
$k_{s,c}, k_{s,w}$	= current and wave-related bed-roughness
u_r	= depth-averaged undertow velocity
α_r	= correction factor

Intermediate layer ($\delta_m < z \leq 0.5h$)

$$\text{Velocity profile: } u_{r,z} = \alpha_r [u_r / (-1 + \ln(h/z_a))] \ln(z/z_a) \quad (44)$$

with: $z_a = k_a / 30$

h = water depth

Upper layer ($0.5h < z \leq h$)

$$\text{Velocity profile: } u_{r,z} = u_{r,\text{mid}} [1 - ((z - 0.5h) / (0.5h))^3] \quad (45)$$

with:

$$u_{r,\text{mid}} = \alpha_r [u_r / (-1 + \ln(h/z_a))] \ln(0.5h/z_a) \quad = \text{velocity at } z = 0.5h$$

Equation 45 yields: $u_{r,z} = u_{r,\text{mid}}$ for $z = 0.5h$ and $u_{r,z} = 0$ for $z = h$.

$$\text{The correction factor } \alpha_r \text{ can be determined from: } q_1 + q_2 + q_3 = u_r h. \quad (46)$$

The q -values are:

$$q_1 = \int_{z_0}^{\delta} u_{r,z} dz \cong 0$$

$$q_2 = \int_{\delta}^{0.5h} u_{r,z} dz = \alpha_r [u_r / (-1 + \ln(h/z_a))] [(\delta_m - 0.5h) + 0.5h \ln(0.5h/z_a) - \delta_m \ln(\delta_m/z_a)]$$

$$q_3 = \int_{0.5h}^h u_{r,z} dz = 0.375h u_{r,\text{mid}}$$



This yields:

$$\alpha_r = C_1 / (C_3 + 0.375 C_2) \quad (47)$$

with:

$$C_1 = -1 + \ln(h/z_a)$$

$$C_2 = \ln(0.5h/z_a)$$

$$C_3 = [(\delta_m/h - 0.5) + 0.5 \ln(0.5h/z_a) - (\delta_m/h) \ln(\delta_m/z_a)] \cong -0.5 + 0.5 \ln(0.5h/z_a)$$

Example case

Input: $h = 5$ m, $H_s = 2$ m, $T_p = 7$ s, $v_{long} = 1$ m/s, $u_r = -1$ m/s, $\Phi = 90^\circ$, $k_{s,c} = k_{s,w} = 0.02$ m, $\delta_m = 0.1$ m, $k_a = 0.08$ m, $z_a = 0.00267$ m

This yields: $\alpha_r = 1.19$

The undertow velocity profile is shown below and for reference a logarithmic velocity profile over the full depth is also shown. In both cases: $u_r = 1$ m/s.

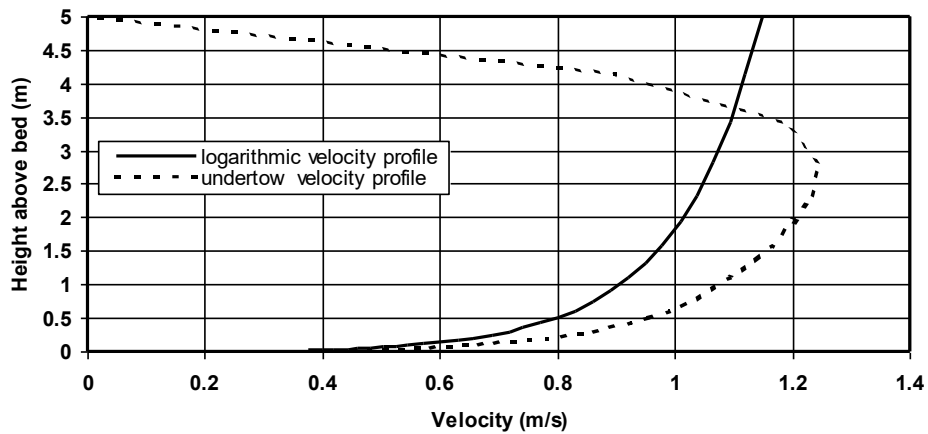


Figure 2.2.6 Undertow velocity profile



2.2.4 Sand transport

Bed load transport

The net bed-load transport rate in conditions with uniform bed material is obtained by time-averaging (over the wave period T) of the instantaneous transport rate using a bed-load transport formula (quasi-steady approach), as follows:

$$q_b = (1/T) \int q_{b,t} dt \quad (48)$$

with $q_{b,t} = F$ (instantaneous hydrodynamic and sediment transport parameters).

The applied bed-load transport formula is a parameterization of a detailed grain saltation model representing the basic forces acting on a bed-load particle for steady flow (Van Rijn, 1984a, 1993). This approach is generalized to the regime of combined current and wave conditions by using the concept of the instantaneous bed-shear stress. The instantaneous bed-load transport rate (kg/s/m) is related to the instantaneous bed-shear stress, which is based on the instantaneous velocity vector (including both wave-related and current-related components) defined at a small height above the bed. The formula applied, reads as:

$$q_b = \gamma \rho_s d_{50} D_*^{-0.3} \left[\left[\tau'_{b,cw} / \rho \right]^{0.5} \left[\tau'_{b,cw} - \tau_{b,cr} \right] / \tau_{b,cr} \right]^\eta \quad (49)$$

in which:

$\tau'_{b,cw}$ = **instantaneous grain-related bed-shear stress** due to both currents and waves = $0.5 \rho f'_{cw} (U_{\delta,cw})^2$,

$U_{\delta,cw}$ = instantaneous velocity due to currents and waves at edge of wave boundary layer,

f'_{cw} = grain friction coefficient due to currents and waves = $\alpha \beta f'_c + (1-\alpha) f'_w$,

f'_c = current-related grain friction coefficient,

f'_w = wave-related grain friction coefficient,

α = coefficient related to relative strenght of wave and current motion,

β = wave-current-interaction coefficient,

$\tau_{b,cr}$ = critical bed-shear stress according to Shields,

ρ_s = sediment density, ρ = fluid density,

d_{50} = particle size, D_* = dimensionless particle size,

γ = coefficient = 0.5, η = exponent = 1.

Detailed information of the critical bed-shear stress and the bed roughness is given by Van Rijn (2007a).



The grain roughness is assumed to be $k_{s,grain} = \epsilon d_{90}$ with $\epsilon=3$ for $d_{50} < 0.5$ mm; $\epsilon=1$ for $d_{50} > 1$ mm and $\epsilon=3$ to 1 for intermediate values (van Rijn, 1993). The bed-load transport is assumed to be mainly affected by the grain roughness, but the overall bed-form roughness also has some (weak) influence on the bed-load transport in case of combined steady and oscillatory flow because of its effect on the near-bed velocity profile. Analysis of sensitivity computations for combined steady and oscillatory flow shows that the bed-load transport is reduced by about 15% for an increase of the bed-form roughness by a factor of 5 ($k_{s,c} = 0.05$ m in stead of 0.01 m).

The measured bed-load transport rates of the wave tunnel tests have been used to determine the γ and η coefficients, yielding $\gamma=0.5$ and $\eta=1$.

Equation (49) is based on the assumption that the sediment particles respond instantaneously (quasi-steady) to the oscillatory fluid motion near the bed. The net transport rate will always be in the direction of the largest peak orbital velocity.

Gravel transport

To show that Equation (2.2.2) can also be used to compute gravel transport, the CROSMOR-model has been used in river mode (no waves; input file GRAVELR.inp) for a channel with a gravel bed. Three values of the d_{50} of the gravel bed have been used: $d_{50}=6, 12$ and 18 mm; $d_{90}=12, 24, 36$ mm. The bed roughness is set to $k_s=1 d_{90}$. The water depth is set to a constant value of $h=1$ m. The depth-averaged current velocity is varied in the range of 1 to 3 m/s. The water temperature is 15 °C and the salinity is 0 promille (fresh water). The computed gravel transport rates are shown in **Figure 2.2.7**. The computed values of the transport equation of Meyer-Peter and Mueller MPM (1948) are also shown in **Figure 2.2.7**. The MPM-equation is especially valid for coarse grains based on a series of flume experiments with gravel material ($d_{50}=5.2$ and 28.7 mm), see **Figure 2.2.7**.

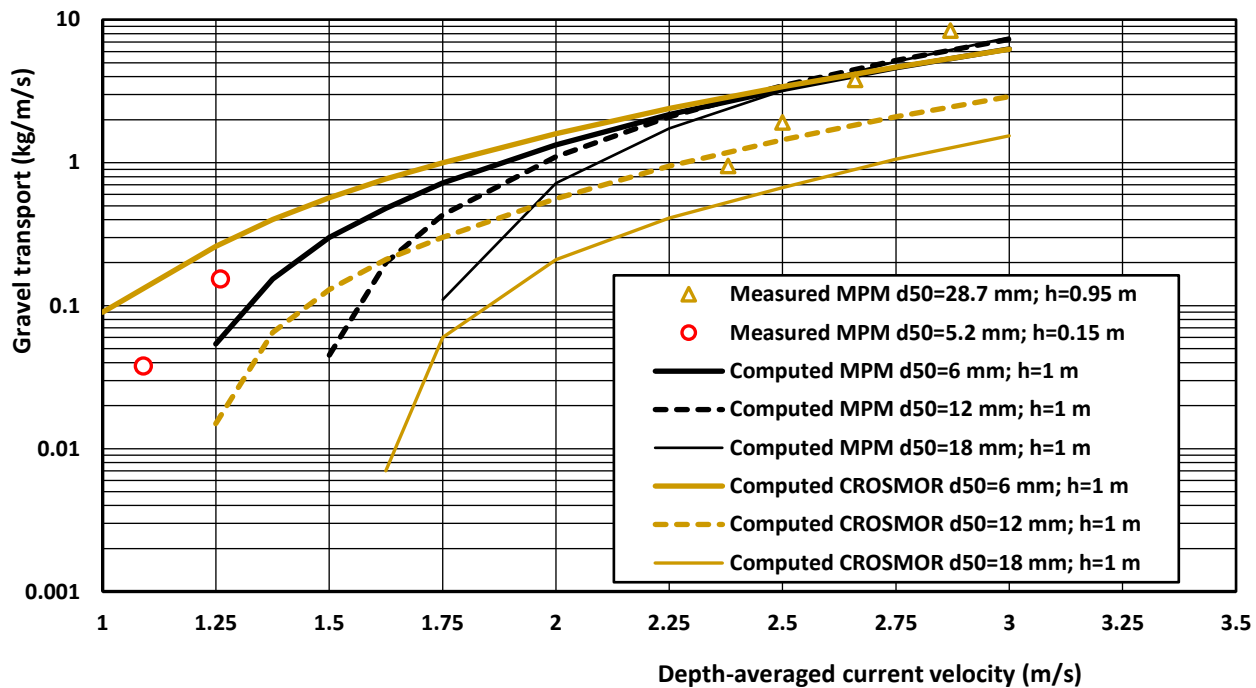


Figure 2.2.7 Gravel transport as function of depth-averaged current velocity



The results of the MPM-equation show that the effect of grain size on the gravel transport is minor for current velocities higher than 2.25 m/s. The transport rates of the CROSMOR-model and the MPM-equation are in good agreement for $d_{50}=6$ mm. The CROSMOR-model underpredicts somewhat for $d_{50}=12$ mm (factor 2) and more severely (factor 5) for $d_{50}=18$ mm.

Suspended load transport (1 fraction)

Definitions

The net depth-integrated suspended sand transport is defined as the sum of the net current-related ($q_{s,c}$) and the net wave-related ($q_{s,w}$) transport components, as follows:

$$q_s = q_{s,c} + q_{s,w} = \int v c \, dz + \int \langle (V-v)(C-c) \rangle \, dz \quad (50)$$

in which: $q_{s,c}$ = time-averaged current-related suspended sediment transport rate and $q_{s,w}$ = time-averaged wave-related suspended sediment transport rate (oscillating component), v = time-averaged velocity, V = instantaneous velocity vector, C = instantaneous concentration and c = time-averaged concentration and $\langle \rangle$ averaging over time, \int the integral from the top of bed-load layer to the water surface.

The current-related suspended transport ($q_{s,c}$) is defined as the advective transport of sediment particles by the time-averaged (mean) current velocities (longshore currents, rip currents, undertow currents). Thus, the transport of sediment which is carried by the steady flow. In conditions with waves superimposed on the current, both the current velocities and the sediment concentrations will be affected by the wave motion. It is known that the wave motion reduces the current velocities near the bed, but the near-bed concentrations are strongly enhanced due to the stirring action of the waves. These effects are included in the current-related transport.

The wave-related suspended sediment transport ($q_{s,w}$) is defined as the transport of sediment particles by the high-frequency oscillating fluid components (cross-shore orbital motion). Low-frequency transport contributions are herein neglected. The wave-related transport components are defined in the plane of orbital motion.

For practical reasons the current-related and the wave-related transport components are studied separately. Furthermore, this allows the evaluation of the relative magnitude of both components, which is of significant importance for modelling purposes.

The CROSMOR-modell can also be applied with multiple fractions (see detailed description).

Wave-related suspended transport

Modelling of the wave-related suspended transport ($q_{s,w}$) for a sand bed covered with ripple type bed forms, basically requires the simultaneous (numerical) solution of both the time-dependent momentum equation for the oscillatory fluid flow and the time-dependent advection-diffusion equation for suspended sediment particles.

For the two-dimensional vertical plane this latter equation reads as:

$$\partial C / \partial t + \partial [UC - (\varepsilon_{s,x} \partial C / \partial x)] / \partial x + \partial [(W-w_s)C - (\varepsilon_{s,z} \partial C / \partial z)] / \partial z = 0 \quad (51)$$



with: C = instantaneous sand concentration (volume); U , W = horizontal and vertical instantaneous fluid velocities; w_s = fall velocity of suspended sand; $\varepsilon_{s,x}$, $\varepsilon_{s,z}$ = sediment mixing coefficient in horizontal x and vertical z directions; t = time; x = horizontal coordinate and z = vertical coordinate.

The oscillatory flow along a rippled bed is rather complicated due to the generation, advection and diffusion of the near-bed vortices including the sediment particles carried by the vortices. Numerical simulation of the detailed vortex motions requires the application of sophisticated turbulence-models on a fine grid structure. Furthermore, the shape and dimensions of the ripples should be known a priori (boundary conditions). Using this approach, the instantaneous fluid flow and suspended transport due to combined steady and oscillatory flow over a rippled bed can be solved in an integrated way, which is a great advantage of this method. A major drawback is the relatively large computational time involved, when it is applied in a numerical morphological model system with feed back to changing bed levels and hence hydrodynamics (loop system). This detailed approach is at an early stage of research and beyond the scope of the present study.

For a plane bed without bed forms the advection-diffusion equation for the suspended concentrations can be simplified to:

$$\frac{\partial C}{\partial t} + \partial[(-w_s)C - (\varepsilon_{s,z} \frac{\partial C}{\partial z}) / \partial z = 0 \quad (52)$$

This unsteady model approach is applied by many researchers to simulate the suspended concentrations inside and outside the wave boundary layer over a plane bed (see overview of Dohmen-Janssen, 1999). This approach may also be used to simulate the time-averaged sand concentrations over a rippled, provided that the overall effect of the bed forms on the sediment mixing coefficients is taken into account (Chung and Grasmeyer, 1999). Their results also show that the wave-related suspended transport can not be simulated accurately by this approach.

Herein, an engineering approach is proposed to estimate the wave-related suspended transport. This method has been introduced by Houwman and Ruessink (1996). Experimental data are required to determine the empirical coefficient involved.

The wave-related suspended transport component is modelled as:

$$q_{s,w} = \gamma [(U_{on})^4 - (U_{off})^4] / [(U_{on})^3 + (U_{off})^3] \int c \, dz \quad (53)$$

with: $U_{on} = U_{\delta,f}$ = near-bed peak orbital velocity in onshore direction (in wave direction) and $U_{off} = U_{\delta,b}$ = near-bed peak orbital velocity in offshore direction (against wave direction), c = time-averaged concentration and γ = phase lag function.

It is based on an instantaneous response of the suspended sand concentrations (C) and transport ($q_{s,w}$) to the near-bed orbital velocity (C proportional to U^3 and q_s to U^4). This may be valid for the near-bed layer (say 1 to 5 times the wave boundary layer thickness), but at higher levels a delayed response of the sand concentrations (phase lag effects) will be more realistic, particularly for fine sediments. For very fine sediment the wave-related suspended transport may even be opposite to the wave propagation direction.

Phase lag effects are supposed to be accounted for by the γ -function. As phase lag effects are related to the wave conditions, sand size and bed geometry, the γ -function is supposed to be a complicated function of the



former parameters (yielding negative values for very fine sand). A detailed discussion of phase lag effects and functions is given by Dohmen-Janssen (1999).

Simulation of the wave-related suspended transport requires computation of the time-averaged sand concentration profile and integration of the time-averaged sand concentration profile in vertical direction. Herein, the integration is taken over a near-bed layer with a thickness equal to about 0.5 m, assuming that the suspended sand above this layer is not much effected by the high-frequency wave motion with periods in the range of $T = 5$ to 10 s. This assumption is satisfied if the fall time of a suspended sand particle over a distance of 0.5 m is much larger than the wave period ($T_{fall} = 0.5/w_s$ yielding about 25 s for $d = 0.2$ mm with $w_s = 0.02$ m/s). Furthermore, the data of the Delta flume (Chung and Grasmeyer, 1999) show that most of the wave-related suspended transport occurs in the near-bed layer with a thickness of about 0.5 m (10 to 20 times the ripple height).

Chung and Grasmeyer (1999) have determined the γ -function by fitting of the measured wave-related transport rates. The peak onshore and offshore orbital velocities as well as the time-averaged sand concentrations were taken from the measured data. Amazingly, the γ -function was found to be a constant value of about 0.2 for all test results (relative standard error of about 30 %). Any influence of the wave conditions and/or the sand size on the γ -function could not be detected, implying relatively small phase lag effects for the five data sets used. It is noted that the γ -value of 0.2 is based on data with rather pronounced ripples observed in a large scale 2D wave tank. The γ -value may be considerably smaller (say between 0.1 and 0.2) for field conditions with less pronounced 3D-ripples (Grasmeyer et al., 2000).

Current-related suspended transport

Modelling of the current-related suspended transport requires modelling of both the time-averaged velocity profile and the time-averaged sand concentration profile. The suspended transport in the main current direction is computed as: $q_{s,c,1} = \int v_{R,z} c_z dz$ with c_z = time-averaged sand concentration at height z and $v_{R,z}$ = current velocity at height z in main current direction.

The current velocity profile in the main current direction is represented as a two-layer system to account for the wave effects in the near-bed layer (Van Rijn and Kroon, 1992; Van Rijn, 1993). In both layers the velocity profile is assumed to be logarithmic.

The suspended transport due to the undertow current is computed as: $q_{s,c,2} = \int u_{r,z} c_z dz$ (54)

with c_z = time-averaged sand concentration at height z and $u_{r,z}$ = undertow velocity at height z above the bed. The current velocity profile of the undertow current (due to breaking waves), which is opposite to the wave direction, is represented as a three-layer system. In the two layers near the bed the velocity profile is assumed to be logarithmic. In the upper layer ($z/h > 0.5$) the velocity profile is assumed to decrease to zero at the water surface according to a third power distribution.

The new three-layer velocity profile for the undertow results in somewhat larger suspended transport rates (about 30%) due to the increase of the near-bed velocities.

Both current-related suspended transport components ($q_{s,c,1}$ and $q_{s,c,2}$) are summed by vectorial addition.

The total suspended transport is obtained by vectorial summation of $q_{s,c}$ and $q_{s,w}$.



The time-averaged (over the wave period) advection-diffusion equation is applied to compute the equilibrium time-averaged sand concentration profile due to the combined effect of steady and oscillatory flow. This equation reads as:

$$w_{s,m} + \varepsilon_{s,cw} \frac{dc}{dz} = 0 \quad (55)$$

in which: $w_{s,m}$ = fall velocity of suspended sediment in a fluid-sediment mixture (m/s), $\varepsilon_{s,cw}$ = sediment mixing coefficient for combined steady and oscillatory flow (m^2/s), c = time-averaged concentration at height z above the bed (kg/m^3); hindered settling and turbulence damping effects are taken into account.

For combined steady and oscillatory flow the sediment mixing coefficient (see Figure 2.2.8) is modelled as:

$$\varepsilon_{s,cw} = ((\varepsilon_{s,c})^2 + (\varepsilon_{s,w})^2)^{0.5} \quad (56)$$

in which: $\varepsilon_{s,w}$ = wave-related mixing coefficient (m^2/s), $\varepsilon_{s,c}$ = current-related mixing coefficient due to main current and undertow current (m^2/s); the effect of the sediment particles on the mixing of fluid momentum is taken into account by the β_c -factor, which depends on the particle fall velocity of the suspended sand particles and the bed-shear velocity ($\beta_c = 1 + 2(w_s/u_{*,c})^2$). Thus: $\varepsilon_{s,c} = \beta_c \varepsilon_{f,c}$ and $\varepsilon_{s,w} = \beta_w \varepsilon_{f,w}$.

$$\delta_s = \max(5\gamma_{br} \delta_w, 10\gamma_{br} k_{s,w}) \text{ with limits } 0.1 \leq \delta_s \leq 0.5 \text{ m} \quad (57)$$

with: δ_s = thickness of effective near-bed sediment mixing layer, δ_w = thickness of wave boundary layer, $k_{s,w}$ = wave-related bed roughness and $\gamma_{br} = 1 + (H_s/h - 0.4)^{0.5}$ = empirical coefficient related to wave breaking ($\gamma_{br} = 1$ for $H_s/h \leq 0.4$).

The wave-related sediment mixing coefficient in the upper half of the water column has been modified into (multiplied by the breaking coefficient γ_{br}):

$$\varepsilon_{s,w,max} = 0.035 \gamma_{br} h H_s/T_p \text{ with } \varepsilon_{s,w,max} \leq 0.05 \text{ m}^2/\text{s} \quad (58)$$

The wave-related sediment mixing coefficient near the bed is described by:

$$\varepsilon_{s,w,bed} = 0.018 \beta_w \delta_s U_\delta \quad (59)$$

in which: U_δ = near-bed peak orbital velocity, δ_s = thickness of mixing layer, $\beta_w = 1 + 2(w_s/u_{*,w})^2$ with $\beta_w \leq 1.5$, w_s = fall velocity of suspended sand, $u_{*,w}$ = wave-related bed-shear velocity.

The near-bed mixing parameter $\varepsilon_{s,w,bed}$ was found to be dependent on the particle velocity (size), based on analysis of sand concentration profiles of experiments with bed material in the range of 0.1 to 0.3 mm (Van Rijn, 1993). The near-bed mixing appears to increase with increasing particle size, which may be an indication of the dominant influence of centrifugal forces acting on the particles due to strong turbulence-induced vortex motions close to the bed resulting in an increase of the effective mixing of sediment particles. This effect is modelled by the β_w -factor. As no information is available for bed materials larger than about 0.3 mm, the application of Eq. (3.3.6b) for these conditions is highly uncertain. More research is necessary for accurate prediction of the wave-induced suspended transport for relatively coarse materials (>0.3 mm; coarse sand and gravel beds).



Numerical solution of the advection-diffusion equation requires the specification of the concentration at a certain elevation above the bed (reference concentration, see Figure 2.2.8).

The reference concentration (volume) is given by:

$$c_a = 0.015 \frac{d_{50}}{a} \frac{T^{1.5}}{D_*^{0.3}} \quad \text{with } c_a \leq 0.05 \text{ (approx. } 130 \text{ kg/m}^3\text{)} \quad (60)$$

in which: D_* = dimensionless particle parameter (-), T = dimensionless bed-shear stress parameter (-), a = reference level (m), a is taken equal to the bed roughness height k_s with a minimum value of 0.02 m.

The T -parameter is:

$$T = (\tau'_{b,cw} - \tau_{b,cr}) / \tau_{b,cr} \quad (61)$$

in which: $\tau'_{b,cw}$ = time-averaged effective bed-shear stress (N/m^2), $\tau_{b,cr}$ = time-averaged critical bed-shear stress according to Shields (N/m^2).

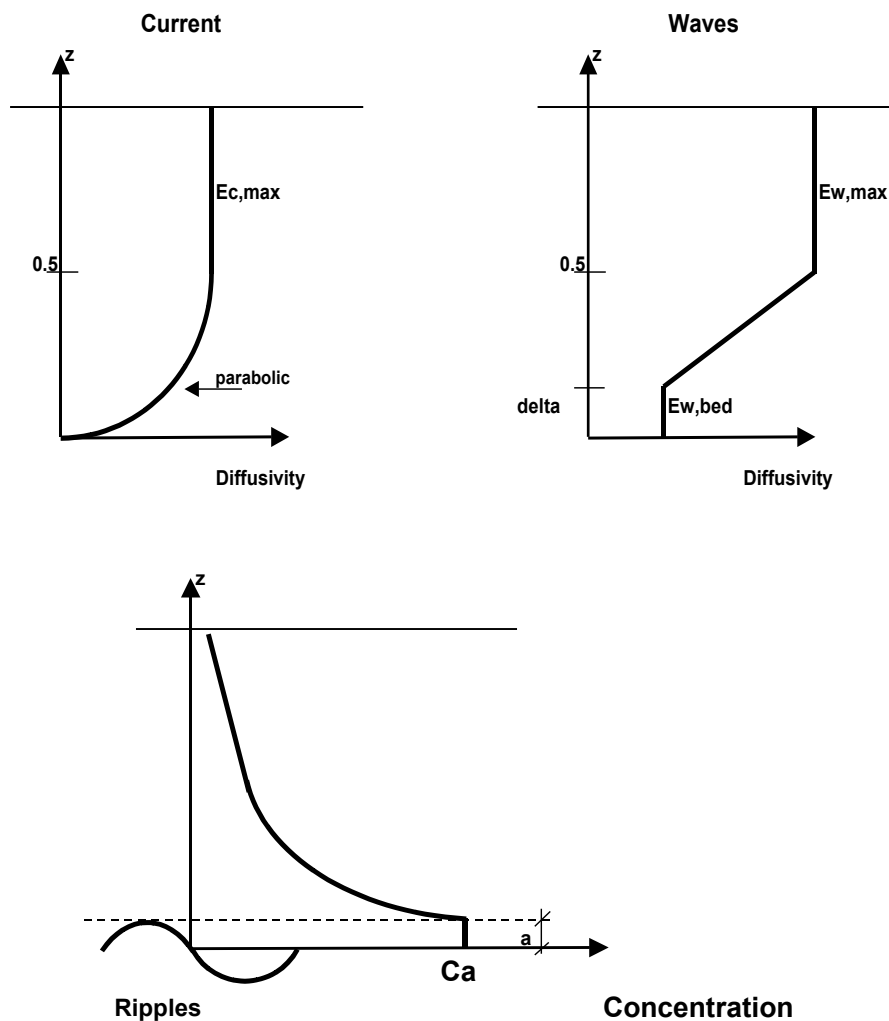


Figure 2.2.8 Vertical distribution of mixing coefficients (upper) and Reference concentration (lower)



The magnitude of the time-averaged bed-shear stress, which is independent of the angle between the wave- and current direction, is given by:

$$\tau'_{b,cw} = \tau'_{b,c} + \tau'_{b,w} \quad (62)$$

in which: $\tau'_{b,c} = \mu_c \alpha_{cw} \tau_{b,c}$ = effective current-related bed-shear stress (N/m²), and $\tau'_{b,w} = \mu_{w,a} \tau_{b,w}$ = effective wave-related bed-shear stress (N/m²), $\mu_{w,a}$ = efficiency factor and α = wave-current interaction factor; grain-related friction factor depends on d_{90} .

The wave-related efficiency factor $\mu_{w,a}$ is an important parameter, because it strongly affects the reference concentration near the bed. This parameter will probably depend on the bed form and bed roughness characteristics, but the functional relationship involved is not yet known. Therefore, the $\mu_{w,a}$ factor has been used as a calibration parameter to get a better estimate of the near-bed concentration. As the bed forms are related to the relative wave height (ripples for small values of H_s/h and plane bed for large values of H_s/h), the $\mu_{w,a}$ factor is supposed to be related to the relative wave height. Based on analysis of experimental data, the $\mu_{w,a}$ factor has been modified into $\mu_{w,a} = 0.125(1.5 - H_s/h)^2$ with minimum value of 0.063. This yields a better description of the reference concentration for relatively small wave heights in the ripple regime.

Important parameters for the suspended load transport are the current-related and the wave-related bed-form roughness ($k_{s,c}$ and $k_{s,w}$). These parameters are directly related to the size and geometry of the bed forms (ripples). The wave-related bed-form roughness is also related to the near-bed orbital excursion. If the ripple length is much larger than the orbital excursion, the wave-related bed-form roughness is relatively small because the ripple-related vortices will be relatively weak. At present stage of research both parameters ($k_{s,c}$ and $k_{s,w}$) are used as input parameters. Research is necessary to get better estimates of these parameters. Basically, bed form and bed roughness predictors are required.

For morphological computations, the effect of the local bed slope on the transport rate must be taken into account, This is done, as follows:

- multiplying the critical bed-shear stress with the Schoklitsch-factor $k_1 = \sin(\phi + \beta) / \sin(\phi)$, in which ϕ = dynamic friction angle ($\tan \phi$ is about 0.6) and β = local slope angle; the angle β is positive for uphill transport yielding $k_1 > 1$ and hence an increase of the critical bed-shear stress and a decrease of the transport rate; β is negative for downhill transport;
- multiplying the net bed-load and suspended load transport with the Bagnold factor $k_2 = (1 / (1 + \tan \beta / \tan \phi))$; $\tan \beta$ is positive for uphill transport yielding $k_2 < 1$ and hence a decrease of the transport rate; $\tan \beta$ is negative for downhill transport.

Basically, the Bagnold-factor should be applied to the instantaneous transport rates within the wave cycle and not to the net time-averaged transport rate. The former approach may lead to a rather strong effect of the bed slope on the net bed-load transport. This is caused by the fact that the net bed-load transport is the difference of two large transport quantities related to the forward and backward phases of the wave cycle.

2.2.6 Erosion of sand beaches and dunes

Processes

The application of a numerical cross-shore profile model to compute the erosion of the beach and duneface poses a fundamental problem which is related to the continuous decrease of the water depth to zero at the runup point on the dune face.



The numerical modelling of the (highly non-linear) wave-related processes in the swash zone with decreasing water depths is extremely complicated and is in an early stage of development. In the CROSMOR-model the numerical method is applied up to a point (last grid point) just seaward of the downrush point, where the mean water depth is of the order of 0.1 to 0.2 m.

The complicated wave mechanics in the swash zone are not explicitly modelled, but taken into account in a schematized way. The limiting water depth of the last (process) grid point is set by the user of the model (input parameter; typical values of 0.1 to 0.2 m). Based on the input value, the model determines the last grid point by interpolation after each time step (variable number of grid points).

Low-frequency waves are present in the swash zone due to spatial and temporal variation of the wave breaking point resulting in spatial and temporal variation of the wave-induced set-up creating low-frequency waves (surf beat). This involves a transfer of energy in the frequency domain: from the high frequency to the low frequency waves. The total velocity variance (total wave energy) consists of high-frequency and low-frequency contributions ($U_{rms}^2 = U_{hf,rms}^2 + U_{lf,rms}^2$). Basically, accurate modelling of low-frequency waves requires the application of a long-wave model on the wave group time scale (Van Thiel de Vries et al., 2006). Such an approach is beyond the present scope of work. Herein, a more pragmatic approach is introduced to crudely represent the low-frequency effects.

The low-frequency significant wave height is related to the high-frequency significant wave height, as follows:

$$H_{s,lf} = (\gamma - \gamma_{tr})^\alpha H_{s,hf} \quad \text{for } H_s/h > 0.5 \text{ and } x < 5 h_{end} \quad (63a)$$

$$U_{lf} = 0.5 (H_{s,lf}/h)(gh)^{0.5} \quad \text{for } H_s/h > 0.5 \text{ and } x < 5 h_{end} \quad (63b)$$

with: $H_{s,lf}$ = low-frequency significant wave height, $\gamma = H_{s,hf}/h$ = relative significant high-frequency wave height, γ_{tr} = threshold value (=0.5), h = water depth, h_{end} = water depth in last grid point, $H_{s,hf}$ = significant high-frequency wave height, $\alpha = 0.3$, U_{lf} = peak velocity of low-frequency waves. The α -exponent is found to be 0.3 based on the data of the Deltaflume experiment T01 (Van Thiel de Vries et al., 2006). The long wave velocity is computed from long wave theory. Using this approach, long wave motion (surf beat) is generated under strongly breaking waves (plunging waves) in the surf zone.

Figure 2.2.9 shows measured and computed values of the low-frequency waves (wave height and peak velocity).

The measured significant low-frequency velocity is related to the measured rms-value of the low-frequency velocity: $U_{lf} = 1.4 U_{lf,rms}$. Reasonable agreement between measured and computed values can be observed. The peak velocity of the low-frequency waves is added to the peak velocity of the high-frequency waves: $U_w^2 = U_{hf}^2 + U_{lf}^2$, with: U_{hf} = peak velocity of high-frequency waves near the bed and U_{lf} = peak-velocity of low frequency waves. **The total velocity (U_w) is used to compute the bed-shear stress and the near-bed concentration for suspended sediment transport (not used in bed load transport).** The maximum amplitude of the low-frequency water level variations is of the order of 0.3 m at $x=200$.

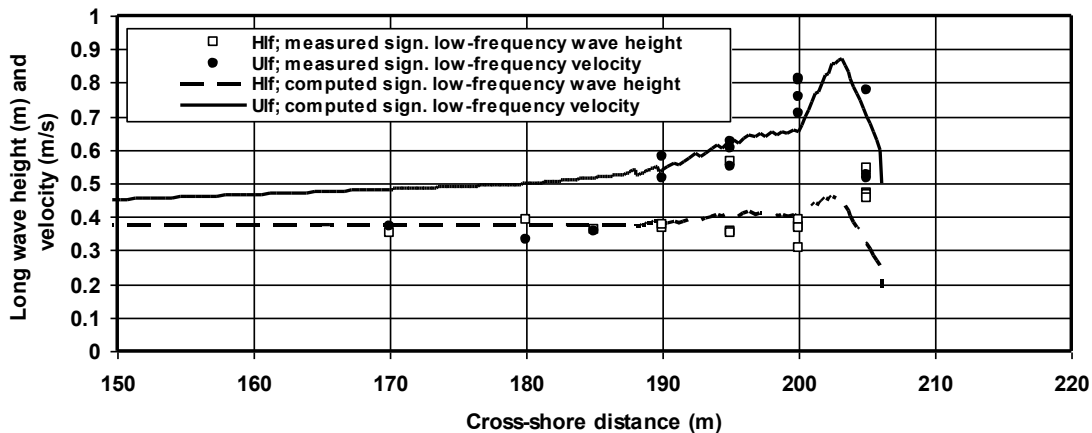


Figure 2.2.9 *Low-frequency wave height and velocity in surf zone of Deltaflume experiment on dune erosion (Test T01)*

The sand transport of the CROSMOR2007-model is based on the TRANSPOR2004 sand transport formulations (Van Rijn, 2006, 2007a,b,c,d). The effect of the local cross-shore bed slope on the transport rate is taken into account (see Van Rijn, 1993, 2006).

The sand transport rate is determined for each wave (or wave class), based on the computed wave height, depth-averaged cross-shore and longshore velocities, orbital velocities, friction factors and sediment parameters. The net (averaged over the wave period) total sediment transport is obtained as the sum of the net bed load (q_b) and net suspended load (q_s) transport rates. The net bed-load transport rate is obtained by time-averaging (over the wave period) of the instantaneous transport rate using a formula-type of approach.

The net suspended load transport is obtained as the sum ($q_s = q_{s,c} + q_{s,w}$) of the current-related and the wave-related suspended transport components. The current-related suspended load transport ($q_{s,c}$) is defined as the transport of sediment particles by the time-averaged (mean) current velocities (longshore currents, rip currents, undertow currents). The wave-related suspended sediment transport ($q_{s,w}$) is defined as the transport of suspended sediment particles by the oscillating fluid components (cross-shore orbital motion). The oscillatory or wave-related suspended load transport ($q_{s,w}$) has been implemented in the model, using the approach given by Houwman and Ruessink (1996). The method is described by Van Rijn (2006, 2007a,b,c,d). Computation of the wave-related and current-related suspended load transport components requires information of the time-averaged current velocity profile and sediment concentration profile. The convection-diffusion equation is applied to compute the time-averaged sediment concentration profile based on current-related and wave-related mixing. The bed-boundary condition is applied as a prescribed reference concentration based on the time-averaged bed-shear stress due to current and wave conditions. An additional calibration factor (sef-factor=suspension enhancement factor) acting on the time-averaged bed-shear stress and hence on the reference concentration in the shallow swash zone (dune erosion zone) in front of the dune face has been used to calibrate the model for dune erosion conditions; sef=1 yields the default model settings; a sef-value in the range of 2 to 3 is found (based on Deltaflume experiments 2005; Van Thiel de Vries et al., 2006) to be valid for the shallow surf zone in front of the dune face. The sef-factor is used to simulate the effects of wave collision and breaking in the shallow surf zone on the bed-shear stress and on the mixing capacity (increased turbulence) of the system resulting in a significant increase of the sand transport capacity. The shallow dune erosion zone is defined as the zone with a length scale of a few meters (of the order of the dune face length scale). To ensure a



gradual transition from $\text{sef}=1$ outside the dune erosion zone, a linear transition is assumed to be present seaward of it.

Wave runup at beach slopes

Maximum wave run-up is an important design criterion for several types of coastal structures such as revetments, breakwaters and dikes. Also, beach processes such as beach/dune erosion and storm flooding are related to wave run-up. Generally, the wave runup for irregular waves is expressed as $R_{2\%}$, which is the runup exceeded by 2% of the waves. On average, the wave runup consists of contributions of wave-setup (25%) and swash-runup (75%).

To prevent wave overtopping and flooding of the hinterland, the crest level of the beach-dune system should be above the maximum runup level which depends on the maximum astronomical tide level (Δh_T), the wave-induced setup, the wind-induced setup (surge Δh_s) and the runup due to short and long waves, see **Figure 2.2.10**.

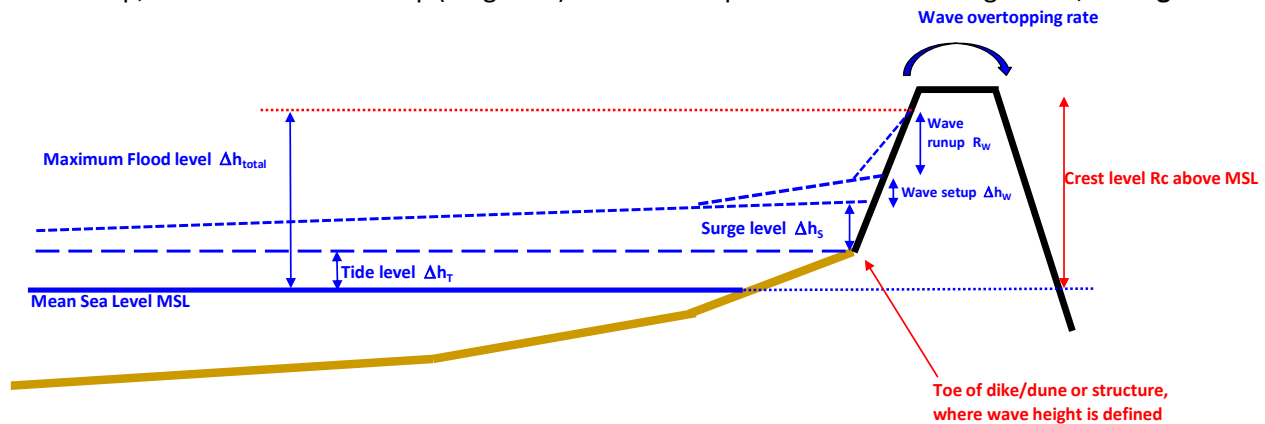


Figure 2.2.10 Maximum water level due to tide, storm surge, wave setup and wave runup.

Three types of relationships are used to describe the total wave runup, as follows:

- $R_{2\%} = \alpha H_o$; wave runup only depends on the offshore wave height;
- $R_{2\%} = \alpha (H_o L_o)^{0.5} = \alpha [H_o T_p^2 g / (2\pi)]^{0.5}$, effect of the wave period is included;
- $R_{2\%} = \alpha \zeta_o H_o$; effect of wave period and beach slope are included ($\zeta_o = \tan\beta / (H_o / L_o)^{0.5}$; $\tan\beta$ =beach slope around water line).

An early practical formula for regular wave run-up on smooth and rough plane slopes and composite slopes was presented by Hunt (1959). His equation can be expressed as (Hughes, 2004):

$$R = H_o \tan\beta / (H_o / L_o)^{0.5} = \tan\beta (H_o L_o)^{0.5} = \zeta_o H_o \quad (64)$$

with: R =vertical runup height above still water level (SWL); H_o =deep water wave height, L_o =deep water wave length based on peak wave period (T_p); β = beach slope angle; $\zeta_o = \tan\beta / (H_o / L_o)^{0.5} = [L_o^{0.5} / H_o^{0.5}] \tan\beta$ = deep water Iribarren number, also known as the surf similarity parameter (Battjes, 1974).

Wave runup has been extensively measured in laboratory flumes and at field sites.



Laboratory wave runup data

The laboratory data are mostly expressed in terms of the ζ_o -parameter. Often, the ζ_o -parameter is calculated using the measured wave height in the horizontal section of the flume seaward of the toe of the slope rather than as the true deepwater value $H_{s,o}$.

Mase (1989) presented results from irregular wave runup (flume) experiments on mild smooth impermeable plane slopes of $\tan\beta=1/5, 1/10, 1/20$ and $1/30$. The water depth in front of the beach was 0.45 m. The wave heights were in the range of 0.03 to 0.11 m. He expressed the runup values for irregular waves by the following expressions:

$$R_{\max}=2.3 (\zeta_o)^{0.77} \quad \text{for } \zeta_o < 3 \quad (65a)$$

$$R_{2\%}=1.9 (\zeta_o)^{0.7} \quad \text{for } \zeta_o < 3 \quad (65b)$$

$$R_{33\%}=1.4 (\zeta_o)^{0.7} \quad \text{for } \zeta_o < 3 \quad (65c)$$

with: R_{\max} =maximum runup level above SWL, $R_{33\%}$ =runup exceeded by 33% ($R_{33\%}\cong 0.7 R_{2\%}$).

Run-up data for nonbreaking breaking waves that surge up steeper slopes do not correlate as well to the Iribarren number, and instead run-up appears in this case to be directly related to wave height. Rearranging Equation (64) of Hunt for breaking wave run-up, it is found that $R\sim H^{0.5} T \tan\beta$ or runup is directly proportional to wave period, slope and the square root of wave height.

Van Gent (2001) has studied the wave runup along steep impermeable dike slopes (between 1 to 2.5 and 1 to 6) in a laboratory scale model and at the field site of Petten sea defense, The Netherlands. The foreshore slopes were 1 to 100 and 1 to 250. Some scale tests were done with the bar-berm bed profile as measured at the Petten field site (with a moderately rough bed). Comparison of measured runup values ($R_{2\%}$) in the scale model and at the field site showed rather good agreement (within 4%). About 25% of the data are in the range of $1 < \zeta_o < 2$, and 75% in the very steep range of $2 < \zeta_o < 30$.

The data of Van Gent which are valid for impermeable, moderately rough slopes can be represented by:

$$R_{2\%}\cong 1.7 \zeta_o^{0.8} H_{s,toe} \quad \text{for } 0.8 < \zeta_o < 2.0 \quad (66a)$$

$$R_{2\%}\cong 2.5 \zeta_o^{0.25} H_{s,toe} \quad \text{for } 2.0 < \zeta_o < 20 \quad (66b)$$

It is noted that Equation (66) is given in terms of $H_{s,toe}$, whereas most runup equations are given in terms of the deep water wave height $H_{s,o}$. Equation (66) is based on flume and field data for which $H_{s,toe}\cong H_{s,o}$. The coefficients of Equation (66) may be somewhat smaller in terms of $H_{s,o}$, particularly for field data.

Equations (65) and (66) are plotted in **Figure 2.2.12** showing close agreement. Equation (66) representing the data of Van Gent (2001) is rather close to Equation (65) of Mase (1989). In terms of $H_{s,o}$, the curve of Van Gent will be somewhat lower. The higher values of Mase may be related to a more smooth slope bottom.

Roberts et al. (2010) have re-analyzed wave runup data from tests in a large scale wave flume and wave basin (wave heights in the range of 0.3 to 1.15 m; beach slopes $\tan\beta$ in the range of 0.0 to 0.2; ζ_o in the range of 0.4 to 2.8). The initial bed profile consisted of an equilibrium profile ($h_x=Ax^{2/3}$ with A =shape parameter for medium fine sand of 0.3 mm; no bars). In some tests, steep dune fronts were present. Mostly, a scarp developed at the dune toe by wave erosion causing the overlying sand to become unstable and collapse.

The wave runup was found to be equal to the height of the breaking waves (and independent of beach slope), as follows:

$$R_{2\%}=H_{s,br} \quad \text{for fairly steep beaches/dunes with } \tan\beta \text{ in the range of } 0.08\text{-}0.20 \quad (67a)$$

$$R_{2\%}\cong 0.7 \text{ to } 0.9 H_{s,o} \quad (67b)$$



with: $H_{s,br}$ = maximum breaking wave height in the surf zone ($\cong 0.7-0.9H_{s,o}$) and $\tan\beta$ = beach slope over 10 m landward and seaward of the still waterline. Equation (67a) was substantiated by theoretical analysis of wave runup on a slope.

Field data of wave runup

Guza and Thornton (1982) analyzed field data on wave runup in the USA and derived a simple expression:

$$R_{2\%} = 0.035 + 0.71 H_{s,o} \quad (68)$$

which is independent of the beach slope. Some researchers (Douglass, 1992; Nielsen and Hanslow, 1991) have questioned the dependence of wave runup on beach slope. Douglass (1992) analyzed runup data of Holman (1986) of natural beaches and argued that beach slope is not an important parameter for predicting wave runup on natural beaches. Given the problem of defining beach slope and the slope variability, Douglass suggested that beach slope can be eliminated from the runup equation when applied to beaches.

Stockdon et al. (2006) analyzed wave runup data (with $0.1 < \zeta_o < 2.5$) of ten different field experiments (west and east coasts of USA and the coast of Terschelling Island of The Netherlands) based on video techniques. Their equation can be represented as:

$$R_{2\%} = 0.043 [H_{s,o} L_{s,o}]^{0.5} = (0.043/\tan\beta) H_{s,o} \zeta_o \quad \text{for } \zeta_o < 0.3 \text{ (dissipative beaches)} \quad (69a)$$

$$R_{2\%} = 0.75 (\sin\beta) [H_{s,o} L_{s,o}]^{0.5} \cong 0.75 H_{s,o} \zeta_o \quad \text{for } \zeta_o > 1.25 \text{ (reflective beaches)} \quad (69b)$$

with: $H_{s,o}$ = significant wave height in deep water.

Senechal et al. (2011) performed field experiments in March-April of 2008 at the barred surf and beach zone at the Truc Vert site (sand 0.35 mm) on the Atlantic coast of France. Video measurements of wave runup were collected during extreme storm conditions characterized by energetic long swells (peak period of 16.4 s and offshore height up to 6.4 m) impinging on relatively steep foreshore beach slopes (0.06-0.08). The measured ζ_o -values are in the range of 0.5 to 0.9.

Figure 2.2.11 shows observations of the wave runup (total; incident wave components < 20 s and infragravity wave components > 20 s). It shows that the vertical wave runup is dominated by the infragravity components with periods > 20 s. The highest measured runup value was about 2.3 m for an offshore wave height of 5 m ($\zeta_o = 0.58$; $\tan\beta = 0.069$), see **Table 2.2.2** and **Figure 2.2.11**. As the total runup (S) is dominated by the infragravityband, **Figure 2.2.11(right)** also suggests that the infragravity component (S_{ig}) becomes saturated for offshore significant wave heights above 4.0 m. For minor storms with $H_o < 4$ m; the total wave runup can be represented as $0.6H_{s,o}$, which is close to the runup-equation of Guza and Thornton (1982). The effect of beach slope on the wave runup was not found to be very important (weak effect).

The total wave runup data consisting of incident and infragravity wave contributions of Senechal et al. (2011) are herein represented by :

$$R_{2\%} = \alpha_s \tanh(0.4H_o) \quad \text{with } \alpha_s = 2.14 \text{ for the best fit and } \alpha_s = 2.6 \text{ for the upper envelope curve} \quad (70a)$$

$$R_{2\%} = \alpha_s (\zeta_o)^{0.5} H_{s,o} \quad \text{with } \alpha_s = 0.9 \text{ for the best fit and } \alpha_s = 1.15 \text{ for the upper envelope curve} \quad (70b)$$

$$R_{2\%} = \alpha_s [H_o L_o]^{0.5} = \alpha_s [H_o T_p^2 g / (2\pi)]^{0.5} \quad \text{with } \alpha_s = 0.06 \text{ for best fit and } \alpha_s = 0.075 \text{ for upper envelope} \quad (70c)$$

Equation (70b) is plotted in **Figure 2.2.12**; it has substantial scatter of the data around the fit curve.

Equation (70c) has less scatter and is close to the wave runup equation (69b) of Stockdon.



Clearly, the runup values for natural beaches are much smaller (factor 2) than those of impermeable slopes for the same value of the surf similarity parameter, mainly due to effects of beach permeability, nonuniform beach slope, wave breaking over sand bars and other factors (Hughes, 2004).

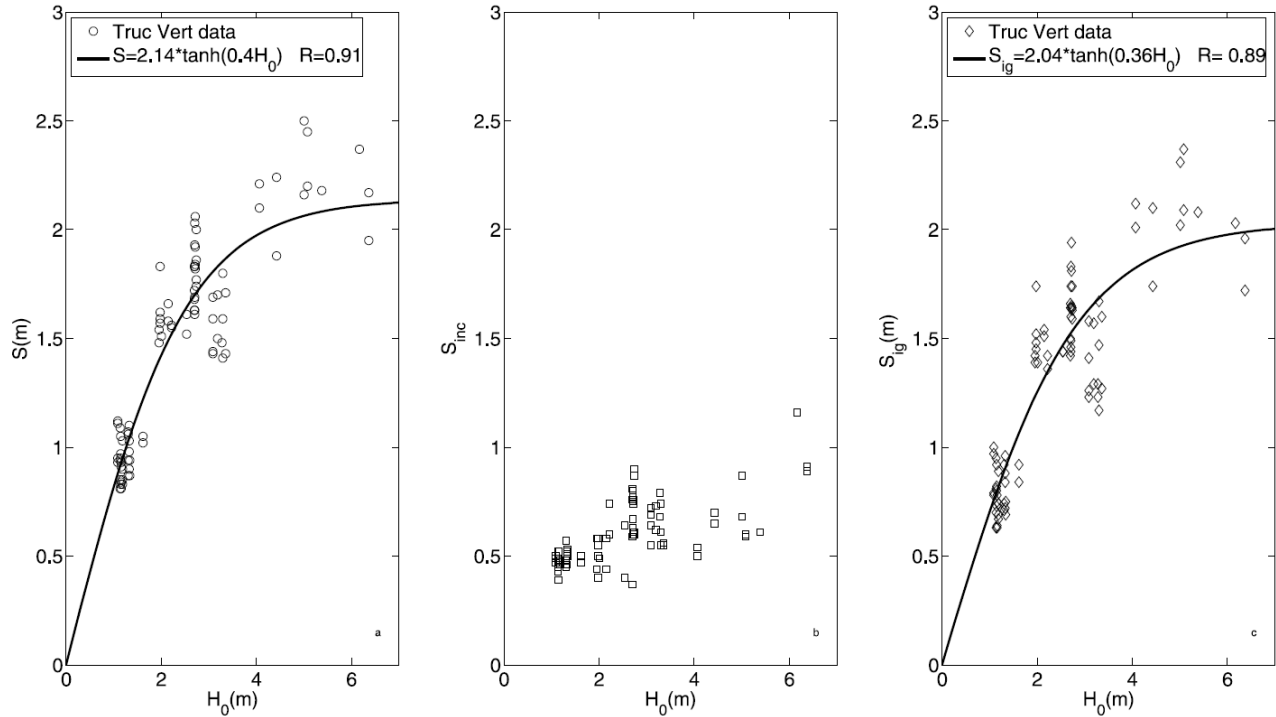


Figure 2.2.11 Left: vertical wave runup (S) versus offshore wave height H_o (left); Middle: vertical wave runup (S_{inc}) related to the incident wave components and Right: vertical wave runup (S_{ig}) related to infragravity components (right); observations are represented by symbols; line is the hyperbolic tangent fit to observations; Senechal et al., 2011

Run	Offshore significant wave height H_o (m)	Offshore wave period T_o (s)	Beach slope $\tan\beta$ (-)	Surf similarity parameter ζ_o (-)	Total wave runup S (m)	Wave runup incident waves < 20 s S_{inc} (m)	Wave runup infra-gravity > 20 s S_{ig} (m)	Ratio S/S_{ig} (-)
85	1.3	12.5	0.059	0.773	0.94	0.57	0.74	1.27
27	2.0	14.3	0.059	0.712	1.62	0.4	1.52	1.07
1	2.5	16.3	0.056	0.687	1.61	0.64	1.44	1.12
18	3.4	14.2	0.068	0.633	1.43	0.56	1.37	1.13
72	4.4	15.4	0.059	0.518	1.88	0.65	1.74	1.08
70	5.0	15.6	0.069	0.575	2.50	0.87	2.31	1.08
23	6.2	14.4	0.081	0.560	2.37	1.16	2.03	1.17
21	6.4	14.3	0.075	0.513	1.95	0.89	1.72	1.13

Table 2.2.2 Some characteristic wave runup data of Truc Vert site, France (Senechal et al., 2011)



Poate et al. (2016) have studied the wave runup at gravel beaches at 6 sites in the UK ($H_{s,o}=2$ to 6 m; $\tan\beta=0.07$ to 0.4; $d_{50}=2$ to 160 mm; $\zeta_o=0.5$ to 5). At each site, the wave runup was measured using video data logged using a temporary camera installation. The leading edge of the uprush of the swash is a distinctive feature which can be easily extracted through automated routines. However, the downrush is less clear, limiting delineation of its position under storm waves. Nearshore wave data were measured by Directional Waveriders owned and managed by the Channel Coastal Observatory and by CEFAS. The wave buoys are deployed in -10 m Chart Datum and provide half-hourly wave statistics accessible online. The deep water wave height ($H_{s,o}$) was obtained by de-shoaling the nearshore significant wave height using the spectral mean wave period to 200 m water depth. The highest runup value of 12.5 m for an offshore wave height $H_{s,o}= 6.5$ m was measured at the very steep Chesil gravel barrier ($d_{50}=50$ mm; $\tan\beta=0.4$ or 1 to 2.5; $\zeta_o\cong 3$; $R_{2\%}/H_{s,o}\cong 0.5$), see **Figure 2.2.12**.



Figure 2.2.12 Wave overtopping at Chesil beach (UK) on 5 February 2014 (about 10 m high gravel barrier); Poate et al., 2016

The $R_{2\%}$ values can be roughly represented by:

$$R_{2\%} = \alpha H_{s,o} \quad \text{with } \alpha = 1.5 \text{ best fit } (\alpha = 2 \text{ for upper data envelope, } \alpha = 1 \text{ for lower envelope)} \quad (71a)$$

$$R_{2\%} = \alpha (\zeta_o)^{0.8} H_{s,o} \quad \text{with } \alpha = 1 \text{ best fit } (\alpha = 1.5 \text{ for upper data envelope, } \alpha = 0.7 \text{ for lower envelope)} \quad (71b)$$

Equations (71b) is shown in **Figures 2.2.13** and **2.2.14**.

Regression analysis of modelled data (XBEACH) showed the importance of key parameters, being: the beach slope, grain size and spectral shape which can be lost when the peak wave period is used (T_p). In cases where spectral wave data is not available, the inclusion of mean wave period (T_z) provides a suitable replacement particularly at sites where bimodality may be present.



Dodet et al. (2018) have studied the wave runup over steep impermeable rocky cliffs (October 2012 to May 2015) at Banneg Island, Brittany, France in conditions with a tidal range of 2 to 8 m. The beach slope between LAT and HAT (distance of about 50 m) was $\tan\beta=0.2$. The offshore wave rider buoy was in 50 m water depth at 1 km from the shore. Four pressure sensors were deployed in the LAT-HAT zone. The highest sensor P4 was at 1.6 m above HAT. The $\eta_{2\%}$ -value was measured which is the 2% exceedance of the water level elevation above the still water level (SWL) in the highest pressure sensor P4. This $\eta_{2\%}$ -parameter is somewhat lower than the $R_{2\%}$ -parameter. The highest measured $\eta_{2\%}$ -value was 5.4 m in 131 events for $H_{s,o}\cong 4.5$ m.

The $\eta_{2\%}$ -values of sensor P4 for a cliff slope of $\tan\beta=0.2$ can be roughly represented by:

$$\eta_{2\%} = \alpha H_{s,o} \quad \text{with } \alpha=1.15 \text{ best fit } (\alpha=1.4 \text{ for upper envelope, } \alpha=0.9 \text{ for lower envelope}) \quad (72a)$$

$$\eta_{2\%} = \alpha (H_{s,o} L_{s,o})^{0.5} \quad \text{with } \alpha=0.16 \text{ best fit } (\alpha=0.18 \text{ upper envelope, } \alpha=0.14 \text{ lower envelope}) \quad (72b)$$

$$\eta_{2\%} = \alpha (\zeta_o)^{0.8} H_{s,o} \quad \text{with } \alpha=0.75 \text{ best fit } (\alpha=0.9 \text{ for upper envelope, } \alpha=0.6 \text{ lower envelope}) \quad (72c)$$

Equations (72c) is shown in **Figures 2.2.13, 2.2.14**.

Equation (72c) for steep cliffs gives somewhat lower values (30%) than Equation (71c) for gravel beaches. For natural steep rocky cliffs, the runup dynamics is more complex with higher reflection due to increased steepness, stronger dissipation due to increased drag over an irregular bottom, enhanced turbulence during the breaking processes affected by impacts, splash-ups, and air entrapment and the volume loss of the swash tongue due to infiltration within fractured bed rock.

The wave runup equations for gravel beaches, rocky cliffs and other impermeable slopes give much higher values (factor 2) than the runup equations for sandy beaches.

CROSMOR-model

The standard runup equation ($R_{33\%}$) used in the CROSMOR-model is:

$$R_{2\%} = 0.85 (\zeta_o)^{0.6} H_{s,o} \quad (73a)$$

$$R_{33\%} = 0.7 R_{2\%} \quad (73b)$$

Equation (73) is only valid for natural sand beaches and is in good agreement with the runup-values of Equation (70b), see **Figure 2.2.13**.

It is noted that the beach erosion in the CROSMOR model is based on $R_{33\%}$ (default setting), which is smaller than the $R_{2\%}$ ($R_{33\%}\cong 0.7 R_{2\%}$). The $R_{33\%}$ -value is most representative for the beach changes of the majority of the waves, while the $R_{2\%}$ is most important for dune crest overtopping by the most extreme wave heights. The model user can also apply the $r_{2\%}$ -value (frunup input parameter should be set to 1.4).

A smaller runup value leads to a shorter wet beach length exposed to erosion (length between the last grid point and the runup point) and thus to a deeper erosion depth at the beach.

Comparison of flume and field data

All flume and field data in terms of the ζ_o -parameter are shown in **Figure 2.2.13**. The most striking results are:

- the wave runup values at mild and steep sand beaches of Stockdon et al. 2006 are somewhat smaller than that of Senechal et al. 2011; the CROSMOR-values for sand beaches are closest to the wave runup values of Senechal et al. 2011;
- the wave runup values at steep gravel beaches are higher (30%) than at sand beaches; the wave runup at rocky cliffs are much lower than at gravel beaches, but are reasonably in agreement with the CROSMOR-equations for wave runup;
- the wave runup values at mild and steep, smooth, impermeable slopes of Mase 1989 and Van Gent 2001 are much higher (factor 1.5 to 2) than those at gravel beaches.

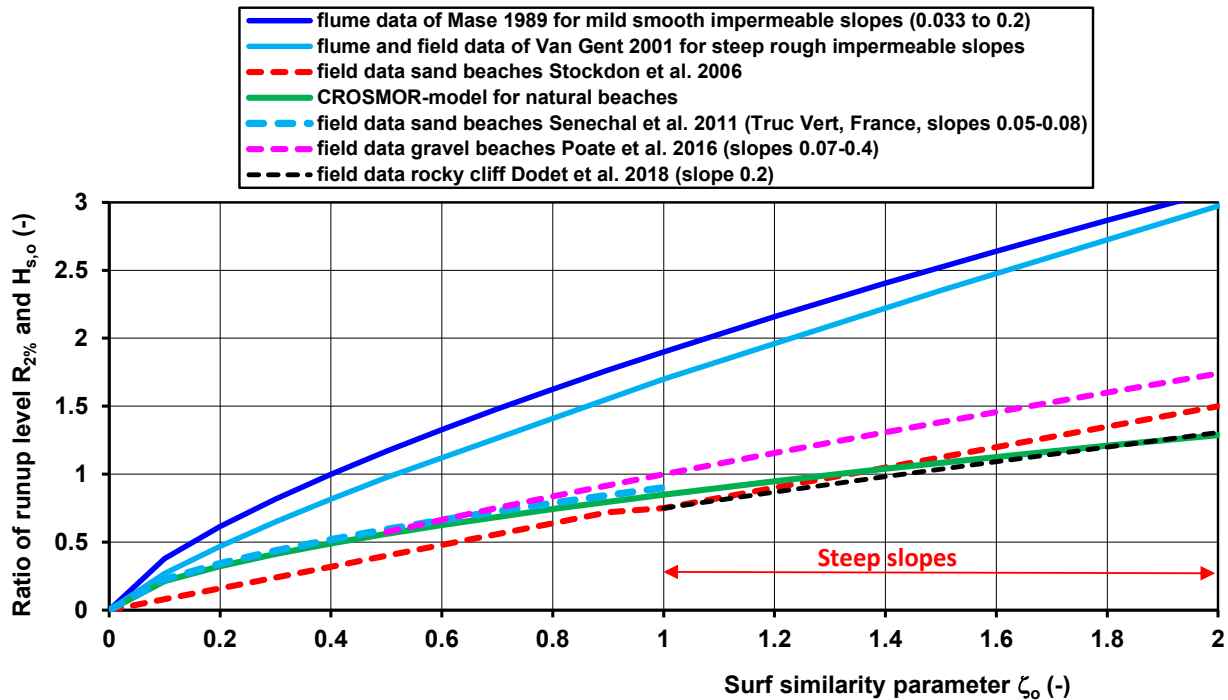


Figure 2.2.13 Dimensionless runup $R_{2\%}/H_{s,o}$ as function of the surf similarity parameter ζ_o

Figure 2.2.14 shows the computed runup levels of Equation (73) in terms of $R_{33\%}$ ($R_{33\%} \cong 0.7R_{2\%}$) as function of the offshore wave height $H_{s,o}=1$ to 7 m ($T_p=6$ to 12 s) for beach slopes of 1 to 1/10/20/40/100. The results of the field data Equation (71b) of Poate et al. (2018) and Equation (72b) of Dodet et al. (2018) are also shown.

The most striking features are:

- the wave runup of Equation (73) of the CROSMOR-model is relatively small (about 1 m for $H_{s,o}=7$ m) for mild slopes between 1 to 100 and 1 to 40;
- the wave runup of Equation (73) increases to 2 m for slope of 1 to 20 and to 4 m for slope of 1 to 5 and to 7 m for slope of 1 to 2.5 in the case of $H_{s,o}=7$ m;
- the wave runup based on the field data of Senechal et al. (2011; dashed yellow line) are smaller (factor 1.5 to 2) than the values of Equation (73) for the same slope and offshore wave height;
- the wave runup for cliff and gravel slopes are relatively high and reasonably represented by the CROSMOR-Equation (73).

Finally, the highest measured wave runup values in field conditions are summarized, as follows:

- sand beach ($\tan\beta=0.06-0.08$): about 2.5 m for an offshore wave height of $H_{s,o} \cong 5$ m (field data of Senechal et al., 2011);
- steep gravel beach: about 12.5 m ($\tan\beta=0.4$) for an offshore wave height of $H_{s,o} \cong 6.5$ m (field data of Poate et al. 2016).

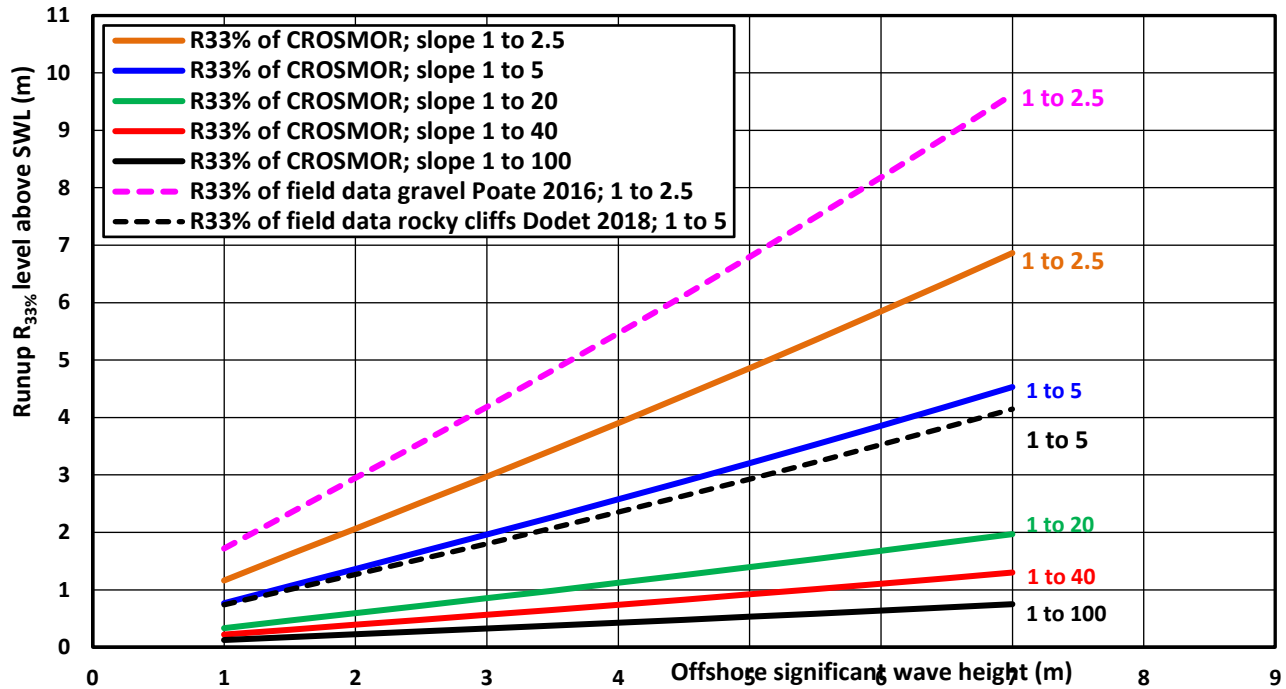


Figure 2.2.14 Runup levels ($R_{33\%}$) above still water level (SWL)
 $(H_{s,o}=1, 1.5, 2, 2.5, 3, 3.5, 4, 4.5, 5, 5.5, 6, 6.5, 7 \text{ m};$
 $T_p= 6, 6.5, 7, 7.5, 8, 8.5, 9, 9.5, 10, 10.5, 11, 11.5, 12 \text{ s}).$

Erosion in swash-runup zone

The dune erosion zone in front of the relatively steep dune face is defined as the zone up to the run-up level which is dominated by breaking bores (swash motions). Herein, the length of the dune erosion zone (L_s) is determined as the maximum value of two length scales.

Hence, $L_s = \max(L_{s1}, L_{s2})$ with:

- 1) $L_s = 6h_{L,m}$ with: $h_{L,m}$ = average water depth of last, five computational grid points. The last computational point is set by the model user by specifying a minimum water depth h_L (input value). This value should be approximately 0.1 times the dune face length ($h_L \approx 0.1L_d$);
- 2) $L_{s,R33\%} = x_R - x_L$ with: x_R = horizontal coordinate of run-up point ($R_{33\%}$) and x_L = horizontal coordinate of last computational point; x_R is the point for which the bed level z_{bn} is just larger than z_{runup} ; $z_{runup} = \text{runup} + \text{hdg}$ in point $x_L + z_{bn}$ of point x_L with hdg = water depth to SWL in point x_L

```
if(zrunup.le.zbn(i).or.i.eq.nx)then
  lgr1=x(min(i+1,nx))-xggr
```

- 3) $L_{s,\text{minimum}} = 6h_{L,m}$ and $L_{s,\text{maximum}} = 30 h_{L,m}$;
- 4) $L_s = f_{runup} L_s$ with f_{runup} = input parameter to modify runup length scale (default=1; range=0.7 to 1.5)

The length of the dune erosion zone is in the range of 0.5 to 1 times the dune face length (L_d , see Figure 5.2.4) above the still water level (SWL). The dune face length is in the range of $L_d = 1$ to 3 m for large-scale laboratory conditions (Deltaflume) and $L_d = 3$ to 5 m for field conditions.

Herein, it is assumed that the runup length ($L_{s,R33\%}$) related to $R_{33\%}$ is most effective for beach erosion. The most extreme runup length ($L_{s,R2\%}$) is related to $R_{2\%}$, but the runup length between the point $R_{33\%}$ and $R_{2\%}$ is a relatively



thin layer of water and strongly effected by percolation of water into the beach sediment. Therefore, the runup length ($L_{s,R33\%}$) defined by $R_{33\%}$ is herein taken as the most representative length for beach erosion ($L_{R,33\%} \cong 0.7 L_{R,2\%}$).

To model dune erosion correctly, a run-up formula is required which is valid for steep slopes (up to 70°). In the CROSMOR-model, the runup level (above SWL plus set-up) associated with significant waves is estimated by Equation 73 (default approach). The maximum runup is limited to 5 m.

The total erosion area (A_E) over the length of the erosion zone is defined as:

$$A_E = q_L \Delta t / ((1-p)\rho_s) \quad (74)$$

with: q_L =cross-shore transport computed at last grid point at the toe of the erosion zone (**Figure 2.2.15**), Δt =time step, p =porosity factor of bed material, ρ_s =sediment density. The cross-shore transport generally is offshore directed during high energy (storm) conditions and onshore directed during low energy conditions. The erosion profile of the erosion zone with length L_s is assumed to have a triangular shape (see **Figure 2.2.15**), yielding $A_E = 0.5eL_s$, with e =maximum erosion depth.

The maximum erosion depth in the swash zone is:

$$e = 2q_L \Delta t / (L_s(1-p)\rho_s) \quad (75)$$

In the case of onshore-directed transport (q_L) at the last grid point, the same procedure is followed resulting in accretion with a triangular shape (swash bar generation). This may occur during low-energy events (post storm conditions).

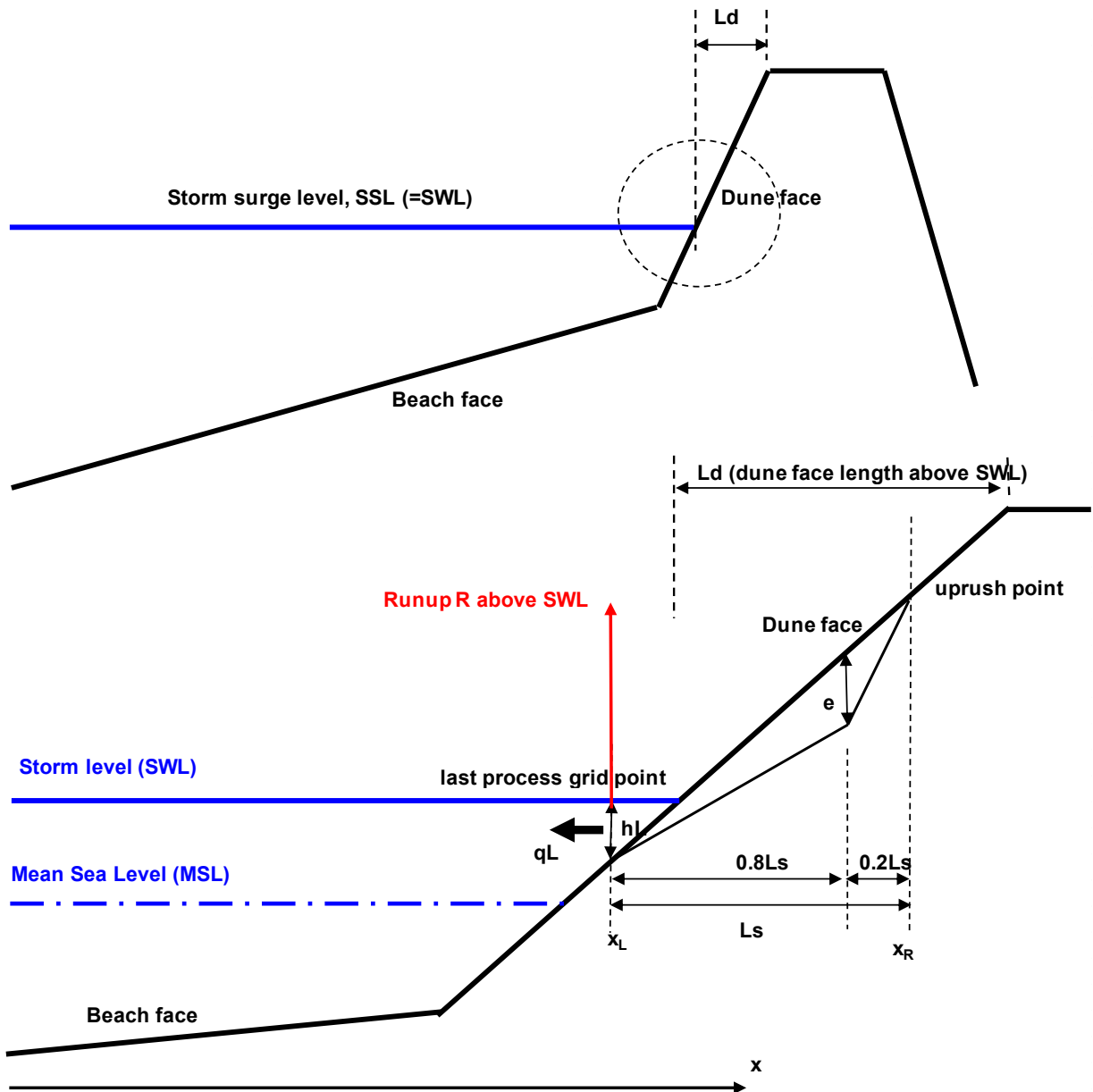


Figure 2.2.15 Definition sketches of bed level changes in swash zone
Top: Beach and dune face
Bottom: Erosion in swash zone at dune face



CODE SUBROUTINE BEACH

```
subroutine beach(stlgr,dt,por,rhos,xggr,x,hdg,nxx,nx,zbn,zm,
*SL,d50,frunup)
common/hcaeb/tanbx,hs0,ls0
dimension x(*),hdg(*),zbn(*)
c hdg=local water depth to MSL at time t
C tanbx=beach slope in last computational grid point
C xggr=x-coordinate of last grid point (nxx=number of last computational grid point)
C nx=number of last point
C zbn=bed level of beach; zm= bed level change at x=0.8L beyond last computational grid point)
C stlgr=sediment transport;mean of transport in last 5 computational points
real ls0,ibar,lgr
if(tanbx.le.0.)then
lgr1=0.1
zm=0.
xgr=xggr
return
endif
pi=4.*atan(1.)
c tanbeta=tan(SL/360.*2.*pi); SL=slope angle
lgr1=0.1
hend1=hdg(nxx)
if(tanbx.gt.2.5)tanbx=2.5
if(tanbx.lt.0.025)tanbx=0.025
Ibar=tanbx/sqrt(hs0/ls0)
Thulp=tanh(3.4*Ibar)
frunup1=frunup
if(Thulp.lt.0.2)Thulp=0.2
if(Ibar.le.0.5)runup=0.4*Hs0*Thulp
if(Ibar.gt.0.5)runup=0.6*Ibar**0.5*Hs0
C
c if(d50.ge.0.002)runup=0.16*(hs0*ls0)**0.5 based on Larsen-method
C Larsen gives higher runup fro steep slopes (factor 1.5)
c
if(runup.ge.5.)runup=5.
```



```
c
c frunup1 is applied to lgr, see below
c runup above point where h is equal to hgrens
C runup of larson et al 2004 runup=0.16*(hs0*ls0)**0.5
c
c zrunup=runup+hdg(nxx)+zbn(nxx)
c
c nx=last point of profile (beach); nxx=last computational point
c
c do 10 i=nxx,nx
c
C nxx= last computational point, nx= last point of grid
c determination of runup length lgr1
C xggr=x-value of last computational point
c
c if(zrunup.le.zbn(i).or.i.eq.nx)then
c lgr1=x(min(i+1,nx))-xggr
c goto 20
c endif
10 continue
20 continue
c
c determination of the HORIZONTAL dune erosion length lgr
C hdg=local total water depth to SWL in last grid point at time t
C hend1=total total water depth at time t in last computational point
c
c hhdg=0.2*(hdg(nxx)+hdg(nxx-1)+hdg(nxx-2)+hdg(nxx-3)+hdg(nxx-4))
c lgr=6.0*hhdg
c
c largest value of lgr1 and lgr is taken
c
c if(lgr.lt.lgr1)lgr=lgr1
```



```
c
  if(lgr.lt.6.0*hhdg)lgr=6.0*hhdg
  if(lgr.gt.30.0)lgr=30.
C   lgr is always between 6hhdg and 30 m
  lgr=frunup1*lgr
  if(d50.ge.0.002)lgr=frunup1*runup/tanbx
  if(d50.ge.0.002.and.lgr.ge.15.0)lgr=15.0
  zm=0.
  xgr=xggr
c
C   stlgr=sediment transport in last grid point
  if(lgr.gt.0.)zm=(stlgr*dt)/(0.5*lgr*(1.-por)*rhos)
c
c
  do 30 i=nxx,nx
  xx=x(i)
  if(lgr.gt.0.)then
  if(xx.ge.xgr.and.xx.le.xgr+0.8*lgr)then
    corbe=((xx-xgr)*zm)/(0.8*lgr)
    zbn(i)=zbn(i)+corbe
c
c
c
  endif
  if(xx.gt.xgr+0.8*lgr.and.xx.le.xgr+lgr)then
    corbe=((xgr+lgr-xx)*zm)/(0.2*lgr)
    zbn(i)=zbn(i)+corbe
c
c
c
  endif
  endif
30 continue
c   correction of erosion area, because xgr+lgr may be outside gridpoint
  corr=0.
```

Bed sliding at steep slopes

The bed level in the swash zone at the dune face may become so steep due to wave-induced erosion and other undermining processes that the local bed becomes unstable resulting in local bed failure, see **Figure 2.2.16**. A wedge-shaped part of the dune face will slide downward to settle at the toe of the dune face, where it can be eroded again by wave-induced processes. The sliding procedure is a post-processing procedure after each time step, which is repeated until the bed is stable everywhere along the profile.

The local bed is assumed to slide out, if :

$$\tan(\beta) > \tan(\alpha_x) \quad (76)$$

with: $\tan(\alpha_x) = (z_{bo,i+1} - z_{bo,i}) / (x_{i+1} - x_i)$ and β = maximum bed slope angle (input parameter), $z_{bo,i+1}$ = old bed level at point $i+1$, $z_{bo,i}$ = old bed level at point i

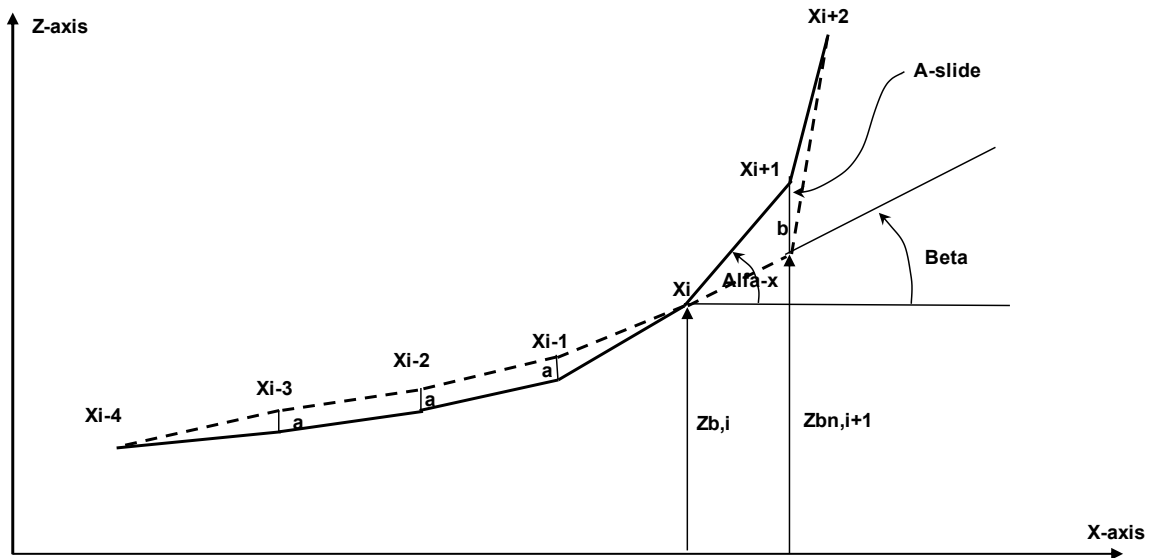


Figure 2.2.16 Sliding mechanism dune front

2.2.7 Erosion of gravel/shingle beaches

Deposition and erosion in the swash zone between the waterline and the uprush point (landward of the last grid point) is a typical morphological feature of wave attack on a steep slope and is represented in a schematized way by using a subgrid model. The length of the swash zone is determined as the distance between the last grid point and the uprush point.

In the case of steep shingle slopes the run-up level can be determined by an empirical expression: $R_s = (H_{s,o} L_{s,o})^{0.5}$ with a maximum value of 5 m above the mean water level. The maximum run-up is set to 5 m because the run-up along a steep, permeable shingle slope with percolation effects will be significantly smaller than along a rigid, smooth slope.

In the most nearshore zone where the water depth is smaller than $3h_{grens}$, an extra onshore directed swah current is assumed to be present (subroutine golf.for), (see $u_{sw,on}$ in **Figure 2.2.17**) :

$$u_{swash,x} = CSW [1 - h_x / (3h_{grens})] u_{bore} \quad \text{for } 3h_{grens} < h_x < h_{grens} \quad (77)$$

with: h_x =local water depth; h_{grens} = water depth in last computational grid point; $u_{bore} = 0.2(gH_{s,o})^{0.5}$ (bore-related velocity at steep gravel beaches); $H_{s,o}$ =significant wave height at $x=0$; CSW =calibration factor (0 to 1.5; default=1). The swash velocity (u_{swash} ; Equation (77)) is only applied when $d_{50} > 2$ mm (steep gravel beaches) and $NHW=1$ (number of wave classes; $H_{s,o} = 1.41 H_{rms,o}$); otherwise $u_{bore} = 0$ m/s.

The total deposition or erosion area (A_D or A_E) over the length of the swash zone is herein defined as:

$A_D = q_p \Delta t / ((1-p)\rho_s)$ with: q_p = cross-shore transport computed at last grid point P at the toe of swash zone including onshore swash velocity component (for $x < 3 h_{grens}$), Δt = time step, p = porosity factor of bed material, ρ_s = sediment density.

The deposition (or erosion) profile in the swash zone is assumed to have a triangular shape, see **Figure 2.2.17**. The maximum deposition or erosion (e) can then be determined from the area A_D . The cross-shore transport on steep shingle slopes is onshore directed during low wave conditions due to the dominant effect of the velocity



asymmetry and the percolation of fluid through the porous bed surface. The cross-shore transport is offshore-directed during storm conditions.

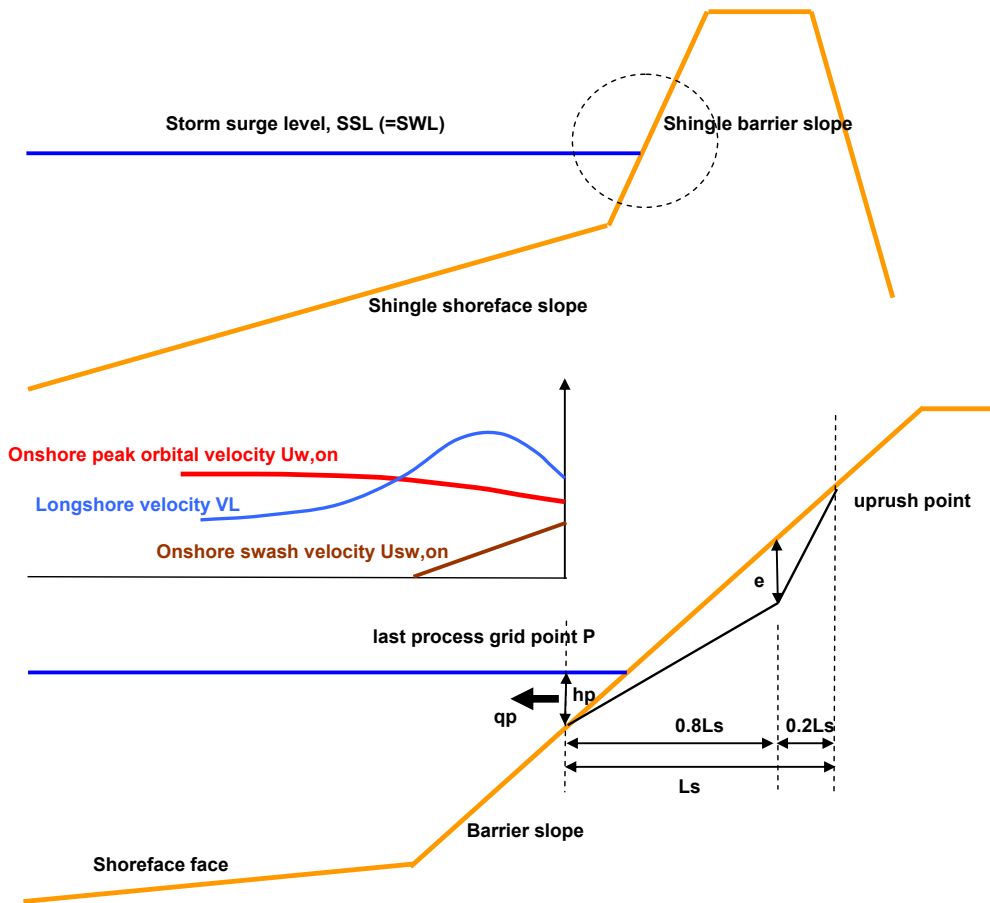


Figure 2.2.17 Schematization of swash erosion zone for shingle beach

2.2.8 Bed level computation

The bed level is computed from the sediment continuity equation (sources and sinks are neglected), as follows:

$$dz_b/dt + \gamma dS/dx = 0 \quad (78)$$

with; z_b = bed level (m) to a datum at location x and at time t ; $S = q_{b,x} + q_{s,x}$ = bed load transport plus suspended load transport (kg/m/s); $\gamma = 1 / ((1-p)\rho_s)$ = coefficient, p = porosity factor of bed material, ρ_s = sediment density (kg/m³).

Various explicit numerical schemes including a smoothing term can be used to solve the bed level equation, as follows:

- Upwind Scheme (U): $z_{b,i,t+\Delta t} - z_{b,i,t} = -\gamma \Delta t / \Delta x [S_{i,t} - S_{i-1,t}] + \alpha [z_{b,i+1,t} - 2z_{b,i,t} + z_{b,i-1,t}]$;
- Upwind BW scheme (UBW): $z_{b,i,t+\Delta t} - z_{b,i,t} = -\gamma \Delta t / (2\Delta x) [3S_{i,t} - 4S_{i-1,t} + S_{i-2,t}] + \alpha [z_{b,i+1,t} - 2z_{b,i,t} + z_{b,i-1,t}]$;
- **Central LW scheme 1 (CLW1):** $z_{b,i,t+\Delta t} - z_{b,i,t} = -\gamma \Delta t / (2\Delta x) [S_{i+1,t} - S_{i-1,t}] + \alpha [z_{b,i+1,t} - 2z_{b,i,t} + z_{b,i-1,t}]$;
- Central LW scheme (CLW2): $z_{b,i,t+\Delta t} - z_{b,i,t} = -\gamma \Delta t / (2\Delta x) [S_{i+1,t} - S_{i-1,t}] + \alpha [z_{b,i+2,t} - 4z_{b,i+1,t} + 6z_{b,i,t} - 4z_{b,i-1,t} + z_{b,i-2,t}]$.



with: Δt = time step, Δx =horizontal grid size, α =smoothing coefficient, LW=Lax-Wendorf scheme; BW=Beam-Warming scheme. The term $\gamma (\Delta t/\Delta x)$ is set to 1. **Scheme CLW1 is used in CROSMOR.**

The smoothing term of U, UBW and CLW1 is based on three bed level values around point i.

The smoothing term of CLW2 is based on five bed level values around point i.

The bed level computation in CROSMOR-model can become unstable easily due to the presence of sediment convergence points (points where sand accumulates due to supply from 2 directions in the surf zone: onshore sand transport seaward side of bar of bar and offshore-directed sand transport at landward side of bar), see **Figure 2.2.18.**

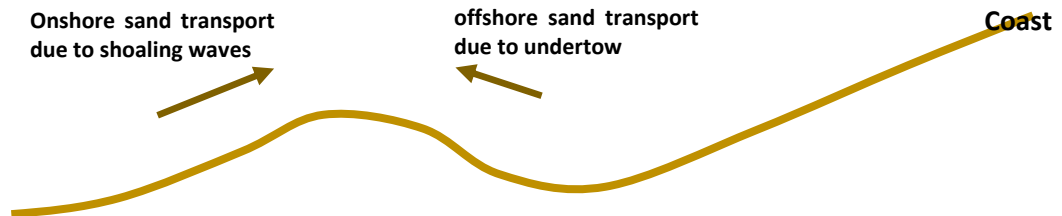


Figure 2.2.18 Sediment convergence point with onshore and offshore sand transport

These schemes are studied for a very irregular sediment transport pattern over a trench. The sediment transport varies around 1 kg/m/s upstream (left) of the trench, decreases in the trench and increases to about 1 kg/m/s in the downstream zone (right).

Figures 2.2.19 shows the bed level change (BLC) based on the four numerical schemes with $\alpha=0$ and the **original** sediment transport pattern.

Figures 2.2.20 shows results for $\alpha=0.2$.

All schemes show wiggles, which are highest for the UBW-scheme, both $\alpha=0$ and $\alpha=0.2$.

The U-scheme has slightly lower wiggles than the CLW-schemes.

The smoothing term has not much effect on the computed bed level change values.

Figure 2.2.21 shows the bed level change (BLC) based on the four numerical schemes with $\alpha=0$ and a **smoothed** sediment transport pattern using a 5 point-averaging scheme (dashed curve).

Figures 2.2.22 shows results for $\alpha=0.2$.

The wiggles are much lower. The UBW-scheme has more wiggles than the other schemes. The CLW1-scheme has slightly lower wiggles than the U-scheme.

The smoothing term with $\alpha=0.2$ has much effect on the computed bed level change values of the CLW2-scheme.

Figure 2.2.23 shows the bed level change (BLC) based on CLW1-scheme and the U-scheme with $\alpha=0$ and a smoothed sediment transport pattern using a 5 point-averaging scheme (dashed curve). The CLW1-scheme has less wiggles.

Figure 2.2.24 shows the results of the CLW1-scheme with $\alpha=0, 0.05$ and 0.2 . Wiggles increase locally for $\alpha=0.2$. Hence, the value of the smoothing coefficient α should be set to a relatively small value (<0.05).

Conclusions:

- 1) irregular sediment transport should be smoothed before computation of bed level change (not done in CROSMOR);
- 2) bed level change can be best computed by the CLW1-scheme or the U-scheme;
- 3) smoothing coefficient should be small ($\alpha < 0.05$).

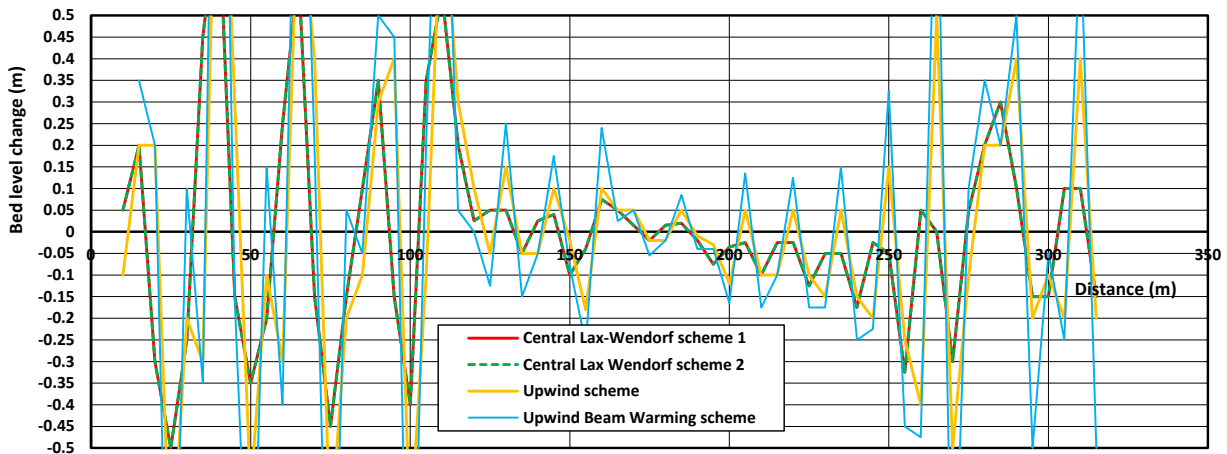
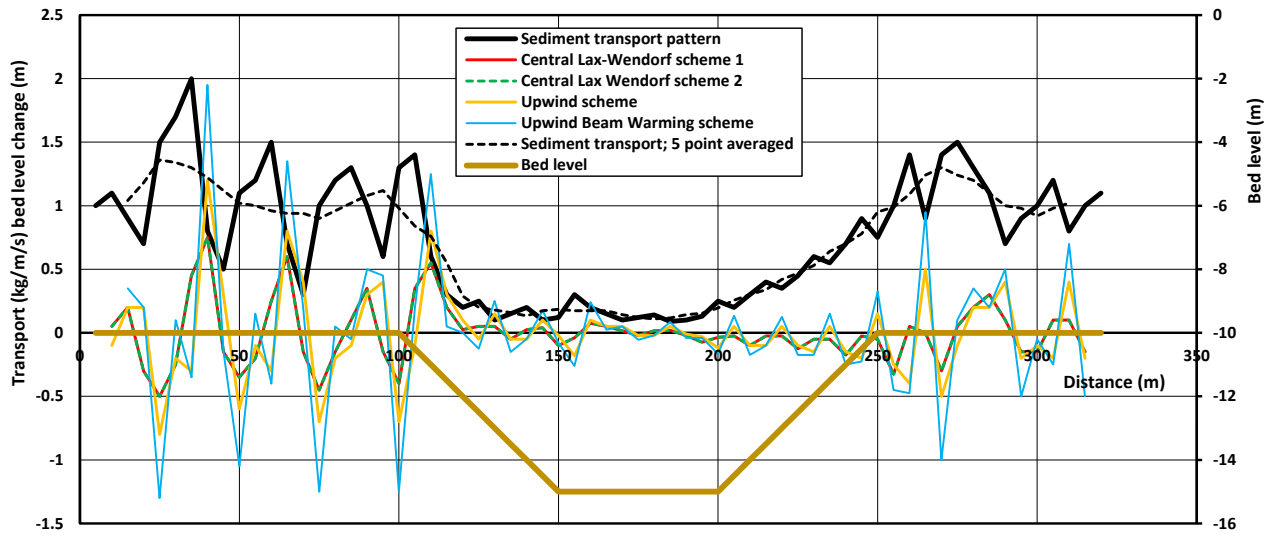


Figure 2.2.19 Effect of numerical schemes on bed level change; sediment transport not smoothed; $\alpha=0$

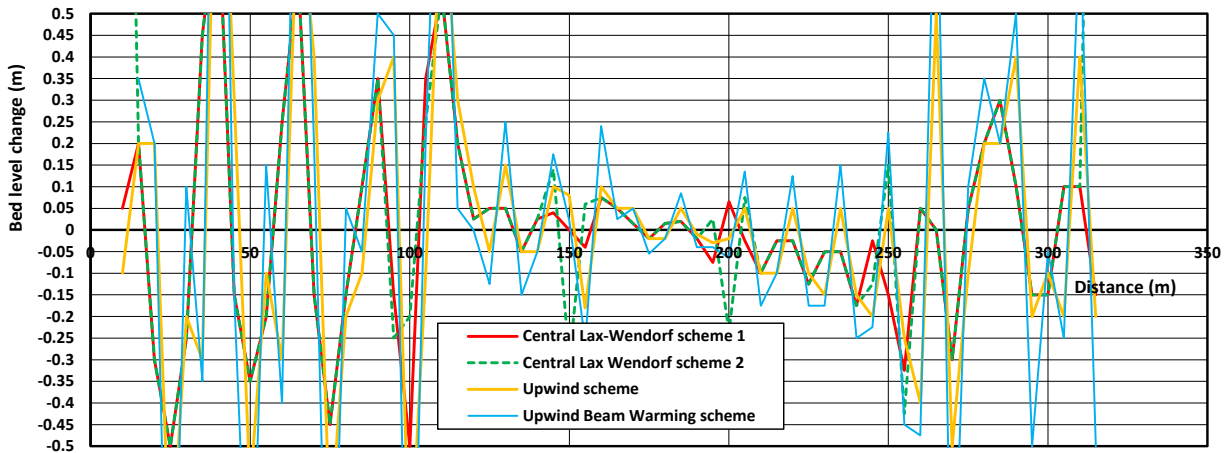


Figure 2.2.20 Effect of numerical schemes on bed level change; sediment transport not smoothed; $\alpha=0.2$

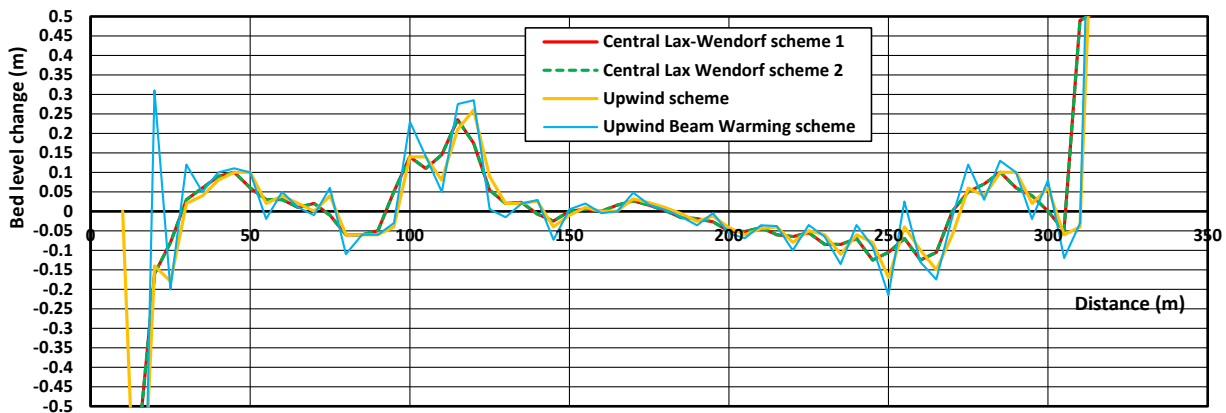
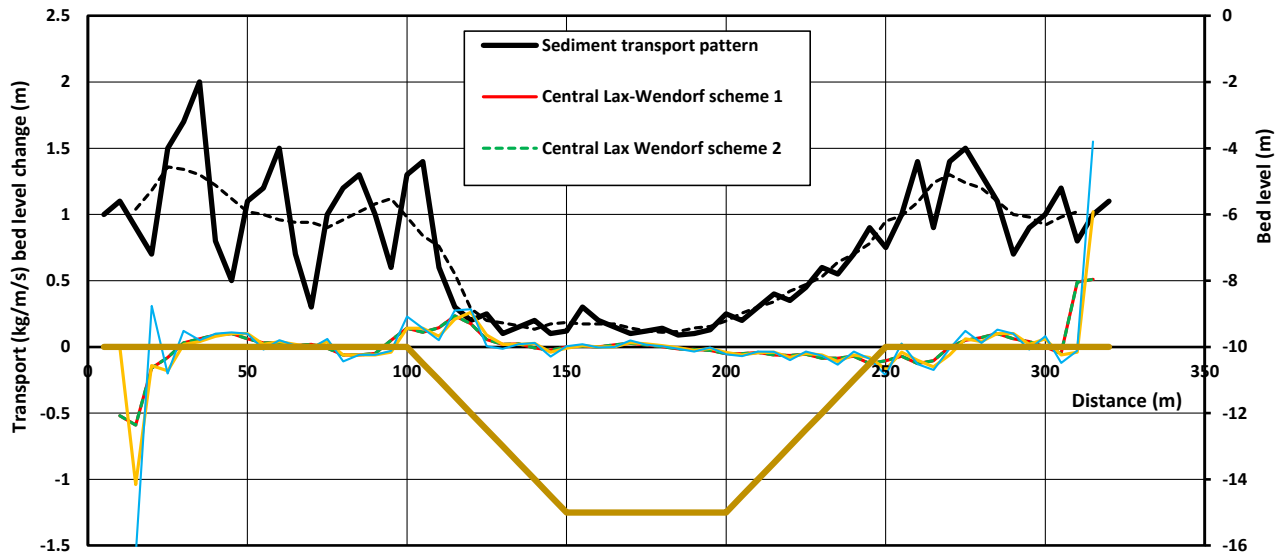


Figure 2.2.21 Effect of numerical schemes on bed level change; sediment transport smoothed; $\alpha=0$

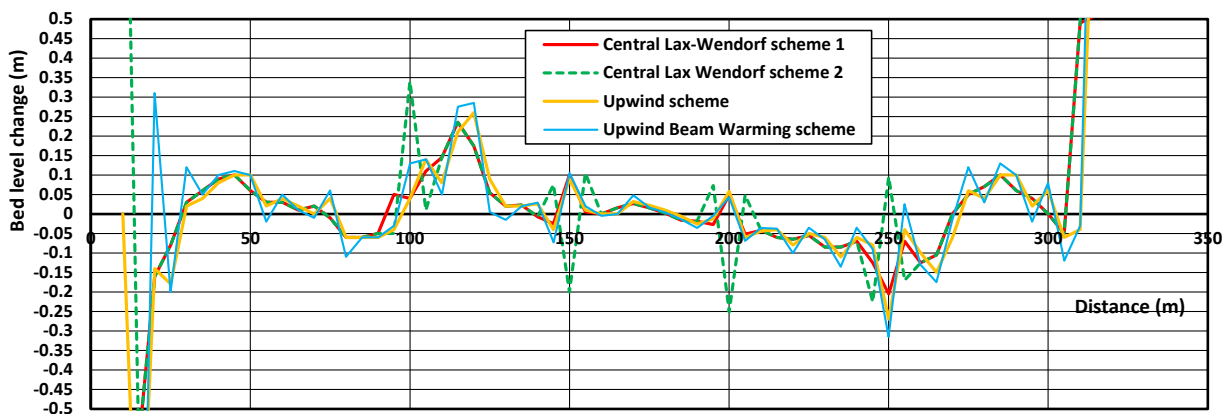


Figure 2.2.22 Effect of numerical schemes on bed level change; sediment transport smoothed; $\alpha=0.2$

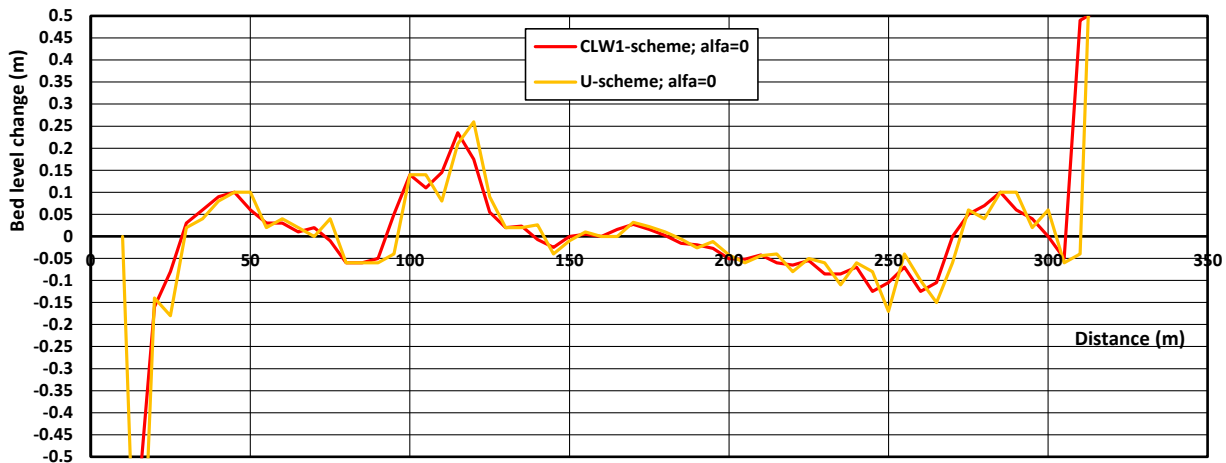


Figure 2.2.23 Effect of CLW1-scheme and U-scheme on bed level change; sediment transport smoothed; $\alpha=0$

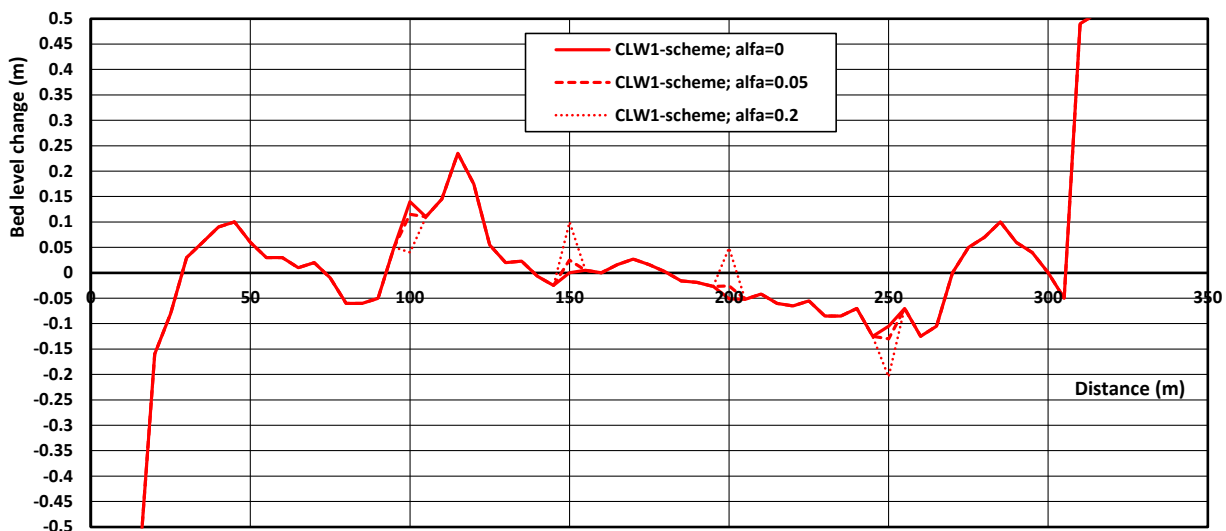


Figure 2.2.24 Effect of CLW1-scheme on bed level change; sediment transport smoothed; $\alpha=0, 0.05, 0.2$



2.2.9 STRUCTURE OF PROGRAM CROSMOR

1	CROSMOR	DISP			
3		SKCOMA			
4		INPUT	SKCOMA		
6		LEES	SKCOMA		
9		RAYL	RINTPL		
13		RINTPL			
14		GOLF	FWL		
20			TOLX		
21			RINTPL		
25			ZEROIN		
32			RK	RK1ST	FKT
33				COMP	
36			STAT	ORDER	
37			SNELH	FVV	
41				TOLV	
48				SMOOTH	
50				ZEROIN	
52		TRANSP			
54			RINTPL		
55			CALC		
57			INIT		
59			FDSTER		
66			SUSPEN		
70			BODEM		
79			SMOOP		
80			BEACH		
81			HARDL		



BEACH	computation (kinematic) of bed level landward of last grid point to run-up level
BODEM	computation of bed load for all fractions
CALC	computation of d50, dm, d90, hiding factor
CALC1	computation of d90
COMP	stop criterion for integration wave height and set-up
CROSMOR	main program
DISP	file crosmor.inf to screen
FDSTER	computation of critical bed-shear stresses τ_{ucr} and τ_{ucr1}
FKT	derivatives of wave height and set-up for numerical integration
FVV	computation of longshore velocity using ZEROIN
FWL	computation of wave length
GOLF	Subroutine for computation of wave data per wave class, postprocessing and transfer of data to transport subroutines
INIT	initialisation of parameters
INPUT	reads input file
HARDL	sand transport at hard layer
LEES	routine for INPUT
ORDER	ordering for determination of statistics Hrms etc.
RAYL	Rayleigh distribution for Hrms
RINTPL	linear interpolation in space and time
RK	routine for numerical integration(runge-kutta, variable step size)
RK1ST	routine for RK (solution first step)
SKCOMA	skipping of commentlines (* at first position of line) in input file
SMOOP	"smoothing" of fraction-values along x-axis
SMOOTH	"smoothing" of DBR and UR parameters
SNELH	computation of longshore velocity and smoothing
STAT	statistical computation of H1/3 H1/10 etc.
SUSPEN	total suspended transport
TOLV	tolerance of velocity in FVV for numerical solution



- TOLX tolerance for wave length solution
- TRANSP transport per wave class, per fraction and bed levels
- ZEROIN routine for determination of positive roots from functions

2.3 Model settings

2.3.1 Numerical and physical settings

The CROSMOR-model (in Fortran-code) is a morphodynamic model for computation of wave heights, wave asymmetry, undertow and longshore currents, bed load and suspended load transport and beach and dune erosion along a cross-shore coastal bed profile. It is noted that morphodynamic models are complex models because of bed instability problems, depending on the choice of the numerical model parameters involved.

The most important numerical parameters are explained in **Table 2.3.1**.

The most recent input files are : ACROS1.inp and ACROS2.inp

If input file does not execute, see file DIAGNOSE.

Parameter	Description	Range	Default
Grid size (DX)	The profile is specified in a number of characteristic sections; the grid size in each section is determined by the parameter NSTAP (integer), which is the number of grid steps in that section	offshore: 10 to 20 m nearshore: 0.5 to 2 m (DX=0.5 m should be applied in very steep section ; steeper than 1 to 10)	
Factime (DT)	Time step; the time step is automatically selected in the model depending on the offshore wave height (see input file); factime is a multiplication of the selected time step	short term storm runs (over 1 to 10 days): factime=0.1-0.5 long term runs (10 to 1000 days): factime=1 to 2	factime=0.5 factime=2
Bed smoothing (Facsmooth)	The bed updating scheme requires slight bed smoothing for stability reasons; the bed smoothing parameter is automatically selected to be 0.005; facsmooth is a multiplication factor to 0.005 (0.5% smoothing); facsmooth=10 means that the bed smoothing factor applied is 0.05 (5% smoothing)	short term storm runs (over 1 to 10 days): facsmooth=1 to 5 long term runs (10 to 1000 days): facsmooth=5 to 10	facsmooth=5 facsmooth=10
Bed smoothing near water line (sw)	Extra bed smoothing to suppress bed instability near the water line	short term storm runs (over 1 to 10 days): sw=0.05-0.1 (5% to 10% extra smoothing) long term runs (10 to 1000 days): sw=0.01-0.05 (1% to 5% extra smoothing)	0.05 0.05

Remark: short-term storm runs are for the erosion due to excessive wave heights (RP=10 to 100 years)
 long term runs are for wave heights up to RP=1 year (no excessive wave heights)

Table 2.3.1 Numerical input parameters of CROSMOR-model (version 15 July 2025)



The modelling (trial and error) procedure is as follows:

- use default values as much as possible for the start run;
- reduce grid size in nearshore section (factor 2) and compare results with the start run;
- reduce factime (factor 2) until model becomes unstable or crashes and compare results to the start run
- reduce facsmooth and sw (factor 2) until model becomes unstable or crashes and compare results with the start run;
- check that the erosion area is approximately equal to the accretion area.;
- for long term runs with NHW=-1, the representative wave height should be determined; make first short term storm runs over 1 day with NHW=7 and also make similar short term runs with NHW=1 varying GAMMAR-coefficient (GAMMAR=1. 1.2 and 1.41) and select the GAMMAR-value which gives the best agreement with NHW=7, see **Figure 2.3.1** and **2.3.2**.

Other important physical input parameters are explained in **Table 2.3.2**.

Parameter	Value	Description
Bed level (m)		Specify initial bed level to Mean Sea Level (MSL; schematize bed profile in a number of characteristic sections (table length is specified separately); grid points are linearly interpolated
Level of hard layer (m)		Specify top of hard layer to MSL; if no hard layer present, use a large value (for example: -100 m) for all sections
hgrens	0.1-0.5	Depth at last computational grid point; default=0.3
Beach	0/1	Model can be run with or without beach (for example: a berm in deeper water can be simulated without beach)
Storm level Hstorm (m)		Specify value to MSL (+ values above MSL) as function of time
NHW (-)	1 to 10	The wave spectrum of each wave condition can be schematized in to a number of Rayleigh waves. Short term run: NHW=6 to 10 (time step should be smaller for relatively high waves of the spectrum; runtime goes up for more waves NHW>1) Long term runs: NHW=1; if NHW=1, the representative wave height is $H_{representative}=(\text{Gamma}R) H_{rms}$
NHT (-)	>2	Specify wave conditions ($H_{rms,0}$; T_p , θ_0 Wave incidence angle at deep water; w_{10} =wind speed at height of 10 m parallel to shore affecting the computed longshore current; if w_{10} is specified, the coefs coefficient related to the shear stress of the wind at the sea surface should be set to a value >0)
Switch1 (-)	0,1,3,4	Selection parameter for method to compute wave asymmetry velocities (default=0= method of Isobe-Horikawa, mostly used)
Switch2 (-)	0,1	Default=0; acceleration effect on shear stress are excluded, 1=acceleration effect of Nielsen are included.
Switch3 (-)	0,1	Default=0; phase lag effects for wave-related suspended transport are excluded, 1= phase lags are included
Roller (-)	0-1	inclusion of roller of breaking waves; default=0.5
Coef6 (-)	laboratory cases=1; field cases=3	related to the undertow velocity, which depends on the local wave height; coef6=1 means that the wave height is averaged over 1 wave length; coef6=3 means averaging over 3 wave lengths (more averaging gives more smoother results); default=3
Coef5 (-)	laboratory cases=1; field cases=3	This coefficient is related to the longshore current velocity, which depends on the local wave height; coef5=1 means that the wave height is averaged over 1 wave length; coef6=5 means averaging over 3 wave lengths (more averaging gives more smoother results); only works if wave incidence angle is larger than 0; default=3



CLH (-)	0-1	Inclusion of onshore streaming near bed of Longuet-Higgins; important for bed load transport (coarser sediments); default=0.5
SL (degrees)	30° to 70°	Slope angle of dune front (last section); bed sliding if local slope is larger than SL
SEF (-)	1 to 2	Extra sand entrainment at steep beach or dune front; default SEF=1 for slopes milder than 1 to 10; SEF=1.25 for slopes of 1 to 5; SEF=1.5 for slopes of 1 to 3; SEF=2 for slopes of 1 to 2 (do not use SEF>2)
COEFLF (-)	0 to 1	COEFLF= coefficient low frequency swash velocity near waterline (range 0 to 1; default=1; 0=no effect)
CSW (-)	0-1	Inclusion of onshore-directed swash-induced velocity (u_{swash}) in swash zone (only for steep gravel beaches); only applied in the zone where the water depth $h < 3$ hgrns; csw can only be used for NHW=1 (1 wave class); $u_{swash}=0$ for NHW>1 csw=0 to 1.5 (default=1) for accretive sediment transport conditions csw=0 for erosive sediment transport conditions
Coefsr (-)	o, or >0	Can be used to model the wind-induced shear at the water surface
Gamma (-)	0 or 0,6-1	Default=0; wave breaking is automatically computed by model (depending on local slope); gamma=0.6: wave breaking coefficient is set to a constant value of 0.6 (use values of 0.6 to 1 only)
GAMMAR	1 to 1.41	Default=1; coefficient for representative wave height in case of NHW=1
Frunup (-)	1	Default=1; runup length on beach can be made shorter or longer (use 0.5 to 2)
CLC (-)	0.5-1	Default=1; coefficient to represent the effect of groin type structures on the longshore current; values <1 give a reduction of the longshore current
ELS (m ² /s)	0.5	Mixing coefficient to compute longshore mixing effect acting on longshore current velocity; default=0.5; range =0.1 to 10 m ² /s
Niteration (-)	300	Number of iterations to compute longshore current velocity
SW (-)		Extra bed smoothing near water line; see Table 2.3.1
DL (m)	0.1 to 1	Thickness of top layer; only used if NFR>1
Rhos (kg/m ³)	2650	Sediment density
Por (-)	0.4	Bed porosity value default Por=0.4 gives bulk density of 1600 kg/m ³
Cu (-)	1.-2.5	Uniformity coefficient of bed material $Cu = d_{60}/d_{10}$
Faced (-)	0.5-2	Default=1; calibration factor of bed load transport; bed-load transport is mostly landward-directed
Facsus (-)	0.5-2	Default=1: calibration factor of suspended load transport due to combined waves and currents (undertow and longshore current velocity); suspended load transport is mostly seaward directed transport
Facsusw (-)	0.1-0.5	Default=0.1; calibration factor of suspended load transport due to wave asymmetry effects; mostly landward-directed transport
Tend (s)		End time of computation (in seconds)
Factime (-); Facsouth (-)		See Table 2.3.1
NFR (-)	1-10	Number of sand fractions; default=1 for long term runs; NFR=5 to 10 for short term runs over 1 day or so (NFR> 1 leads to increase of run time) if NFR> 1 the hard layer function cannot be used (hard layer is automatically set to -100 m)
TE (°C)	°Celsius	Sea water temperature; used for computation of settling velocity and fluid density
SA (promille)	0-30 promille	Salinity of seawater; used for computation of fluids density (SA=30 promille gives fluid density of 1025 to 1020 kg/m ³)
RC (m)	0; 0.01-0.5	Current-related bed roughness; default=0 RC is computed by model; RC is specified as function of x



RW (m)	0; 0.01-0.05	Wave-related bed roughness for friction factor; default=0; RW is computed by model; RC is specified as function of x
Pmud (%)	0-30%	Percentage of mud < 63 μm in bed material; can be specified as function of x; default=0
Frip (-)	0.5-1.5	Multiplication factor of undertow current ; can be specified as function of x; default=1; use value of 0.5 to suppress erosion or 1.5 to enhance erosion
Fsand (-)	1-5	Multiplication factor of bed concentration near hard structure; can be specified as function of x; default=1; use value >1 to represent the effect of extra structure-generated turbulence on the bed concentration
Dsi (m)		d_{50} if NFR=1; fraction values in NFR >1

Table 2.3.2 Physical input parameters of CROSMOR-model (version 15 July 2025)

Determination of representative wave height (GAMMAR) in the case of NHW=1 (1 wave class)

A record of irregular non-breaking waves of say 30 minutes is mostly represented by the rms-wave height H_{rms} . Generally, the wave height of this record has a Rayleigh-type of distribution with higher and smaller waves. It is not, a priori, clear what is the representative wave height for sediment transport. The CROSMOR-model has been used to study this problem. Each wave height condition can be represented by either 1 (representative) wave height or by a series of Rayleigh-distributed waves. The number of wave classes to be used can be selected by the model user (input parameter NHW=1 or NHW>1). If NHW>1, the sediment transport is computed for each individual wave height and then summed over all wave heights taking the frequencies of occurrence into account. It is noted that NHW> 1 is not very suitable for long term runs because of excessive run times. If NHW=1, the representative wave height is set to $H_{representative}=\gamma_r H_{rms}$ with $\gamma_r =1, 1.2$ and 1.41 . Sensitivity runs have been made to assess the most appropriate γ_r -value compared to similar run with NHW=7. Two different cases are considered: 1) a storm with $H_{rms,o}=7.45$ m ($T_p=14$ s, $\theta_o=10^\circ$, duration=1 day) attacking a relatively steep beach profile of 1 to 5 between -10m and -1 m and 2) a storm with $H_{rms,o}=3.55$ m ($T_p=14$ s, $\theta_o=10^\circ$, duration=2 day) attacking a relatively mild beach profile of 1 to 20 between -3 m and 0 m.

Figure 2.3.1 for case 1 shows that the computed beach erosion is substantially smaller than for NHW=7. Using NHW=1, the γ_r -value should be set to 1 to have the best agreement with the profile for NHW=7.

Figure 2.3.2 for case 2 shows that that the computed beach erosion is somewhat larger than for NHW=7. Using NHW=1, the γ_r -value should be set to 1.41 to have the best agreement with the profile for NHW=7. Similar results were obtained for a run with $d_{50}=0.25$ mm and for a run with $H_{rms,o}=2.12$ m.

Based on these 2 cases, the type of bed profile (steep or mild slope) affecting the wave breaking processes has a significant effect on the most appropriate γ_r -value. The best approach for practical cases is to determine the best γ_r -value for a short duration storm run. This value can then be used for long term runs.

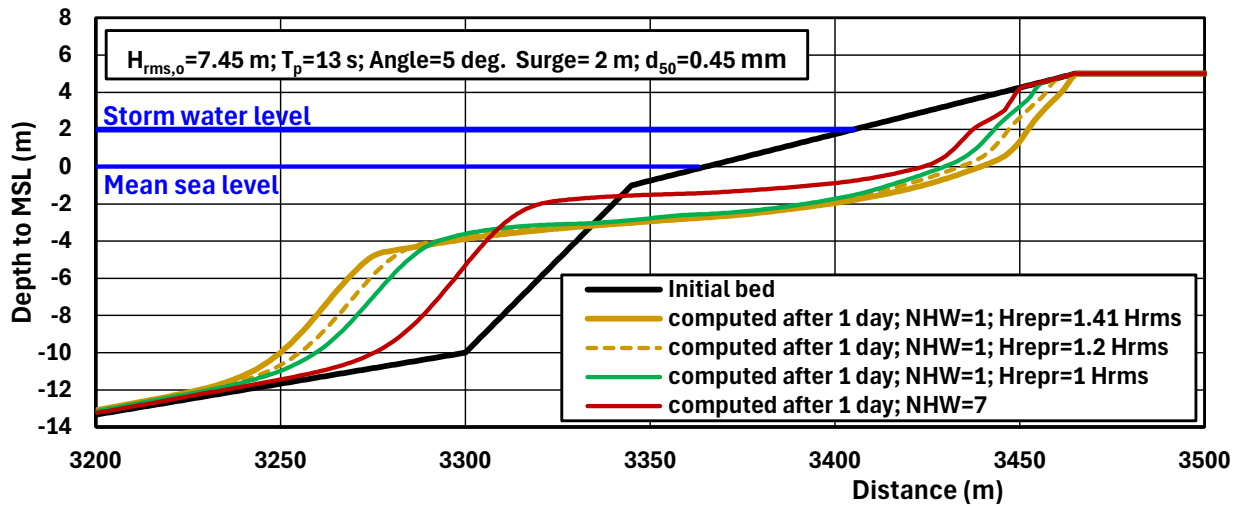


Figure 2.3.1 Effect of representative wave height (number of wave classes); storm case 1

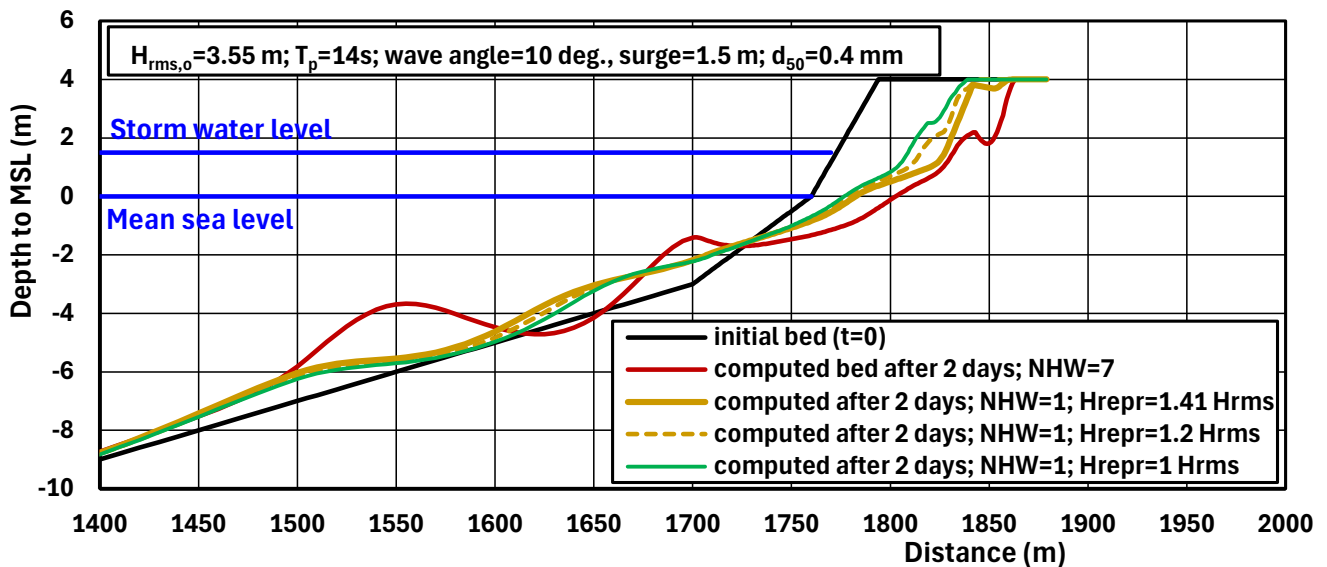


Figure 2.3.2 Effect of representative wave height (number of wave classes); storm case 1

Table 2.3.3 shows an example table with main settings for a practical project.

PARAMETERS	Values
Tide	tide; varying -4 to 2.6 m; longshore tidal current=0
Water depth at deep water (m)	-6.25 m below MSL
RMS-wave height, period and wave incidence angle at deep water	H_{rms} =1.6 to 4.8 m, T_p =4 to 7.3 s, angle= 5°



Storm level above MSL (m)	4.1 m
Beach slope above MSL	1 to 90 (-4 to 0 m); 1 to 70 (0 to +3 m); 1 to 5 (dune front above +6 m)
Dune level above MSL (m)	+16 m
Maximum dune slope SL (sliding when slope is larger)	25°
Boundary depth near beach (last grid point, m)	0.3 m
Grid size (m)	10 m offshore; 2 m nearshore
Hard layer	none
Number of wave classes per wave height	6
Wave asymmetry	Isobe-Horikawa
Wave breaking coefficient (-); roller coefficient (-)	auto; 0.5
Runup coefficient frunup (-)	1 (default)
Coefficients wave averaging for undertow (coef6=1 for lab cases and 3 for field case) and longshore current (coef5=1 for lab cases and 3 for field cases)	coef6=1 coef5=1
Coefficient Longuet-Higgins streaming (-); roller effect (-)	1 (default=1); 0.5 (default=1)
Grain diameter sand d_{50} ; C_u -coefficient	0.23 mm; 2
Coefficients sand transport formulas facbed; facsus; facsusw (-)	0.7; 0.7; 0.7 (default 1)
Coefficient extra sand entrainment in dune zone, sef (-; range 1 to 2)	1.5
Coefficient bed concentration landward of hard layer fsand (-)	1 (default)
Coefficient longshore current CLC (-) and undertow frip (-)	1; 1 (default)
Bed roughness (m)	Automatic
Bed smooth factor facsmooth (-); sw (-)	10 (default=5); 0.2 (default=0.05)
Time step factor factime (-)	0.1 (default=0.5)
Temperature (°C) and salinity (promille)	15° C and 30 promille
Files	case2.inp

Table 2.3.3 *Input data of CROSMOR-model*

Output examples are given in Tables 2.3.4 to 2.3.9.

*TIME (S) =	0.0									
* X	HD	S	HRMS	TRMS	H1/3	T1/3	H1/10	HMAXS	QB	
*(m)	(m)	(m)	(m)	(s)	(m)	(s)	(m)	(m)	(-)	
B001										
482	10									
0.00	41.500	0.000	5.450	13.385	7.633	14.811	9.822	16.600	0.000	
5.00	41.400	0.000	5.450	13.385	7.633	14.811	9.821	19.241	0.000	
10.00	41.300	-0.000	5.450	13.385	7.634	14.811	9.823	20.646	0.000	
15.00	41.200	-0.000	5.450	13.385	7.634	14.811	9.824	21.377	0.000	

Table 2.3.4 Output of wave data; case with NW=7

HD= water depth; S=wave setup; QB= percentage breaking waves
 if NHW>1, HRMS, H1/3, H1/10 and HMAXS; TRMS and T1/3= wave height and period data averaged over all Rayleigh-waves; sediment transport is computed for each Rayleigh wave and summed;
 if NHW=1, HRMS=H1/3=H1/10; H1/3=1.4 HRMS is used for sediment transport



```
*TIME (S) =          0.0
* X      UBWF1/3 UBWB1/3  UCRmn UBmean UBWF-rms UBWB-rms  UCR-rms UB-rms(+/-)
*(m)     (m/s)  (m/s)   (m/s) (m/s)  (m/s)   (m/s)   (m/s)   (m/s)
B002
  482     9
    0.00  1.376  1.179  -0.160  0.000  0.958  0.836  -0.218  0.000
    5.00  1.379  1.181  -0.161  0.000  0.960  0.837  -0.218  0.000
   10.00  1.382  1.183  -0.161  0.000  0.963  0.839  -0.218  0.000
   15.00  1.385  1.184  -0.161  0.000  0.965  0.840  -0.219  0.000
```

Table 2.3.5 Output of wave and current data; case with NW=7

UBWF1/3= peak forward orbital velocity; UBWB1/3=peak backward orbital velocity
 UBWRMS= peak forward orbital velocity; UBWBRS=peak backward orbital velocity
 UCRmn=mean undertow velocity; UBmean= near-bed streaming velocity

```
*TIME (S) =          0.0
* X      L      TETAS  DBR   V(no mix)  V(mix)  C1(ka)  C2(ks)  Kw  Kc
*(m)     (m)  (degree) (N/(SM)) (m/s)   (m/s)   (m0.5/s)  (m) (m)
B003
  482     8
    0.00 226.06  5.00  0.00  0.001  0.001  50.29  68.29  0.080  0.080
    5.00 225.89  5.00  0.00  0.001  0.002  68.28  68.28  0.080  0.080
   10.00 225.79  4.99  0.00  0.001  0.002  68.26  68.26  0.080  0.080
   15.00 225.62  4.99  0.00  0.001  0.003  68.24  68.24  0.080  0.080
```

Table 2.3.6 Output of wave and current data; case with NW=7

L= wave length; TETAS= wave angle to shore normal; DBR= wave dissipation energy;
 V(no mix)= longshore current velocity without horizontal mixing
 V(mix)= longshore current velocity with horizontal mixing
 C1= Chezy-coefficient based on overall roughness
 C2= Chezy-coefficient based on current-related roughness
 KW= wave-related bed roughness
 KS= current-related bed roughness



```

*TIME (S) =          0.0
*      Summed over wave classes
*      X      SBCROSS   SSCROSS   STCROSS   STHARD   SBLONG   SSLONG   STLONG
*      (M)    (KG/SM)  (KG/SM)  (KG/SM)  (KG/SM)  (KG/SM)  (KG/SM)  (KG/SM)
B011
      482          7
0.000      0.000    -0.000    -0.000    -0.000     0.000    -0.000    -0.000
5.000      0.000    -0.000    -0.000    -0.000     0.000    -0.000    -0.000
10.000     0.000    -0.000    -0.000    -0.000     0.000    -0.000    -0.000
15.000     0.000    -0.000    -0.000    -0.000     0.000    -0.000    -0.000
20.000     0.000    -0.000    -0.000    -0.000     0.000    -0.000    -0.000

```

Table 2.3.7 Output of sediment transport data; case with NW=7

SBcross= cross-shore bed load transport
 SSCross= cross-shore suspended load transport
 STcross= cross-shore total load transport
 SBlong= longshore bed load transport
 SSLong= longshore suspended load transport
 STlong= longshore total load transport

```

*TIME (S) =          0.0
*      Integrated longshore transport and CA
*      X      SBLONG   SSLONG   STLONG   CA
*      (M)    (KG/S)   (KG/S)   (KG/S)  (KG/M3)
B012
      482          4
0.000      0.000     0.000     0.000     0.000
5.000      0.000    -0.000    -0.000     0.000
10.000     0.000    -0.000    -0.000     0.000
15.000     0.000    -0.000    -0.000     0.000

```

Table 2.3.8 Output of sediment transport data; case with NW=7

SBlong= longshore bed load transport integrated along x-axis
 SSLong= longshore suspended load transport integrated along x-axis
 STlong= longshore total load transport integrated along x-axis (value in last x-point is the total longshore transport in the surf zone with breaking waves)
 Ca= bed concentration along x-axis



*TIME (S) =	79200.0				
* X	DZ	DZ(last)	Z(t=0)	Z-NEW	
* (m)	(m)	(m)	(m)	(m)	(m)
B025					
	536	5			
	0.0	0.0000	0.00000	-40.000	-40.000
	5.0	-0.0006	-0.00000	-39.900	-39.901
	10.0	-0.0005	-0.00000	-39.800	-39.800
	15.0	0.0000	0.00000	-39.700	-39.700

Table 2.3.9 Output of bed level changes; case with NW=7
 DZ = total bed level change over the computational time
 DZ (last) = total bed level change in last time step
 Z(t=0)= initial bed level to datum (MSL)
 Z(new)=bed level to datum at end of computation

2.3.2 Input files

Various input files are available (see also areadme file):

ACROS1.inp with extended explanations

AATEST1.inp: waves from file; 1 fraction, sand is represented by d50

AATEST2.inp: wave spectrum according to Rayleigh; sand is represented by d50

AATEST3.inp: wave spectrum (free) specified in N classes; sand represented by N fractions; not for hard layer

AATEST4.inp: wave spectrum according to Rayleigh; sand represented by 1 fractions;

AATEST5.inp: wave spectrum according to Rayleigh; sand represented by N fractions; not if hard layer is present

Copy of input file ACROS1.inp

Name of input file is free; use no more than 7 characters; extension .inp is required



```

* table length of bottom schematization and hard layer
19
* X=cross=shore coordinate,
* HMSL=depth of bed to Mean Sea Level MSL (neg below MSL),
* HRMSL= bed level of top of hard layer to MSL; use very lage negative value -100)if no hard layer
* NSTAP=INTEGER=number of space steps between table points of depth
*
* X(m)   HMSL(m)  HRMSLm(m)  NSTAP
* 0       -40.    -100.      100
* 500.    -30.    -100.      60
* 800.    -20.    -100.      200
* 1800.   -10.    -100.      100
* 2000.   -1.     -100.      5
* 2002.5  -0.9    -100.      5
* 2007.5  -0.3    -100.      5
* 2012.5  0.2    -100.      5
* 2017.5  0.9    -100.      5
* 2020.   1.2    -100.      5
* 2022.5  1.9    -100.      5
* 2025.   2.9    -100.      5
* 2027.5  4.0    -100.      5
* 2030.   5.1    -100.      5
* 2031.2  5.7    -100.      5
* 2032.5  5.8    -100.      5
* 2035.   6.0    -100.      5
* 2037.5  6.3    -100.      30
* 2067.5  6.3    -100.

* hgrens= water depth at last grid point (wave and transport computation up to 1/2hgrens)
* beach      beach=1; no beach=0
0.5          1

* table length storm (wind-induced) set-up HSTORM
2
* HSTORM is constant along profile and specified as a function of time;
* interpolation at each time step and cyclic repetition if end time is smaller tah total time
*
* T(s)      HSTORM(m)
* 0.         2.0
* 864000.    2.0
*
* NHW=number NHW of wave classes per wave condition=1/2/-2, if NHW=1, HRMS is multiplied with 1.4 for sediment transport
* 1= specify wave classes for 1 condition (ouput HYDRODYNAMICS see above);
* 2= compute wave classes according to Rayleigh for nht conditions (output HYDRODYNAMICS see above)
* 2= same as 2 but NHT, Time, Hrms, T, Teta, w10 from read from a separate file; comes after NHW see below (file is Awavedat.inp; Atest1.inp)
2
* In case of option 1,
* specify Number of wave classes of spectrum, H= wave height at x=0, T=period, P=percentage of occurrence, TETA= wave angle to coast normal; w10=longshore wind vel.
* NHW
* 3
* In case option -2, specify name of wave data file (maximum 12 characters; no space in first column); check that other wave data must have * (inactive)
*awavedat.inp
*
* H      T      P      TETA  W10
*
*          H = wave height(m)
*          T = wave period(s)
*          P = perc entage of occurrence
*          TETA = angle wave incidence w.r.t. coast normal
*                (positive or negative)
*          W10= longshore wind velocity at 10 m parallel coast (pos. or neg.)
*                pos.=same direction as waves; neg. against waves
*
* 0.4  9.   0.50  10.  0.
* 0.8  9.   0.40  10.  0.
* 1.2  9.   0.10  10.  0.
*

```



```

* In case of option 2
* NHW=number of wave classes
  7
* NHT=number of wave conditions
  2
* Specify wave height Hrms, Tp, TETA and W10=longsh. wind vel. as function of time; values are
* interpolated linearly at each time step (if end time is smaller than total
* computation time, the cycle is repeated)
*
*   TIME(s)   HRMS   Tp   TETA (degrees)   W10 (m/s; if w10>0, then coefsr >0)
*
*   0.         5.45  13.9  5.0             0.
* 90000.      5.45  13.9  5.0             0.
*
* Parameters for hydrodynamics (friction, breaking, currents)
*
* Switch1 0/1/2; 0=velocity asymmetry Isobe-Horikawa (default); 1= Ruessink 2008; 2= Ruessink 2010
* Roller-coefficient (0=maximum roller effect; 1= no roller; default=0.5)
* COEF6=distance for averaging of wave parameters of wave length in undertow model; 3=field cases (averaging over 3 wave lengths); 1= laboratory cases
* CLH= coefficient for Longuet-Higgins streaming near the bed (0-1; default=0.5)
* CSW= coefficient to include effective swash velocity near water line for grave/shingle beach (0-1; default=0 only for gravel; NHW must be 1)
* Switch2 0/1; 0=excl. acceleration effect on shear stress, 1=incl. acceleration effect of Nielsen
* Switch3 0/1; 0=excl. phase lag effects for wave-related suspended transport, 1= including phase lags
* SL=Maximum slope angle of dune front (default=50 in degrees); sliding occurs if local bed angle is larger than SL
* SEF=suspension enhancement factor at steep fronts=1 to 3;
*   SEF=1 without dune erosion (default=1); SEF=2 for dune erosion; SEF=2.5-3 for steep gravel under extreme storms
* Switch4 0/1 (INTEGER); 0=excluding long waves in surf zone; 1= included (default).
* CLC=coefficient (0.5-1.5) to increase or decrease longshore current (default=1); use CLC=0.7 if groins are present
*
* Switch1 ROLLER COEF6 CLH CSW Swit2 Swit3 SL SEF Switch4 CLC
* 0 0.5 1. 0.5 0. 0. 0. 50 1.5 1 1.0
*
* COEFSR=coefficient roller shear stress at water surface (0=default, gives zero stress; use COEFSR=0.001-0.003 if W10>0 m/s)
* GAMMA=breaking index (0=default=gamma is computed by model; otherwise specify value gamma=0.5-1.0; constant gamma is used)
* ELS=horizontal mixing coefficient for longshore current (0.1 to 3 m2/s);
* COEF5= parameter related to averaging of wave height over wave length for longsh. current; 3= field cases; 1 =laboratory basins
* Frunup= multiplication factor of wave runup (default=1; range=0.5-2);
* ELS=horizontal mixing coefficient for longshore current (default=1; 0.1 to 10 m2/s);
* Niteration=number of iterations for longshore velocities (default=300; 1 if TETA=0)
* SW=0.01 to 0.2= extra smoothing near waterline (over 10 points on both sides of last point; default=0.05)
* COEFSR GAMMA coef5 Frunup ELS(m2/s) Niteration SW
* 0.0 0.0 1.0 1.0 0.5 300 0.05
*
* Options OUTPUT TRANSPORT AND BED LEVELS 0/1/2 and Nout
* Output to screen:0=no output; 1= run infomation; 2= maximum erosion/sedimentation interval 10 timesteps
* Output parameters: 0= no output transport; 1= bed levels t=0 and t=end and every Nout;
* 2= transport and bed levels at t=0 and t=end and every Nout
* Outputscreen Output parameters NOUT= output of bed levels after any NOUT time steps
  2 2 10000
*
* Sediment transport parameters
* DL = thickness of active transport layer only used for sediment fractions (0.1-1.0 m)
* RHOS = sediment density (2650 kg/m3)
* POR = porosity of bed ( 0.4 )
* CU = uniformity coefficient=d60/d10
* facbed= calibration factor bed load transport (default=1)
* facsusc= calibration factor current-related susp.load transport (default=1)
* facsusw= calibration factor wave-related susp.load transport (default=1)
* T-END = total computation time (s)
*
* DL(m) RHOS(kg/m3) POR(-) CU facbed (-) facsusc (-) facsusw (-) T-END (s)
* 0.5 2650 .4 2.0 1.0 1.0 .0 79200.
*

```



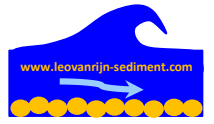
```

* factime;(DEFAULT=1)
* DT=factime*3600 seconds if 0<Hrms,off<1 m
* DT=factime*2400 if 1<Hrms,off<2 m
* DT=factime*1200 if 2<Hrms,off<3 m
* DT=factime*600 if 3<Hrms,off<3.5 m
* DT=factime*300 if 3.5<Hrms,off<4 m
* DT=factime*200 if 4<Hrms,off<4.5 m
* DT=factime*100 if Hrms,off<4.5 m
* facsmooth; Smoothing factor of bed=facsmooth*0.005; facsmooth may be as large as 30 (DEFAULT=10)
* facsgrain; Smoothing-fractions=facsgrain*0.2 (default=1)
* factime facsmooth facsgrain
* 0.1 10. 1.
* NFR = NUMBER OF SAND FRACTIONS (NFR>1 only for short term runs 1-7 days)
* NSED = NUMBER OF X-COORDINATES FOR SEDIMENT DATA
* TE = WATER TEMPERATURE (CELSIUS)
* SA = SALINITY OF FLUID (PROMILLE)
* NFR NSED TE SA
* 1 5 10 30
* 4 5 10 30
* X = X-COORDINATE (m); values are linearly interpolated
* RC = CURRENT-RELATED ROUGHNESS (m);if RC=0.; RC is computed by model
* RW = WAVE-RELATED ROUGHNESS (m);if RW=0.; RW is computed by model
* PMUD = PERCENTAGE OF MUD IN BED [ % ] =
* Frip=multiplication of undertow velocity (default=1; range=0.5-3)
* Fsand=multiplication of bed concentration near structures; only for structures (hard layers); (default=1)
* X(m) RC(m) RW(m) PMUD(%) FRip Fsand(-)
* 0. .0 .0 0. 1.0 1.
* 1000. .0 .0 0. 1.0 1.
* 2000. .0 .0 0. 1.0 1.
* 3000. .0 .0 0. 1.0 1.
* 5000. .0 .0 0. 1.0 1.
* Dsi = GRAIN DIAMETER OF FRACTION I (MAX 10) [ M ]
* Ds1 Ds2 Ds3 Ds4 Ds5 Ds6 Ds7 Ds8 Ds9 Ds10
* .0003
* .0001 .0002 .0003 .0004
* X Psi = PART OF TOTAL FOR FRACTION I ( SOM(Psi+PMUD/100 +/- =1 ) [ - ]
* X Ps1 Ps2 Ps3 Ps4 Ps5 Ps6 Ps7 Ps8 Ps9 Ps10
* 0. 1.
* 1000. 1.
* 2000. 1.
* 3000. 1.
* 5000. 1.
* 0. .25 .25 .25 .25
* 1000. .25 .25 .25 .25
* 2000. .25 .25 .25 .25
* 3000. .25 .25 .25 .25
* 5000. .25 .25 .25 .25
* NDC = Number of depth contours for partial sediment integration; either depth contours or between x-coordinates (maximum 10)
* results are printed at the end of the output file
* 5
* Depth contours (NDC values )
* -6. -4. -2. -1. 6.
* NDX = Number of x-coordinates for partial sediment integration (maximum 10)
* ( 10 maximum )
* 7
* x-coordinates (NDX values)
* 0. 50. 1500. 1780. 2000. 2300. 2900.

```



Memo: Crosmor modelling and applications
Date: 6 December 2025





2.3 Model runs for testing of numerical and physical parameters

2.3.1 Dune erosion in Deltaflume; Cases1A, Case 1B

Case1A (T5)

The data of both flume cases (Deltaflume of Deltares) are taken from the PhD report of H. Steetzel. The input data of Case1A (base case, short term storm run over 6 hours) are given in **Table 2.3.1**.

The following input parameters have been varied:

- effect of grid size; $dx=0.25$ m in stead of 0.5 m for $x>150$ m; effect is marginal, see **Figure 2.3.1**;
- effect of smoothing near water line; $SW=0.05$ in stead of 0.2 ; effect is marginal for short term run, see **Figure 2.3.2**;
- effect of wave breaking coefficient; a constant or a slope-dependent wave breaking coefficient (default) can be used; the base case has a constant value of $\gamma_{br}=0.65$; the erosion is substantially less for the default slope-dependent wave breaking coefficient, see **Figure 2.3.3**;
- effect of wave averaging (for undertow (coef6)); $coef6=3$ in stead of 1 leads to less erosion ($coef6=1$ is more appropriate for laboratory conditions), see **Figure 2.3.4**;
- CROSMOR-version: version 15 July 2025 in stead of 14 July 2024; new version gives slightly less erosion, see **Figure 2.3.5**.

Overall conclusion: schematization and selected input parameters are sufficiently adequate (fresh water is used in Deltaflume; so salinity should be set to 0 promille; effect is small); bed smoothing parameters (facsmooth and sw) are not so important for short term runs, as long as default values (facsmooth=10; sw=0.05 for short term runs) are used.

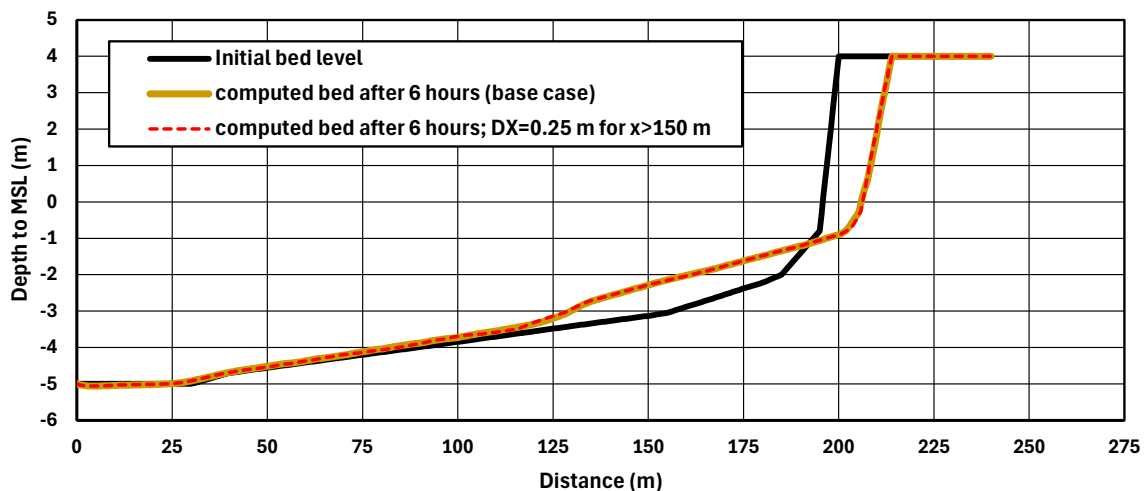


Figure 2.3.1 Effect of grid size; 0.25 m in stead of 0.5 for $x > 150$ m.

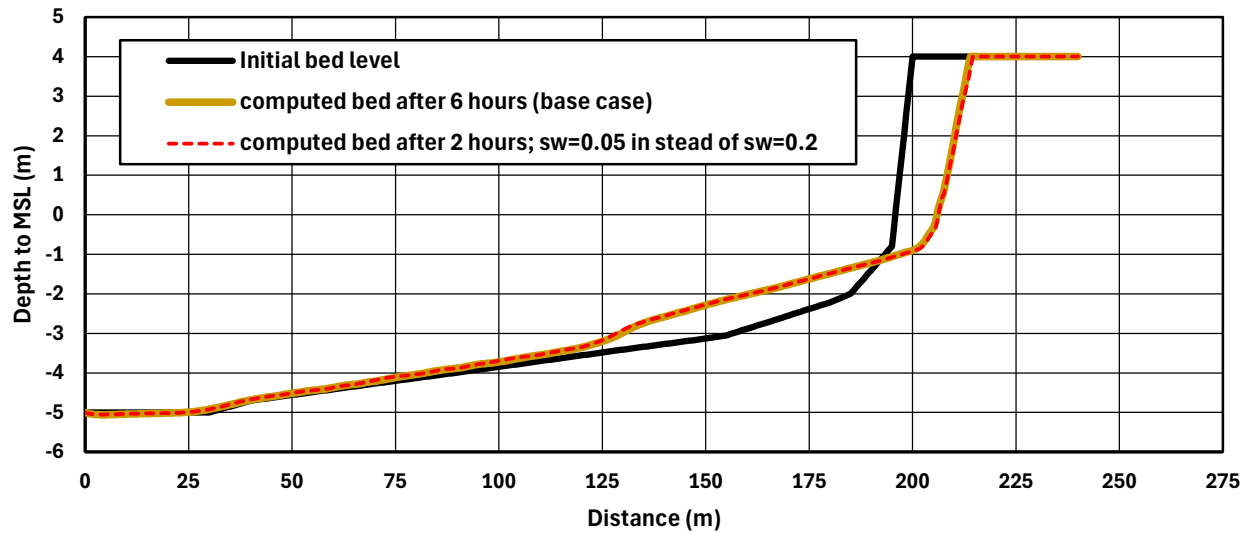


Figure 2.3.2 Effect of bed smoothing near water line; $sw=0.01$ in stead of 0.2

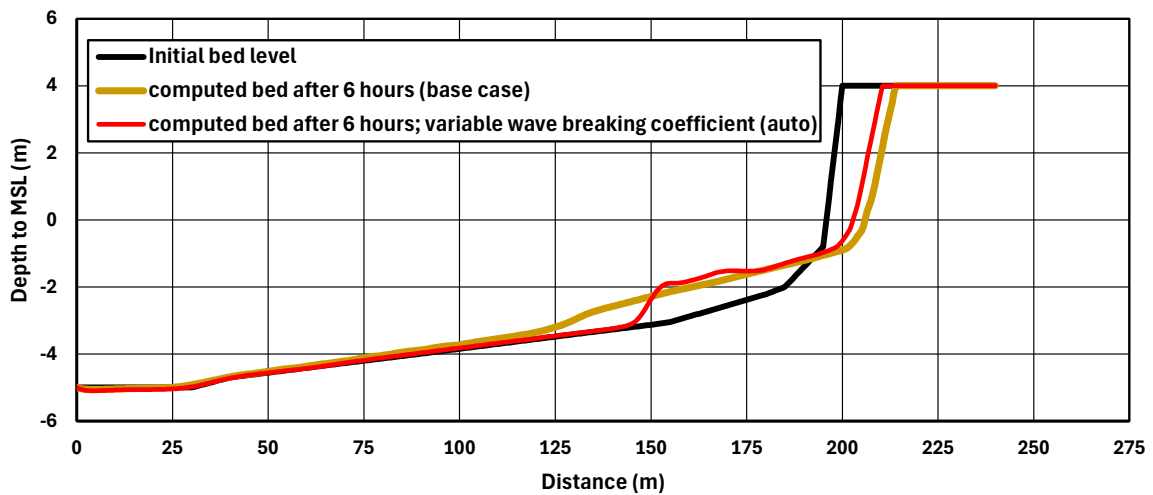


Figure 2.3.2 Effect of wave breaking coefficient (γ_{br}); variable depending on bed slope in stead of constant

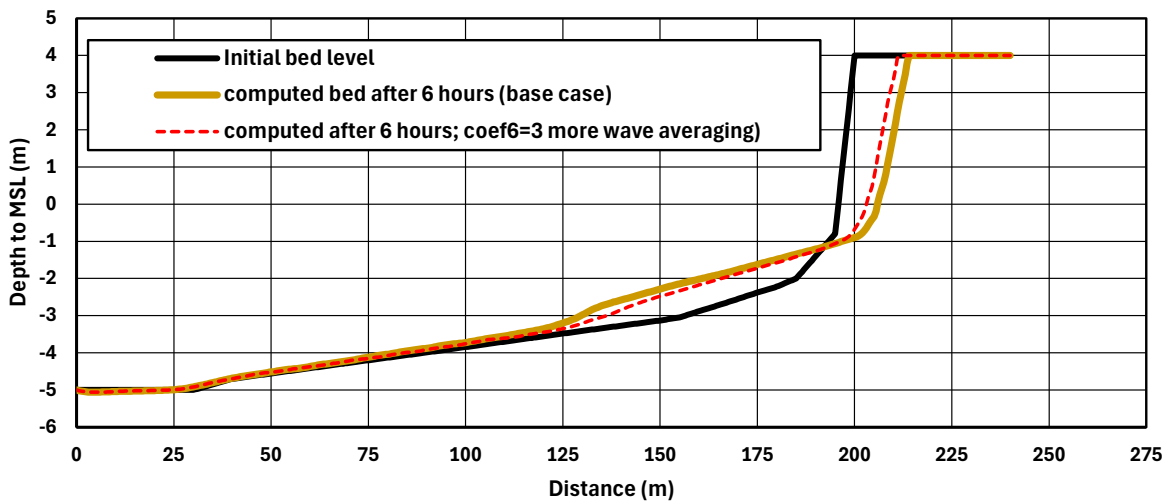


Figure 2.3.4 Effect of coefficient coef6 (undertow); coef6=3 in stead of 1

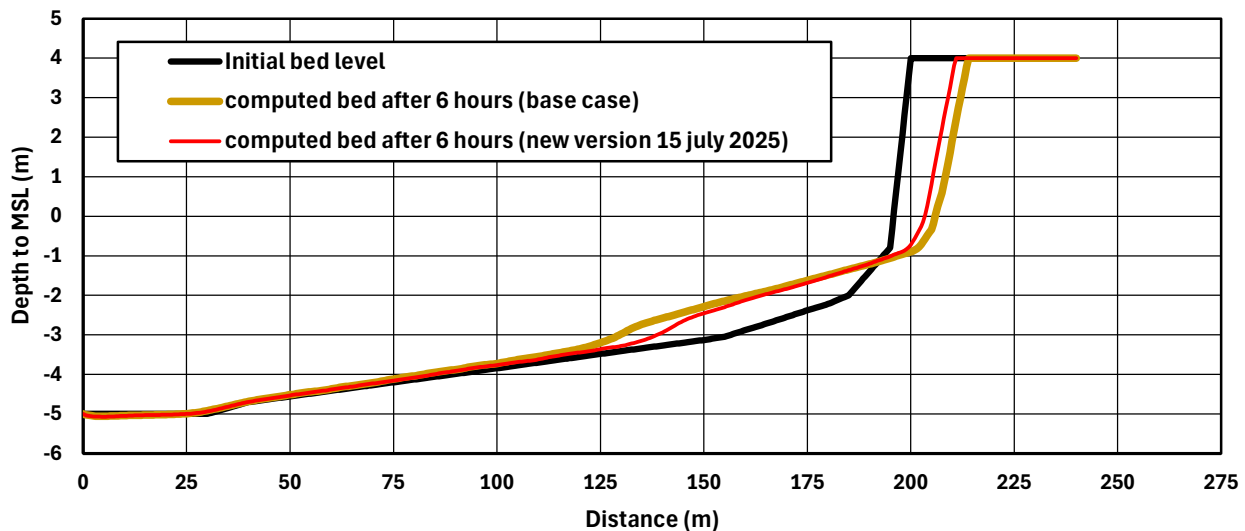


Figure 2.3.5 Effect of new CROSMOR-version; version 15 July 2025 in stead of version 14 July 2024

PARAMETERS	Values
Tide	no tide; constant water level
Water depth at deep water (m)	-5 m below MSL
RMS-wave height, period and wave incidence angle at deep water	$H_{rms}=2.2$ m, $T_p=7.5$ s, angle= 0°
Storm level above MSL (m)	0
Beach slope above MSL	approx. 1 to 30 (-3 to -2 m); approx. 1 to 8 (-2 to -0.8 m); approx. 1 to 1 (dune front)
Dune level above MSL (m)	4 m
Maximum dune slope SL (sliding when slope is larger)	30°
Boundary depth near beach (last grid point, m)	0.3 m
Grid size (m)	0.5 m
Hard layer	none
Number of wave classes per wave height	6



Wave asymmetry	Isobe-Horikawa
Wave breaking coefficient (-); roller coefficient (-)	0.65; 0.5
Runup coefficient frunup (-)	1 (default)
Coefficients wave averaging for undertow (coef6=1 for lab cases and 3 for field case) and longshore current (coef5=1 for lab cases and 3 for field cases)	coef6=1 coef5=3 (not relevant in flume)
Coefficient Longuet-Higgins streaming (-); roller effect (-)	1 (default=1); 0.5 (default=1)
Grain diameter sand d_{50} ; c_u -coefficient	0.225 mm; 2
Coefficients sand transport formulas facbed; facsus; facsusw (-)	1; 1; 1 (default 1)
Coefficient extra sand entrainment in dune zone, sef (-; range 1 to 2)	1.25
Coefficient bed concentration landward of hard layer fsand (-)	1 (default)
Coefficient undertow frip (-)	1 (default)
Bed roughness (m)	Automatic
Bed smooth factor facsmooth (-); sw (-)	10 (default=5); 0.2 (default=0.05)
Time step factor factime (-)	0.1 (default=0.5)
Temperature (°C) and salinity (promille)	15° C and 30 promille
Files	case1A.inp

Table 2.3.1 *Input data of CROSMOR-model; Case1A (test T5)*

Case1B (Test T2)

The input data (base case, short term storm run over 10 hours) of Case1B are given in **Table 2.3.2**.

PARAMETERS	Values
Tide	no tide; constant water level
Water depth at deep water (m)	-4 m below SWL (bed level is defined to SWL)
RMS-wave height, period and wave incidence angle at deep water	$H_{rms}=1.3$ m, $T_p=4.5$ s, angle= 0°
Storm level above MSL (m)	0.2
Beach slope above MSL	approx. 1 to 30; 1 to 25, 1 to 10 (beach) approx. 1 to 1.25 (dune front)
Dune level above MSL (m)	2.4 m
Maximum dune slope SL (sliding when slope is larger)	70°
Boundary depth near beach (last grid point, m)	0.3 m
Grid size (m)	0.5 m
Hard layer	none
Number of wave classes per wave height	6
Wave asymmetry	Isobe-Horikawa
Wave breaking coefficient (-); roller coefficient (-)	automatic; 0.5
Runup coefficient frunup (-)	1 (default)
Coefficients wave averaging for undertow (coef6=1 for lab cases and 3 for field case) and longshore current (coef5=1 for lab cases and 3 for field cases)	coef6=1 coef5=1 (not relevant in flume)
Coefficient Longuet-Higgins streaming (-); roller effect (-)	1 (default=1); 0.5 (default=1)
Grain diameter sand d_{50} ; c_u -coefficient	0.225 mm; 2
Coefficients sand transport formulas facbed; facsus; facsusw (-)	1; 1; 1 (default 1)
Coefficient extra sand entrainment in dune zone, sef (-; range 1 to 2)	1.25
Coefficient bed concentration landward of hard layer fsand (-)	1 (default)
Coefficient undertow frip (-)	1 (default)



Bed roughness (m)	automatic
Bed smooth factor facsmooth (-); sw (-)	10 (default=5); 0.2 (default=0.05)
Time step factor factime (-)	0.1 (default=0.5)
Temperature (°C) and salinity (promille)	15° C and 30 promille
Files	case1B.inp

Table 2.3.2 Input data of CROSMOR-model; Case1B (base case)

The following input parameters have been varied:

- smoothing of bed levels (facsmooth; sw): facsmooth=1 in stead of 10; almost no effect on results; facsmooth=10 is sufficiently accurate; sw=0.05 in stead of 0.2 gives almost similar results, see **Figure 2.3.6**;
- sediment erosion at dune front (sef): sef=1.5 in stead of 1.25; gives more erosion, see **Figure 2.3.7**;
- suspended transport capacity (facsus): facsus=2 in stead of 1; gives more erosion, see **Figure 2.3.8**;
- number of wave classes of wave spectrum (NHW): NHW=10 in stead of 6; almost no effect; NHW=6 is sufficiently accurate (less computation time), see **Figure 2.3.9**;
- CROSMOR-version: version 15 July 2025 in stead of 14 July 2024; new version gives slightly less erosion, see **Figure 2.3.10**.

Overall conclusion: schematization and selected input parameters are sufficiently adequate (fresh water is used in Deltaflume; so salinity should be set to 0 promille; effect is small); bed smoothing parameters (facsmooth and sw) are not so important for short term runs, as long as default values (facsmooth=10; sw=0.05 for short term runs) are used.

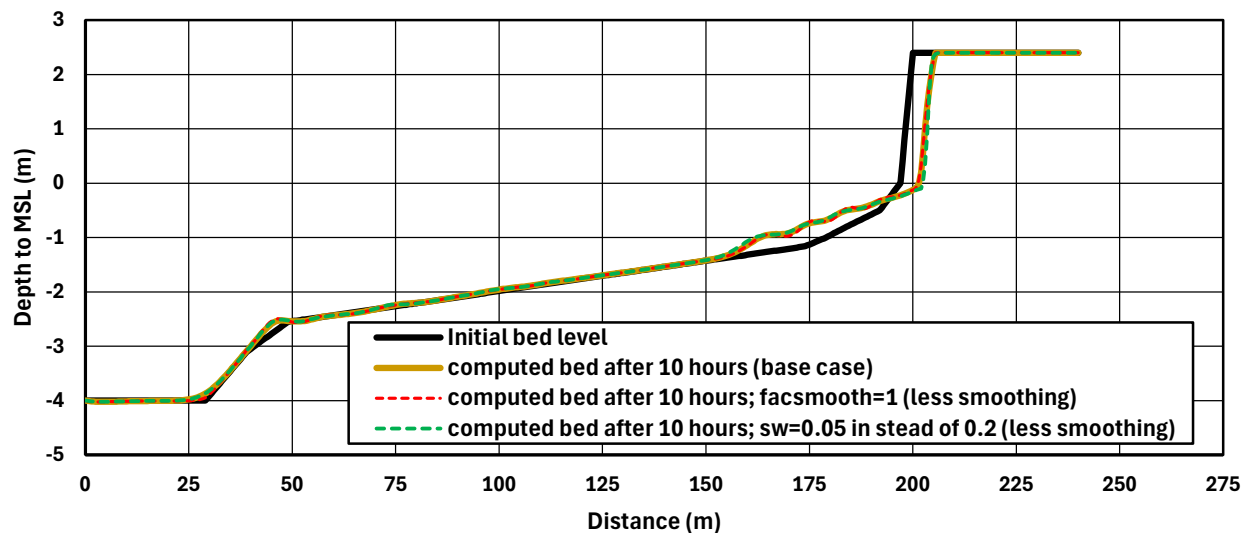


Figure 2.3.6 Effect of bed smoothing factor (facsmooth); facsmooth=1 in stead of 10

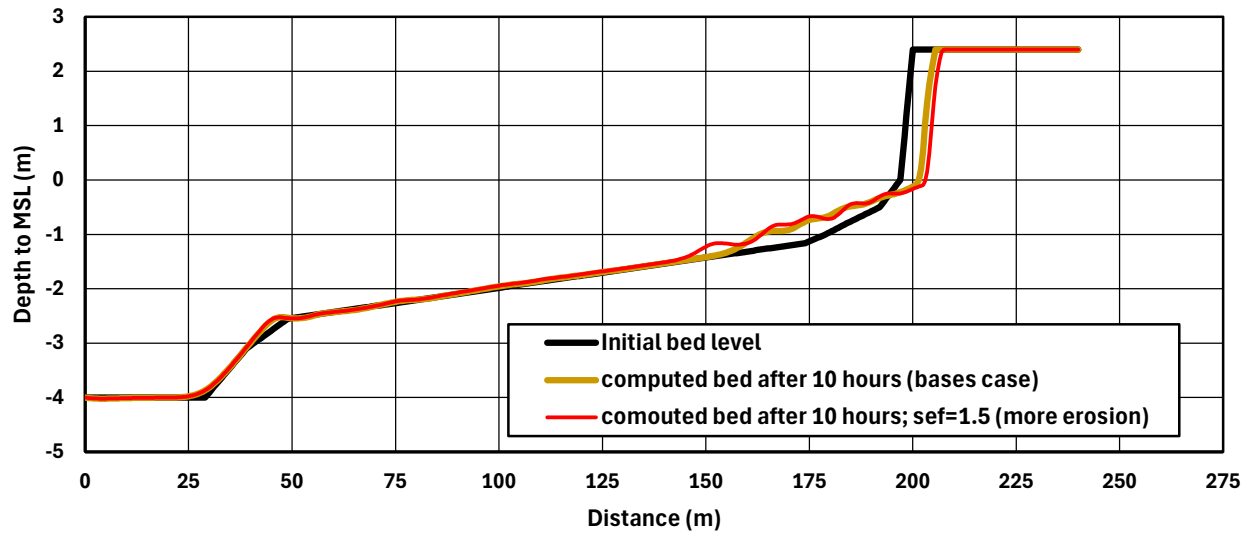


Figure 2.3.7 Effect of sediment entrainment at dune front (sef); $sef=1.5$ in stead of 1.25

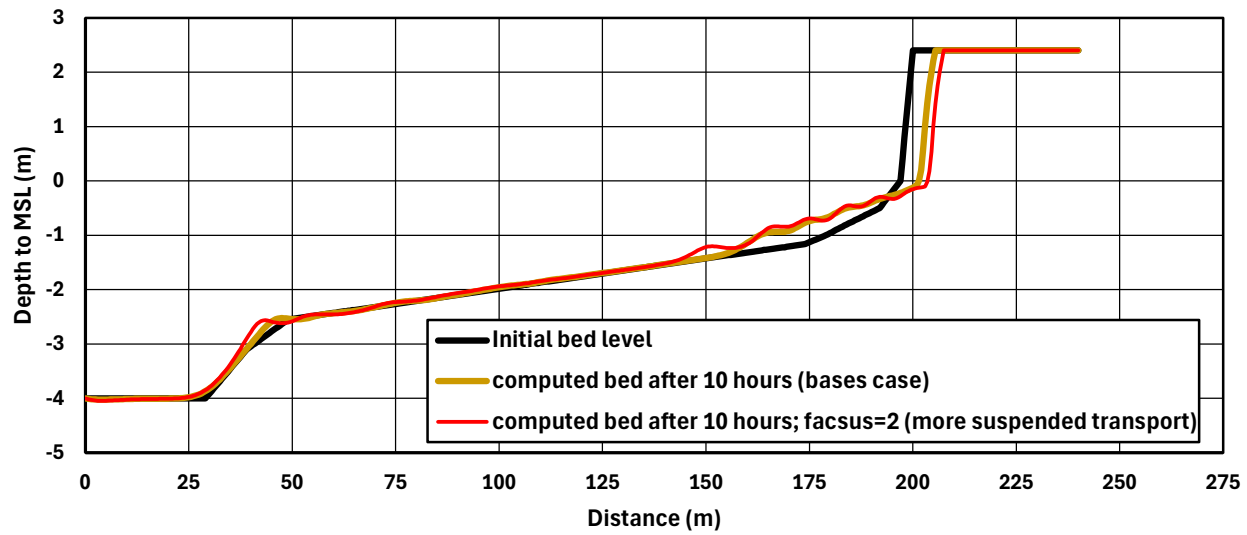


Figure 2.3.8 Effect of suspended transport ($facsus$); $facsus=2$ in stead of 1

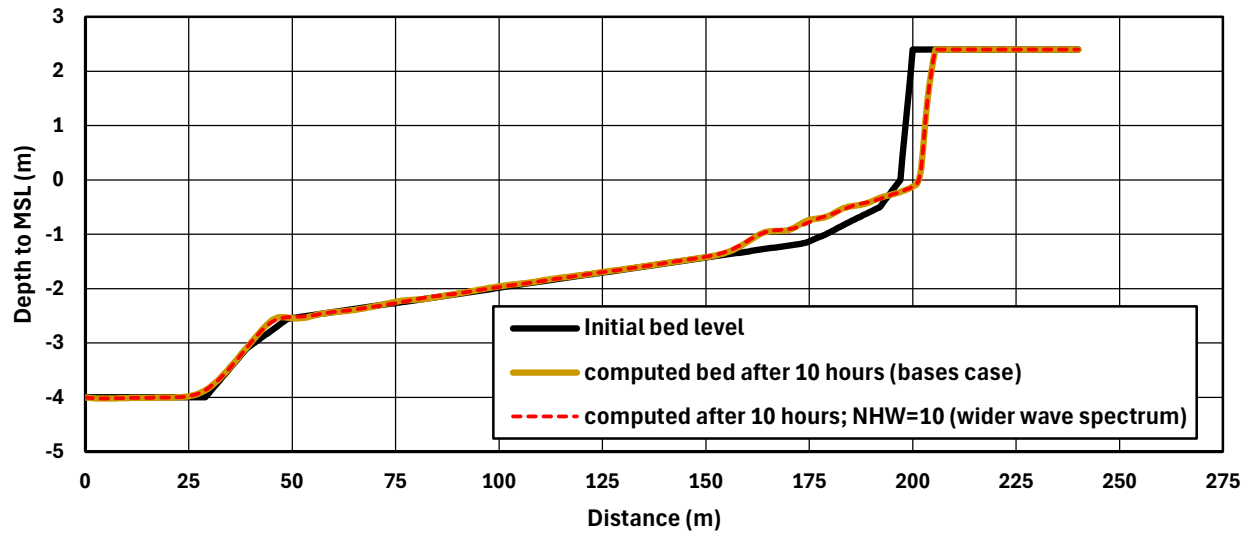


Figure 2.3.9 Effect of wave spectrum (NHW=number of Rayleigh wave classes); NHW=10 in stead of 6

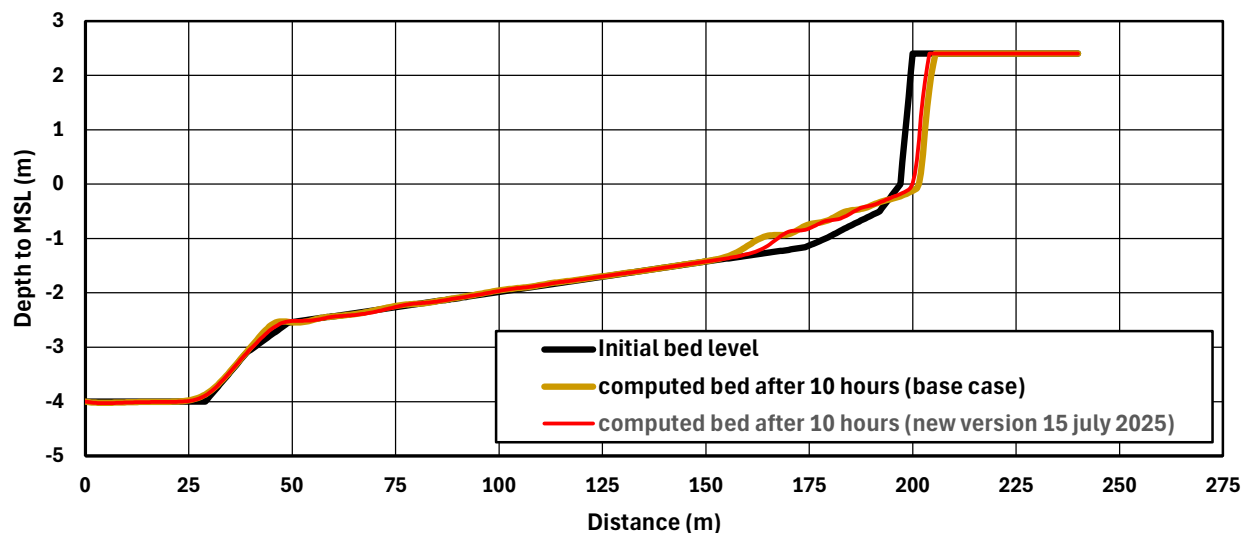


Figure 2.3.10 Effect of new CROSMOR-version; 15 July 2025 in stead of 14 July 2024

Dune erosion at site De Haan, Belgium; Case 2

The input data of Case2 (base case, short term storm run over 5.3 days) are given in **Table 2.3.3**.

The following input parameters have been varied:

- number of grid points (NSTAP must be specified as an INTEGER, not REAL); effect is marginal, see **Figure 2.3.11**;
- time step (factime); factime=0.5 in stead of 0.1; effect is marginal, see **Figure 2.3.11**;
- bed smoothing near water line (SW); sw=0.05 in stead of 0.2 gives almost the same results (not shown);
- wave averaging procedure for longshore current (coef5): coef5, coef6=3 in stead of 1; effect is marginal, see **Figure 2.3.12**;
- onshore sand transport (facsusw): facsusw=0.1 in stead of 0.7; smaller onshore transport leads to slightly more erosion, see **Figure 2.3.13**;



- CROSMOR-version: version 15 July 2025 in stead of 14 July 2024; new version gives slightly less erosion, see **Figure 2.3.14**.

Overall conclusion: schematization and selected input parameters are very adequate; factime=0.1, facsmooth=10 and sw=0.05 are good settings of the numerical parameters.

PARAMETERS	Values
Tide	tide; varying -4 to 2.6 m; longshore tidal current=0
Water depth at deep water (m)	-6.25 m below MSL
RMS-wave height, period and wave incidence angle at deep water	H_{rms} =1.6 to 4.8 m, T_p =4 to 7.3 s, angle= 5°
Storm level above MSL (m)	4.1 m
Beach slope above MSL	1 to 90 (-4 to 0 m); 1 to 70 (0 to +3 m); 1 to 5 (dune front above +6 m)
Dune level above MSL (m)	+16 m
Maximum dune slope SL (sliding when slope is larger)	25°
Boundary depth near beach (last grid point, m)	0.3 m
Grid size (m)	10 m offshore; 2 m nearshore
Hard layer	none
Number of wave classes per wave height	6
Wave asymmetry	Isobe-Horikawa
Wave breaking coefficient (-); roller coefficient (-)	auto; 0.5
Runup coefficient frunup (-)	1 (default)
Coefficients wave averaging for undertow (coef6=1 for lab cases and 3 for field case) and longshore current (coef5=1 for lab cases and 3 for field cases)	coef6=1 coef5=1
Coefficient Longuet-Higgins streaming (-); roller effect (-)	1 (default=1); 0.5 (default=1)
Grain diameter sand d_{50} ; c_u -coefficient	0.23 mm; 2
Coefficients sand transport formulas facbed; facsus; facsusw (-)	0.7; 0.7; 0.7 (default 1)
Coefficient extra sand entrainment in dune zone, sef (-; range 1 to 2)	1.5
Coefficient bed concentration landward of hard layer fsand (-)	1 (default)
Coefficient undertow frip (-)	1 (default)
Bed roughness (m)	Automatic
Bed smooth factor facsmooth (-); sw (-)	10 (default=5); 0.2 (default=0.05)
Time step factor factime (-)	0.1 (default=0.5)
Temperature (° C) and salinity (promille)	15° C and 30 promille
Files	case2.inp

Table 2.3.3 *Input data of CROSMOR-model; Case2*

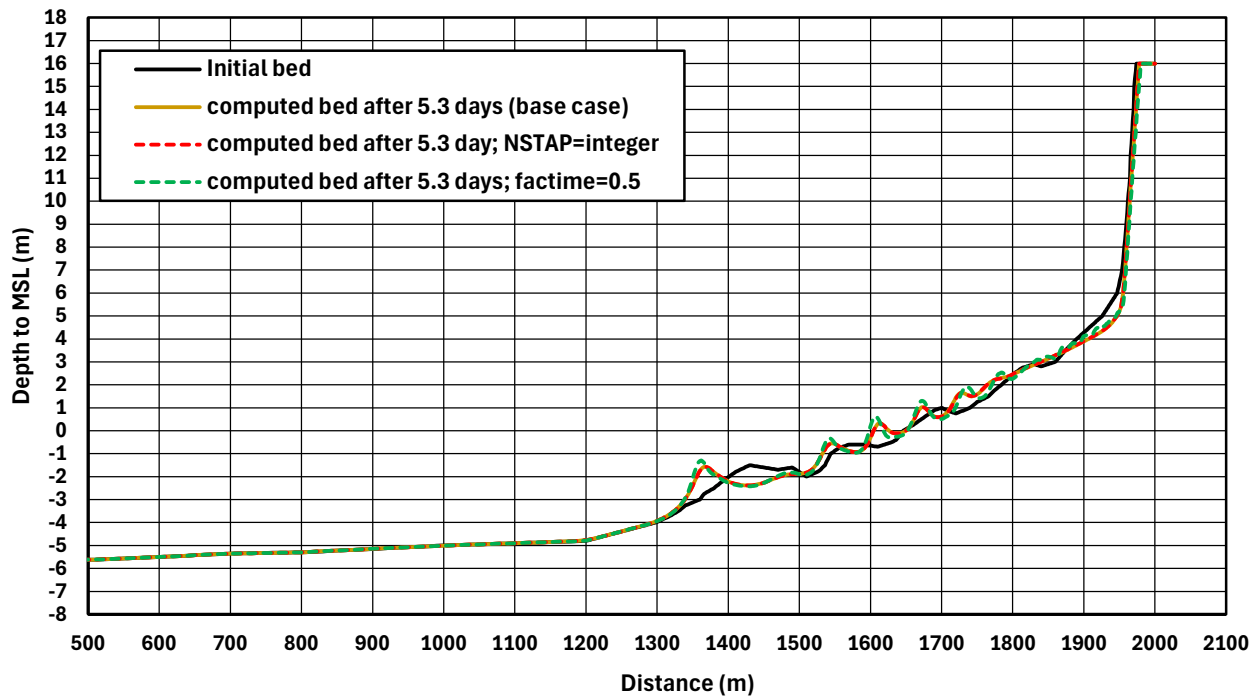


Figure 2.3.11 Effect of time step (*factime*); *factime*=0.5 in stead of 0.1

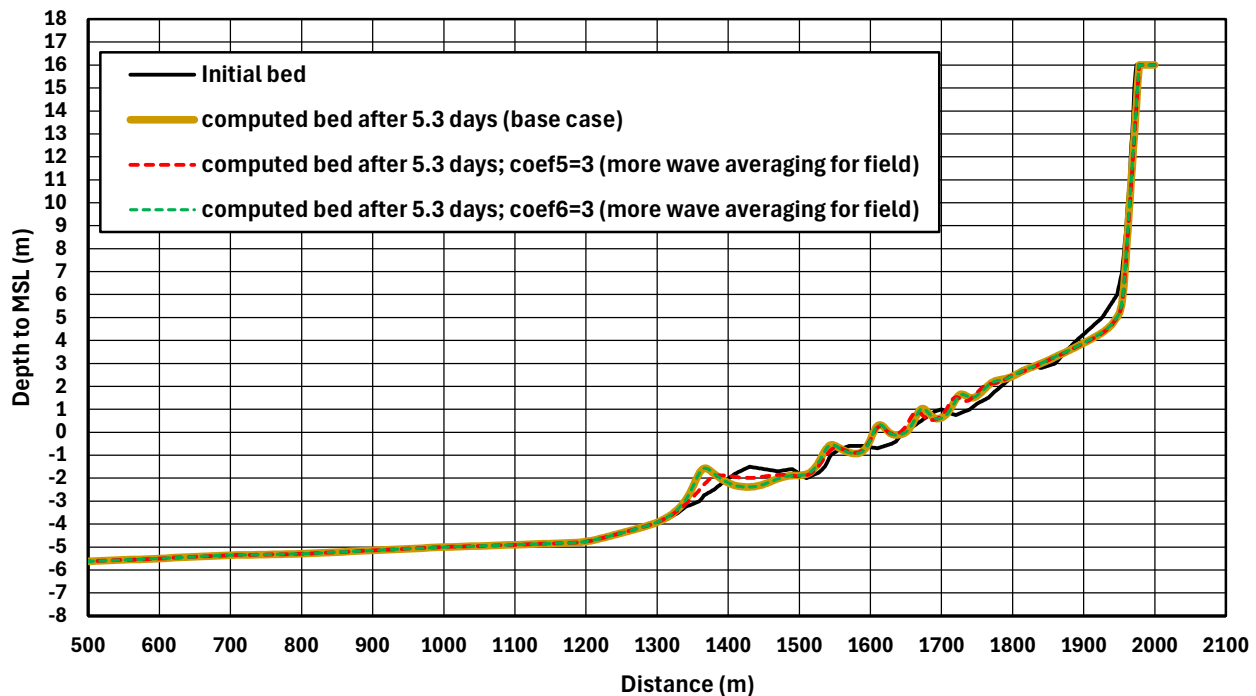


Figure 2.3.12 Effect of wave averaging for longshore current (*coef5*) and undertow (*coef6*); *coef5*=3 in stead of 1; *coef6*=3 in stead of 1

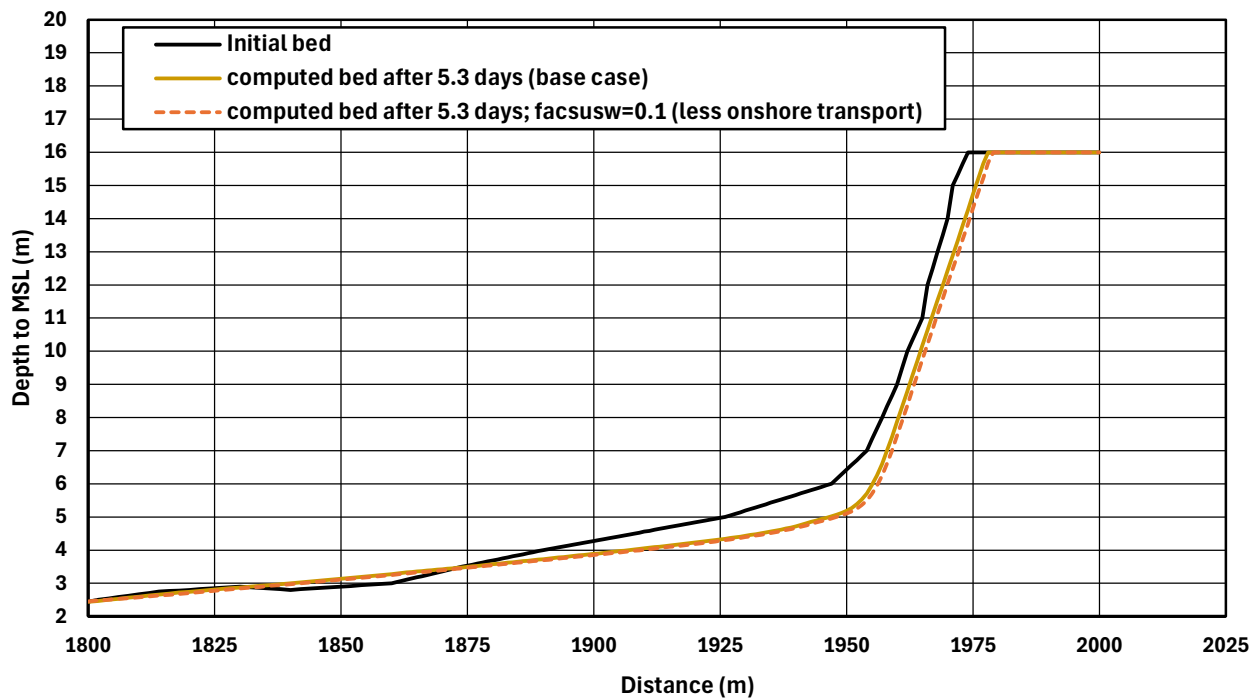
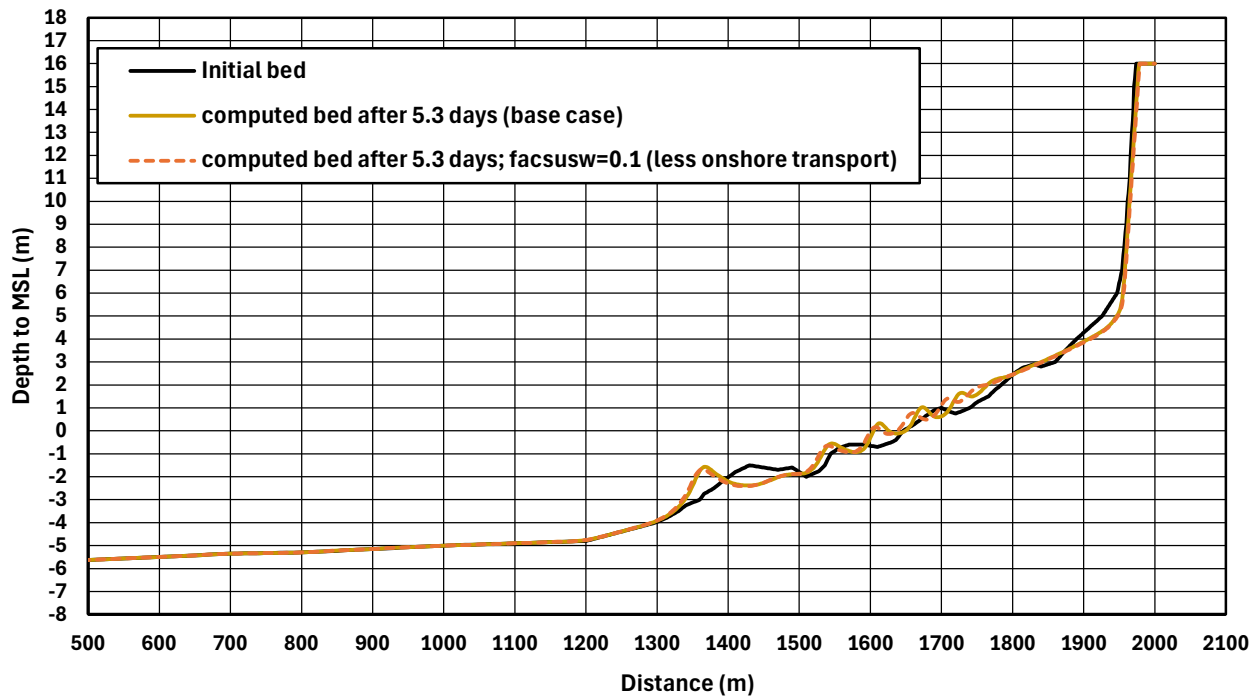


Figure 2.3.13 Effect of onshore sand transport (*facsusw*); *facsusw*=0.1 in stead of 1.

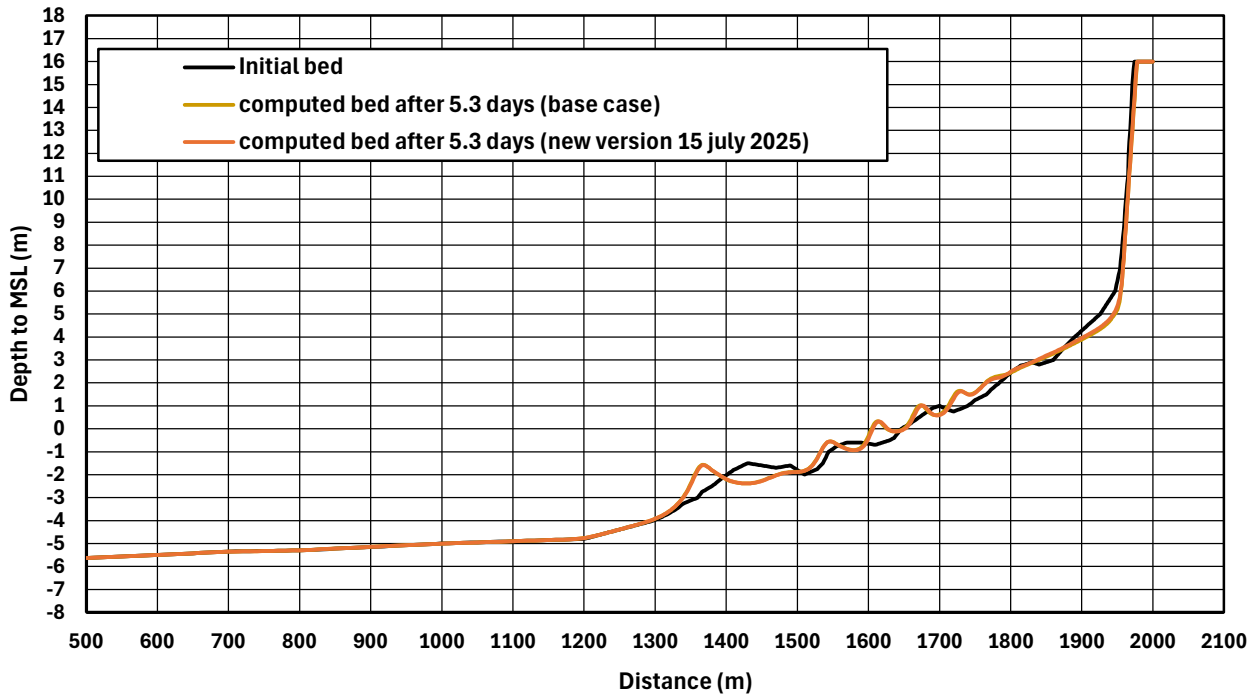


Figure 2.3.14 Effect of new CROSMOR-version; version 15 July 2025 in stead of version 14 July 2024



Beach-dune erosion at site in Egypte; Case 3

The input data of Case3 (base case, long term run over 730 days) are given in **Table 2.3.4**. This case represents a very complex long term case with a rather steep bed section of 1 to 5 between $x=3300$ m and 3345 m in combination with an excessive wave height of $H_{s,o}=10.5$ m in the wave file. It is a very severe test of the CROSMOR-model.

The long term bed level is strongly influenced by the grid size (DX), the time step (factime) and the bed-smoothing parameters (facsmooth, sw). The grid size is particularly important at the steep bed sections, where the grid size should be in the range of 0.5 to 2 m. The time step should be as small as possible (factime in range of 0.5 to 2; default=1), but it should be realized that a smaller time step also means the bed-smoothing procedure is applied more often. The bed smoothing parameter should also be as small possible (factime in range of 5 to 15; default=10). Facsmooth-values smaller than 5 may easily result into bed level instability and model failure; facsmooth-values larger than 15 may result in inaccurate results.

The most appropriate values of DX, factime and facsmooth can only be determined by trial and error making a series of runs with systematic variation of these parameters.

The following input parameters have been varied:

- time step and bed smoothing parameters (factime and facsmooth); factime and facsmooth should be as small as possible; the base case run (red line) with the old version 14 July 2024 is not sufficiently accurate because the bed smoothing effect is too large (see point $x=3000$, where the sediment transport is low and where accretion should be low, see **Figure 2.3.15**); the accuracy increases by reducing the facsmooth-coefficient to 10 in stead of 30; the accuracy can be further increased by using factime=2 (larger time step and smoothing procedure is applied less, factor 2); the most accurate run is for factime=2 and facsmooth=10; see dashed red line in **Figure 2.3.15** and also **Figure 2.3.16**; the combinations factime=2 and facsmooth-values in the range of 10 to 30 give sufficiently accurate results (facsmooth=10 is best);
- effect of bed smoothing near water line (sw); $sw=0.001$ and 0.01 in stead of $sw=0.05$ gives somewhat more erosion, because less smoothing is applied; $sw=0.01$ is sufficiently accurate, see **Figure 2.3.17**;
- grid size; the accuracy can be further improved by reducing the grid size from 1 m to 0.5 m at the steep section $x=3300$ to 3345 m; see **Figure 2.3.18**; this run (blue line) gives more accurate results; the run with factime=2 and facsmooth=10 (dashed blue line) gives slightly more accurate results because the bed smoothing procedure is applied less (factor of 2) which can be seen at point $x=3000$ m (dashed blue line is most close to the initial bed);
- onshore sand transport (facsusw): $facsusw=0.1$ in stead of 0.3; smaller onshore transport leads to slightly more erosion, see **Figure 2.3.19**;
- CROSMOR-version: version 15 July 2025 in stead of version 14 July 2024; new version gives slightly less erosion, see **Figure 2.3.20**; it is noted that the facsmooth can be as low as 5 in the new CROSMOR-version; **Figure 2.3.21** shows that the runs with factime=1 are less accurate, although the run with factime=1 and facsmooth=5 is still acceptable; **Figure 2.3.22** shows the effect of $frunup=0.5, 1$ and 2 ; more erosion occurs for $frunup=2$; erosion is similar for $frunup=1$ and 2 .

Overall conclusion: schematization and selected input parameters of the base case file are not optimal; the grid size should be 0.5 m (in stead of 1 m) in the steep bed section between $x=3300$ and 3345 m; the factime parameter should be set to 2 for most accurate results; the facsmooth-coefficient should be set to 5 or 10; the sw-coefficient should be set to 0.01; it is better to do long term runs with maximum wave height equal to the wave height with return period of 1 year; the effect of extreme storms (return periods of 10 to 100 year) can be better studied in short-duration storm runs.



PARAMETERS	Values
Tide	tide -0.15 and +0.15 m; longshore tidal current=0.1 m/s
Water depth at deep water (m)	-50 m below MSL
RMS-wave height, period and wave incidence angle at deep water	H_{rms} =0.35 to 7.45 m, T_p =7 to 13 s, angle= 5°
Storm level above MSL (m)	0 to 2 m
Beach slope above MSL	approx. 1 to 5 (-10 to -1 m); approx. 1 to 20 (beach front -1 to +5 m)
Dune level above MSL (m)	+5 m
Maximum dune slope SL (sliding when slope is larger)	50°
Boundary depth near beach (last grid point, m)	0.3 m
Grid size (m)	20 m offshore; 1 m nearshore
Hard layer	none
Number of wave classes per wave height	1
Wave asymmetry	Isobe-Horikawa
Wave breaking coefficient (-); roller coefficient (-)	auto; 0.5
Runup coefficient frunup (-)	0.5 (default =1)
Coefficients wave averaging for undertow (coef6=1 for lab cases and 3 for field case) and longshore current (coef5=1 for lab cases and 3 for field cases)	coef6=3 coef5=3
Coefficient Longuet-Higgins streaming (-); roller effect (-)	0.5 (default=1); 0.5 (default=1)
Grain diameter sand d_{50} ; c_u -coefficient	0.45 mm; 2
Coefficients sand transport formulas facbed; facsus; facsusw (-)	0.7; 0.7; 0.3 (default 1)
Coefficient extra sand entrainment in dune zone, sef (-; range 1 to 2)	1 (default=1)
Coefficient bed concentration landward of hard layer fsand (-)	1 (default)
Coefficient undertow frip (-)	1 (default)
Bed roughness (m)	Automatic
Bed smooth factor facsmooth (-); sw	30 (default=10); 0.05 (default=0.05)
Time step factor factime (-)	1 (default=2)
Temperature (°C) and salinity (promille)	10° C and 30 promille
Files	case3-k.inp

Table 2.3.4 *Input data of CROSMOR-model; Case3*

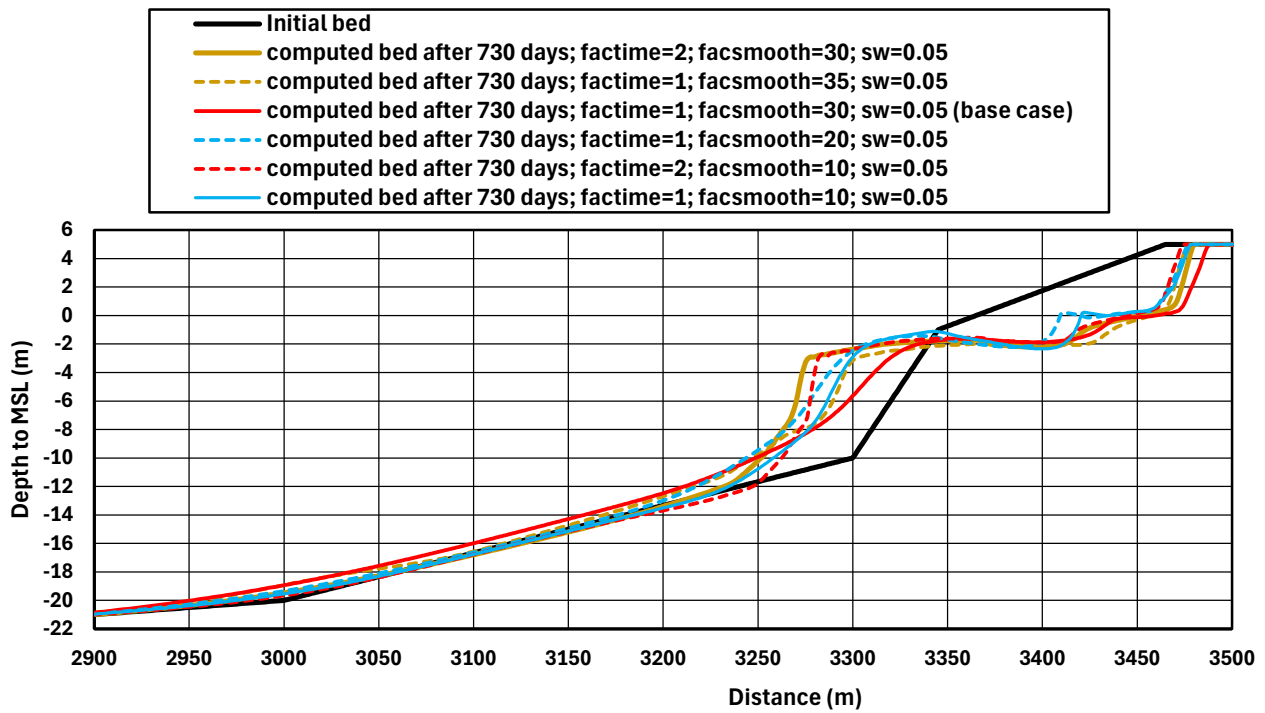


Figure 2.3.15 Effect of factime and facsmooth; factime=1 and 2; facsmooth=10, 20, 30, 35; old version

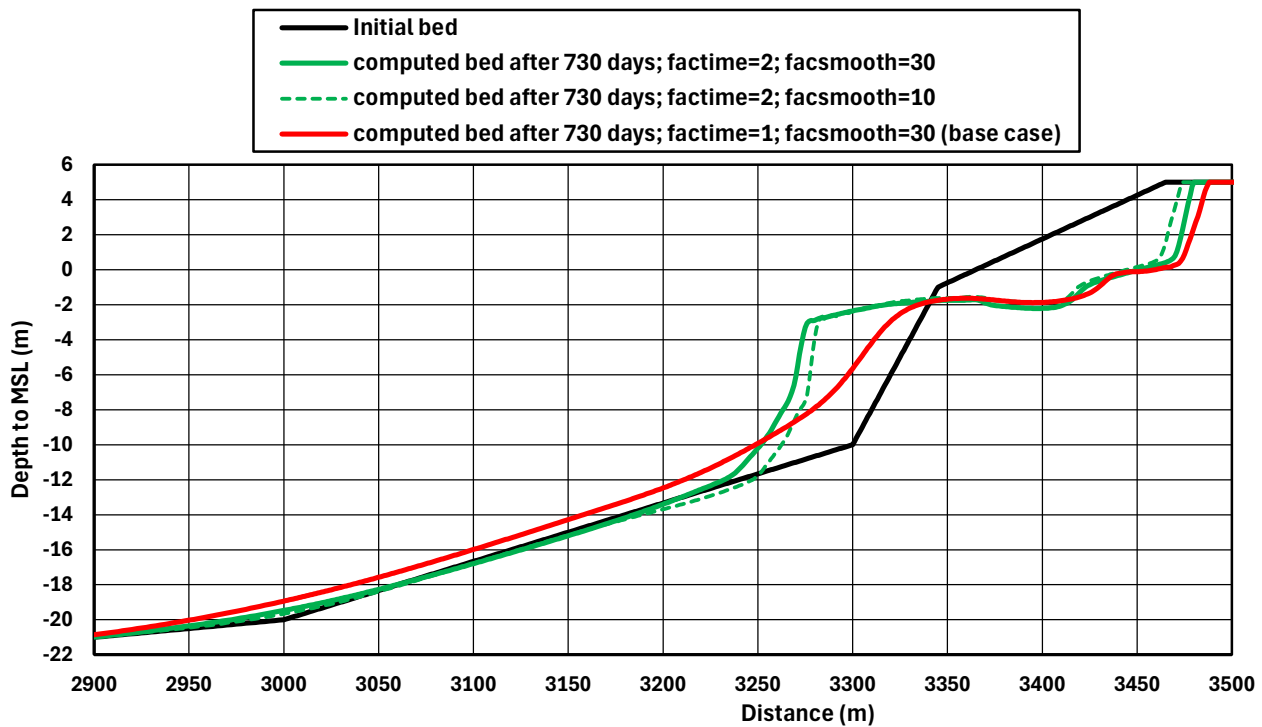


Figure 2.3.16 Effect of bed smoothing facsmooth; facsmooth=10, 30; old version 14 July 2024

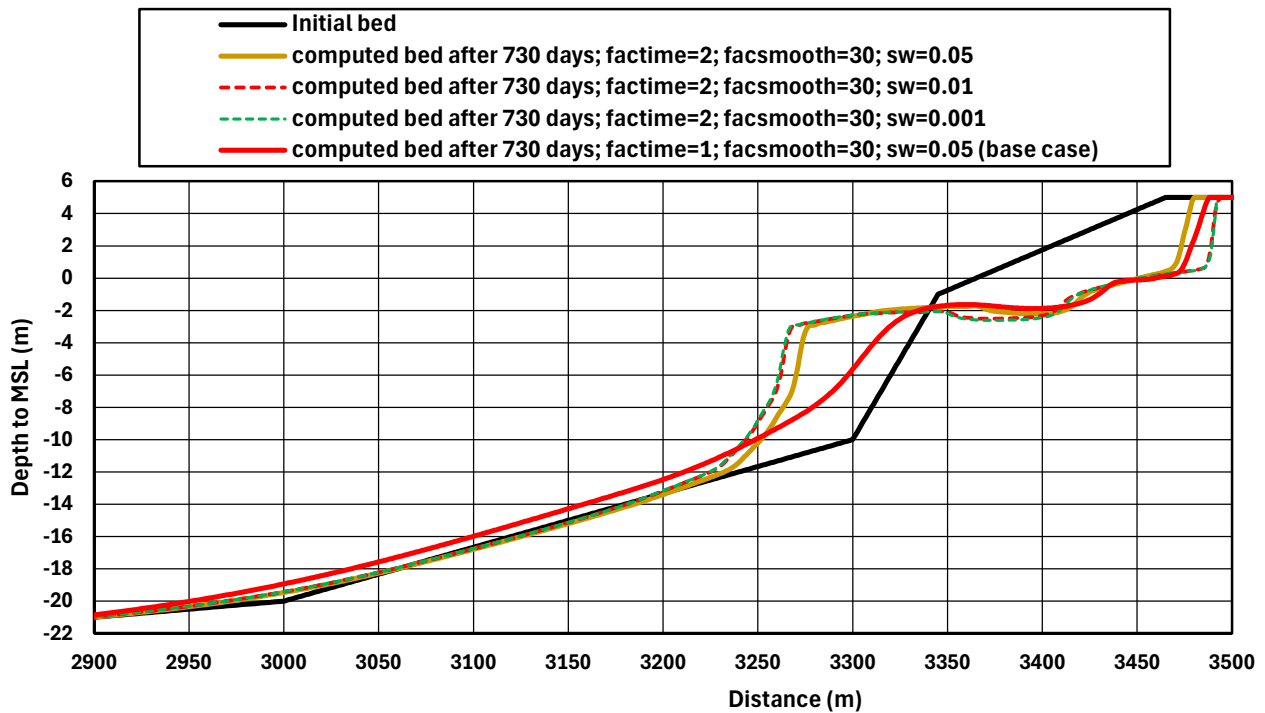


Figure 2.3.17 Effect of bed smoothing near water line (sw); $sw=0.001, 0.01$ in stead of $sw=0.05$; old version

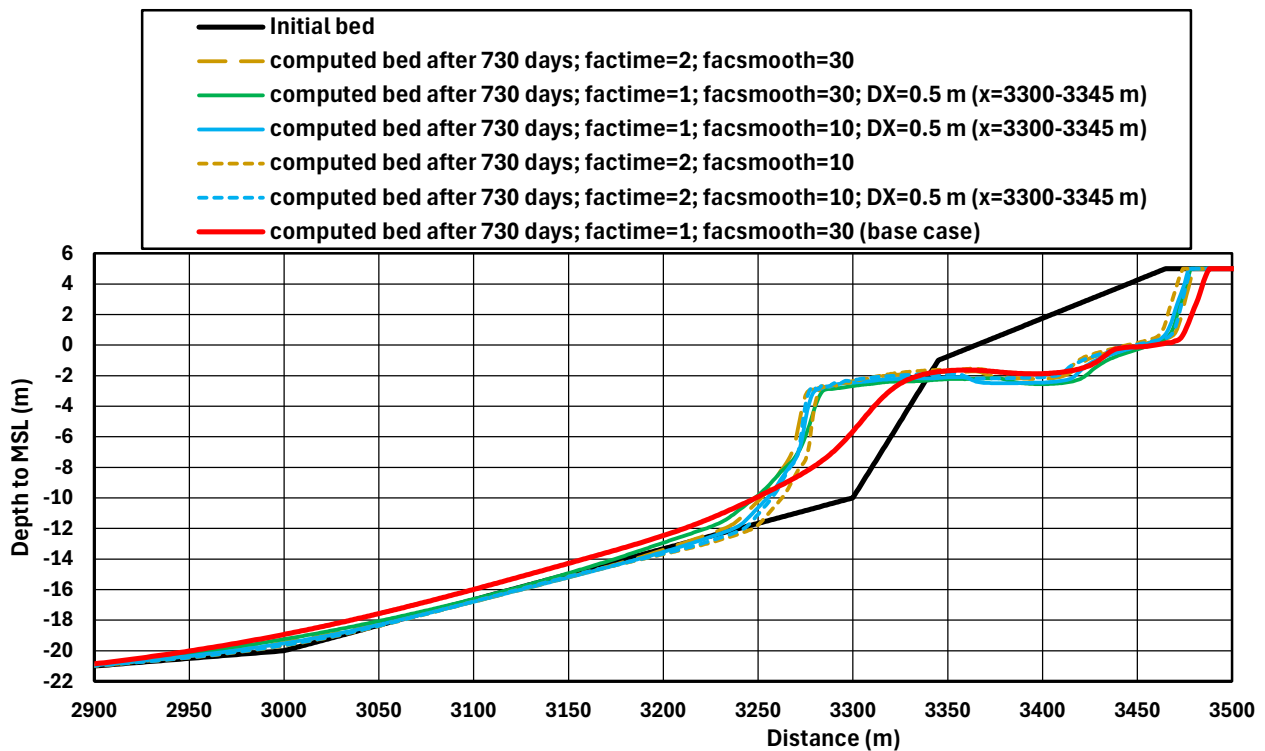


Figure 2.3.18 Effect of grid size; grid size was reduced from 1 m to 0.5 m at the steep section $x=3300$ to 3345 m; old version 14 July 2024

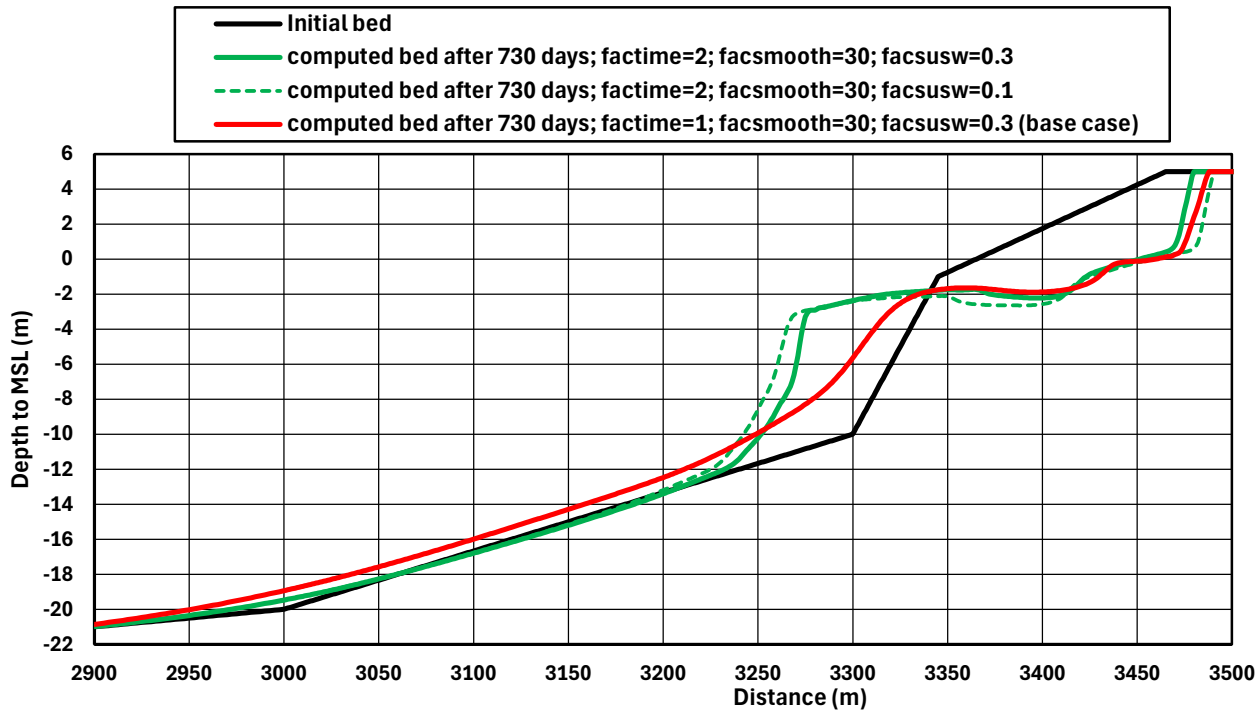


Figure 2.3.19 Effect of onshore sand transport (*facsusw*); *facsusw*=0.3 in stead of 1; old version 14 July 2024

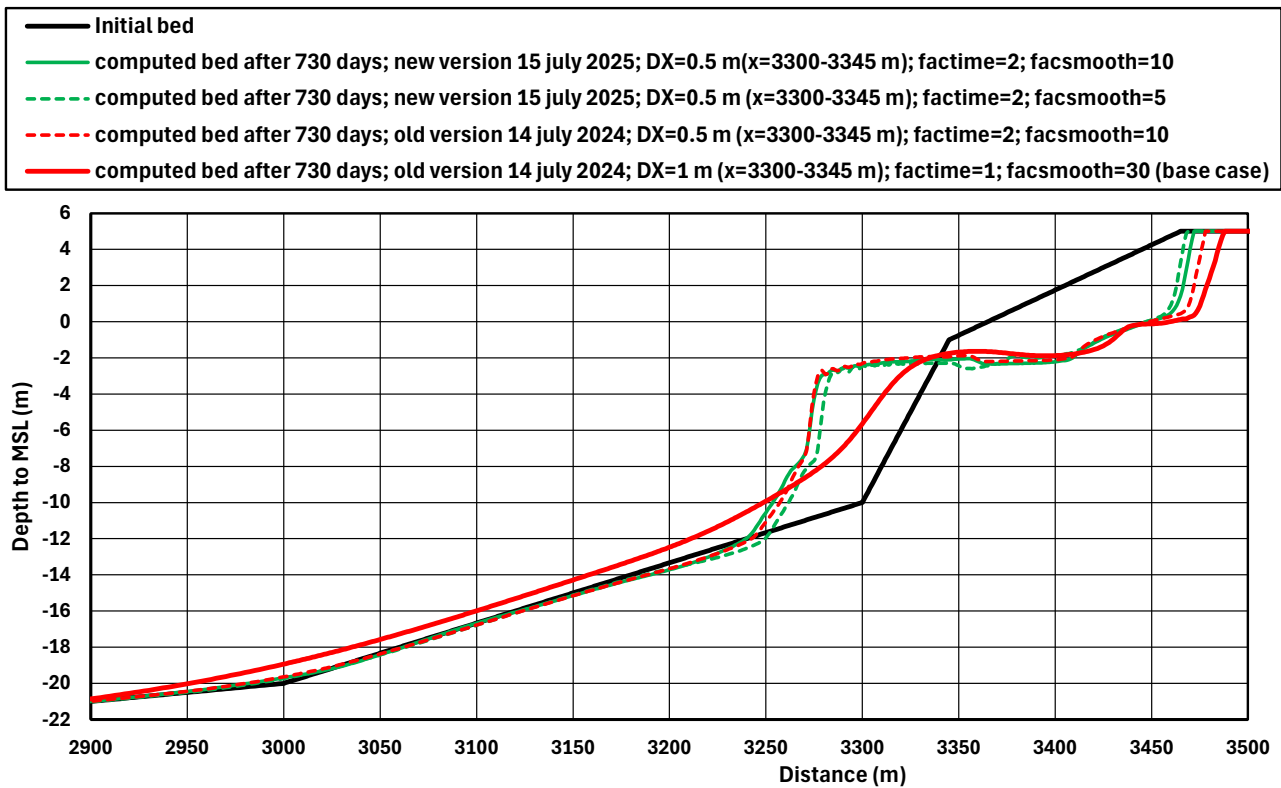


Figure 2.3.20 Effect of new CROSMOR-version; version 15 July 2025 in stead of version 14 July 2024

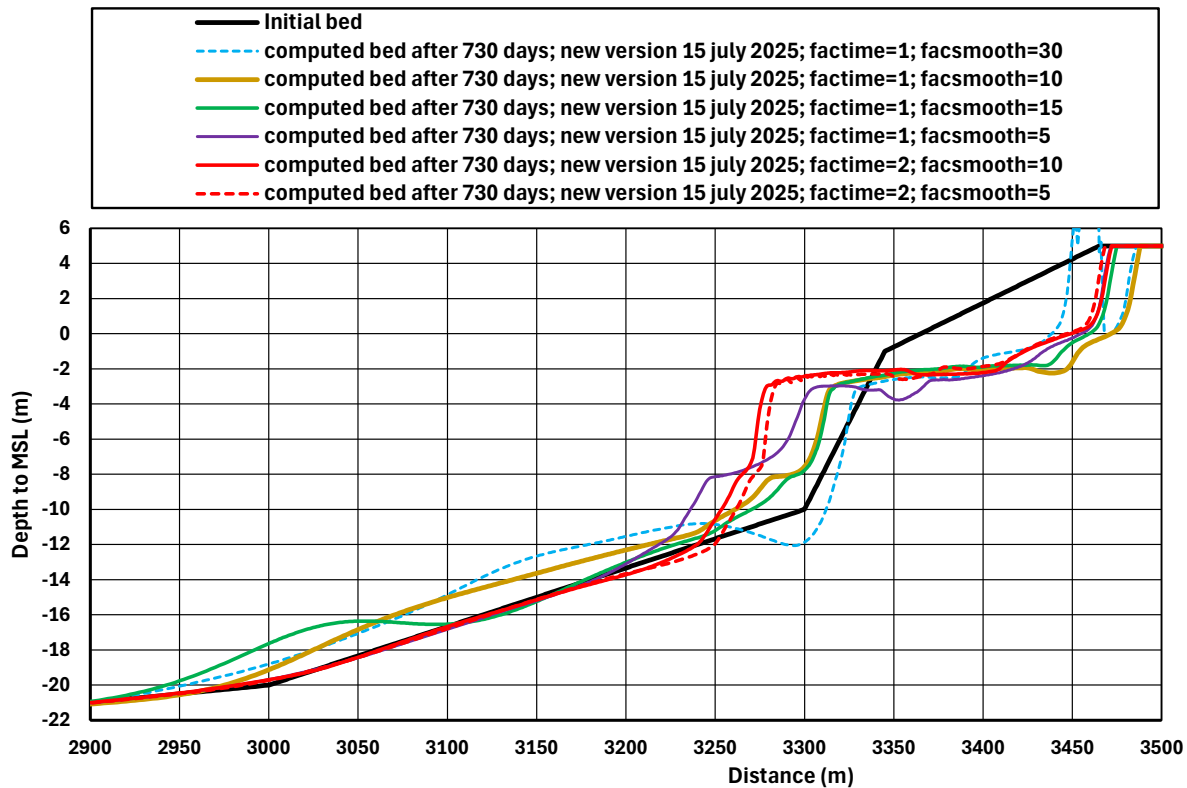


Figure 2.3.21 Effect of new CROSMOR-version; version 15 July 2025 in stead of version 14 July 2024; factime=1 and 2

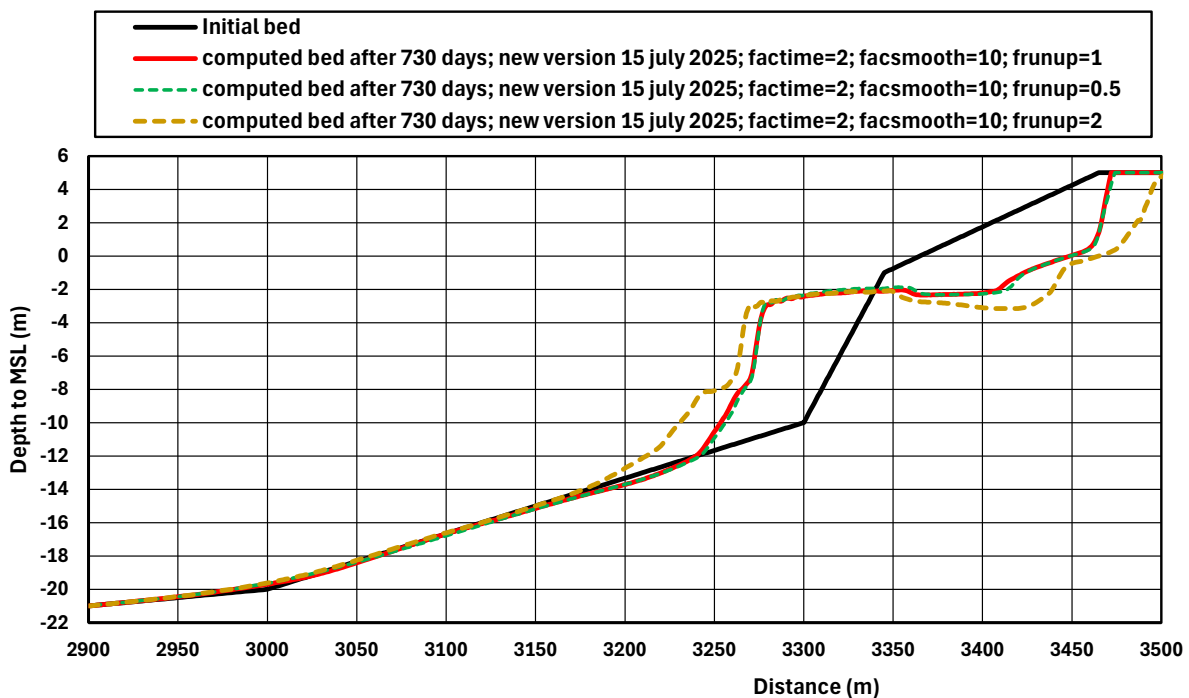


Figure 2.3.22 Effect of new CROSMOR-version; version 15 July 2025 in stead of version 14 July 2024; facrunup=0.5, 1, 2



The new CROSMOR version 15 July 2025 has also been used to study the effect of an extreme storm on the bed profile.

The storm characteristics are:

- $H_{s,o}=10.5$ m ($H_{rms,o}=7.45$ m), $T_p=13$ s, Offshore wave incidence angle $\theta_o=5$ degrees to shore normal;
- storm duration 1 day (24 hours).

The basic data are given in **Table 2.3.4**.

The following input parameters have been varied:

- time step and bed smoothing parameters (factime and facsmooth); **Figure 2.3.23** shows that factime=0.1 to 0.5 with facsmooth=5 and 10 give almost the same results; factime=1 gives inaccurate results;
- runup parameter (frunup); **Figure 2.3.24** shows that frunup=2 gives more erosion near the dune crest; frunup=0.5 gives almost the same results as frunup=1; frunup=0.1 and 0 give much less erosion;
- sediment transport (facbed, facsus and facsusw); **Figure 2.3.25** shows that the erosion at the beach and dune face increases slightly (10% to 15%) if the sediment transport (facbed, facsus) increases and the onshore sediment transport (facsusw) decreases;
- CROSMOR-version: version 15 July 2025 in stead of version 14 July 2024; new version gives slightly less erosion, see **Figure 2.3.26**.

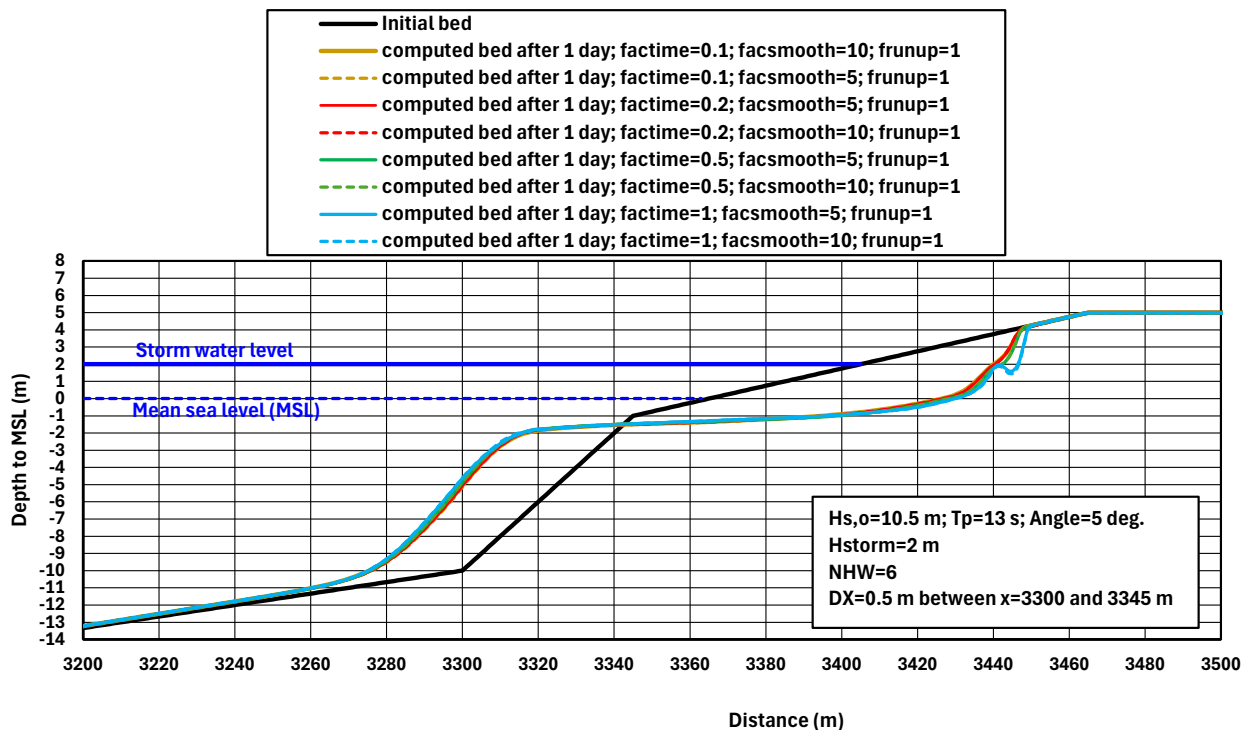


Figure 2.3.23 Effect of factime and facsmooth; new version 15 July 2025

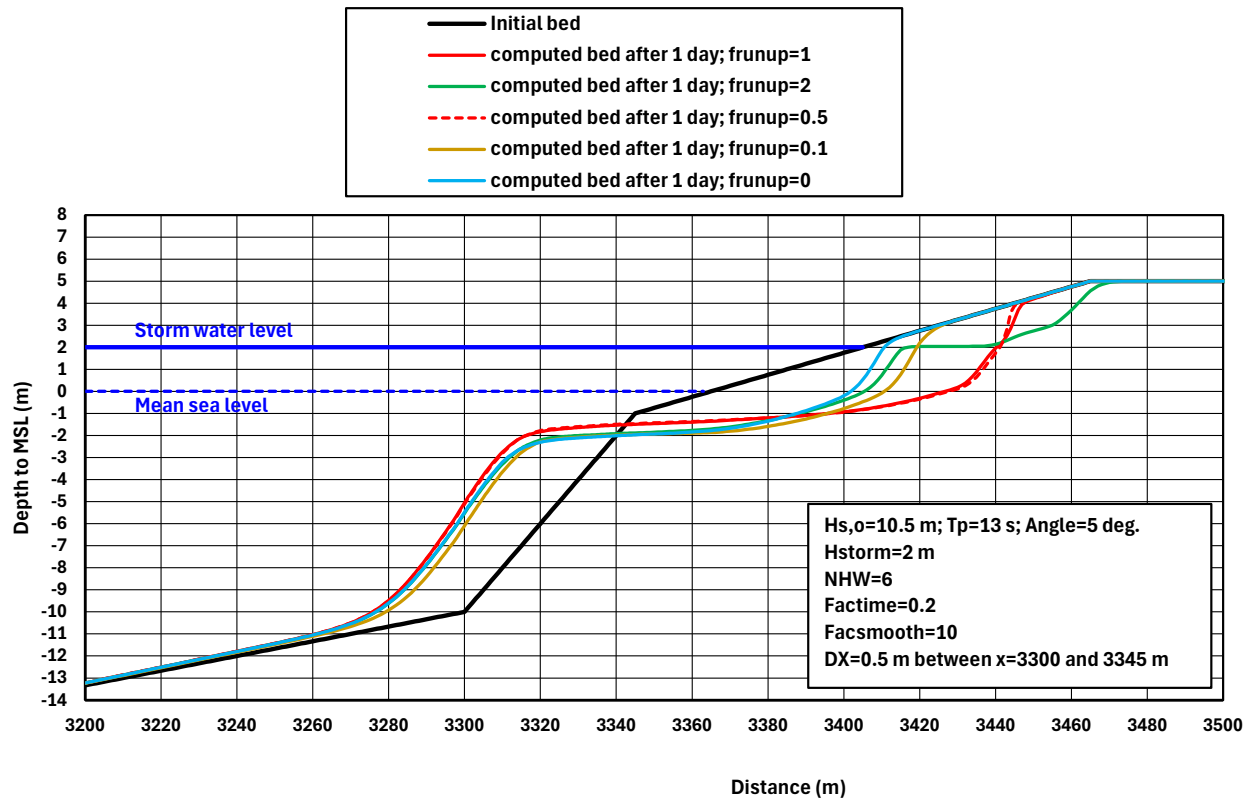


Figure 2.3.24 Effect of *frunup*; new version 15 July 2025

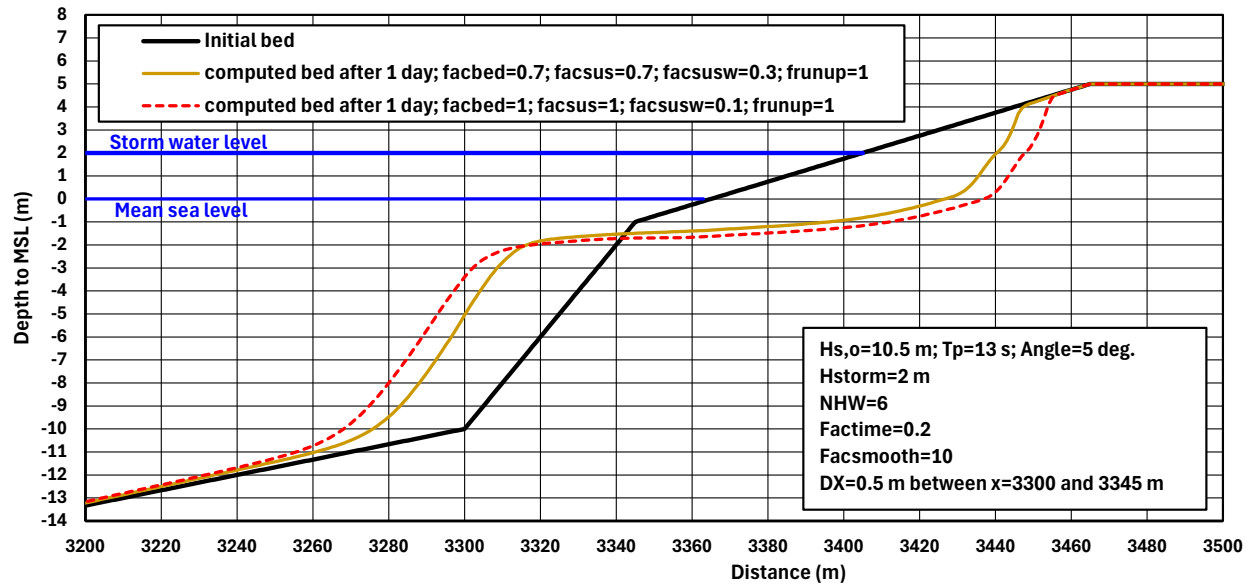


Figure 2.3.25 Effect of sediment transport (*faced*, *facsus* and *facsusw*); new version 15 July 2025

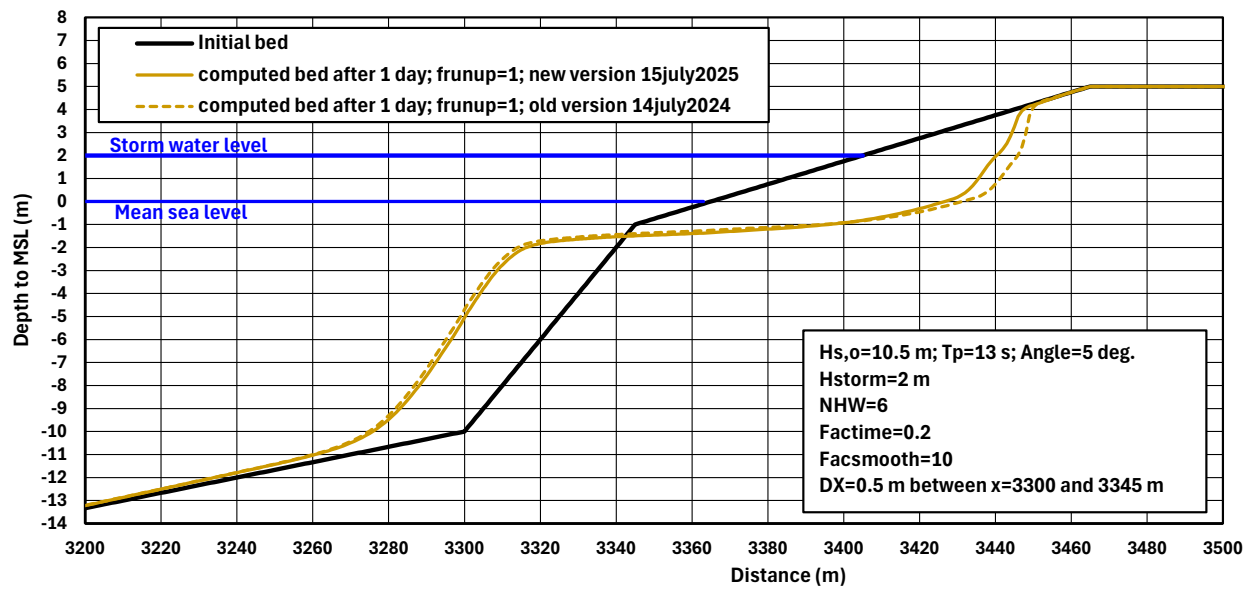


Figure 2.3.26 Effect of CROSMOR-version



Beach-dune erosion at site in Benin/Togo project site; Case 4

The input data of Case4 (base case, long term run over 60 days) are given in **Table 2.3.5**.

The following input parameters have been varied:

- time step and bed smoothing parameters (factime and facsmooth, sw); the results are inaccurate for sw=0.2 (too much smoothing near the water line), see **Figure 2.3.27**; the run with sw=0.01 gives substantially more erosion; the results of the run with smaller values of factime and facsmooth give somewhat more accurate results;
- effect of SEF-factor; a smaller SEF-factor leads to less dune erosion; SEF=1.1 is a realistic value for a slope of 1 to 8.5, see **Figure 2.3.28**;
- onshore sand transport (facsusw): a smaller value of facsusw leads to more dune erosion because the onshore-directed suspended load transport (accretion) is reduced, see **Figure 2.3.29**;
- CROSMOR-version: version 15 July 2025 in stead of 14 July 2024; new version gives slightly less erosion, see **Figure 2.3.30**;

Overall conclusion: schematization and selected input parameters of the base case file are not optimal; the bed smoothing parameter should set to sw=0.01 in stead of sw=0.2 (base case).

PARAMETERS	Values
Tide	tide -0.9 and +0.9 m; longshore tidal current=0 m/s
Water depth at deep water (m)	-37 m below MSL
RMS-wave height, period and wave incidence angle at deep water	$H_{rms,o}=1.3m$ ($H_{s,o}=1.85 m$), $T_p=12.3 s$, angle= 5°
Storm level above MSL (m)	0 m
Beach slope above MSL	approx. 1 to 20 (-3 to 0 m); approx. 1 to 8.5 (beach front 0 to +4 m)
Dune level above MSL (m)	+4 m
Maximum dune slope SL (sliding when slope is larger)	50°
Boundary depth near beach (last grid point, m)	0.3 m
Grid size (m)	10 m offshore; 1 m nearshore
Hard layer	none
Number of wave classes per wave height	1
Wave asymmetry	Isobe-Horikawa
Wave breaking coefficient (-); roller coefficient (-)	auto; 0.5
Runup coefficient frunup (-)	0.5 (default =1)
Coefficients wave averaging for undertow (coef6=1 for lab cases and 3 for field case) and longshore current (coef5=1 for lab cases and 3 for field cases)	coef6=3 coef5=1
Coefficient Longuet-Higgins streaming (-); roller effect (-)	1 (default=1)
Grain diameter sand d_{50} ; c_u -coefficient	0.5 mm; 2
Coefficients sand transport formulas facbed; facsus; facsusw (-)	0.7; 0.7; 0.7 (default 1)
Coefficient extra sand entrainment in dune zone, sef (-; range 1 to 2)	1.5 (default=1)
Coefficient bed concentration landward of hard layer fsand (-)	1 (default)
Coefficient undertow frip (-)	1 (default)
Bed roughness (m)	Automatic
Bed smooth factor facsmooth (-), sw (-)	10 (default=10); 0.2 (default=0.05)
Time step factor factime (-)	0.1 (default=1)
Temperature ($^\circ C$) and salinity (promille)	$10^\circ C$ and 30 promille



Files

case4.inp

Table 2.3.5 Input data of CROSMOR-model; Case4

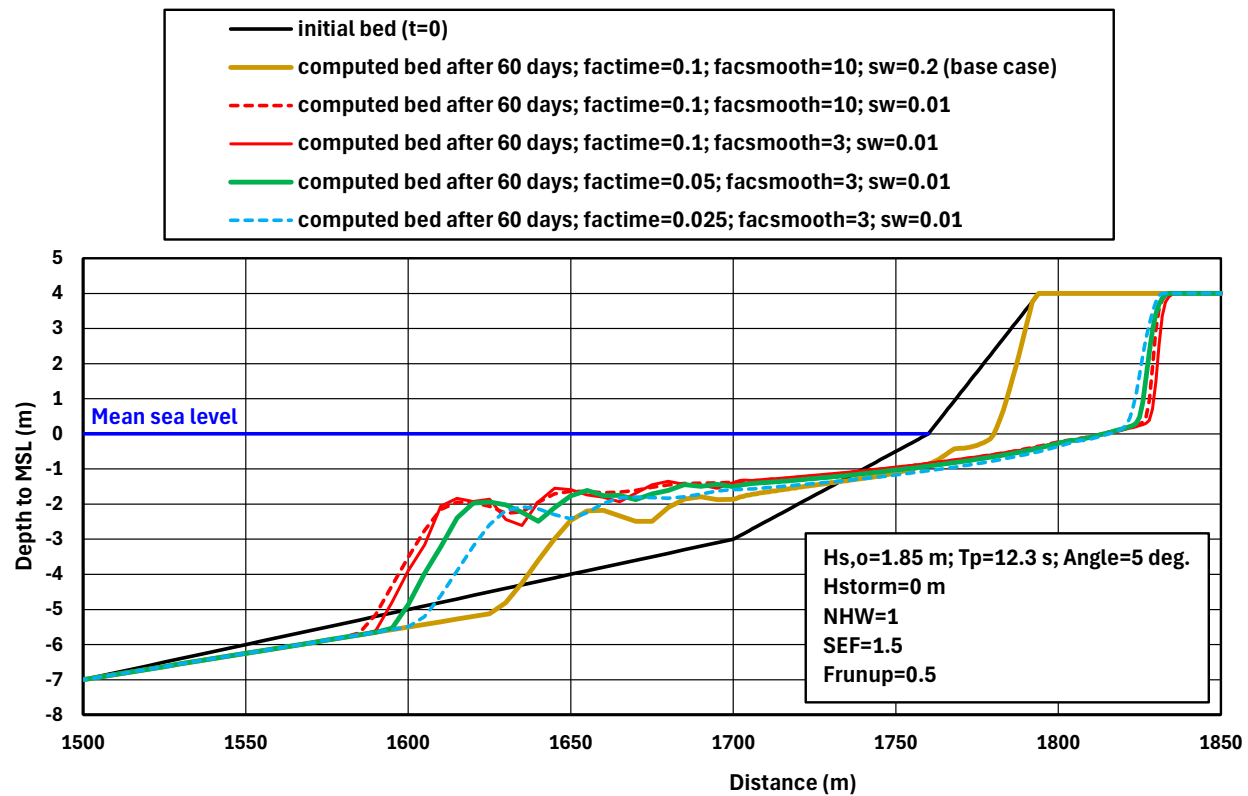


Figure 2.3.27 Effect of factime and facsmooth

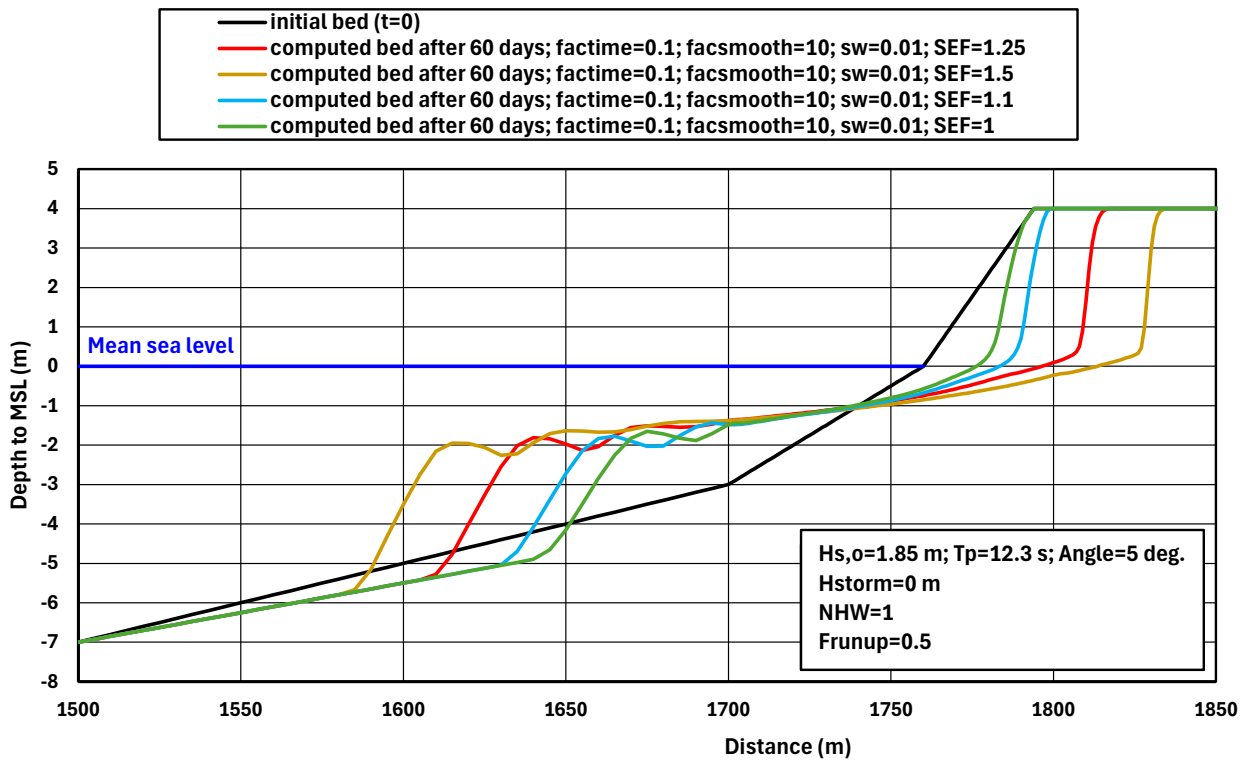


Figure 2.3.28 Effect of SEF-factor

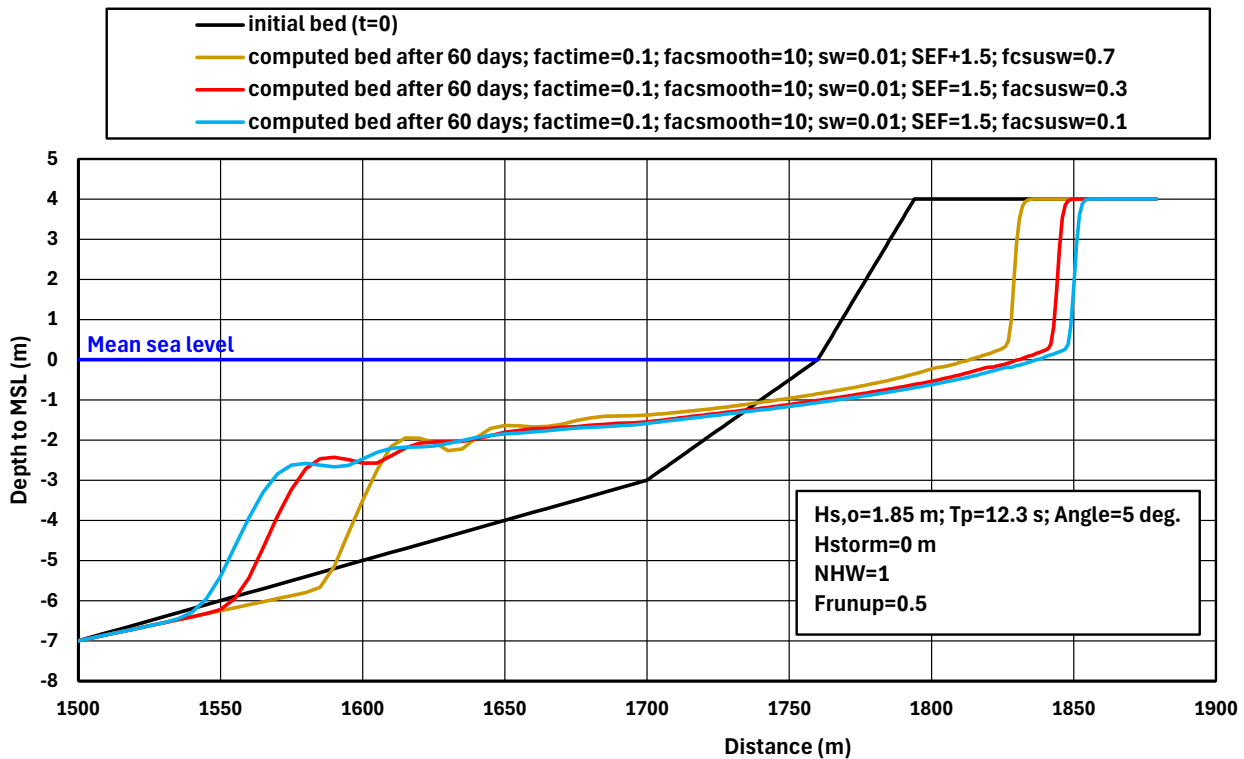


Figure 2.3.29 Effect of onshore suspended load transport (facsusw)

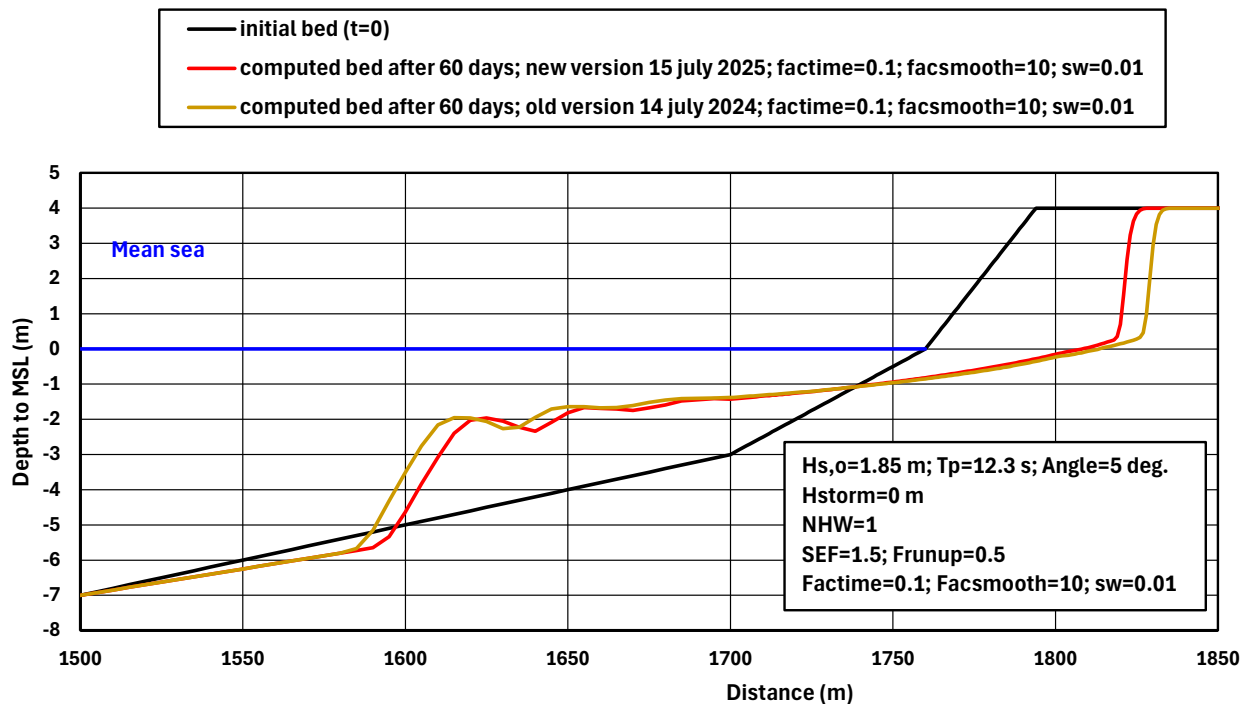


Figure 2.3.30 Effect of CROSMOR -version

2.4 Example wave heights Payra channel Bangladesh

The CROSMOR-model has been used to compute the significant wave heights along a line normal to the shore (between KP60 and KP6), see **Figures 2.3.1, 2.3.2**. A large shallow area with many shoals and flats is present on the westside of the channel between KP0 and KP20.

The propagation and transformation of individual waves (wave by wave approach) including wave shoaling, wave refraction, wave damping by bottom friction and wave breaking along the cross-shore profile is described by a probabilistic model solving the wave energy equation for each individual wave. The individual waves shoal until an empirical criterion for breaking is satisfied. The maximum wave height is given by $H_{max} = \gamma_{br} h$ with γ_{br} = breaking coefficient and h = local water depth. The default wave breaking coefficient is represented as a function of local wave steepness and bottom slope. The default breaking coefficient varies between 0.4 for a horizontal bottom and 0.8 for a very steep sloping bottom.

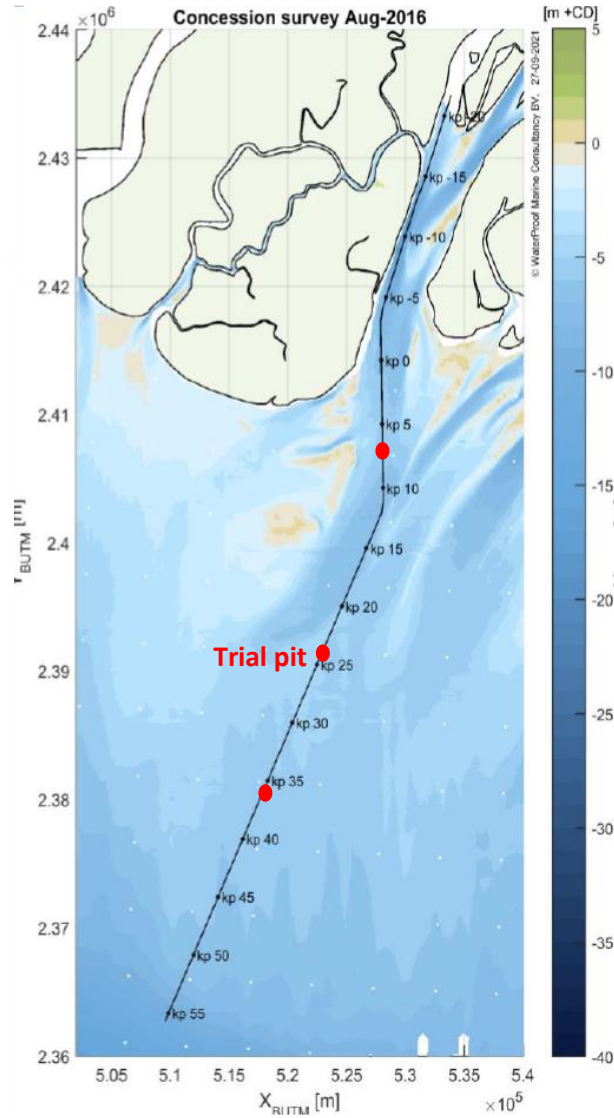


Figure 2.3.1. Plan view of channel alignment; Trial Pits at KP6-7, KP24-25 and KP35-36 km

Model input: $H_{rms,o}$ =0.71, 1.42, 2.13 and 3.55 m; 10 wave classes for each condition (Rayleigh-distribution)
Peak wave periods: T_p =8 and 15 s;
Wave angle at offshore depth: θ =10° to shore normal;
Bottom friction mud bed: k_s =1 and 10 mm.

Table 2.3.1 shows the computed significant wave heights (H_s) at various locations from offshore to nearshore.

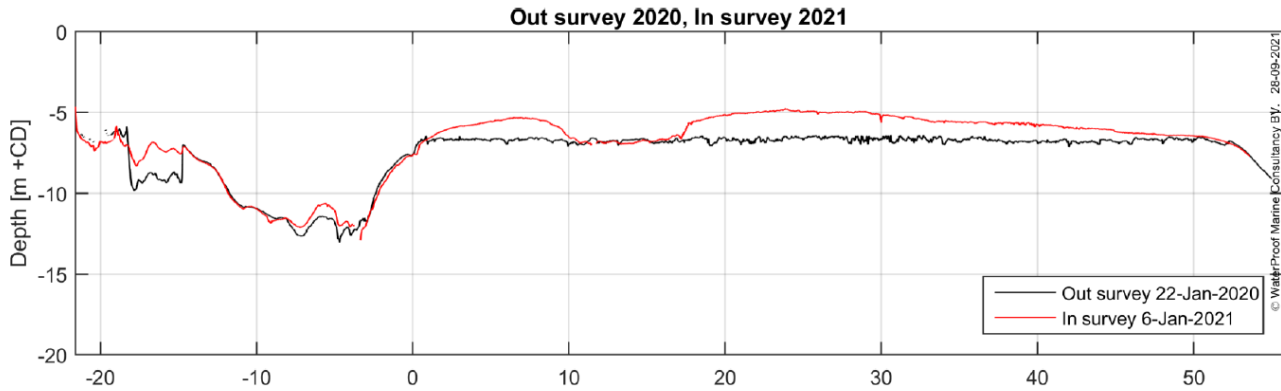


Figure 2.3.2. Bed levels along channel axis (2020-2021)

The variation ranges express the effect of the wave period, bottom roughness and tidal range (LW and HW). The effect of the wave period is about 5% to 10%; a higher wave period yields a slightly higher wave height. The effect of bed roughness is about 10% to 30%; a higher bed roughness yields a lower wave height (more wave damping).

The lowest wave heights values are based on $T_p=8$ s, $k_{s,bed}=10$ mm and water level at LW.

The highest wave heights values are based on $T_p=15$ s, $k_{s,bed}=1$ mm and water level at HW.

The maximum wave heights at KP35 and KP6 during a severe storm with offshore wave heights of 5 m in deep water are about 2.5 to 1.5 m, and in good agreement with the measured wave data.

KP (km)	Depth to MSL (m)	Significant wave height H_s (m) and effect of wave period (8 and 15 s) and bed roughness (1 and 10 mm); Water level at MSL				Significant wave height H_s (m) and effect of LW (-1 m) and HW (+1 m) $T_p=10$ s; $k_s=5$ mm		
		1	2	3	5	2	3	5
60	-10							
55	-9.5	0.93 ±0.03	1.77 ±0.07	2.6 ±0.08	3.7 ±0.10	1.75 ±0.05	2.7 ±0.10	3.6 ±0.25
50	-9.0	0.85 ±0.05	1.57 ±0.10	2.25 ±0.15	3.25 ±0.25	1.55 ±0.07	2.4 ±0.12	3.15 ±0.3
45	-8.5	0.8 ±0.08	1.42 ±0.17	2.0 ±0.20	2.8 ±0.30	1.40 ±0.10	2.2 ±0.13	2.75 ±0.3
35	-7.8	0.7 ±0.1	1.15 ±0.20	1.55 ±0.25	2.1 ±0.35	1.10 ±0.12	1.8 ±0.15	2.15 ±0.3
25	-7.5	0.55 ±0.12	0.87 ±0.22	1.15 ±0.30	1.6 ±0.35	0.8 ±0.13	1.4 ±0.20	1.7 ±0.3
10	-8.5	0.45 ±0.12	0.65 ±0.23	0.85 ±0.30	1.2 ±0.35	0.6 ±0.13	1.05 ±0.20	1.3 ±0.3
6	-8.6	0.42 ±0.12	0.6 ±0.23	0.8 ±0.30	1.1 ±0.35	0.55 ±0.13	1.0 ±0.20	1.2 ±0.3

Table 2.3.1 Computed wave height along line normal to shore; CROSMOR-model

Figure 2.3.3 shows the computed wave heights along a line normal to the shore for storm wave conditions with $H_{s,o}=5$ m and $T_p=10$ s (based on CROSMOR-model).

Blue values represent the effect of LW and HW ($k_s=5$ mm); the significant wave height is about 0.5 m lower at LW (depth is 2 m lower).

Red values represent the effect of bed roughness ($k_s=0.1, 1$ and 10 mm); the significant wave height is about 1 m lower for a rough bed with $k_s=10$ mm compared to a smooth bed with $k_s=0.1$ mm; the maximum wave height.

Green values represent the highest significant wave height during a storm with HW-conditions, a smooth bed with $k_s=0.1$ mm and a high wave period of $T_p=15$ s; the significant wave height is maximum 2.5 m at KP35 and maximum 2 m at KP6, in good agreement with the measured values.



Wave growth due to wind has been neglected; exploring computations using the Brettschneider method (SP Manual 1984) yields a wave height growth of 1 to 1.5 m over 25 to 50 km during storms with BF 6 to 7 (wind speeds between 10 to 17 m/s)

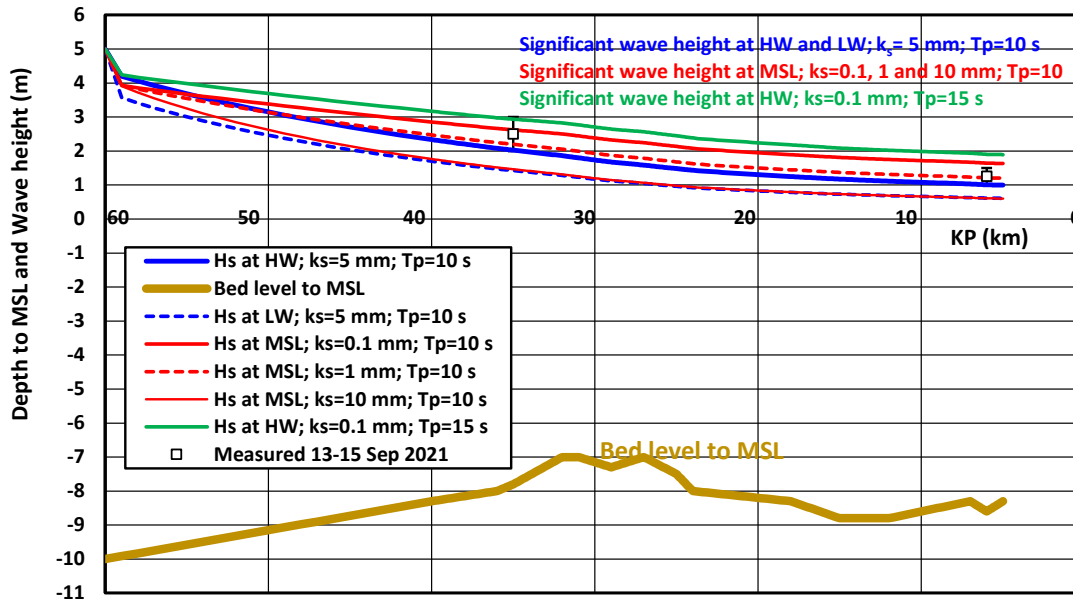


Figure 2.3.3 Computed and measured significant wave heights along line normal to shore during storm wave conditions ($H_{s,0} = 5$ m); CROSMOR-model



3. Dune zone cases

3.1 Erosion of sand dune due to extreme storms; exposed Holland coast, The Netherlands

The standard case of dune erosion for the Holland coast refers to extreme storm conditions as given in **Table 3.1.1**. The median sediment diameter along the Dutch coast is set to 225 μm (0.225 mm). The high storm surge level (SSL) of 5 m above mean sea level (MSL) is assumed to be constant over the storm duration of 5 hours during the peak of the storm. This equivalent duration of 5 hours yields approximately the same overall dune erosion volume as a complete storm cycle with growing and waning phases.

Parameter	Prototype conditions
Offshore wave height/period (m) (s)	7.6 (Pierson and Moskowitz spectrum); 12
Offshore water depth (m)	21 m
Storm surge level above MSL (m)	+5 m NAP during 5 hours (NAP is about 0.1 below MSL)
Median sediment diameter (μm)	225
Median fall velocity (m/s)	0.0267 (temperature= 10° C)
Cross-shore profile	a) dune height at +15 m NAP, b) dune face with slope of 1 to 3 down to a level of +3 m NAP, c) slope of 1 to 20 between +3m and 0 m NAP, d) slope of 1 to 70 between 0 and -3 m NAP, e) slope of 1 to 180 seaward of -3 m NAP line

Table 3.1.1 Parameters of Dutch coastal profile (Reference Case Dune erosion)

Figure 3.1.1 shows computed dune erosion profiles for different values of the storm surge level (SSL) above mean sea level (MSL). The storm duration is 5 hours with constant significant wave height of $H_{s,0}=7.6$ m. The dune erosion volume strongly increases with increasing storm surge level. The computed dune erosion is about 170 m^3/m for $\text{SSL}=5$ m above MSL.

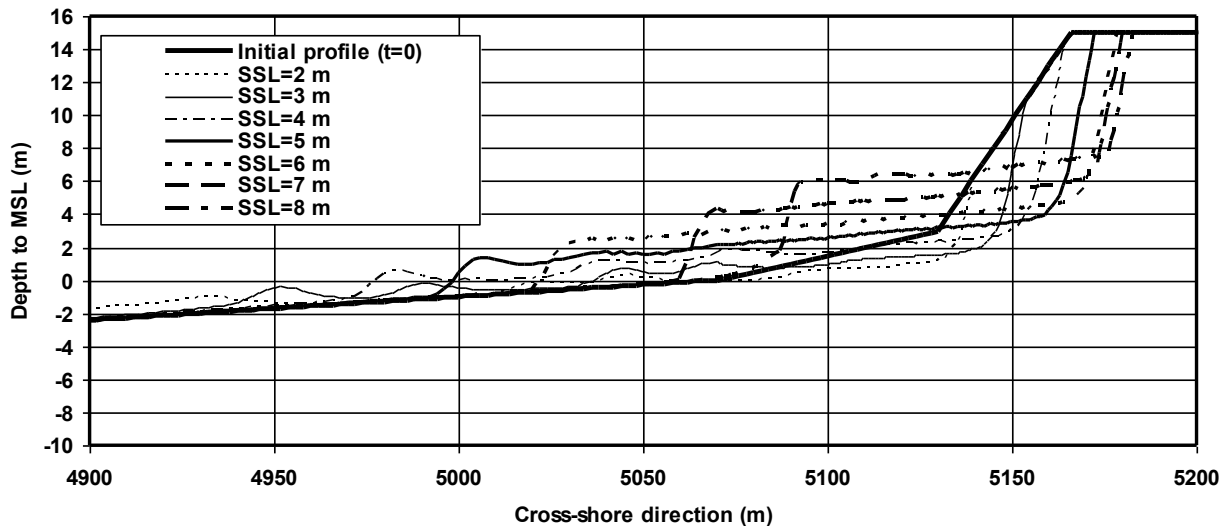


Figure 3.1.1 Effect of storm surge level on computed bed profile after 5 hours for Reference Case



3.2 Erosion of high berm in front of hard dike; sheltered lake coast Markermeer, The Netherlands

The old hard dike is reinforced with a sand berm in front of the (Houtrib) dike. The initial bed profile of sand ($d_{50}=0.21$ mm) has a slope of 1 to 32. Profile and boundary conditions are given in **Table 3.2.1**.

The design storm with return period of 10000 years has a trapezoidal shape in time with a total duration of 47 hours. The maximum significant wave height is 1.8 m. The maximum surge level is 1.92 m above NAP-datum.

PARAMETERS	Values
Water depth at deep water; waterlevel	4 m to NAP (NAP=0.1 m below mean sea level) 1,92 m above NAP (constant)
Significant wave height, period and wave incidence angle at deep water	t=0 hr: $H_s=0$ m, $T_p=6.5$ s, angle= 0° ; 30° t=21 hr: $H_s=1.8$ m, $T_p=6.5$ s, angle= 0° ; 30° t=27 hr: $H_s=1.8$ m, $T_p=6.5$ s, angle= 0° ; 30° t=47 hr: $H_s=0$ m, $T_p=6.5$ s, angle= 0° ; 30°
Bed slope; crest	1 to 32; 2 m above NAP
Boundary depth near beach	0.2 m
Grid size; total length	0.5 tot 1 m; 350 m
Number of wave classes per wave height	1 and 10
Wave asymmetry	Isobe-Horikawa
Coefficient Longuet-Higgins streaming; roller effect	0.5 (default=1); 0.5 (default=1)
Grain diameter sand d_{50}	0.21 mm
Coefficients sandtransportformulas	1 (default= 1)
Coefficient sandtransport wave asymmetry	0.2 (default= 1)
Coefficient sand entrainment beach zone	1 (default)
Coefficient undertow	1 (default)
Extra entrainment at dune front (sef)	1.5
Bed roughness	Automatic
Temperature and salinity	10 degrees and 0 promille
Files	HDIJKS.inp; HDIJKG.inp

Table 3.2.1 Input data of CROSMOR-model

Figure 3.2.1 shows the bed profile after an extreme storm with duration of 47 hours.

The erosion volume is:

- 50 m³/m above 1 m NAP for a wave incidence angle of 30° and 60 m³/m above 0 m NAP;
- 35 m³/m above 1 m NAP for perpendicular waves (no longshore current and less transport capacity).

The recession at the berm crest is about 70 m. The erosion volume is slightly larger using a spectrum of waves (10 wave classes). The erosion is substantially smaller for perpendicular waves (no longshore current).

The beach steepens to 1 to 15. The erosion is relatively large because the waves can wash over the crest.

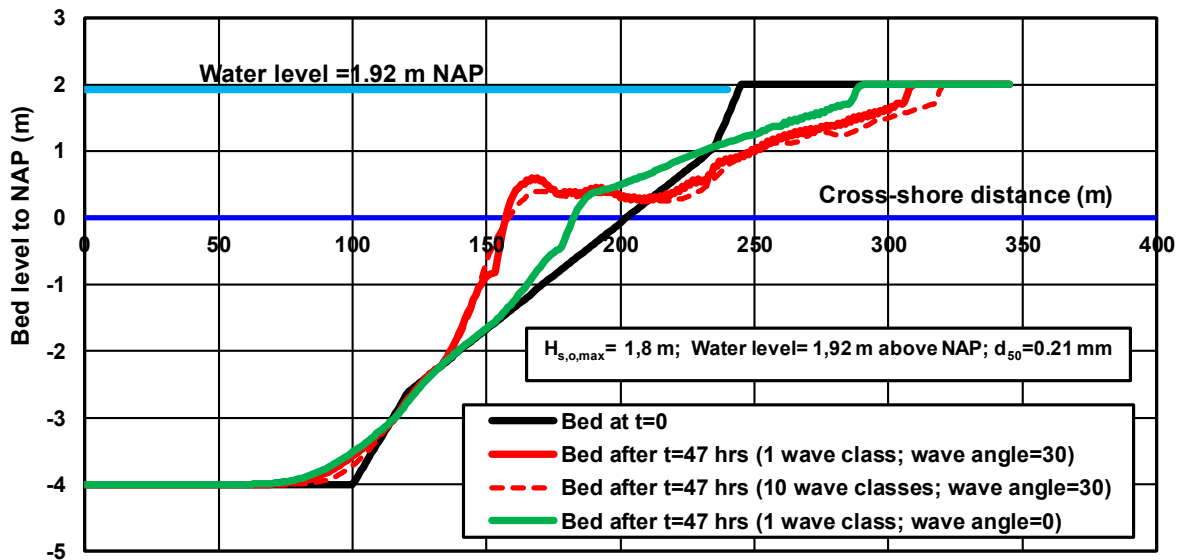


Figure 3.2.1 Bed profile development after a storm of 1x 10.000 years

3.3 Overwash over dune crest; Lagos coast, Nigeria

The CROSMOR-model has been used to compute the cross-shore morphological behaviour of the beach ridge during a storm event with overwash conditions. The wave height at the toe of the beach is set to $H_s = 2.1$ m with $T_p = 15$ s and normal to the shore. The water level is assumed to vary between 2.2 and 2.8 m above mean sea level (MSL). The beach crest is at 2 m above MSL. The beach material is varied in the range of 0.2 to 0.55 mm. The input data are given in **Table 3.3.1**.

Figure 3.3.1 shows the computed bed levels after 1 and 2 days for beach material of 0.55, 0.3 and 0.2 mm. The beach crest is strongly eroded due to overwash processes during the storm event. The beach crest erosion is about $50 \text{ m}^3/\text{m}$ after 1 day and $d_{50} = 0.55$ mm. The erosion volume after 1 day is somewhat larger for finer sediment. Based on these results, it can be concluded that the breach crest can move landward over a cross-shore distance of 40 to 50 m due to overwash processes during a storm event.

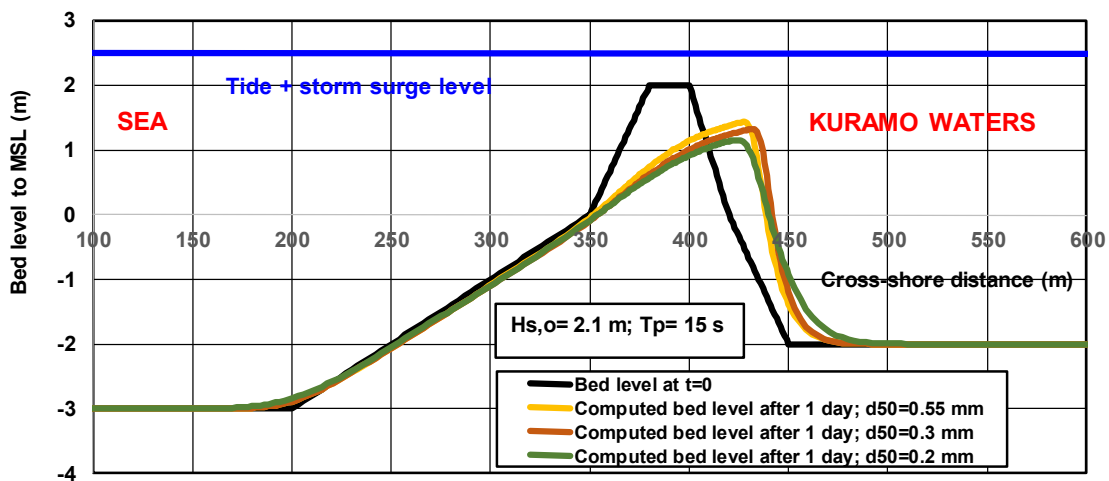


Figure 3.3.1 Cross-shore beach profile changes during storm event; $d_{50} = 0.55, 0.3$ and 0.2 mm; $sef = 1$



PARAMETERS	VALUES
Tidal conditions at x=0	Time(s) Cross-Current (m/s) Waterlevel (m)
	0 0.2 0
	3600 0.2 0.15
	10800 0.2 0.3
	18000 0.2 0.15
	21600 0.2 0
	25200 0.2 -0.15
	32400 0.2 -0.3
	39600 0.2 -0.15
	43200 0.2 0
Water depth at deep water	3 m
Storm surge level above MSL	2.5 m
Slope of sea bottom in the surf zone between -3 m and 0 m below MSL	1 to 50
Beach crest	2.0 m above MSL
Water depth at last grid point	0.1 m
Grid size and time step	1 to 3 m; 100 to 200 s
Total traject length	600 m
Significant wave heigth at x=0; wave period	2.1 m; 15 s
Wave direction at x=0 (to shore normal)	0 degrees
Number of wave classes per condition (to represent wave spectrum)	10
Wave asymmetry	Yes, based on Isebe-Horikawa
Coefficient Longuet-Higgins streaming roller effect	0.5 (default=1); 0.5 (default=1)
Sand grain size d_{50}	0.2 mm; 0.3 mm; 0.55 mm
Coefficients sand transportformulations	1 (default= 1)
Coefficient sand transport wave asymmetry	0 (default= 1)
Coefficient return flow (undertow)	1 (default)
Coefficient additional stirring of sand in beach-dune zone (sef)	1 (default; no effect) and 1.5
Bed roughness	Automatic
Temperature and salinity	20 degrees and 30 promille
Files	Nigerb.inp

Table 3.3.1 *Input data of CROSMOR-model*

3.4 Beach-dune erosion of Test Dunes at site Sand Motor, The Netherlands

In the winter period of October 2021 to March 2022, two test dunes of sand ($d_{50} \approx 0.3$ mm) have been constructed and monitored along the coastline of the Sand Motor site in the south-west part of the Holland coast (Van Wiechen et al, 2022). The crest of the dunes is at +5 m NAP (Dutch Ordnance Datum \cong -1m below MSL). Dune 2 has a slightly different orientation with more oblique incoming waves. Three minor storm events with maximum offshore significant wave heights of $H_{s,o,max} = 3.04$ m ($T_p = 8.3$ s), 4.27 m ($T_p = 9.5$) and 4.03 m ($T_p = 9.6$ s) occurred in the period 6 November 2021 to 6 January 2022. The offshore wave incidence angle to the shore normal was about 10° for Dune 1 and 20° for Dune 2 to the local shore normal. Herein, it is assumed that each storm consists of 6 hours with $H_{s,o} = 0.5 H_{s,o,max}$, 3 hours with $H_{s,o} = H_{s,o,max}$ and 3 hours with $H_{s,o} = 0.5 H_{s,o,max}$ (total duration $3 \times 12 = 36$ hours). The local tidal range is about 2 m. The maxim water level was about 2.2 m (storm setup of about 1.5 m). The most important model settings for both cases are: $f_{aced} = 0.5$, $f_{acsmooth} = 1.1$, $SEF = 2$; slope angle dune



front=50°. Figures 3.4.1 and 3.4.2 show measured and computed bed profiles bed before and after the storm period. Quite good agreement can be observed. The computed and measured dune erosion is about 23 m³/m. The Brier Skill Score [8] is 0.9 for Dune 1 and 2, which means an excellent hindcast prediction.

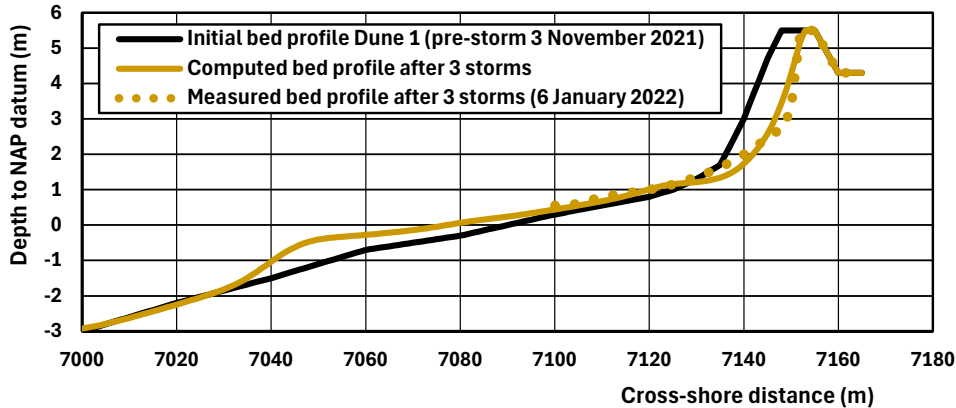


Figure 3.4.1 Measured and computed beach-dune profiles for Test Dune 1 at Sand motor site

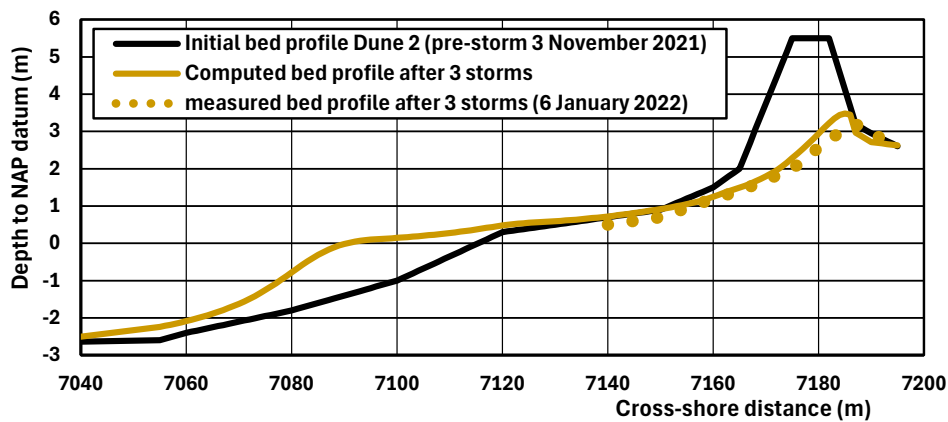


Figure 3.4.2 Measured and computed beach-dune profiles for Test Dune 2 at Sand motor site

3.5 Beach-dune erosion at site De Haan, Belgium

Between January 25 and the night of February 28 to March 1 of 1990, the coast of Belgium was hit by a record number of storms with maximum wind gusts up to 165 km/h in a period of just over a month. The coastal damage was substantial along the entire coastline of about 60 km. The retreat of the dune profile at the beach village of De Haan in Belgium due to the winter storms was measured in March 1990, see Figure 3.5.1. The maximum dune retreat is about 7 m, the total eroded volume is about 85 m³/m. The CROSMOR-model was applied for a storm period of 5.5 days with maximum wave height of $H_{s,0}=5$ m ($T_p \approx 8$ s). The tidal range is about 4.5 m. The sediment size is $d_{50}=0.23$ mm. The key model settings are: SEF=1.5; $f_{bed}=f_{acus}=0.7$. The computed beach-dune profile is in good agreement with the measured profile, see Figure 3.5.1. The Brier Skill Score is 0.82, which means an excellent hindcast prediction.

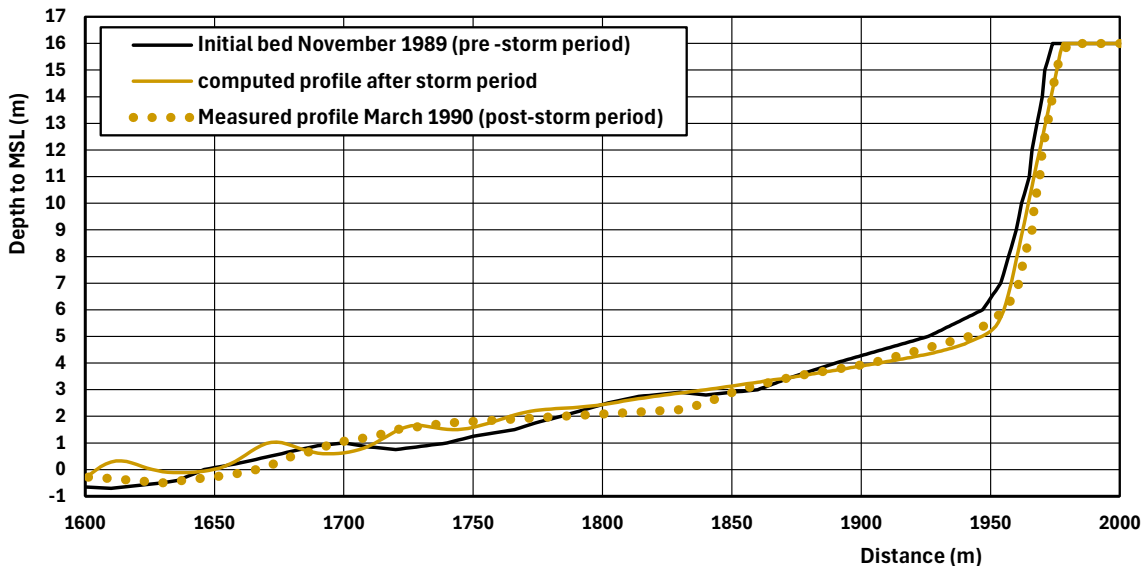


Figure 3.5.1 Measured and computed beach-dune profiles for storm period 1990, site De Haan, Belgium

3.6 Beach-dune erosion at the site HBZ Petten, Netherlands

Before 2015, the section Petten to Camperduin of the Holland coast was protected by an asphalt-type of dike over an alongshore distance of about 6 km. Around 2015, a new natural sand dune was constructed in front of the dike. As this section has been protected since 1600, while the adjacent coastal suffered from chronic erosion and retreat, the new sand dune protrudes into the sea over a distance of about 200 m with respect to the adjacent coastlines. This leads to erosional losses requiring regular maintenance nourishments. The CROSMOR-model has been used to estimate the erosion losses.

The wave climate is schematized into 8 wave conditions with $H_{s,0}$ between 1.5 and 3.2 m and 1 storm condition with $H_{s,0} = 5$ m and duration of 12 hours. The storm represents an event with a recurrence period of 5 years, which is applied each year over the computation period of 3 years. The vertical tide is between +1 and -0.8 m NAP. The maximum flood velocity in deep water is set to 0.3 m/s; the maximum ebb velocity is set to 0.25 m/s. The median particle size is set to $d_{50} = 0.3$ mm. The measured bed profile at km 25 of 2015 is used as the initial bed profile, which has a flat beach at +2 m over about 100 m (JARKUS-database Rijkswaterstaat).

Figure 3.6.1 shows the measured and the computed bed profiles after 3 years. The computed erosion volume is landward of $x = 1900$ m about 300 to 330 m^3/m after 3 years, which is in reasonable agreement with the measured value of 340 m^3/m . However, the computed erosion profile shows more erosion in the upper beach zone ($x > 2200$ m) compared to the measured profile. The eroded sediments are in the model deposited in the bar trough zone at $x = 1900$ m which is not observed in nature. This is caused by the relatively strong longshore current around the new protruding sand dune, which continuously removes the deposited sediments in the bar trough zone carrying it along the coast. This 3D mechanism is absent in the 2D model, which has a closed sand balance in cross-shore direction. The measured profile only shows erosion without deposition (no closed sand balance). Nevertheless, the CROSMOR-model predicts a reasonable erosion loss from the new sand dune, which can be used to estimate the maintenance volume and re-nourishment cycle time

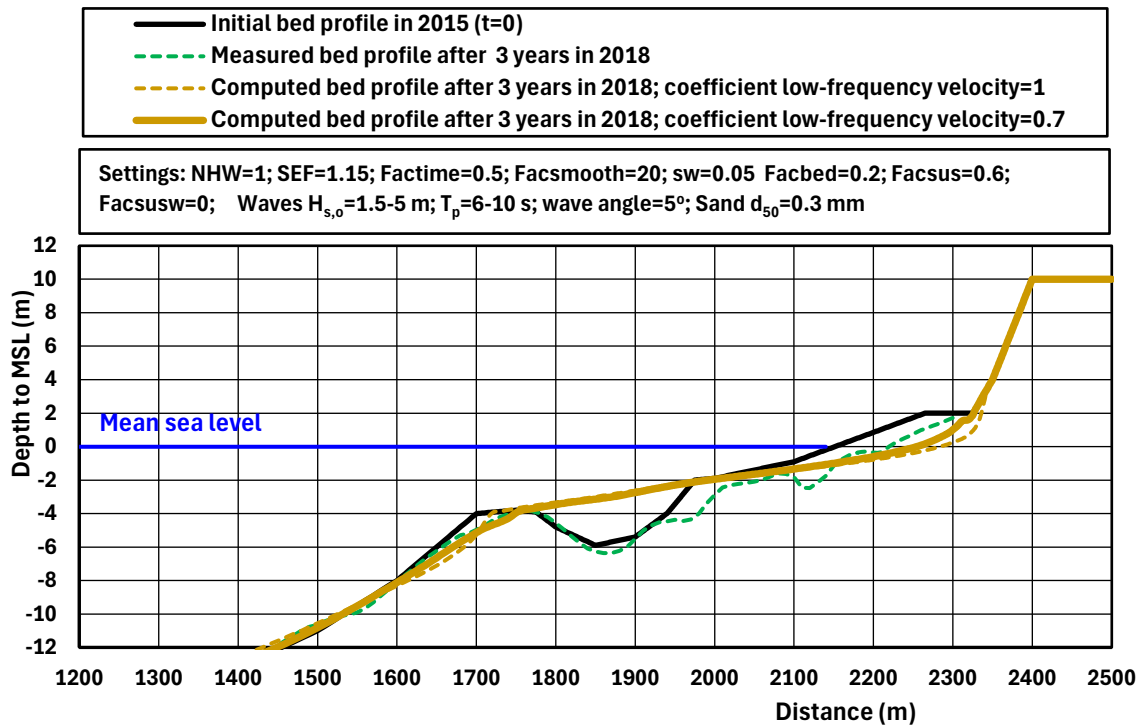


Figure 3.6.1. Measured and computed bed profiles, km 25, North-Holland, the Netherlands



4. Beach and surf zone cases

4.1 Beach stability under daily waves; sheltered coast Lake Markermeer, The Netherlands

The CROSMOR-model which includes both onshore- and offshore-directed transport processes, has been used to get information of the beach deformation during daily wave conditions.

A small beach with an alongshore length of about 450 m was made in the summer period of 2014. The beach was made of sand with d_{50} -value of 0.265 mm (mean value of many samples). Measured wave heights at a depth of 2.5 m are up to $H_s = 1.2$ m, mostly from west to south-west. The lake level varies between -0.2 m and -0.4 m NAP. Water level setup is up to 0.4 m. Wind-induced circulation currents to the east may be as large as 0.4 m/s during stormy periods. The measured wave climate is schematized to 6 wave classes for model input.

Figure 4.1.1 shows the initial beach profile in the middle of the beach and computed bed profiles after 2 years for $d_{50} = 0.25$ and 0.3 mm. The measured erosion above -1 m NAP is about $20 \text{ m}^3/\text{m}$ after 2 years. The computed erosion of about $10 \text{ m}^3/\text{m}$ after 2 years is less than the measured value, but it is a fairly good result given the fact that some of the measured erosion is caused by longshore transport processes which are not taken into account by the model.

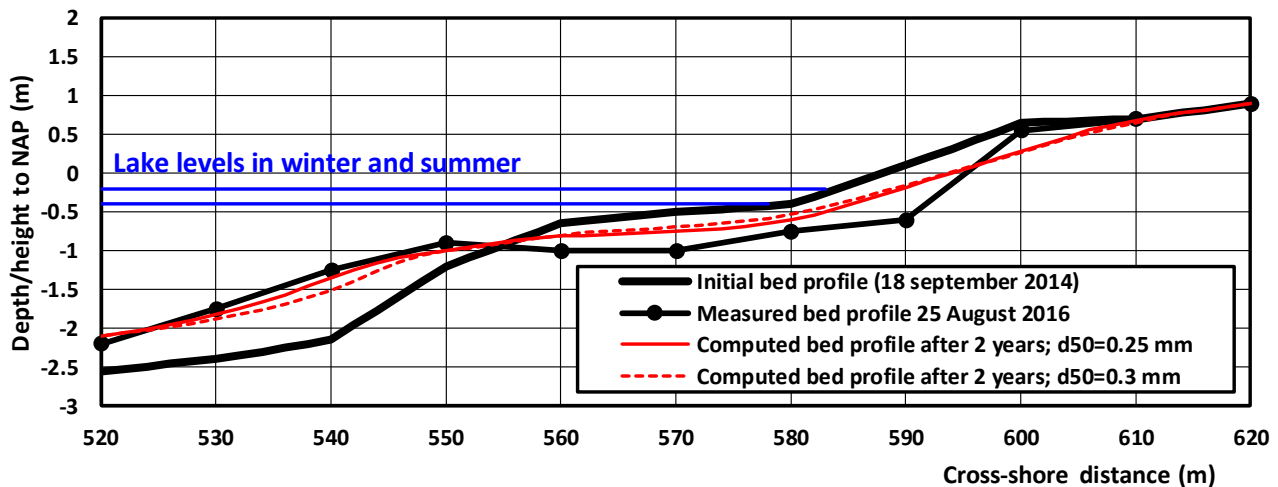


Figure 4.1.1 Computed beach profiles for daily wave conditions; validation case CROSMOR-model

4.2 Beach stability under daily waves; sheltered south-east coast of Texel island, The Netherlands

The CROSMOR-model has been applied to find out what is the most stable beach of a new sand dike/dune at the the south-east coast of Texel (bordering the Wadden Sea). A stable beach is close to equilibrium conditions with almost no erosion and maintenance for daily wave conditions. Daily waves at the project site are in the range of 0.3 and 1 m (periods of 3 to 5 s) with wave incidence angles of about 10° . The nearshore tidal current is set to 0.1 m/s. Many runs have been done for a range of beach slopes between 1 to 15 and 1 to 50 to study the most optimum beach slope minimizing the erosional losses on the seasonal time scale. A relatively steep beach of 1 to 15 is attractive because it gives a relatively small construction volume of sand. However, a steep beach slope leads to significant erosion of sand at the upper beach and accretion at the lower beach, ultimately creating a much milder beach slope. The best result (least erosion) was obtained for a beach slope consisting of a mild slope of 1 to 50 below NAP (about mean sea level) and a slope of 1 to 15/20 above NAP up to the dune toe level at +3 m NAP.

Figure 4.2.1 presents the computed bed profiles showing beach accretion due to onshore sand transport. The top layer of the beach consists of a relatively coarse wear layer (erosion buffer) layer with grain sizes of 0.4 to



0.5 mm extending to the -1.5 m NAP depth line. The sea bottom seaward of the -1.5 m depthline consists of fine sand with grain size of about 0.2 mm. This was simulated by running the CROSMOR-model over 3 years with two sand fractions, as follows:

- seaward of -1.5 m NAP: 90% sand of 0.2 mm and 10% sand of 0.5 mm;
- landward of -1.5 m NAP: 10% sand of 0.2 mm and 90% sand of 0.5 mm.

The CROSMOR-model was also run over 3 years with one sand fraction of 0.4 mm. Beach erosion is hardly present. The total beach accretion volume is of the order of 10 to 20 m³/m/year coming from the lower beach zone. The shallow foreshore consisting of fine sand of 0.2 mm is slightly eroded and a minor part is deposited seaward.

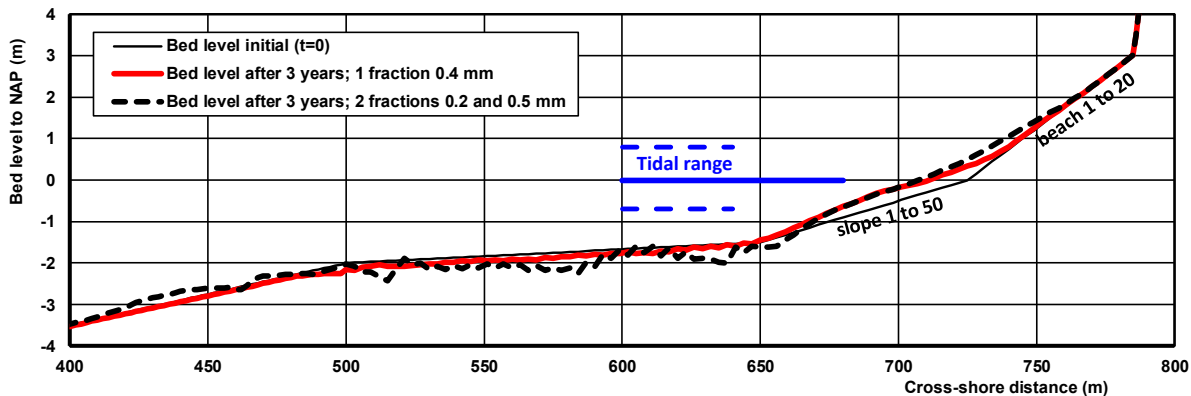


Figure 4.1.2 Computed beach accretion for daily wave conditions; CROSMOR-model

4.3 Erosion of beach nourishment for annual wave climate; Holland coast, The Netherlands

The section Petten to Camperduin of the Holland coast was protected by an asphalt-type of dike. Around 2010, it was decided to construct a sand beach-dune system in front of the dike. This coastal section is known as the 'Hondbossche and Pettemer' Sea dike with a length of about 6 km. The sea dike section protrudes into the sea over a distance of about 200 m with respect to the surrounding coastline.

The wave climate is a yearly-averaged wave climate based on observations in the period 1980-1988 and has 8 wave height classes ($H_{\text{significant}}$) between 1.5 and 3.2 m. A storm with a deep-water wave height of $H_{s,0} = 6$ m and a duration of 12 hours is added. This is an extreme wave height with a recurrence period of 100 years, which is applied 5 times over the computation period of 5 years. Two storm surge levels (including tide levels) of +3 and +4 m NAP have been used. The wave asymmetry of the near-bed velocities is computed by the method of Isobe-Horikawa. The vertical tide is between +1 and -0.8 m NAP. The maximum flood velocity in deep water is set to 0.6 m/s; the maximum ebb velocity is set to 0.5 m/s. Two median particle sizes have been used: $d_{50} = 0.21$ and 0.25 mm. Model settings are given in **Table 4.3.1**.

Figure 4.3.1 shows the initial bottom and the computed bed levels after 1, 2 and 5 years for $d_{50} = 0.25$ mm of Profile 21.230 km (final design).

In the first year a new sand bar with a width of about 150 m and a height of about 4 m is generated between $x = 500$ m en 700 m. The erosion at the upper beach is caused by the storm waves with a surge level of +4 m. Most of the erosion takes place at the lower beach.

Based on all CROSMOR-results, the average annual erosion volume during the initial phase of about 5 years after construction is estimated to be in the range of 55 to 85 m³/m/year (70±15 m³/m/year; uncertainty of about 20%). The sand material is eroded from the beach zone and deposited into the surf zone beyond the -3 m NAP-line. The maximum recession due to cross-shore transport processes after 5 years is estimated to be about 100±30 m.

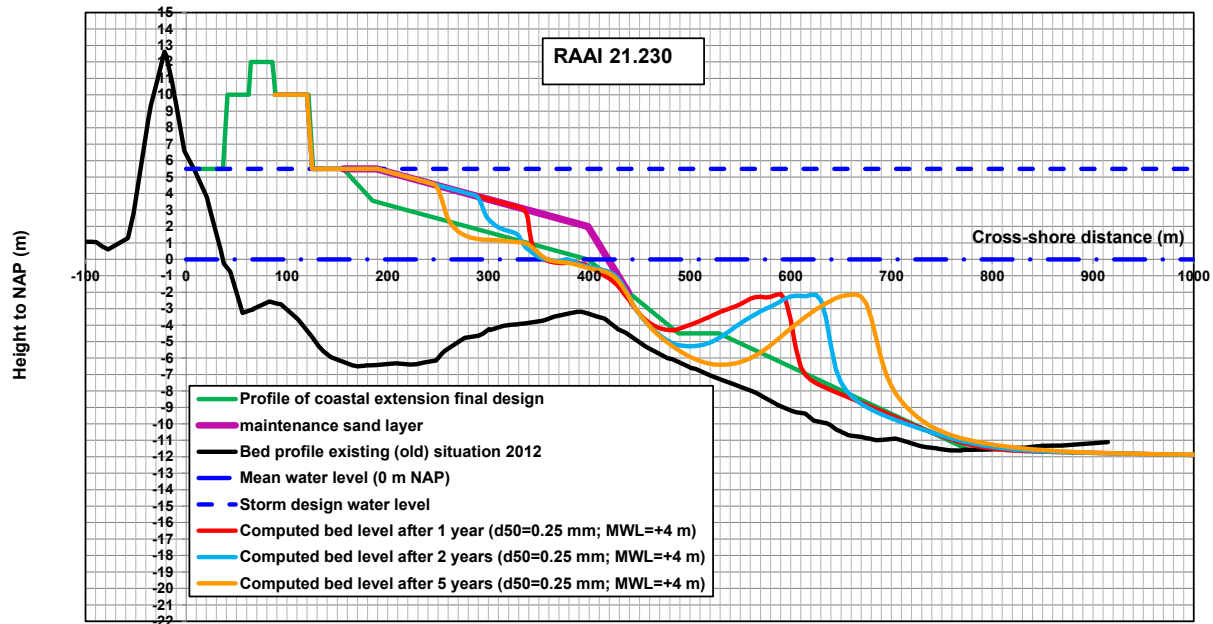


Figure 4.3.1 Computed bed level of cross-shore profile 21.230 km; CROSMOR; $d_{50} = 0.25$ mm; maximum water level = +4 m.

Parameters	Values
Tidal conditions	Time (sec) Current velocity (m/s) Water level (m)
	0 0 0
	3600 0.3 0.5
	10800 0.6 1.0
	18000 0.3 0.5
	21600 0 0
	25200 -0.2 -0.4
	32400 -0.5 -0.8
	39600 -0.2 -0.4
	43200 0 0
Limiting depth = water depth in last grid point	0.5 m
Grid size; total length	50 m (deep water) to 2 m (beach zone); 5000 m
Time step	Automatic
Number of wave classes	1
Wave asymmetry	Isobe-Horikawa
Coefficient Longuet-Higgins streaming roller effect	0.5 (default=1); 0.5 (default=1)
Grain size d_{50}	0.25 mm
Coefficients sand transport equation	1 (default= 1)
Coefficient sand transport wave asymmetry	0.2 (default= 1)
Bed roughness	Automatic
Temperature and salinity	10 degrees and 30 promille
Filenames	PB21.inp (coastal extension 300 m) PBB21.inp (coastal extension 300 m and extra bar) P2B21.inp (coastal extension 220 m) P3B21.inp (coastal extension 260 m) Pbb360.inp (coastal extension 360 m and extra bar)

Table 4.3.1 Model settings



4.4 Sediment sorting in beach and surf zone; Katwijk beach, The Netherlands

Detailed information of cross-shore grain size variations at the Katwijk-site (about 20 km north of The Hague) along the North Sea coast of The Netherlands has been presented by Terwindt (1962). He studied grain size variations and the effect of a storm event on the cross-shore particle size distribution. The results of Terwindt (1962) for the location Katwijk are based on the analysis of samples collected in a summer period under different hydraulic conditions (fairweather and minor storm event; 1 to 2 weeks). The maximum significant wave height outside the surf zone was estimated to be about 3 m during summer storm conditions. The summer storm period has been modelled by assuming offshore significant wave heights between 1 and 3 m during 1 week (see input data below).

The observed cross-shore grain size variations (Figure 4.4.1) show the following features:

Before summer storm period

- relatively coarse material (d_{50} of about 300 μm) in the shallow swash zone near the water line;
- systematic fining of sediment material in seaward direction over the width of the surf zone; seaward of the outer breaker bar the d_{50} has reduced to a value of about 140 micron during periods with calm weather;
- fining of sediment from the swash zone (300 micron) to the dune top (220 micron);

After summer storm period

- the sediments in the outer surf zone are found to be somewhat coarser (10% to 20%; d_{50} is about 180 micron) after a summer storm period; the fraction 105-150 micron shows the greatest variations; during calm periods the fraction 105-150 micron is dominant (50% to 70%) in the bed material; after the storm period the contribution of the 105-150 fraction is reduced to about 20%; thus the finer material is washed out during conditions with higher waves and is most probably transported in suspension to deeper water where it is deposited.

The CROSMOR-model has been used to simulate the Katwijk-measurements. The input data are:

Significant wave height at depth=10 m

t= 0 hrs	$H_{1/3,0}$	= 1 m
t= 24 hrs (1 day)	$H_{1/3,0}$	= 1 m
t= 36 hrs (1.5 days)	$H_{1/3,0}$	= 3 m
t= 60 hrs (2.5 days)	$H_{1/3,0}$	= 3 m
t= 72 hrs (3 days)	$H_{1/3,0}$	= 1 m
t= 168 hrs (7 days)	$H_{1/3,0}$	= 1 m
Water depth (x=0 m)	h_0	= 10 m
Wave incidence angle (x=0 m)	θ	= 10 degrees
Longshore tidal velocity (x=0 m)	v_0	= 0.6; -0.5 m/s
Tide levels (x=0 m)	Δh	= 0.8; -0.8 m
Peak period	T_p	= 8 s
Number of wave classes	NW	= 5
Fluid density	ρ_w	= 1030 kg/m^3
Bottom friction	$k_{s,w}$	= 0.02 m
Water temperature	Te	= 15 degrees C
Salinity	Sa	= 30 promille
Current-related bed roughness	$k_{s,c}$	= 0.02 m
Wave-related bed roughness	$k_{s,w}$	= 0.02 m



Multi fraction method (N=5)	d_{50}	= 0.14 to 0.28 mm ($d_i = 0.1; 0.15; 0.2; 0.3; 0.4$ mm)
Thickness of bed surface layer	δ	= 0.2 m
Factor high-freq. susp. transport	γ	= 0.2

Figure 4.4.1 shows the computed distribution of the d_{50} along the cross-shore profile after 7 days based on the multi fraction method. The initial particle size distribution (model input) is represented by a variation between 0.14 and 0.28 mm based on the trend of the measured d_{50} -values before the summer storm period.

The computed results are:

- during the storm event the computed suspended transport is dominant and offshore-directed in the swash zone ($670 \text{ m} < x < 720 \text{ m}$); on the landward flank of the inner bar ($560 \text{ m} < x < 620 \text{ m}$) and at the outer bar ($x < 470 \text{ m}$), where the longshore and cross-shore currents are relatively large;
- bed-load transport is dominant and onshore-directed in the troughs landward of the inner and outer bars ($470 \text{ m} < x < 560 \text{ m}$; $620 \text{ m} < x < 670 \text{ m}$);
- deposition can be observed in the swash zone ($650 \text{ m} < x < 690 \text{ m}$) where a swash bar is generated just seaward of the mean waterline (MSL-line); deposition also occurs around the crest of the inner bar ($550 \text{ m} < x < 580 \text{ m}$) and just landward of the outer bar ($390 \text{ m} < x < 420 \text{ m}$);
- erosion can be observed around the mean waterline ($680 \text{ m} < x < 720 \text{ m}$); in the trough landward of the inner bar ($580 \text{ m} < x < 650 \text{ m}$) and at the crest of the outer bar ($330 \text{ m} < x < 390 \text{ m}$);
- the changes in particle size (d_{50}) correspond strongly to the computed deposition and erosion patterns; coarsening of the bed surface does occur in the erosion zones where the finer particles are winnowed from the bed and are transported to the deposition zones resulting in fining of the bed surface; the beach shows a tendency for coarsening of the bed surface;
- the computed coarsening effects in the trough between the inner and outer bar are in reasonably good agreement with the observed pattern; the coarsening effect observed seaward of the outer bar is not represented by the model; the coarsening effect in the trough zone landward of the inner bar and the fining effect seaward of the mean waterline are in reasonable agreement with the observed patterns.

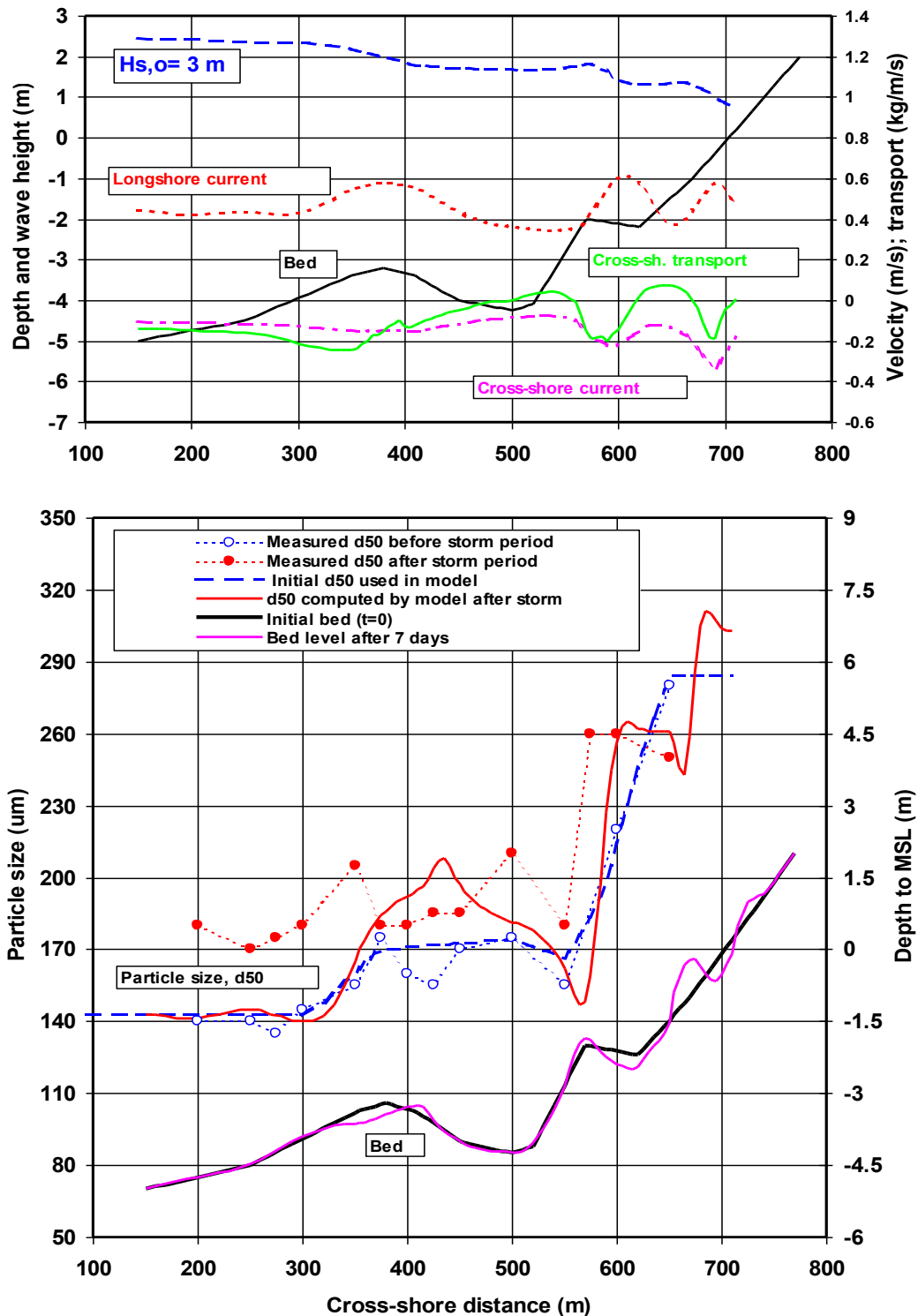


Figure 4.4.1 Effect of storm event on cross-shore particle size distribution, Katwijk-site, The Netherlands
Top: Wave heights and currents
Bottom: Particle size and bed profile



4.5 Sedimentation and erosion of mining pit for land reclamation; China

The City of Dong Ying (China) has planned the construction of a large-scale land reclamation site (approximately $4 \times 14.5 \text{ km}^2$), just south of the mouth of the Yellow River in China. The project site is characterised by a very shallow nearshore area (with a slope in the range between 1 to 1500 and 1 to 2000), meso tidal water level movement of the Bohai Sea, large sediment supply to the coastal zone originating from the Yellow River (although greatly reduced in recent years as a consequence of river training works upstream) and large amounts of very fine, non-cohesive sediments in the coastal zone. The sediment for the land reclamation site is taken from a nearshore borrow area (sediment extraction mining pit).

The CROSMOR-model has been run for a period of 6 months with waves (no waves in the other 6 months). The tide is schematized into 13 blocks of 1 hour with quasi-steady flow. The tidal range is 1 m; the peak tidal velocities are 0.5 m/s in the flood and in ebb directions.

The pit (borrow area) is situated between the -5 m and -2 m depth lines, the bottom of the pit is at -10 m, the seaward side slope is 1 to 200 and the landward side slope is 1 to 125. The length of both side slopes is 1000 m. The initial (at $t=0$) bed profile of the pit is shown in **Figure 4.4.1**. One constant, representative wave height of $H_{s,o}=2 \text{ m}$ ($H_{rms,o}=1.4 \text{ m}$) was used over a period of 6 months (183 days).

Runs with and without tidal filling velocities have been made. The tidal filling velocities are associated with the velocities required to generate the tidal water level changes (rising and falling of tide). These velocities may be quite large due to the large horizontal scale of the bed profile (20 km). Assuming a water level rise of 0.15 m per hour (3600 s), the tidal filling and emptying velocity at 2 km (2000 m) from the shore (water depth= 2 m) is: $v=0.15 \times 2000 / (2 \times 3600) = 0.042 \text{ m/s}$. This latter velocity is of the same order of magnitude as the offshore-directed undertow generated by the waves. It should be realized, however, that the modelling of the rising and falling of the tide in the cross-shore direction is not fully realistic. Generally, the tides are propagating parallel to the shore. Therefore, runs with and without this effect have been made.

Figure 4.5.1 shows the computed bed profiles after 1 year. The main results are:

- erosion occurs in the nearshore zone and is of the order of -1 m over a length of about 1500 m;
- deposition occurs on the landward side slope of the pit; in reality this deposition will be much more spread out due to the delayed settling of the fine sediments;
- erosion occurs at the seaward edge of the pit and is of the order of -1 m;
- erosion and deposition is about 50% less if the cohesive effects of the clay fraction (30% clay) is taken into account;
- tidal filling has not much effect on the erosion and deposition values.

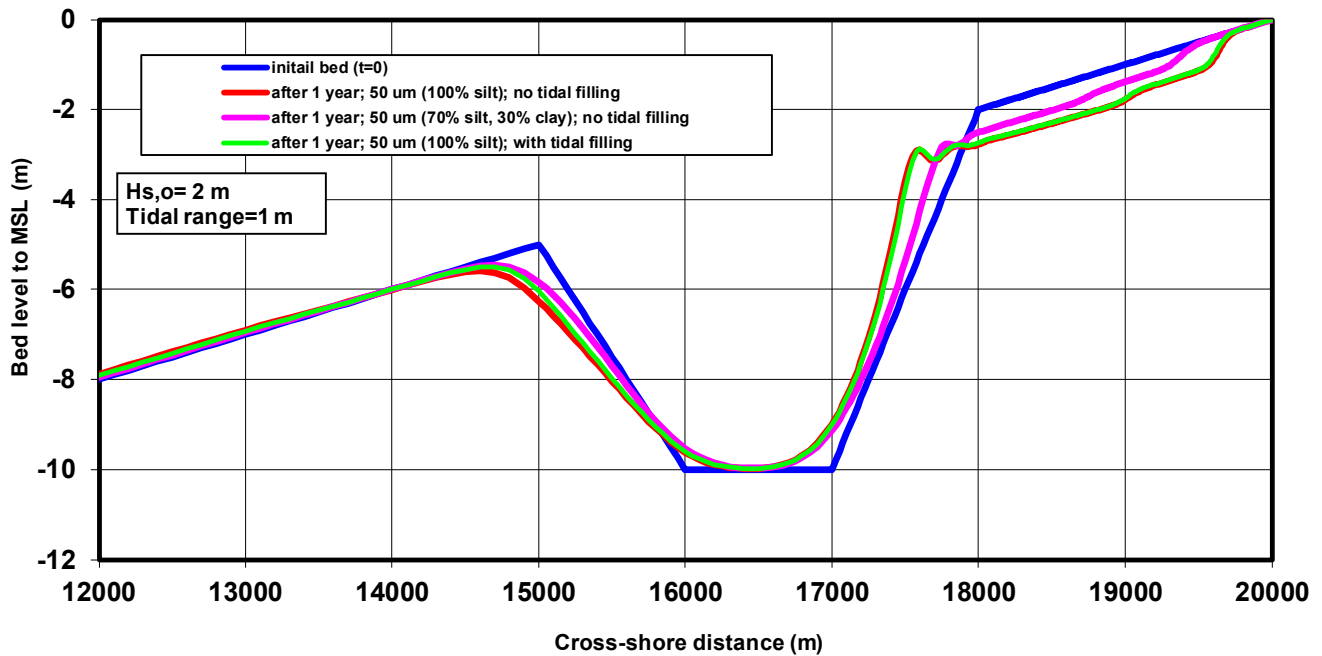


Figure 4.5.1 Computed bed profiles after 1 year for nearshore mining pit; Dong Ying, China

4.6 Onshore bar migration at beach; Duck beach , USA

The present data were obtained during the Duck94 field experiment conducted near Duck, North Carolina (USA) on a barrier island exposed to the Atlantic Ocean (Gallagher et al., 1998). The data period covered is 21 September to 20 October 1994.

The presence of a breaker bar can be observed around the cross-shore position of 200 m from the reference line. The bathymetry characteristics can be described as:

- 21 September: minor storm on 21 Sept., $H_{s,offshore} = 2.5$ m (maximum); the bar has a reasonably straight alignment between the main transect 945 m and the transect 1200 m; an oblique (crescentic) pattern can be observed between transects 700 m and 945 m;
- 21 September - 4 October: significant wave height $H_{s,offshore}$ between 1 and 1.5 m; the bar has moved offshore (about 25 m) between transects 700 and 800 m; the bar has moved onshore slightly between transects 875 and 975 m; bar alignment is almost straight;
- 4 October - 10 October: $H_{s,offshore}$ is maximum 1 m; bar movement is minor;
- 10 October - 14 October: $H_{s,offshore}$ between 1 and 1.5 m; bar has moved offshore (about 30 to 40 m); bar alignment is almost straight;
- 14 October - 16 October: $H_{s,offshore}$ is between 2 and 3 m (storm period);
16 October - 20 October: $H_{s,offshore}$ is between 1.5 and 2 m; bar has moved offshore (about 50 m) between transects 875 and 975 m; bar has moved onshore near transects 700-850 m; bar has moved onshore near transects 1050-1200 m; bar alignment is crescentic.

During the period September 21-26, the bar crest around the main transect at 945 m moved onshore over a distance of about 15 m. Longshore variations of the bar are minor over a distance of 50 m on both sides of the main transect 945 m. The significant wave height at a depth of about 5 m varied between 0.5 and 2.5 m; a



minor storm with a duration of about 12 hours occurred on September 21; most of the time (5 days) the wave height varied between 0.5 and 1 m.

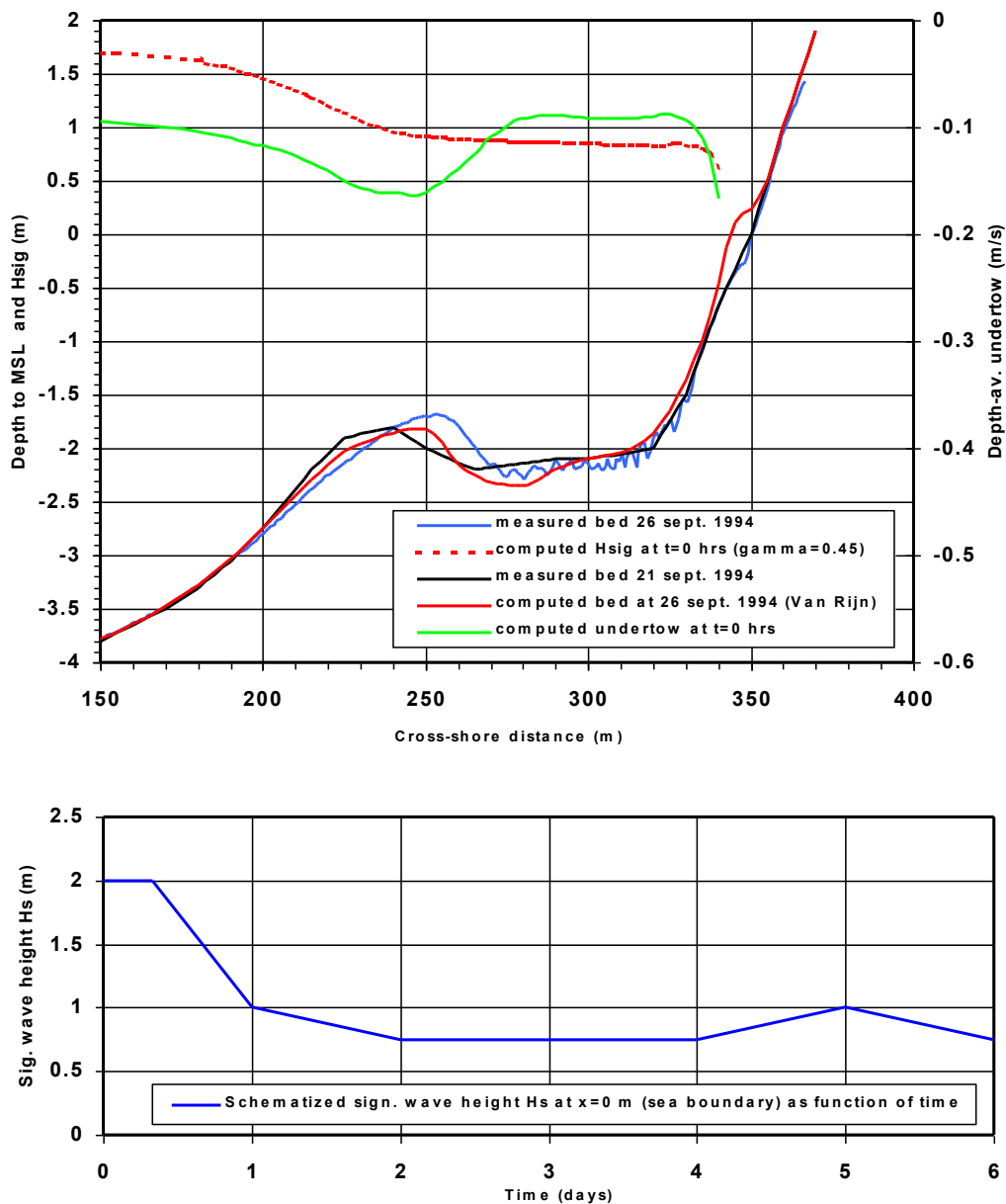


Figure 4.6.1 Measured and computed bed levels for 21-26 September 1994 event and schematized offshore significant wave height

The profile model CROSMOR has been applied to simulate the bed level changes in the main transect at 945m. Relatively large wave-induced ripples are assumed to be present in the trough zone, having a wave-related bed roughness value of 0.05 m. The bed material is represented by $d_{50} = 0.15$ mm and $d_{90} = 0.3$ mm. Preliminary runs have been made to calibrate the transport factor (multiplication factor to standard sand transport) yielding 0.5. The wave breaking coefficient is taken as $\gamma = 0.45$. The sand transport model of Van Rijn has been used to compute the morphologic development of the cross-shore profile.



The computed results (**Figure 4.6.1**) show the following features:

- slight onshore migration of the bar, which is considerably smaller than the observed values; the sand transport due to the wave asymmetry and the undertow creates a convergence point just landward of the bar crest resulting in onshore bar migration; the relatively large bed roughness in the trough zone is necessary to generate sufficiently large offshore-directed sand transport by the undertow in the trough zone;
- generation of beach bar (about $4 \text{ m}^3/\text{m}$) near the mean waterline, which is not observed in the field data.

4.7 Erosion of steep slope

Sand dam

A sand dam with a steep slope of 1 to 7 in the coastal zone of Egypt is attacked by waves over a period of 1 year

Slope: 1 to 7

Sand: $d_{50}=0.2 \text{ mm}$

Waves: H_{rms} up to 0.95 m over 1 year.

Tides: tidal range of 0.2 m

Input file: aqer291.inp

Computed bed profiles for two conditions are shown in Figure 4.7.1.

Condition 1: higher waves $H_{rms} > 0.6 \text{ m}$ over 19 days; highest wave $H_{rms}=0.95 \text{ m}$.

Condition 2: all waves ($H_{rms} 0.2 \text{ to } 0.95 \text{ m}$) of 1 year.

Estimated erosion after 1 year: $70 \text{ to } 80 \text{ m}^3/\text{m}$ after 1 year

Maximum recession at crest: 25 m

Strategy running Crosmor:

1. grid size 1 to 2 m in nearshore;
2. factime=0.1; facsmooth=10;
3. susw=0 or 0.1 (extra onshore transport; mostly for coarse sand and gravel);
4. susb=0.5 to 1; susc=0.5 to 1.
5. run the model first for the higher waves over a short period of time (1 month)
6. reduce facsmooth to 1 (factime=0.1) to get less smoothing, see profiles;
7. run model for longer period with all waves;
8. increase factime to 0.3 and 0.5 (as high as possible); smoothing procedure is applied less for higher factime.

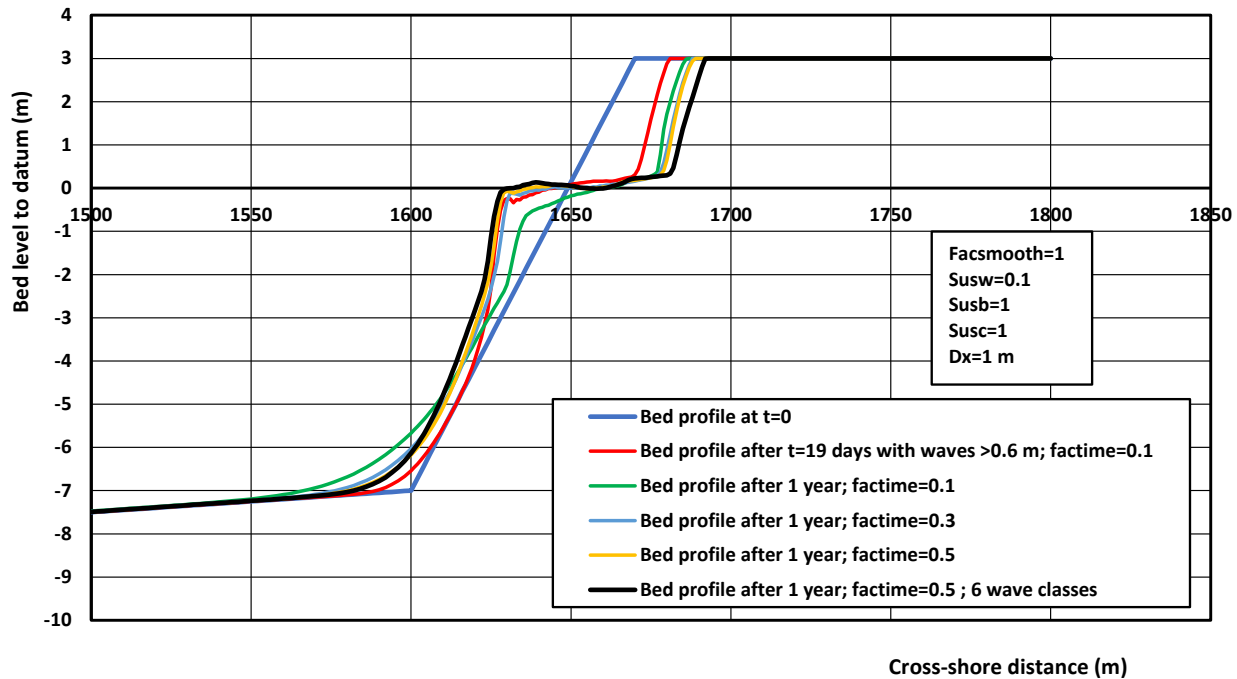


Figure 4.7.1 Erosion of steep slope of 1 to 7

Erosion of steep pit slope

The basic input data of the CROSMOR-model for the nearslope slope of Profile 2 are:

- water depth at $x=0$: $h=9$ m to MSL; no beach (profile ends a depth of -1 m);
- annual: maximum depth-averaged longshore current at $x=0$: 0.3 m/s for annual conditions;
- annual: maximum cross-shore depth-averaged current at $x=0$: -0.01 m/s (seaward directed during ebb);
- storm: maximum depth-averaged longshore current at $x=0$: 0.5 m/s;
- storm: maximum depth-averaged cross-shore current=-0.2 m/s (seaward directed during ebb);
- no phase shift between vertical and horizontal tide;
- tidal amplitude=0.6 m; tidal period=12 hours;
- waves at $x=0$: $H_s=0.35$ m $T_p=3$ s for annual conditions 1 m, $H_s=1$ m; $T_p=3.5$ s for storm event;
- wave approach angle at $x=0$: 30° with respect to the local shore normal;
- $d_{50}=0.17$ mm; $d_{90}=0.5$ mm; bed roughness: automatic;
- scaling coefficient bed reference concentration $\alpha_c=1$; a=reference level=0.05 m;
- settling velocity $w_{sand}=0.015$ m/s;
- density: $\rho_s=2650$ kg/m³, $\rho_w=1025$ kg/m³, water temperature=20° C; $\nu=0.000001$ m²/s,
- porosity=0.4;
- wave breaking: automatic; $f_{rip}=0$ for $x>350$ m (current=0 m/s);
- timestep: automatic; horizontal grid size=1 m at slopes;
- input files: abudha1.inp for storm conditions; abudha2.inp for annual conditions.

Remark: the frip-parameter is set to 0 for $x>350$ m so that the cross-shore currents are zero to prevent the import of sand from the beach zone. The cross-hore current at $x=0$ m need to be set at relatively high negative values (during ebb) to get erosion.



Figure 4.7.2 shows the bed level changes at a steep landward (nearshore) slope for annual conditions. The maximum erosion after 1 year is of the order of 2 m at the upper part of the slope. The eroded sediment is deposited at the toe of the slope

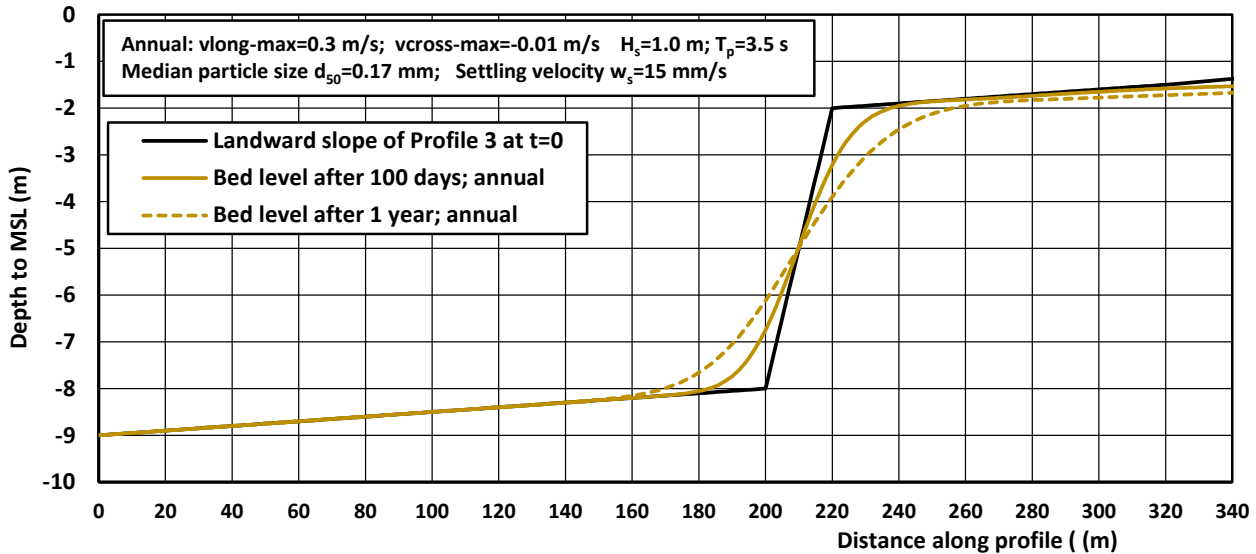


Figure 4.7.2 Computed bed profiles for annual conditions

Figure 3.3.8 shows the bed level changes for an extreme storm event of 2 days. The shallow nearshore area is eroded away of a distance of 150 m. The maximum erosion depth is about 0.4 m after 2 days. The eroded sediment is deposited at the upper part of the slope.

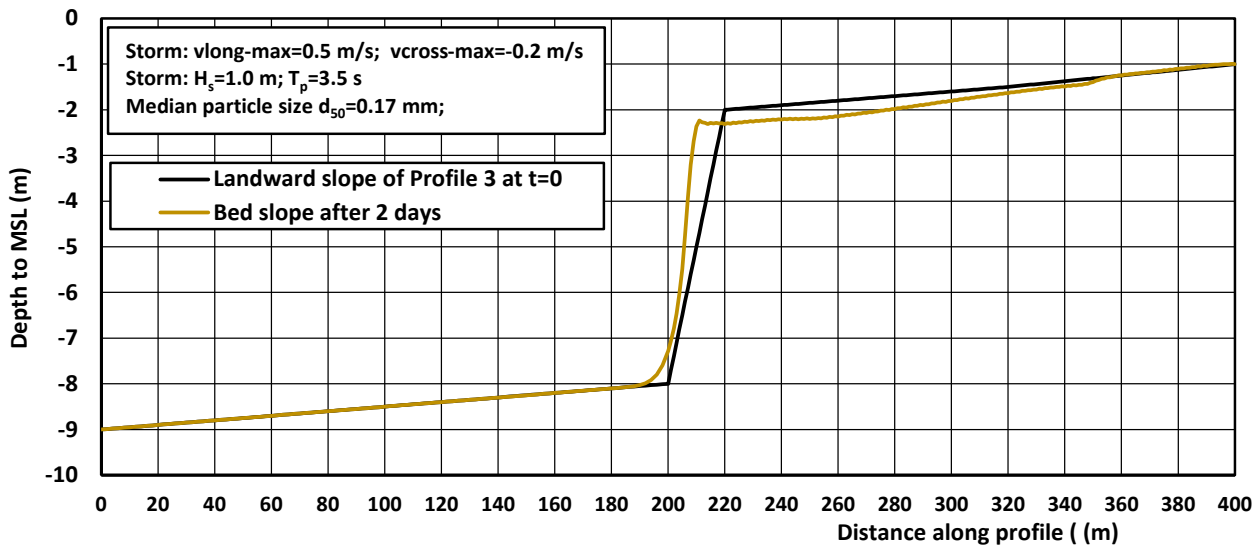


Figure 4.7.3 Computed bed profiles for storm conditions



4.8 Long term bed level changes Black Sea Coast of Romania

Bed profiles along the Romanian Black Sea coast are studied.

Tidal range ≈ 0.1 m

Mean sea level/Still water level (MSL/SWL) is 0.11 m above datum level MN₇₅.

Figure 4.8.1 shows the annual wave rose at the -10 m depth contour.

The annual wave rose data are schematized to a wave table of 9 conditions, see **Table 4.8.1**.

The extreme storm waves with return period of 1 and 100 years are given in **Table 4.8.2**. The other data are obtained by logarithmic interpolation. The storm duration is set to 1 day (24 hours).

The wave runup levels are computed from the equations of Stockdon et al. (2006) for natural beaches. The beach slope is assumed to be 1 to 20. The wave runup level including tide and surge is about 1.65 m during annual wave conditions (SLE), which is below the crest level at +3 m SWL.

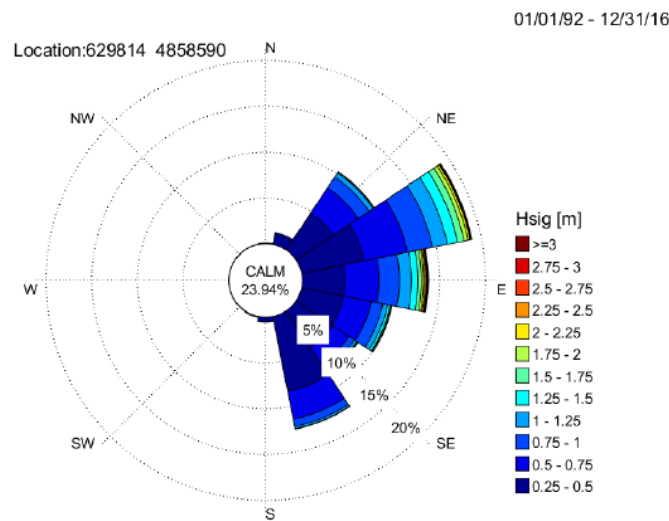


Figure 4.8.1 Wave rose at -10 m depth contour

Time period (days)	Significant wave height offshore $H_{s,o}$ (m)	Peak wave period T_p (s)	Wave direction to coast normal (°)	Surge water level above still water level (m)
0-75 (75)	0.6	5	-20	0
75-93 (18)	1.25	6	-20	0
93-102 (9)	2.0	7	-20	0.3
102-177 (75)	0.6	5	0	0
177-187 (10)	1.25	6	0	0
187-192 (5)	2.0	7	0	0.3
192-277 (85)	0.6	5	30	0
277-280 (3)	1.25	6	30	0
280-283 (3)	2.0	7	30	0.3



283-365 (82)	Calm < 0.5			
--------------	------------	--	--	--

Table 4.8.1 Schematized annual wave conditions offshore (no storms)

Return period (years)	Significant wave height offshore $H_{s,o}$ (m)	Peak wave period T_p (s)	Surge level above SWL (m)	Wave run up level above SWL including tide and surge levels (m)
1	3.5	9	0.6	1.65
10	5.8	10	0.7	2.20
25	6.6	11	0.8	2.60
50	7.4	13	0.9	3.10
100	8.0	15	1.05	3.60

Table 4.8.2 Extreme water level and wave data offshore location

The initial beach profile is shown in **Figure 4.8.2**.

Sand with a median diameter (d_{50}) of 0.2 mm is used as nourishment material.

The beach profile consists of:

- flat upper beach crest at about 3 to 3.5 m;
- beach slope of 1 to 20 above SWL (beach length of 60 to 70 m);
- sea bed slope of 1 to 60 between SWL and -4 m depth contour;
- transition slope of 1 to 15 between -4 m and -6.75 m depth at seaward end of nourishment zone;
- sea bed slope of 1 to 125 seaward of -6.75 m depth contour to offshore depth of -30 m.

The initial, artificial beach profile will be modified into a more natural profile by cross-shore and longshore transport processes.

Cross-shore transport processes are onshore-directed transport due to asymmetric shoaling waves and offshore-directed transport processes due to breaking waves generating a return current.

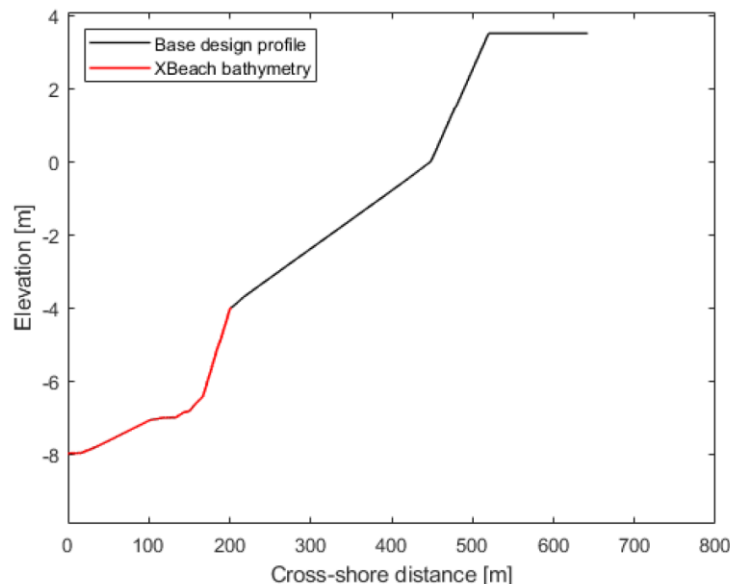




Figure 4.8.2 Typical beach profile

The beach profile requirements for a lifespan of 50 years are:

- beach width at level of + 2 m above SWL (Still Water Level) larger than 60 m in any section within the compartments between the groins during SLS-conditions;
- initial beach slope of 1 to 20 or milder above SWL;
- beach crest at minimum +3 m above SWL;
- initial beach slope of 1 to 60 or milder between 0 and -4 m below SWL;
- initial transition slope of 1 to 15 or milder between -4 m and original sea bed;
- uprush level ($R_{2\%}$) below + 3 m above SWL during SLE-conditions;
- beach recession less than 10 m at +2 m above SWL during SLE-conditions and less than 25 m during SLS-conditions.

SLE-conditions: Operation Limit State being the annual wave climate plus storm with return period of 1 year.

SLS-conditions: Service Limit State being the annual wave climate plus storm with return period of 100 years.

The following CROSMOR-runs have been made:

- short term runs over 1 day for storms with return period of 1 to 100 years;
- long term runs over 1, 3 and 5 years for annual wave climate (**Table 4.8.1**) with and without a storm with return period of 1 year;
- long term runs with a sequence of storm wave events with return periods between 1 and 100 years, representative for a period of 50 years.

The basic input data of the CROSMOR-model are given in **Table 4.8.3**.

PARAMETERS	VALUES
Tidal conditions at x=0	Time(s) Longshore-Current (m/s) Water level (m)
	no tide
	0 0.1 0.
	86400 0.1 0.
Water depth at deep water	30 m
Storm surge level above SWL (Still Water Level)	0 to 1.05 m
Slope of sea bottom	see Figure 3.1.1
Beach crest	3 to 3.5 m above SWL
Water depth at last grid point	0.3 m
Grid size and time step	1 to 10m; 100 to 900 s
Total traject length	3650 m (0, -30; 2000,-15; 3000, -8; 3160, -6.75; 3200, -4; 3440, 0; 3510, 3.5; 3650, 3.5)
Significant wave height at x=0; wave period	up to 8 m; up to 15 s
Wave direction at x=0 (to shore normal)	-20, 0 and +30 degrees
Number of wave classes per condition (to represent wave spectrum)	1
Wave asymmetry	Isobe-Horikawa
Coefficient Longuet-Higgins streaming roller effect	0.5 (default=1); 0.5 (default=1)
Sand grain size d_{50}	0.2 mm
Coefficients sand transport formulations	0.7 (default= 1)
Coefficient sand transport wave asymmetry	0.3 (default= 1)
Coefficient return flow (undertow)	1 (default)



Coefficient additional stirring of sand in beach-dune zone	1 (default; no effect)
Bed roughness	Automatic
Temperature and salinity	20 degrees and 30 promille
Files Rlot8-2.inp Rlot8-3.inp Rlot8-S.inp Rlot8SS.inp Rlot8SL.inp Rlot8SM.inp Rlot6S.inp Rlot11S.inp	long term; annual wave climate + 1 storm long term; annual wave climate; no storm short term; storm 1 day long term; storms 10 days (10 storms); each storm 24 hrs long term; storms 60 days (60 storms); each storm 24 hrs long term; storms 60 days (60 storms); each storm 12 hrs storm for Lot 6 storm for Lot11

Table 4.8.3 *Input data of CROSMOR-model*

Figure 4.8.3 shows the computed beach profiles after 1 day. Most changes occur in the nearshore nourishment zone (landward of $x=3200$ m). Minor changes occur at the seabed seaward of $x=3200$ m, where the onset of breaker bar formation can be seen. Minor storms create a breaker bar in the nourishment zone, whereas major storms carry most of the sand to the toe of the nourishment zone. The beach erosion is not very high for a short-duration period of 1 day, not even for the highest storm with $r=100$ years and a setup of 1.05 m as the beach slope is very flat 1 to 20 (dissipative beach). During the highest storm, a breaker bar is created at $x=3350$ m with crest at level of -1.7 m giving a water depth plus setup of $1.7+1.05=2.75$ m with a wave breaker height of about 1.5 m at about 100 m from the water line (at $x=3475$ m). These broken waves will lose some energy passing the nearshore bottom trough giving a wave breaker height at the -1 m of about 1 m. These conditions are not very severe for a fairly flat beach of 1 to 20. In practice, the beach erosion may be somewhat higher as the effect of long swash waves resulting in a higher uprush level are not included in the CROSMOR-model.

Beach erosion and recession values are given in **Table 4.8.4**.

The beach erosion above -1 m SWL is in the range of 7 to 60 m^3/m after 1 day.

The maximum beach recession at the still water line is about 25 m after 1 day.

Figure 4.8.4 shows beach profile changes after 2 to 10 days with extreme waves. The onset and development of breaker bars in the nearshore and offshore zone can be clearly seen.

Case (Lot 8)	Type of Storm	Erosion between -4 m SWL and -1 m SWL after 1 day (m^3/m)	Erosion above -1 m SWL after 1 day (m^3/m)	Recession at SWL after 1 day (m)	Recession at +2 m SWL after 1 day (m)
A1	Return period 1 year	70	7	2	0
A2	Return period 10 year	100	15	5	0
A3	Return period 25 years	100	25	10	0
A4	Return period 50 years	80	45	15	0
A5	Return period 100 years	80	60	25	1



Table 4.8.4 Erosion and recession values for extreme storms with duration of 1 day

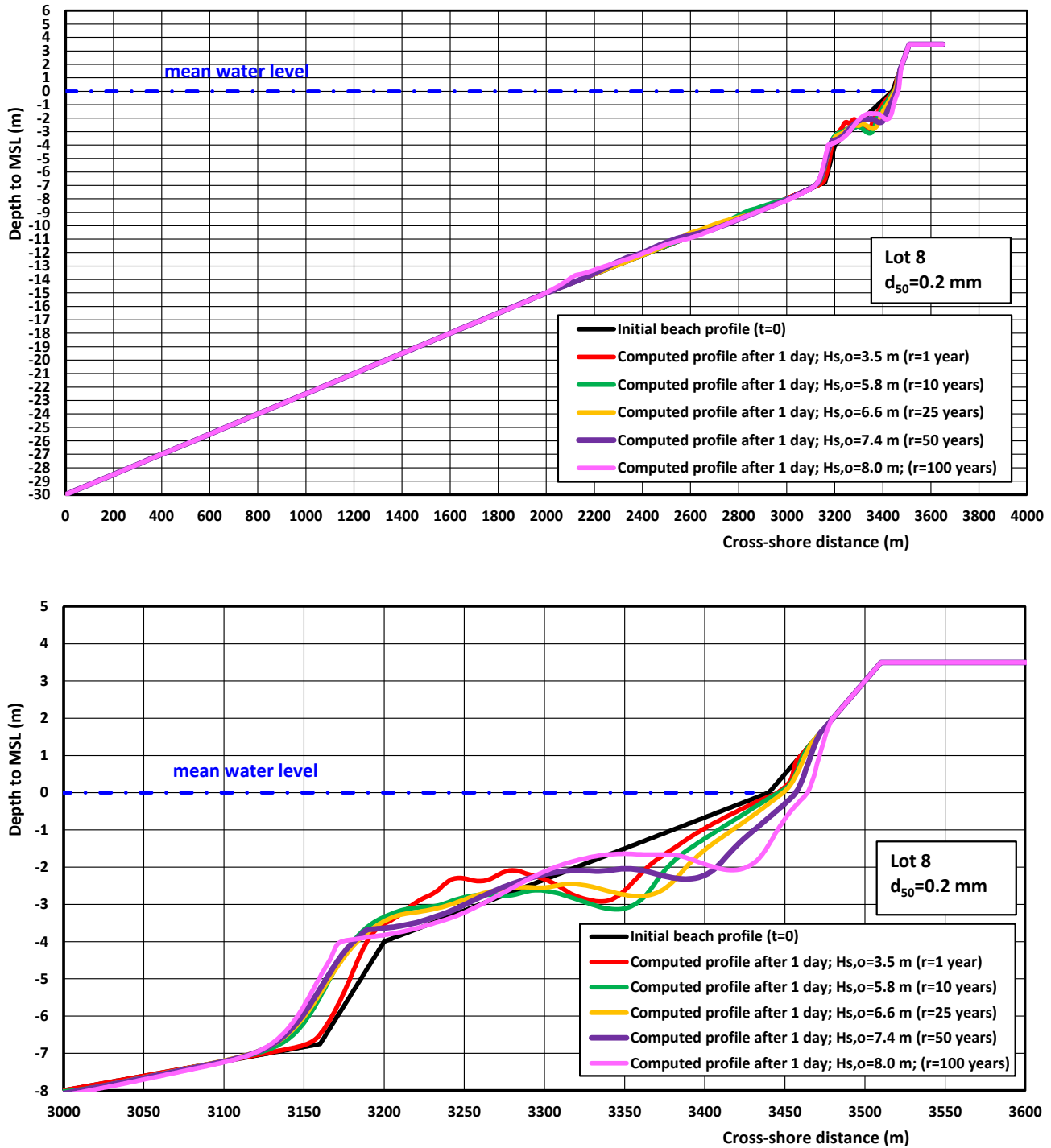


Figure 4.8.3 Computed beach profiles for extreme storms with duration of 1 day (Case A1 to A5); Upper: nearshore-offshore zone; Lower: nearshore zone

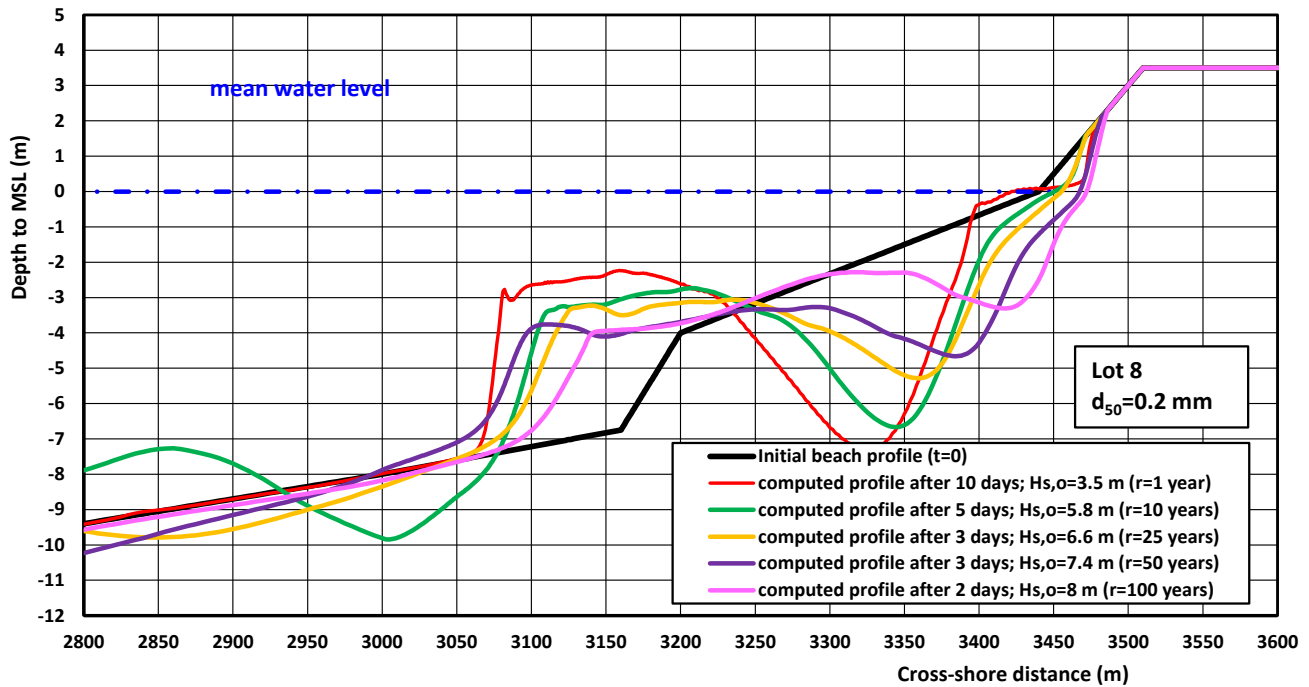
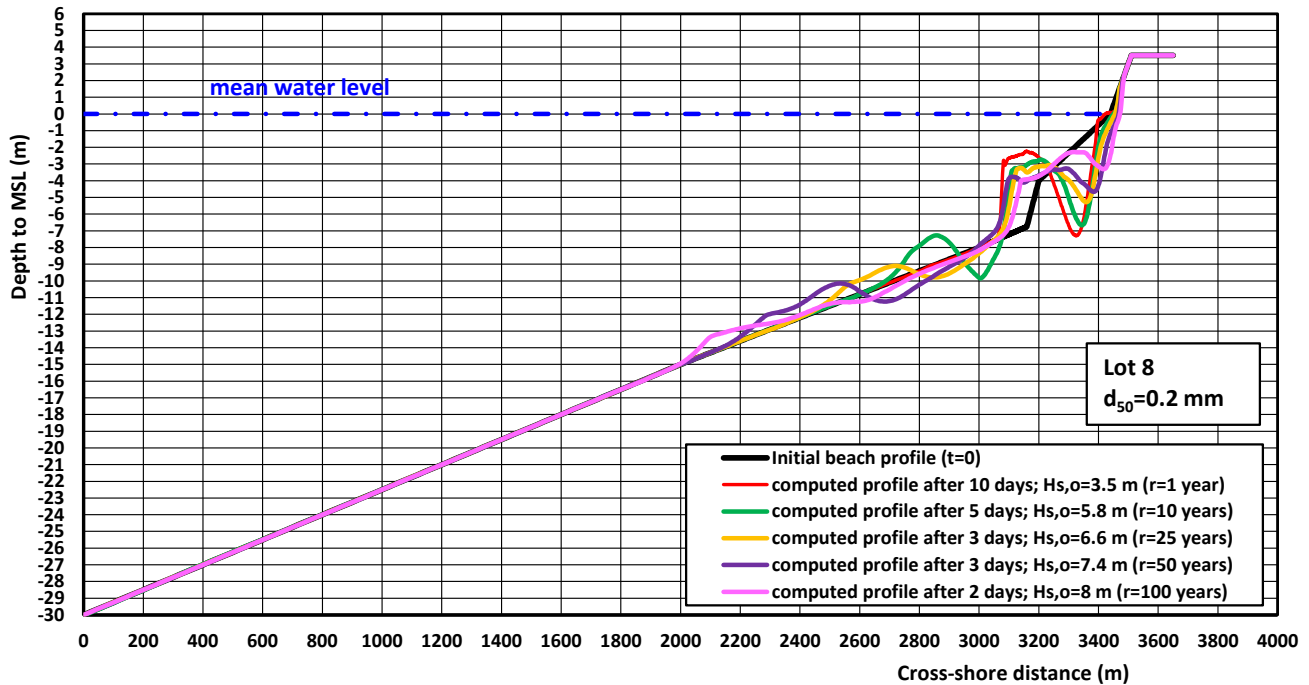


Figure 4.8.4 Computed beach profiles for extreme storms with duration of 2 to 10 days (Case A1 to A5);



Long-term erosion due to annual waves and storms

Long-term runs over a time scale of 50 years cannot yet be made by using the CROSMOR-model, because this leads to unrealistic results as the (smoothing) effects of alongshore transport processes are not included.

Therefore, a schematized approach has been used, as follows:

- Case B1, B2, B3: model run over 1, 3 and 5 years with annual wave climate of **Table 4.8.1**;
- Case C1, C2, C3: model run over 1, 3 and 5 years with annual wave climate + 1 storm (return period=1 year)
- Case D1, D2, D3: model run with 50 minor storms and 10 major storms: 50 storms with $r=1$ year; 6 storms with $r=10$ years, 2 storms with $r=25$ years, 1 storm with $r=50$ years and 1 storm with $r=100$ years; each storm has duration of 24 hours for D1 and D2 and 12 hours for D3; 2 different sequences of wave events have been used (wave input data are given in **Table 4.8.5**).

Figure 4.8.5 shows the computed beach profiles after 1, 3 and 5 years for an annual wave climate without storms. The erosion volumes and beach recession values are largest after the first year and are less for a period of 3 and 5 years, see **Table 4.8.6**. This reduction effect is caused by the growth of a pronounced breaker bar at the toe of the nourishment zone ($x=3200$ m), which becomes a focus point for wave breaking and thus protects the beach against extreme erosion. The breaker bar grows by onshore-directed transport at the seaward flank due to shoaling waves and offshore-directed transport on the landward flank of the bar due to breaking waves plus return currents (see yellow arrows in **Figure 4.8.5**). Onshore transport in the zone between -1 and -3 m may also occur during conditions with low waves, but this effect is overruled by seaward transport due to higher waves resulting in net erosion in this zone. The time scale of bar generation is of the order of 0.5 to 1 year based on the CROSMOR-results. The bar migrates slowly in seaward direction, which is a typical phenomenon of breaker bar along the Dutch North Sea coast and also elsewhere. The height of the offshore breaker bar is overestimated (by about 30%) by the CROSMOR-model as various smoothing effects are not taken included (alongshore transport and redistribution of sand within the compartment between the groins).

A fairly stable terrace with a length of about 50 m is formed in the nearshore zone (at depth of about -0.5 m). The beach face is steepening in the zone above -1 m SWL due to erosion processes. Terrace formation and beach face steepening (even beach scarping) are typical features after nourishment at sites with a constant water level (lakes, non-tidal seas). In practice, the beach face slope will be somewhat milder (1 to 7) due to the smoothing effect of swash processes, not included in the model. The nearshore terrace may also move onshore during a long period with very low waves <0.6 m. This process with long periods of low waves has been neglected in these simulations.

The predicted beach erosion above -1 m SWL after 5 years is about $50 \text{ m}^3/\text{m}$ or $10 \text{ m}^3/\text{m}/\text{year}$ (**Table 4.8.6**).

Figure 4.8.6 shows the computed beach profiles after 1, 3 and 5 years for an annual wave climate plus a storm with a return period of 1 year (Case C). The beach erosion volumes are somewhat higher ($75 \text{ m}^3/\text{m}$ or $15 \text{ m}^3/\text{m}/\text{year}$) than those of Case B ($50 \text{ m}^3/\text{m}$) due to the inclusion of a minor storm, see **Table 4.8.6**.

Figure 4.8.7 shows the computed beach profiles for a series of storm waves representative for a period of 50 years. The sequence of the storm wave events has been varied (Case D1 with a sequence of low to high storm waves over time and Case D2 with a more variable sequence of storm events over time). Beach erosion and beach recession are given in **Table 4.8.6**. The beach erosion is substantially smaller (160 m^3) for Case D1 compared to that (380 m^3) for Case D2, because a major breaker bar is already present before the occurrence of major storm at the end of the period for Case D1. In Case D2, major storm events also occur in the early phase of the sequence of wave events when the breaker bar is not yet fully developed. The outer bar is a new bar generated by the storm waves and is positioned more offshore of the bars in **Figure 4.8.5** and **4.8.6**. The sand of this outer bar is eroded from the zone below the -6 m depth line and does not require compensation by nourishment. The outer bar trough below -6 m may even be redeposited during conditions with milder waves.



In reality, the outer breaker bar will be lower and more rounded compared to the computed bar which becomes peaked to the onshore transport at the seaward flank.

Case D1				Case D2			
Time (s)	Time (days)	Hs,o (m)	Return period (years)	Time (s)	Time (days)	Hs,o (m)	Return period (years)
0- 4320000	50	3.5	1	0-864000	10	3.5	1
4320001-4838400	6	5.8	10	864001-1036800	2	5.8	10
4838401-5011200	2	6.6	25	1036801-1123200.	1	6.6	25
5011201-5097600	1	7.4	50	1123201-1987200.	10	3.5	1
5097601-5184000	1	8.0	100	1987201-2160000.	2	5.8	10
				2160001-2246400.	1	6.6	25
				2246401-3110400.	10	3.5	1
				3110401-3283200.	2	5.8	10
				3283201-3369600.	1	7.4	50
				3369601-4233600.	10	3.5	1
				4233601-4320000.	1	8.0	100
				4322001-5184000.	10	3.5	1

Table 4.8.5 Wave input data for CROSMOR-model; Case D1 and D2

Case	Wave climate	Time period (years)	Nearshore erosion between -1 m SWL and crest at +3 m SWL (m ³ /m); (m ³ /m/year)	Beach recession at SWL (m); (m/year)	Beach recession at SWL+2 (m); (m/year)
B1	Annual wave climate	1	20; 20	20; 20	0; 0
B2	Annual wave climate	3	35; 12	25; 8	0; 0
B3	Annual wave climate	5	50; 10	30; 6	3; <1
C1	Annual wave climate + 1 storm with return period of 1 year	1	30; 30	25; 25	0; 0
C2	Annual wave climate + 1 storm with return period of 1 year	3	50; 17	35; 12	0; 0
C3	Annual wave climate +1 storm with return period of 1 year	5	75; 15	35; 7	3; <
D1	Sequence of 60 storms (60 days) representative for 50 years; duration of each storm=24 hrs	50	160; 3 (0 between -1 and -3 m)	50; 1	30; < 1
D2	Sequence of 60 storms (60 days) representative for 50 years; duration of each storm=24 hrs	50	380; 7.5 (110 between -1 and -3 m)	100; 2	70; 1.5
D3	Sequence of 60 storms (30 days) representative for 50 years; duration of each storm=12 hrs	50	220; 4.6 (250 between -1 and -4 m)	60; 1.2	30; 0.6

Table 4.8.6 Predicted erosion and recession values for Case B, C and D

Each storm of Case D1 and D2 has a duration of 24 hours, which is quite conservative. A more realistic storm duration is 12 hours, which is used for Case D3. This yields a much smaller erosion volume of 220 m³/m above the -1 m depth line. The beach recession at + 2 m is maximum 70 m for D2 and maximum 30 m for D1 and D3. Case D3 yields the highest erosion (250 m³/m) between -1 m and -4 m.

The average erosion of Cases D1 to D3 between -4 m and +3 m is $(160+490+470)/3= 380\pm 150$ m³/m.



An estimate of the total beach erosion over a period of 50 years due to cross-shore transport processes can be best obtained by quadratic summation of the erosion results for the annual waves (Case B3) and the storm waves (Case D2) yielding: $[(50 \times 10)^2 + 380^2]^{0.5} \cong 650 \pm 250 \text{ m}^3/\text{m}$. The maximum erosion is obtained by linear summation giving a value of about $900 \text{ m}^3/\text{m}$ for 50 years.

Most of the erosion is estimated to occur above the -3 m depth line. The predicted beach erosion results are conservative values, as a storm duration of 12 to 24 hours is fairly long. The peak of the storm generally has a duration of 6 to 12 hours (Vellinga, 1986). Furthermore, a sequence of 60 successive storms is not very realistic and does not include beach recovery due to daily waves. In practice, a beach terrace in the zone between the -1 and -2 m depth line will be present creating a sand buffer for the stormy seasons.

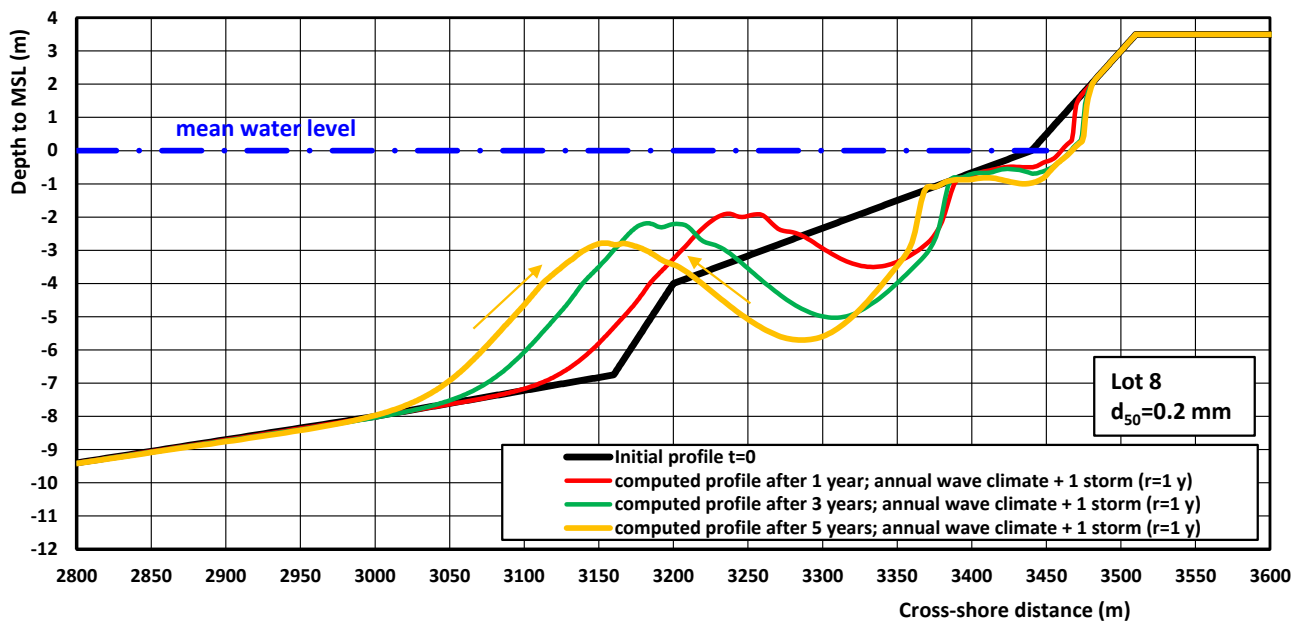
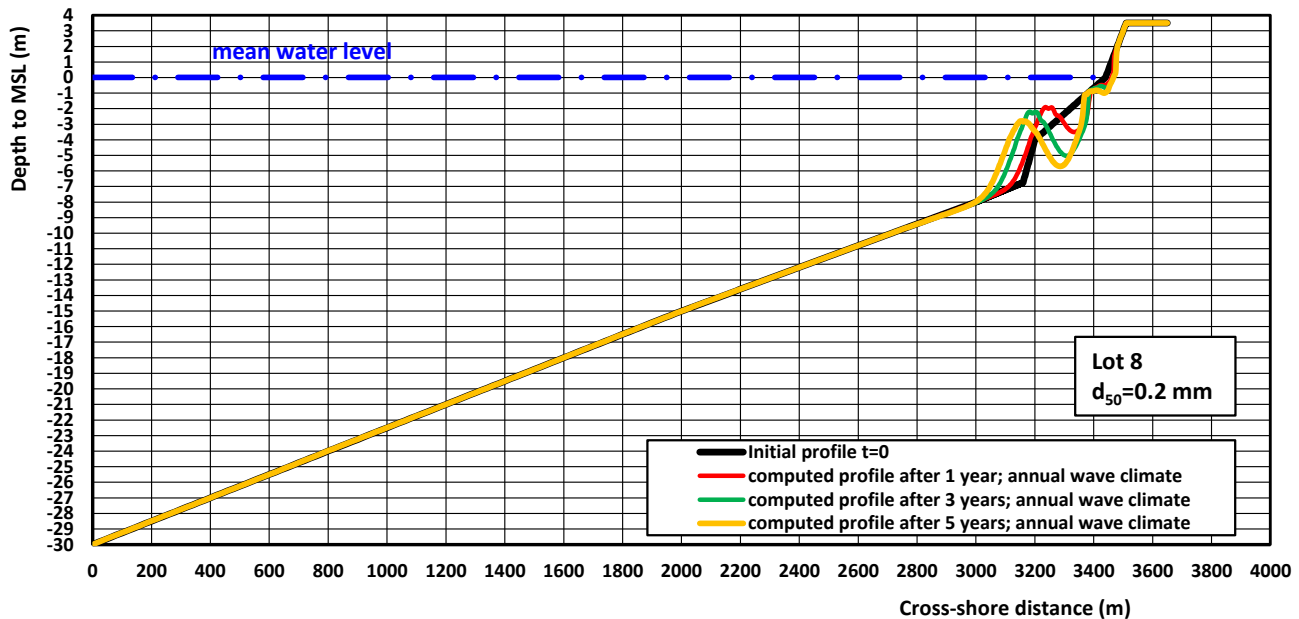


Figure 4.8.5 Computed beach profiles for 1 to 5 years for annual wave climate (no storms); Case B

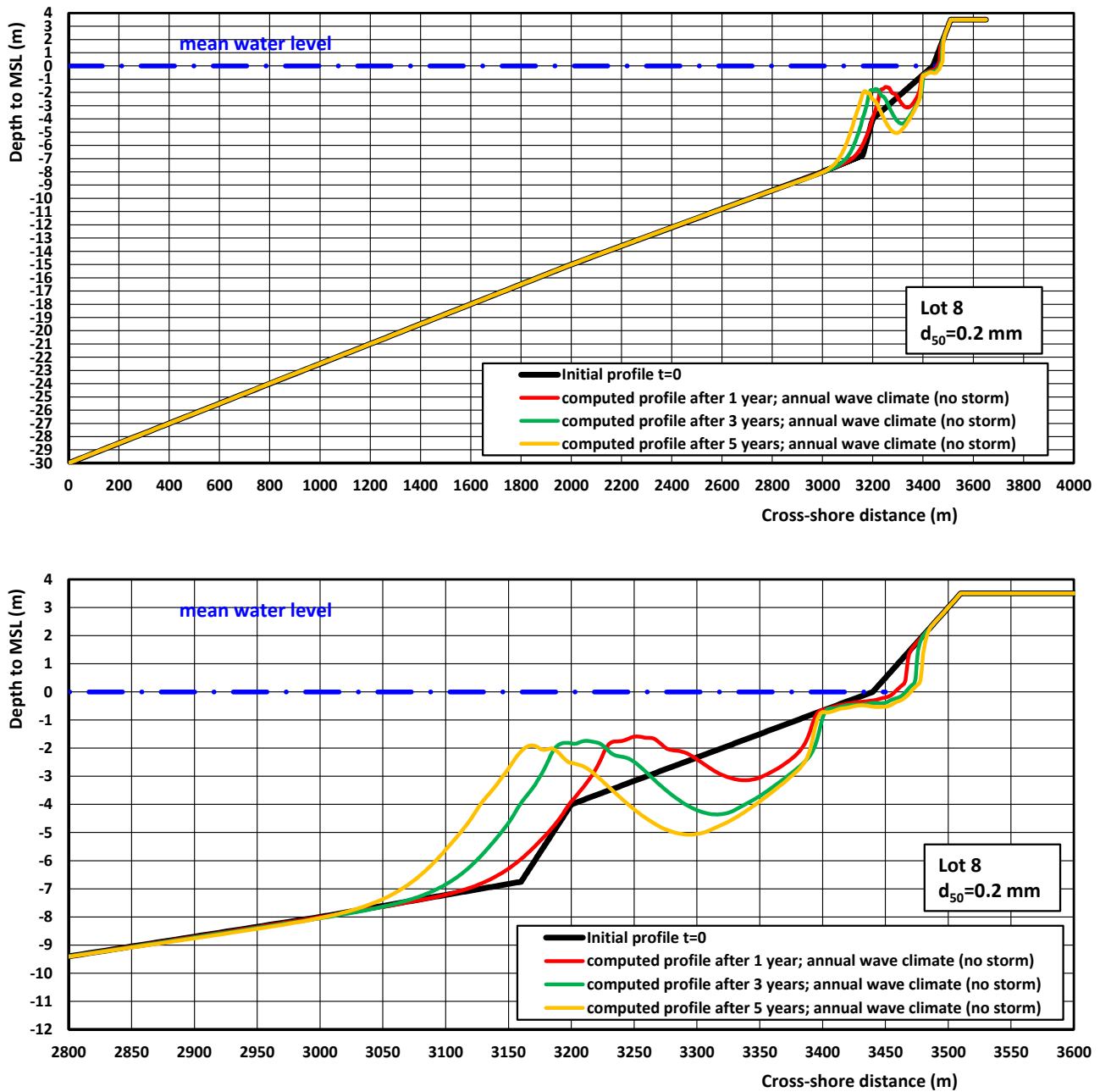


Figure 4.8.6 Computed beach profiles for 1 to 5 years annual wave climate + 1 storm ($r=1$ year); Case C

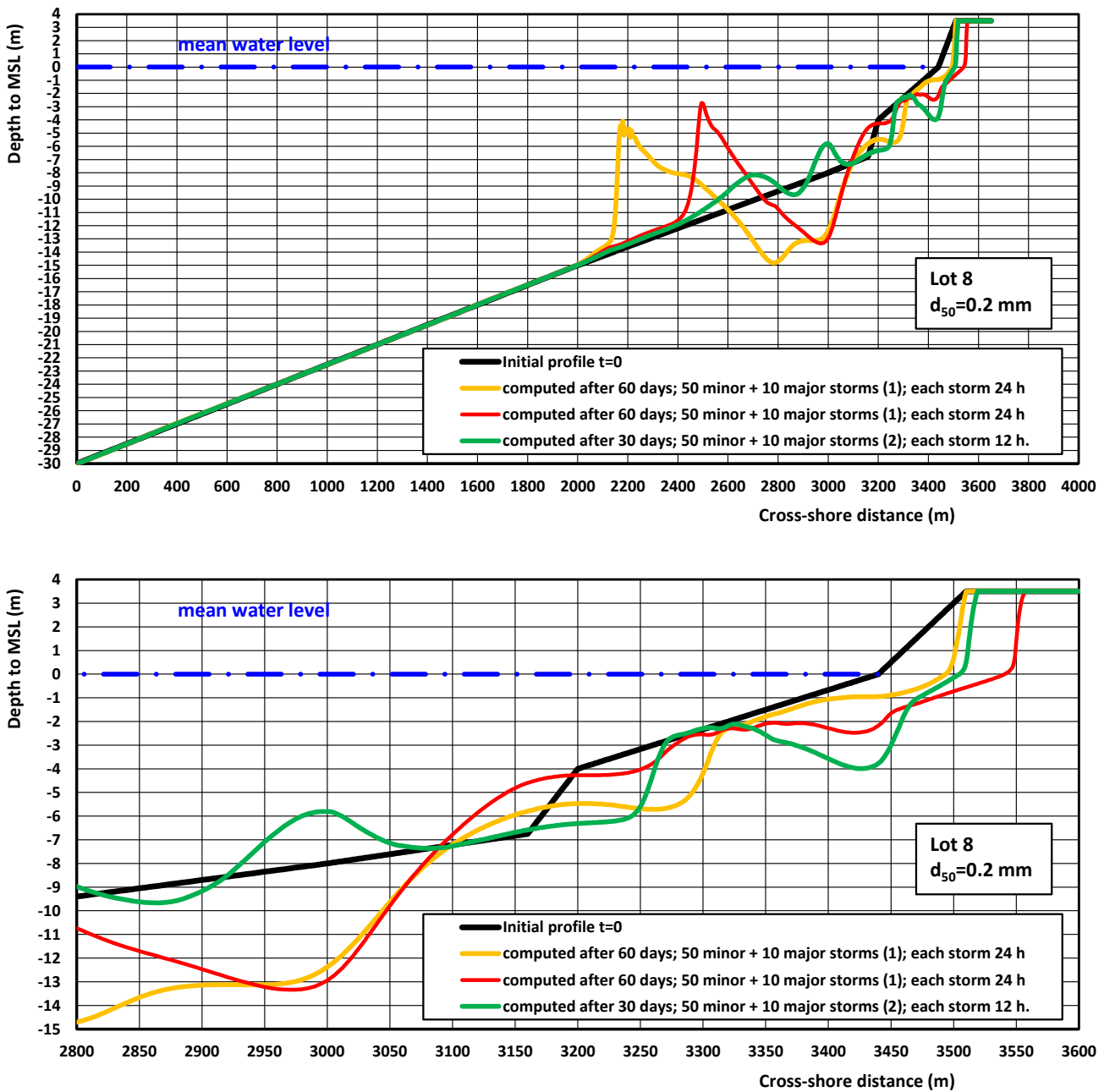


Figure 4.8.7 Computed beach profiles for 60 storms representative for a period of 50 years



4.9 Effect of runup level, sand particle size and gradation coefficient on beach erosion

4.9.1 Introduction

Many artificial beaches of sand are designed along the Arabian Gulf, see **Figure 4.9.1**. The Arabian Gulf is a strategically important and very active marine area that includes the largest offshore oil and gas fields in the world. The Arabian Gulf is an extension of the Indian Ocean through the Strait of Hormuz. The total area of the gulf is approximately 226,000 km². It is 990 km long and varies in width from 56 to 338 km with an average depth of about 35 m, separating Iran from the Arabian Peninsula. In the UAE's territorial waters in the Arabian Gulf, the water depths extend to a maximum of 50 m.

An important aspect of artificial beach design is the beach erosion due to annual waves and extreme storm waves and associated beach maintenance.

Parameters influencing the beach erosion are: i) runup level, ii) particle size of beach sand and iii) gradation coefficient (c_u) of beach sand.



Figure 4.9.1 Dubai coast; Elkersh et al. (2022)

4.9.2 Environmental conditions

Tidal currents

The tides along the coast of Dubai are semi-diurnal with a mean tidal range of about 1.3 m; MHHW is 0.7 m above MSL, MLLW is -0.6 m MSL; LAT is -1.2 m MSL (MSL is 1 m above Chart Datum (mCD); Dubai Municipality Datum (mDmd) is 1.1 m above Chart Datum). Storm surge levels are roughly estimated to be about 0.5 m (annual) up to 1.0 m (once per 100 years). Sea Level Rise over 50 years may be about 0.5 m.

Based on tidal modelling results in various other projects, the maximum tidal currents near the shore are up to 0.3 m/s during springtide and below 0.1 m/s during neap tide.



Waves

A broad understanding of the wave climate at the Dubai coast can be obtained from the work of Elkersh et al. (2022). This paper presents the results of extreme wave analysis distribution methods applied to a long-term wave hindcast at a point (at depth of 15 m) in the Arabian Gulf near the coastline of Dubai, United Arab Emirates. The wave data were hindcasted for a total period of 40 years, starting from 1 January 1979 to 31 December 2018. The numerical model is forced with Climate Forecast System Reanalysis (CFSR) wind fields from the National Centers for Environmental Prediction (NCEP) reanalysis dataset, which is available from January 1979 to 2010. The hindcast is developed using a SWAN wave model, which is validated against a set of field measurements and satellite altimeter data. This hindcast is composed of hourly spectral wave data that specify significant wave height, peak wave period, and peak wave direction. A 2.5 m threshold is selected using the Peak Over Threshold method to filter the storm data for the extreme wave analysis. Different distribution methods are used for this analysis such as Log-normal, Gumbel, Weibull, Exponential, and Generalized Pareto Distribution (GPD). The significant wave heights are predicted for different return periods. The GPD distribution appears to fit the data best compared to the other distribution methods. The main wave direction is from north-west (sector 270°-300° to North). In general, the northwest direction is the most dominant wave direction in the Arabian Gulf. Therefore, the wave data are filtered by wave direction to consider only the waves coming from the most critical direction (northwest) to be used in the extreme wave analysis, which makes the analysis more specific. On the other hand, by considering all directions, minor or no changes might be seen in the results as the waves coming from the other directions are much smaller compared to the northwest direction.

Figure 4.9.2 shows a plot of the significant wave heights of the ordered 113 storm events. Each isolated storm is represented by its peak wave height. The distribution models were used to extrapolate and predict the wave heights for different return periods as shown in **Table 4.9.1**. It is herein assumed that the nearshore wave height (say at depth of 5 to 10 m below MSL) are 50% of the offshore wave heights at depth of 20 to 30 m.

Return period	Offshore wave climate 270°-300°	Nearshore wave climate 270°-300°
Annual	$H_{s,o} = 2.95\text{-}3.05\text{ m}; T_p = 8.0\text{ s}$	$H_{s,nearshore} = 1.5\text{ m}; T_p = 8.0\text{ s}$
20 years	$H_{s,o} = 3.8\text{-}4.2\text{ m}; T_p = 8.5\text{ s}$	$H_{s,nearshore} = 2.0\text{ m}; T_p = 8.5\text{ s}$
50 years	$H_{s,o} = 4.0\text{-}4.6\text{ m}; T_p = 8.5\text{ s}$	$H_{s,nearshore} = 2.15\text{ m}; T_p = 8.5\text{ s}$
100 years	$H_{s,o} = 4.1\text{-}4.9\text{ m}; T_p = 9.0\text{ s}$	$H_{s,nearshore} = 2.25\text{ m}; T_p = 9.0\text{ s}$

Table 4.9.1 Wave statistics

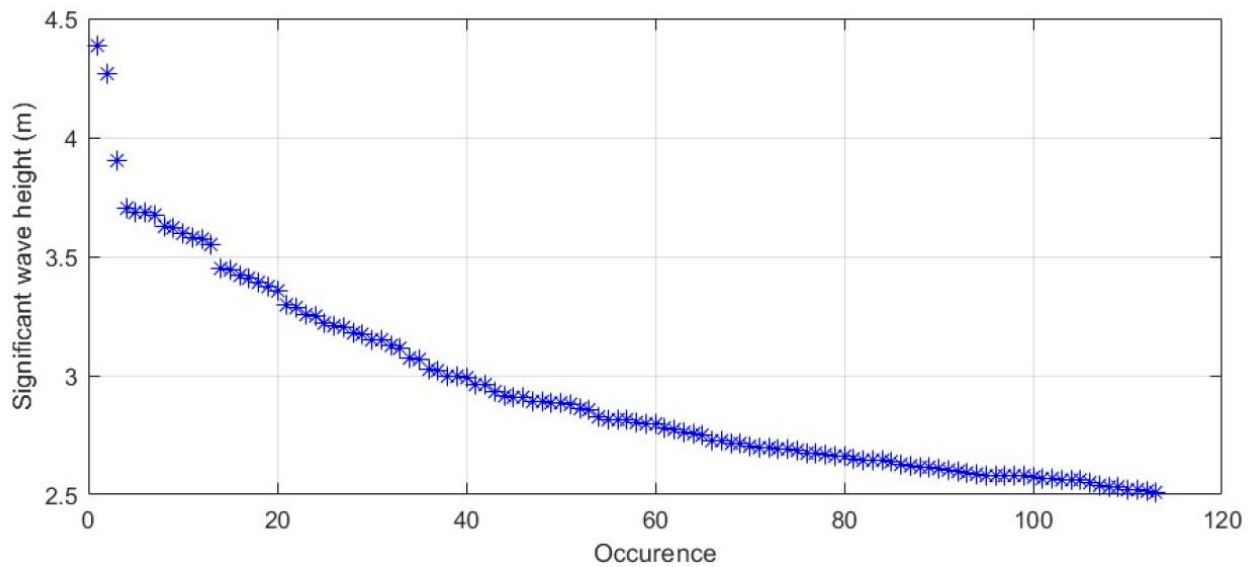


Figure 4.9.2 Offshore significant wave height for 113 storm events; Elkersh et al. (2022)

4.9.3 General requirements for artificial beach sand

Generally the requirements for good quality beach sand for artificial beaches are as follows:

- good permeability for drainage of the beach sand in a tidal regime with rising and falling water levels;
- stable material with high erosion resistance;
- aesthetic appearance in accordance with that of local beaches (generally: white sands with low content of gravels and silts).

Natural sand mixtures are inherently non-uniform, which means that the sand mixture consists of several (multiple) sand fractions with slightly different particle sizes, as expressed by the particle size distribution (psd-curve). To compare different types of beach materials, usually the particle size distribution (psd) is used.

Basic parameters of the psd-curve are: 1) median particle diameter (d_{50}), 2) uniformity coefficient ($c_u = d_{60}/d_{10}$) and 3) grading coefficient $c_c = (d_{30})^2 / (d_{60} d_{10})$. Poorly graded (or well-sorted) sand has $c_u < 3$ and $c_c < 1.3$.

The uniformity of natural sands strongly depends on the median particle size (d_{50} -value). Practice shows that finer sands are more uniform than coarser sands. Thus, the c_u -value increases for increasing median particle sizes (coarser sand). Practical values are given in **Table 4.9.2**. From this table you can observe:

- very fine sands with $d_{50} < 0.2$ mm generally have c_u -values < 2.5 .
- coarser sands with d_{50} of about 0.5 mm generally have c_u -values ≥ 3 .

Very uniform coarse sand with d_{50} of about 0.5 mm and $c_u < 2$ is very difficult to find in nature. It can be made artificially by removing (sieving) the very fine and the very coarse fractions, but this is an intensive and time-consuming operation.

The requirement of the client: $0.3 < d_{50} < 0.5$ mm with $c_u < 2$ is too strict for natural sands and may be better replaced by:

- $0.2 < d_{50} < 0.3$ mm with $c_u < 2.5$;
- $0.3 < d_{50} < 0.4$ mm with $c_u < 2.75$;
- $0.4 < d_{50} < 0.5$ mm with $c_u < 3$.



Sand	d_{10} (mm)	d_{30} (mm)	d_{50} (mm)	d_{60} (mm)	d_{90} (mm)	c_u (-)	c_c (-)
fine	0.1	0.15	0.2 (0.1-0.25)	0.25	0.5	2.5	0.45
medium fine	0.15	0.2	0.3 (0.25-0.5)	0.4	0.8	2.7	0.7
coarse	0.25	0.45	0.6 (0.5-1)	0.75	1.5	3.0	1.1
very coarse	0.35	0.7	1.0 (1-1.5)	1.2	2.0	3.4	1.2

Table 4.9.2 Practical sand parameters

Beach permeability: The permeability of beach sand strongly depends on the porosity of the sand and the porosity in turn depends on the uniformity coefficient (c_u) of the sand material, see **Figure 4.9.3**. The porosity is fairly constant at about 0.34-0.36 for sand with $c_u < 3$. The porosity decreases rapidly for more graded sand with fine particles in the voids of larger particles, particularly for $c_u > 4$.

Graded sand with some content of fines have a very low porosity and thus a low permeability. The beach sand will then drain slowly or may even remain wet at beach depressions promoting algae development etc.

From this it can be concluded that the c_u values in the range from $2 < c_u < 3$ the beach permeability is not strongly affected and will have negligible impact on the drainage capacity of the beach.

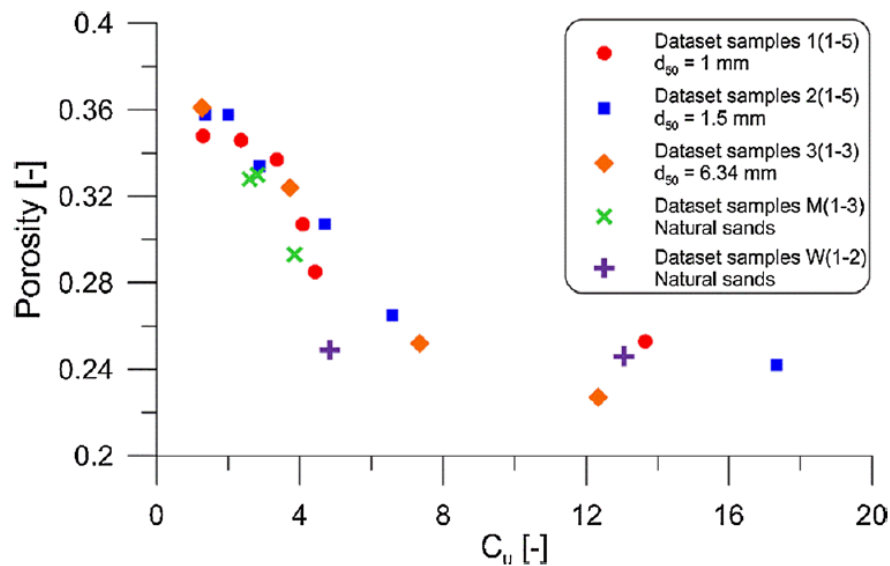


Figure 4.9.3 Relationship between porosity of sand and uniformity coefficient c_u (Lopik et al, 2019.)

Beach stability: Beaches are more stable with less erosion if the beach material consists of coarser sand ($d_{50} \approx 0.5$ mm). Beaches of medium fine sand ($d_{50} \approx 0.2-0.3$ mm) are less stable with more erosion under the same wave climate and thus require more maintenance (sand nourishment).

Natural sands are non-uniform with different size fractions and thus the sand transport and erosion/deposition processes should be computed by using multi-fraction methods (MF-method), which is rather problematic as



simple and generally-accepted MF-methods are not available. The MF-approach was explored by Van Rijn (2007) in comparison with the single fraction (SF) method based on the d_{50} of the psd. Van Rijn (2007) found that the results of MF-methods are fairly similar (somewhat higher) to that of the SF-method for sands with $d_{50} < 0.5$ mm. Generally, the sand transport of slightly more graded sand (higher c_u -value of 2.5 instead of 2) is somewhat higher, but this is mostly within the inaccuracy range of the sand transport formulae involved. It is noted that present methods for computation of sand transport and beach erosion are based on the assumption of almost uniform sand represented by the d_{50} of the psd-curve. The c_u -value is not taken into account by most models.

As regards beach stability, it is better to use coarse sand with $0.4 < d_{50} < 0.5$ mm and $c_u < 3$ than fine sand with $0.2 < d_{50} < 0.3$ mm and $c_u < 2$, because the impact of the median grainsize (d_{50}) is much bigger than the impact of the c_u (see also next sections)

4.9.4 Effect of graded sand on sand transport

General

Sand transport and coastal erosion of artificial beaches with slightly graded beds are studied in this section. Three types of graded beds are distinguished and methods to compute the sand transport rate and coastal erosion are given for each type of bed. Coastal erosion of beaches consisting of graded sand is studied by performing a series of CROSMOR-model runs with different values of the c_u -coefficient.

Graded beds

Three types of sand beds are herein distinguished (see also **Table 4.9.3**):

- uniform sand beds with c_u in the range of 2 to 2.5;
- quasi-uniform sands bed with c_u in the range of 2.5 to 4;
- non-uniform sand beds with $c_u > 4$.

Bed load transport (q_b) and Suspended sand transport (q_s)	Uniform sand $c_u=2$ to 2.5	Quasi-uniform sand $c_u=2.5$ to 4	Non-uniform sand $c_u > 4$
Approach	Single fraction method (SF) based on median diameter d_{50} and fall velocity w_s of bed material $q_s = \text{function}(d_{50}, w_s, \dots)$	Single fraction method based. Bed load depends on median diameter d_{50} and fall velocity w_s of bed material. Suspended load depends on d_{50} of bed material and on suspended sediment size d_s and corresponding fall velocity w_{ss} $q_s = \text{function}(d_{50}, d_s, w_{ss}, \dots)$	Multi-fraction method (MF) $q_s = \sum_{i=1}^N (d_{i,\text{mean}}, w_{si,\text{mean}}, \dots)$ summation over N-fractions

Table 4.9.3 Sand transport along a bed of uniform, quasi-uniform and non-uniform sand particles

In the case of a sand bed consisting of uniform sand particles, all sand particles have approximately the same size and the sand transport (bed load and suspended load) only depends on the median sand diameter (d_{50}) and



fall velocity (w_s) of the bed material. The d_{50} and the fall velocity of the single fraction (SF) are used to compute the sand transport rate (SF-method).

In the case of a sand bed consisting of non-uniform sand particles (graded sand), there is a relatively large proportion (fraction) of finer and coarser particles, which cannot be represented by the median sand diameter. In these conditions it is necessary to compute the overall sand transport for each individual sand fraction using the mean sand diameter of each fraction and make a summation of each transport contribution over all fractions. This procedure is known as the multi-fraction method (MF-method). At present stage of research, no generally accepted MF-method is available (Van Rijn 2007). Given the complexity of this method and the associated book-keeping process of fractions in the bed, it is not much applied in most numerical morphodynamic coastal models. In the case of a sand bed consisting of quasi-uniform sand particles, the SF-method is mostly applied with a correction to include the effect of the finer fraction resulting in slightly higher sand transport rates (Van Rijn, 1984). The correction factor for river flow conditions was determined by Van Rijn (1984) using the multi-fraction method (MF) for a medium fine sand bed with $d_{50}=0.25$ mm. Two types of gradings were distinguished: $\sigma_s=0.5(d_{84}/d_{50}+d_{16}/d_{50})=1.5$ and 2.5 ($\sigma_s \cong 0.6c_u$; thus: $c_u \cong 2.5$ and 4). The MF-method was applied to both types of sand for a range of depth-averaged flow velocities (0.5 to 1.5 m/s). Using the SF-method for the same cases, it was tried to find the same transport rates by varying the representative size (d_s) of the suspended sediments. The d_s -values for river flow conditions can be described by:

$$d_s/d_{50}=1+0.011(\sigma_s-1)(T-25) \quad (4.9.1)$$

with: d_s =representative size of suspended sediments; σ_s =gradation parameter, $T=(\tau_b-\tau_{cr})/\tau_{cr}$, τ_b =bed-shear stress, $\tau_{b,cr}$ = critical bed-shear for initiation of motion based on Shields' curve.

Depending on the gradation parameter and the flow strength (bed-shear stress parameter), the suspended size d_s varies approximately in the range of $d_s \cong 0.6d_{50}$ to $d_s \cong d_{50}$. At low flow strength and a wide grading, only the very fine sand particles are winnowed from the bed resulting $d_s \cong 0.6d_{50}$. At very high flow strength ($T \cong 25$), all sand particles from the bed go into suspension resulting in $d_s \cong d_{50}$.

Using this correction SF-method, a better representation of the suspended load can be obtained in the case of a weakly graded bed (quasi-uniform sand).

Two similar functions are implemented in the CROSMOR-model (single fraction approach) for the computation of coastal erosion, as follows:

$$d_s/d_{50}=1 + 0.0006(c_u-1)^{0.5}(M-550) \quad (4.9.2a)$$

$$d_s/d_{50}=1 - 0.2(c_u-1)^{0.5} \quad (4.9.2b)$$

with: $c_u=d_{60}/d_{10}$ =uniformity coefficient, $M=[(U_R^2+V_L^2)^{0.5}]/[(s-1)gd_{50}]$ =mobility parameter, U_R =cross-shore return current; V_L =longshore current, $s=\rho_s/\rho_w$ =relatively density, g =acceleration of gravity, d_{50} =median particle diameter.

The reference suspended sand concentration (c_a) is multiplied with a factor $f=(c_u-1)^{0.1}$ resulting in a small increase of the c_a -value for increasing c_u -values (more graded sand; 15% increase for $c_u=5$).

Equation (4.9.2a) being the standard function of the CROMOR-model is shown in **Figure 4.9.4** for various values of the c_u -coefficient. The ratio d_s/d_{50} is relatively small for low mobility parameters and increases to 1 for very high mobility parameters. The ratio d_s/d_{50} decreases for increasing c_u -values (more graded sand), because more fine sediments of the bed material are available for erosion and entrainment into suspension (winnowing of fines).



Using Equation (4.9.2b), the d_s -value only depends on the c_u -coefficient and not on the mobility parameter. This gives: $d_s=d_{50}$ for $c_u=1$, $d_s=0.8d_{50}$ for $c_u=2$, $d_s=0.6 d_{50}$ for $c_u=5$ and $d_s=0.4 d_{50}$ for $c_u=10$.

In coastal conditions with wave attack on a sloping beach, the mobility parameter M generally is fairly high in the range of 250 to 500 for medium fine sediments with c_u of 2 to 3, particularly in storm conditions. Most likely, the representative particle d_s is close to the value of the d_{50} ($d_s=0.8$ to $1 d_{50}$) resulting in slightly higher sand transport values for coastal conditions. Equation (3.2a) is most valid for coastal conditions. Both functions are used herein for comparative computations.

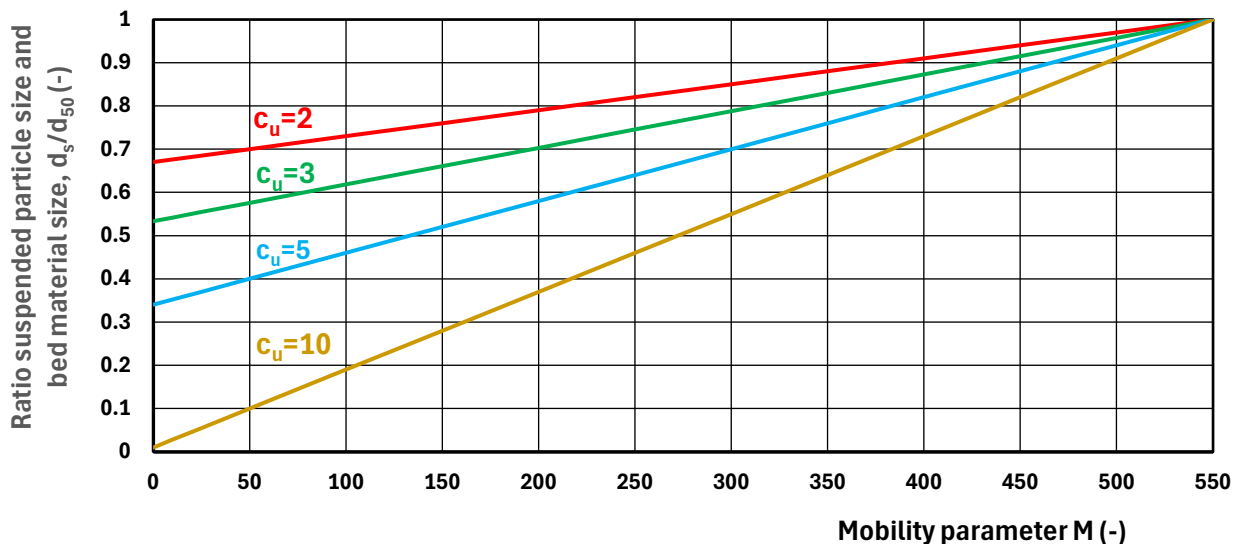


Figure 4.9.4 Dimensionless suspended particle size as function of uniformity coefficient and mobility parameter (Equation 4.9.2a)

4.9.5 Model, boundary conditions and settings

The detailed CROSMOR-model of LVRS-Consultancy has been used to compute the beach erosion for various alternative cases of exposed beaches, see **Table 4.9.4**.

Annual wave conditions for 1 year and storm wave conditions for 1 day are considered, see **Table 4.9.5**.

The CROSMOR-model is a 1D-numerical (Fortran) model comprising sub-models for wave propagation, tidal currents, cross-shore and longshore sediment transport and cross-shore bed level changes on time scales up to 5 years (Van Rijn et al., 2003).

The propagation and transformation of individual waves (wave by wave approach) along the cross-shore profile is described by a probabilistic model solving the wave energy equation for each individual wave. The individual waves shoal until an empirical criterion for breaking is satisfied. The default wave breaking coefficient is represented as a function of local wave steepness and bottom slope. Wave height decay after breaking is modelled by using an energy dissipation method. Wave-induced set-up and set-down and breaking-associated longshore currents are also modelled. Laboratory and field data have been used to calibrate and to verify the model. The complicated wave mechanics in the swash zone is not explicitly modelled, but taken into account in a schematized way.

The cross-shore wave velocity asymmetry under shoaling and breaking waves is described by the semi-empirical method of Isobe and Horikawa (1982). Near-bed streaming effects are modelled by semi-empirical expressions. The velocity due to low-frequency waves in the swash zone is also taken into account by an empirical method.



The depth-averaged return current under the wave trough of each individual wave (summation over wave classes) is derived from linear mass transport and the water depth under the trough.

The sand and gravel transport of the CROSMOR2007-model is based on the TRANSPOR2004 transport formulations. Bed load and suspended load transport are both taken into account. The suspended transport is computed from the computed sand concentration profiles and current velocity profiles. The sediment transport rate is determined for each wave (or wave class), based on the computed wave height, depth-averaged cross-shore and longshore velocities, orbital velocities, friction factors and sediment parameters. The sediment composition can be taken into account (c_u -coefficient is input parameter).

The general model settings used herein are:

- artificial beach with straight slope of 1 to 20 between +4 m above MSL on land ad -10 m below MSL in the offshore zone;
- median sand diameter $d_{50} = 0.3$ to 0.5 mm; uniformity coefficient $c_u = 2$ to 3 ;
- water temperature = 25°C ; sea water salinity = 30 promille ($\cong 1030 \text{ kg/m}^3$);
- longshore current deep water = 0.2 m/s
- maximum tidal levels 0.6 and -0.6 m to MSL; storm surge level = 1.0 m
- number wave classes NHW = 10 (spectrum based on Rayleigh-distribution) per wave condition;
- sef = 1 ; roller = 0.5 ; coef5 = coef6 = 3 ; facsmooth = 10 ; facbed = 0.5 ; facsus = 1 ; facsusw = 0 .

Cases (d_{50})	Conditions	Uniform sand	Quasi-uniform sand
0.4 mm	Annual 1 year	Case U1: File DUBU1.inp $c_u = 2$	Case QU1: File DUBQU1.inp $c_u = 2.6$
	Storm 1 day	Case U2: File DUBU2.inp $c_u = 2$	Case QU2: File DUBQU2.inp $c_u = 2.6$
0.5 mm	Annual 1 year	Case U3: File DUBU3.inp $c_u = 2$	Case QU3: File DUBQU3.inp $c_u = 3$
	Storm 1 day	Case U4: File DUBU4.inp $c_u = 2$	Case QU4: File DUBQU4.inp $c_u = 3$
0.3 mm	Annual 1 year	Case U5: File DUBU7.inp $c_u = 2$	Case QU5: File DUBQU7.inp $c_u = 2.3$
	Storm 1 day	Case U6: File DUBU8.inp $c_u = 2$	Case QU6: File DUBQU8.inp $c_u = 2.3$

Table 4.9.4 Model run cases CROSMOR

Days	Annual wave climate in sector			Days	Storm in sector 270°-300° (return period=100 years)			
	H_{rms} (m)	T_p (s)	Dir (°)		H_{rms} (m)	T_p (s)	Dir (°)	Surge (m)
0.	0.5	4.0	10	0	1.5	8.5	10	1.0
200; 17,280,000 s	0.5	4.0	10	1; 86400 s	1.5	8.5	10	1.0
201; 17,280,001 s	0.7	6.0	10					
300; 25,920,000 s	0.7	6.0	10					
301; 25,920,001 s	0.9	7.0	10					
360; 31,104,000 s	0.9	7.0	10					
361; 31,104,001 s	1.1	8.0	10					
365; 31,536,000 s	1.1	8.0	10					

Table 4.9.5 Nearshore wave climates (annual waves and storm wave; depth 10) of CROSMOR-model runs



4.9.6 Effect of runup level on beach erosion

First, the runup level is computed. **Figure 4.9.5** shows the computed runup level as function of the offshore significant wave height (depth of 10 m) for a beach slope of 1 to 20. Both the standard equation and an alternative equation have been used (See CROMOR model description Section 2). Given an offshore significant wave height in the range of 1 to 2 m at depth of 10 m for Dubai coast, the runup level is of the order of 0.4 to 0.6 m. The surge level during extreme storm conditions is about 1 m. The maximum tide level is about 0.6 m. Thus, the maximum runup point is approximately $1+0.6+0.6 \cong 2.2$ m above MSL. Thus, beach erosion can be expected up to a level of 2 to 2.5 m above MSL. The runup length above the still water at time t is of the order $L_{R33\%} = R_{33\%}/\tan\beta = 0.6/0.05 = 12$ m.

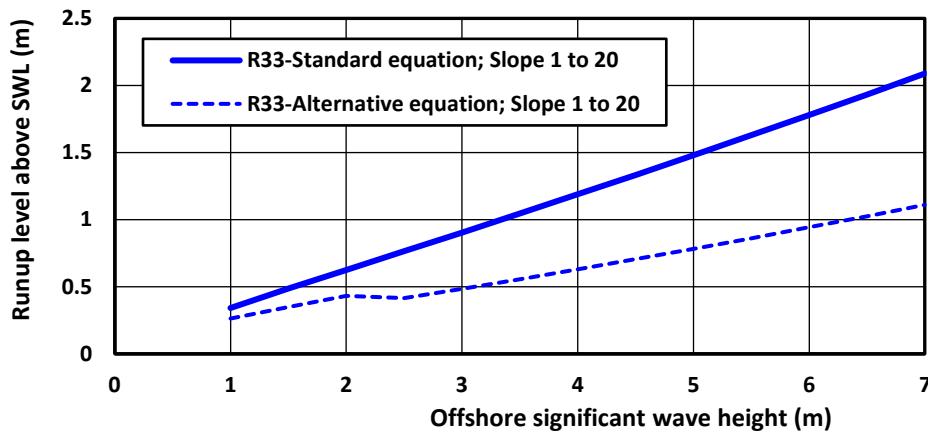


Figure 4.9.5 Runup level above still water level (SWL) as function of offshore significant wave height

The CROMOR-model has been used to compute the beach erosion volume at upper beach for an extreme storm event of 1 year (return period of 100 years) and for annual waves over 1 year. The median sand diameter is $d_{50} = 0.4$ m with uniformity coefficient $c_u = d_{60}/d_{10} = 2.6$. Other model parameters are given in **Section 4.9.5**.

Figure 4.9.6 shows the computed beach erosion volume for three different runup levels due to an extreme storm event of 1 day (**Table 4.9.5**). The maximum significant wave height is $H_s = 2.1$ m. The standard runup equation refers to $frunup = 1$ and gives a total beach erosion volume of about $25 \text{ m}^3/\text{m}$ after 1 day (see **Table 4.9.5**). The maximum erosion depth is about 1 m. The eroded sand is deposited in a bar just below the mean sea level (MSL). The bar toe is at -3 m below MSL. Using $frunup$ of 1.5 and 2 (input values) means that the runup values are multiplied by 1.5 and 2 resulting in higher runup levels. The computed beach erosion remains approximately the same, but it is more spread out over a longer runup length resulting in less deep erosion (maximum 0.5 m).

Figure 4.9.7 shows the computed beach erosion volume for three different runup levels due to annual waves over 1 year (**Table 4.9.5**). The wave heights are much lower ($H_s = 0.7$ to 1.55 m) than for an extreme storm event ($H_s = 2.1$ m) thus the runup levels are lower. The standard runup equation refers to $frunup = 1$ and gives a total beach erosion volume of about $35 \text{ m}^3/\text{m}$ after 1 year. The maximum erosion depth is about 1.1 m. The eroded sand is deposited in a bar just below the mean sea level (MSL). The bar toe is at -4 m below MSL. Using $frunup$ of 1.5 (input value) gives a slightly higher runup level and erosion volume (15%). Using $frunup = 2$, gives almost the same erosion volume as for $frunup = 1.5$. (= no further increase),

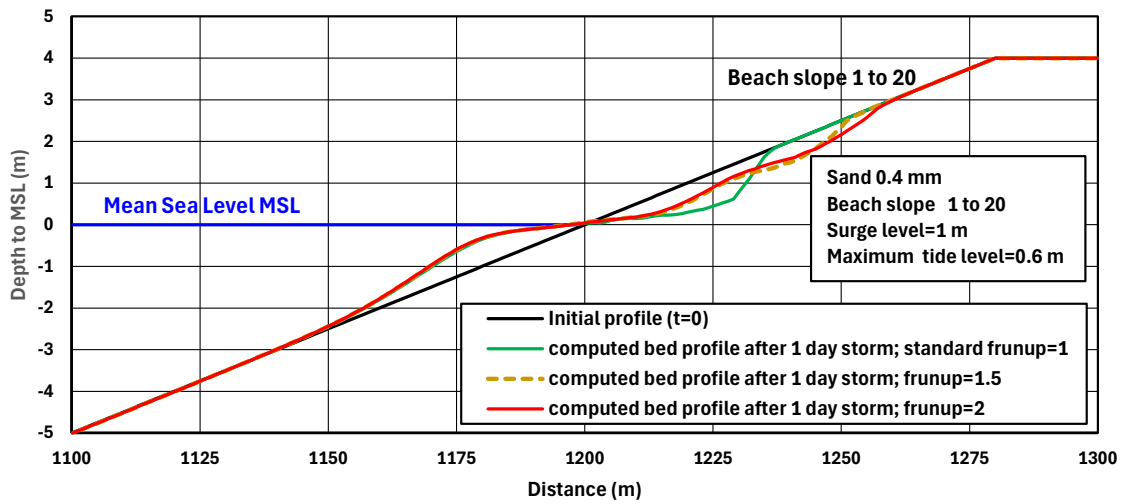


Figure 4.9.6 Computed beach erosion for different runup levels; extreme storm 1 day

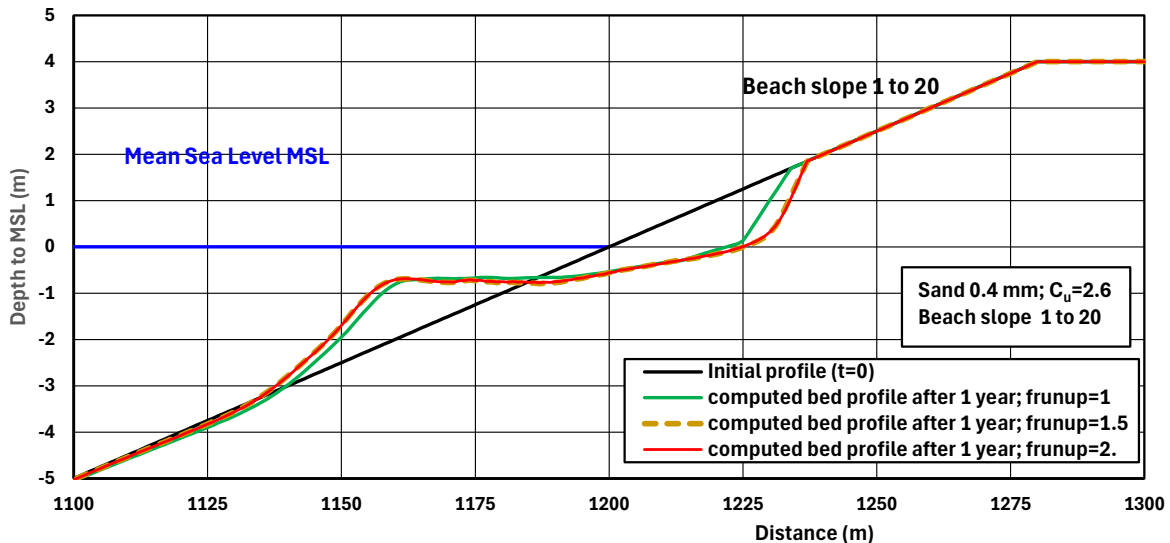
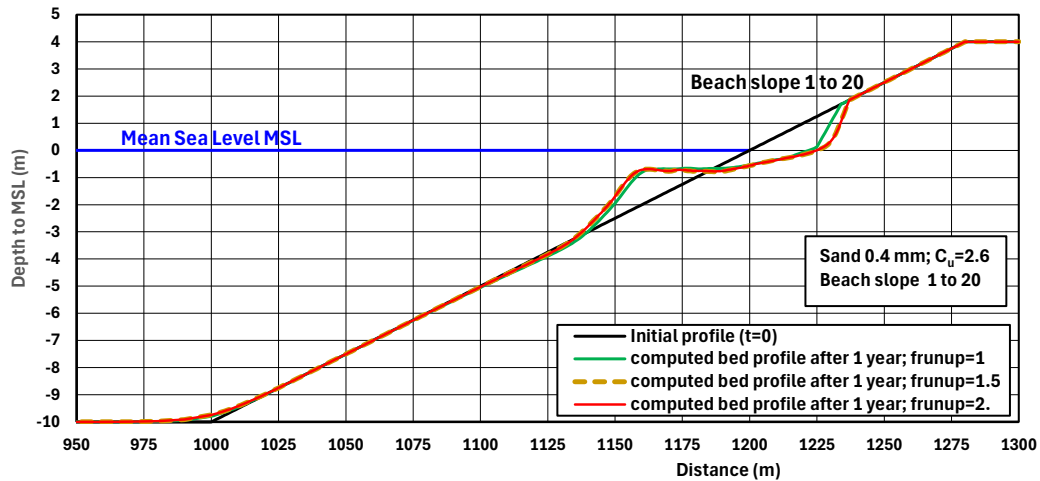


Figure 4.9.7 Computed beach erosion for different runup levels; annual waves over 1 year



4.9.7 Effect of median particle size (d_{50}) and uniformity coefficient (c_u) on beach erosion

The coastal erosion of a beach profile consisting of quasi-uniform natural sand depends on the median sand diameter d_{50} of the bed material and the representative size d_s of the suspended sediments. This latter parameter depends on the grading of the bed material (c_u -coefficient). The sand transport increases for more graded sand with higher c_u -coefficient and thus a smaller d_s -value (more fine sediment in suspension).

The effect of the c_u -coefficient on the computed coastal erosion along an artificial beach with slope of 1 to 20 has been studied for an extreme storm event (see **Table 4.9.5**) of 1 day by performing a series of CROSMOR model runs with sand in the range of 0.3 to 0.5 mm and c_u -values in the range of 2 to 10.

The results are shown in **Figures 4.9.8 to 4.9.11**.

Figure 4.9.8 presents the computed coastal erosion based on using Equation (4.9.2b) to represent the d_s -parameter. The d_s -parameter only depends on the c_u -value and independent of the wave conditions. The erosion volume for the most extreme storm event of 1 day with return period of 100 years is about $25 \text{ m}^3/\text{m}$ for $d_{50}=0.5 \text{ mm}$ with $c_u=2$. The erosion volume increases slightly for $c_u=3$ and 5. The erosion volume increases substantially to about $50 \text{ m}^3/\text{m}$ for $c_u=10$, because more fine sediments are available in the case of a very graded bed. It is noted that the seabed activity is minimum below -4 m MSL , which means that the high-quality upper beach layer can be terminated at -4 m MSL ; the seabed below -4 m MSL can be made of coarse beach fill.

Figures 4.9.9 to 4.9.11 show similar results based on Equation (3.2a). The erosion volume increases for increasing c_u -values (more graded sand). The effect of the c_u -value in the range of 2 to 5 on the computed erosion volume is relatively small (10%-15%). The erosion volume increases substantially (>50%) for very graded sand with $c_u=10$. It is noted that the computed erosion volumes are smaller than those based on Equation (3.2b), because the d_s -values are closer to the d_{50} of the bed material due to the mobility parameter (M) effect.

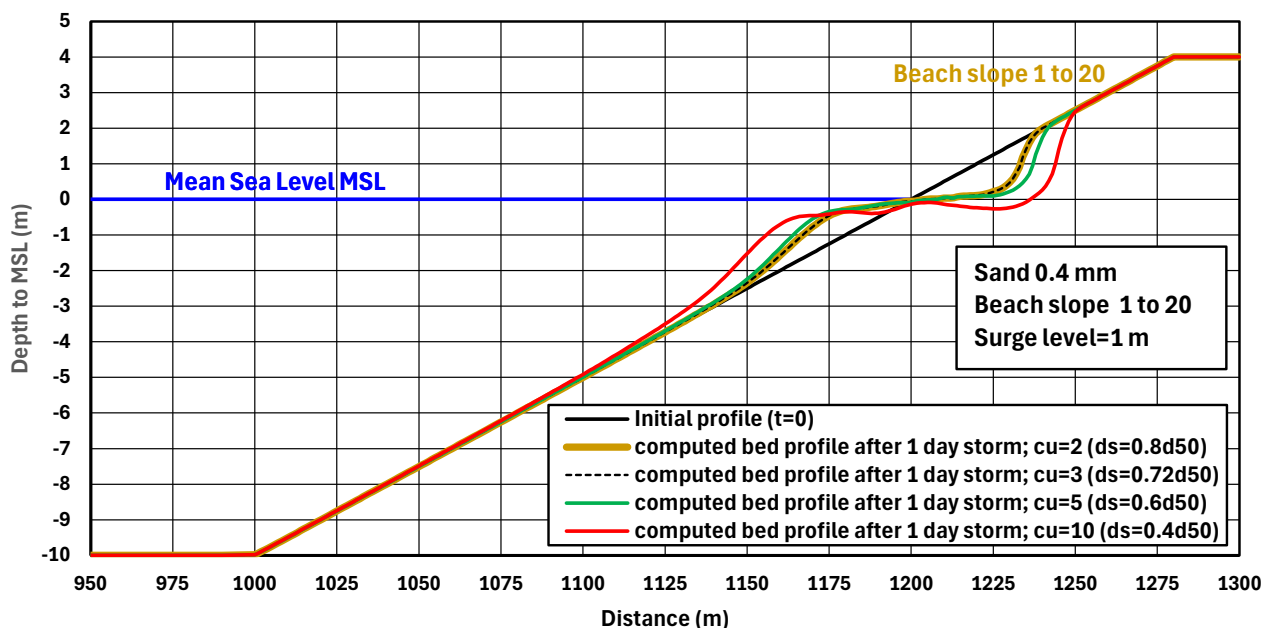


Figure 4.9.8 Computed beach erosion after 1 day (Equation 4.9.2b); 0.4 mm sand; $c_u=2$ to 10; storm event.

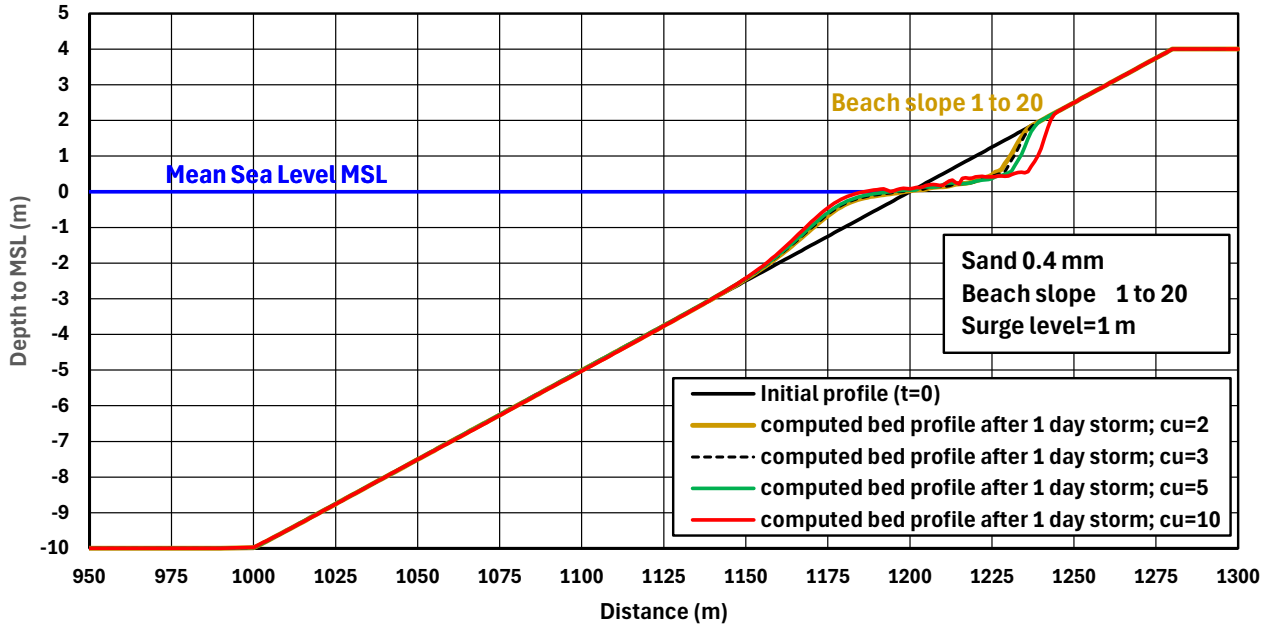


Figure 4.9.9 Computed beach erosion after 1 day (Equation 4.9.2a); 0.4 mm sand; $c_u=2$ to 10; storm event.

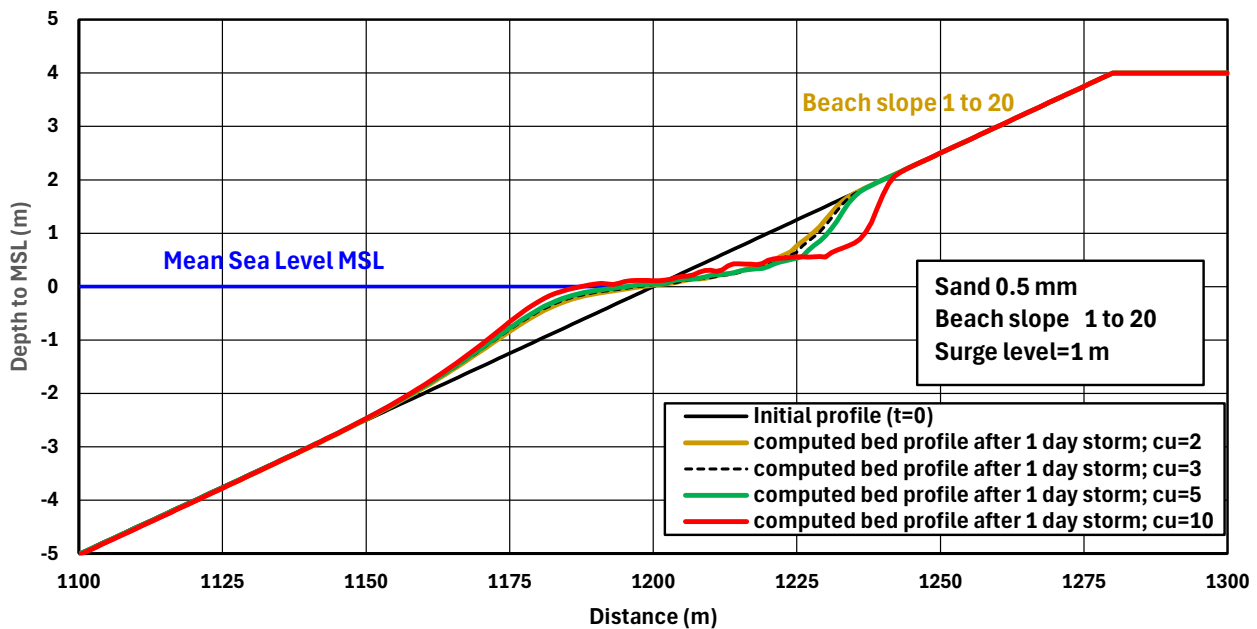


Figure 4.9.10 Computed beach erosion after 1 day (Equation 4.9.2a); 0.5 mm sand; $c_u=2$ to 10; storm event.

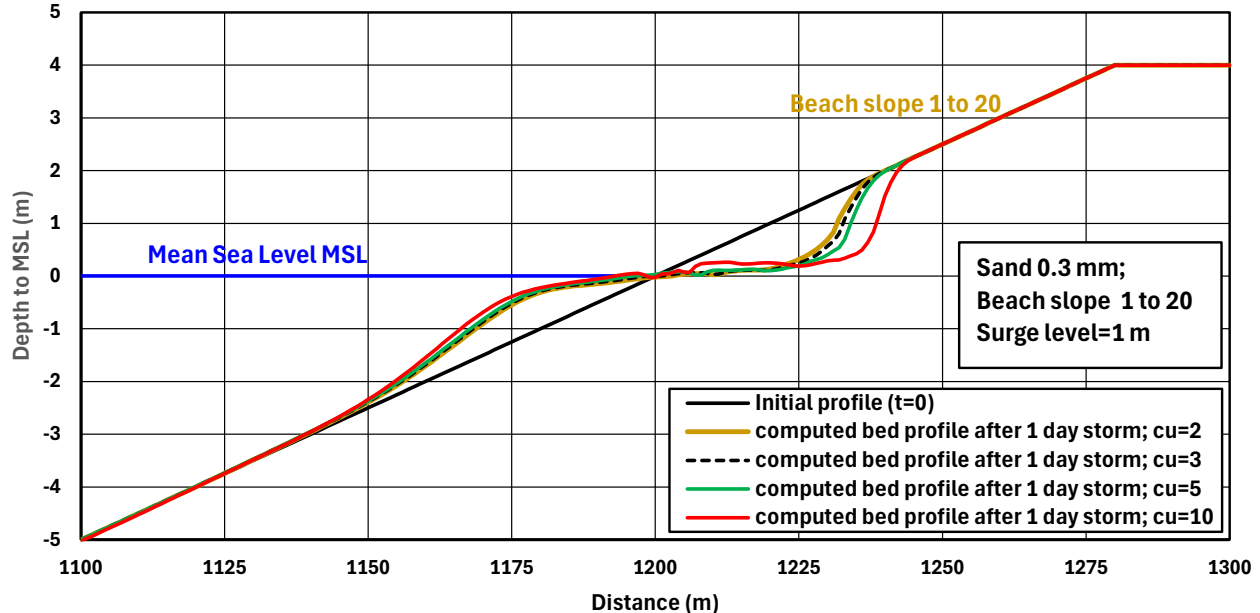


Figure 4.9.11 Computed beach erosion after 1 day (Equation 4.9.2a); 0.3 mm sand; $c_u=2$ to 10; storm event

In addition, long term model runs over 1 year with annual waves have been performed for:

- 0.3 mm sand with $c_u=2.5$;
- 0.4 mm sand with $c_u=2.6$;
- 0.5 mm sand with $c_u=3$.

The results are presented in Figures 4.9.12 to 4.9.14.

The most striking features are:

- $d_{50}=0.3$ mm; the computed erosion after 1 year is relatively large ($\cong 35$ m³/m/year) for uniform sand with $c_u=2$; the erosion volume increases marginally (10%) for quasi-uniform sand with $c_u=2.3$;
- $d_{50}=0.4$ mm; the computed erosion after 1 year is smaller ($\cong 25$ m³/m/year) for uniform sand with $c_u=2$; the erosion volume increases slightly (20%) for quasi-uniform sand with $c_u=2.6$;
- $d_{50}=0.5$ mm; the computed erosion after 1 year is very small ($\cong 12$ m³/m/year) for uniform sand with $c_u=2$; the erosion volume increases substantially to about 22 m³/m/year (80% increase) for quasi-uniform sand with $c_u=3$.

Figure 4.9.15 clearly shows that the beach erosion is much lower for coarser sand with $d_{50}=0.5$ mm and $c_u=3$ than that for sand with $d_{50}=0.3$ mm and $c_u=2.3$. Thus, it is more economic (less maintenance) to use coarse sand with $d_{50}=0.5$ mm and $c_u=3$ than to use finer sand with $d_{50}=0.3$ mm and $c_u=2.3$.

Ideally, almost uniform coarse sand with $d_{50}=0.5$ mm and $c_u=2$ should be used to obtain a stable beach with minimum erosion and maintenance. However, this type of almost uniform sand cannot easily be found at natural borrow sites. It can be produced artificially by removing the coarse fraction ($>0.6-0.7$ mm) from the stockpile sand of the contractor DBB through special (expensive) sieving operations.



Conclusions

Practice shows that finer sands are more uniform than coarser sands. Thus, the c_u -value increases for increasing median particle sizes (coarser sand). Very fine sands with $d_{50} < 0.2$ mm generally have c_u -values < 2.5 . Coarser sands with d_{50} of about 0.5 mm generally have c_u -values $\cong 3$.

Very uniform coarse sand with d_{50} of about 0.5 mm and $c_u < 2$ is very difficult or even impossible to find in nature. It can be produced artificially by removing (sieving) the very fine and the very coarse fractions, but this is an intensive and time-consuming operation.

Herein, it is proposed to use slightly less strict requirements for artificial beach sand, as follows:

- $0.2 < d_{50} < 0.3$ mm with $c_u < 2.5$;
- $0.3 < d_{50} < 0.4$ mm with $c_u < 2.75$;
- $0.4 < d_{50} < 0.5$ mm with $c_u < 3$.

A process-based numerical model (CROSMOR) has been used to demonstrate the effects of the c_u -uniformity coefficient on the beach erosion along an artificial beach of sand with d_{50} of 0.3, 0.4 and 0.5 mm with slope of 1 to 20 in annual wave and in storm wave conditions, representative for the Dubai coast.

The erosion volume increases for increasing c_u -values (more graded sand). The effect of the c_u -value in the range of 2 to 5 on the computed erosion volume is relatively small (10%-15%). The erosion volume increases substantially ($> 50\%$) for very graded sand with $c_u = 10$.

Comparison of the erosion for a beach consisting of relatively coarse sand with $d_{50} = 0.5$ mm and $c_u = 3$ than that of a beach with sand of $d_{50} = 0.3$ mm and $c_u = 2.3$ shows much lower erosion for the coarse beach sand. Thus, the beach will be more stable (and less maintenance) with applying coarse sand with $d_{50} = 0.5$ mm and $c_u = 3$ compared to finer sand with $d_{50} = 0.3$ mm and $c_u = 2$.

Following the requirements an almost uniform coarse sand with $d_{50} = 0.5$ mm and $c_u = 2$ should be used to obtain a stable beach with minimum erosion and maintenance. However, this type of almost uniform sand cannot be found at natural borrow sites. It can be produced artificially by removing the coarse fraction (> 0.6 - 0.7 mm) from natural sand through special (expensive) sieving operations, but that inherently means the d_{50} shall also decrease having negative impact on the beach stability.

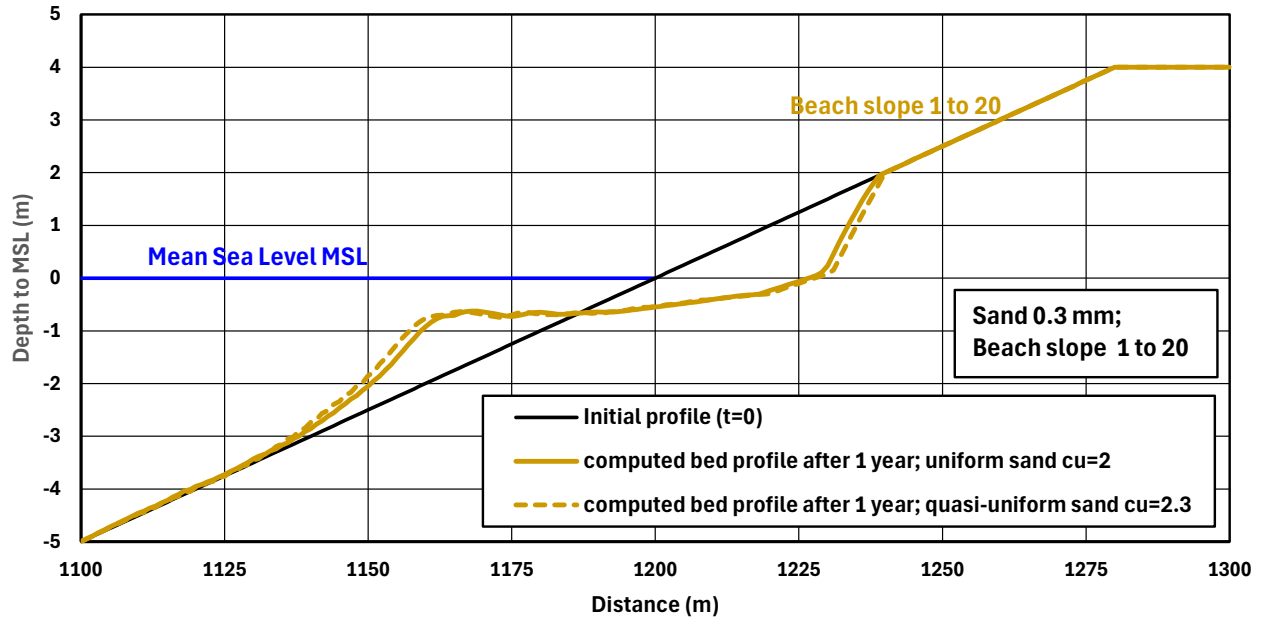


Figure 4.9.12 Computed beach erosion after 1 year annual waves (equation 3.2a); 0.3 mm sand; $c_u=2$ and 2.3;

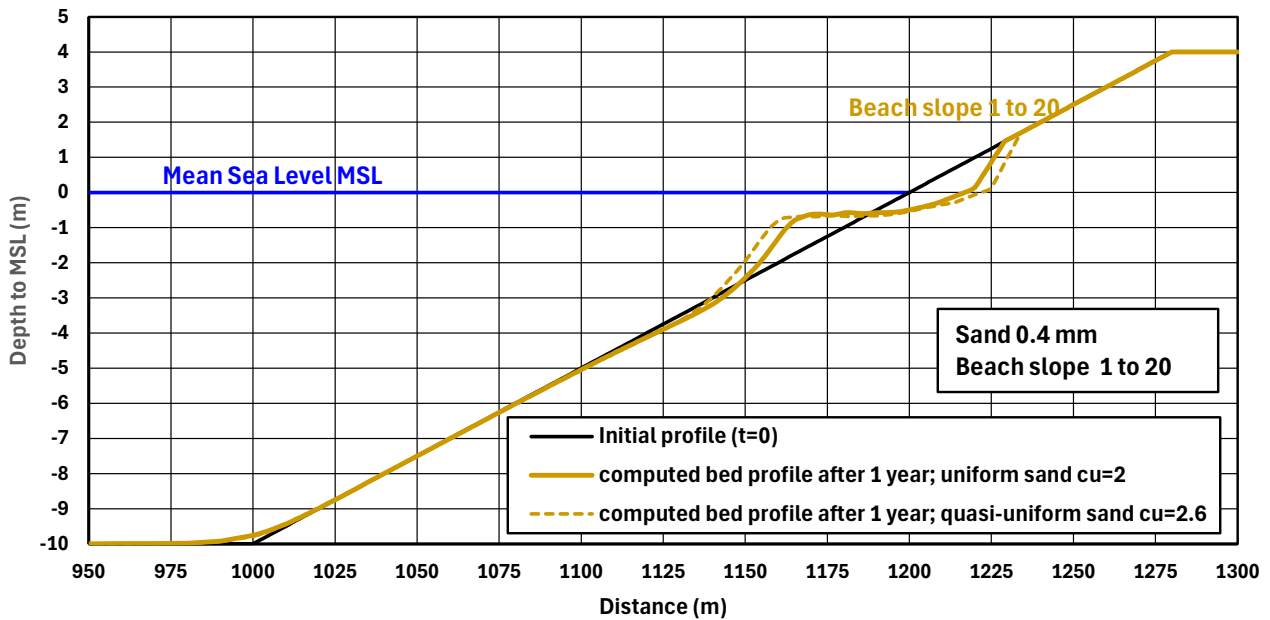


Figure 4.9.13 Computed beach erosion after 1 year annual waves (equation 3.2a); 0.4 mm sand; $c_u=2$ and 2.6;

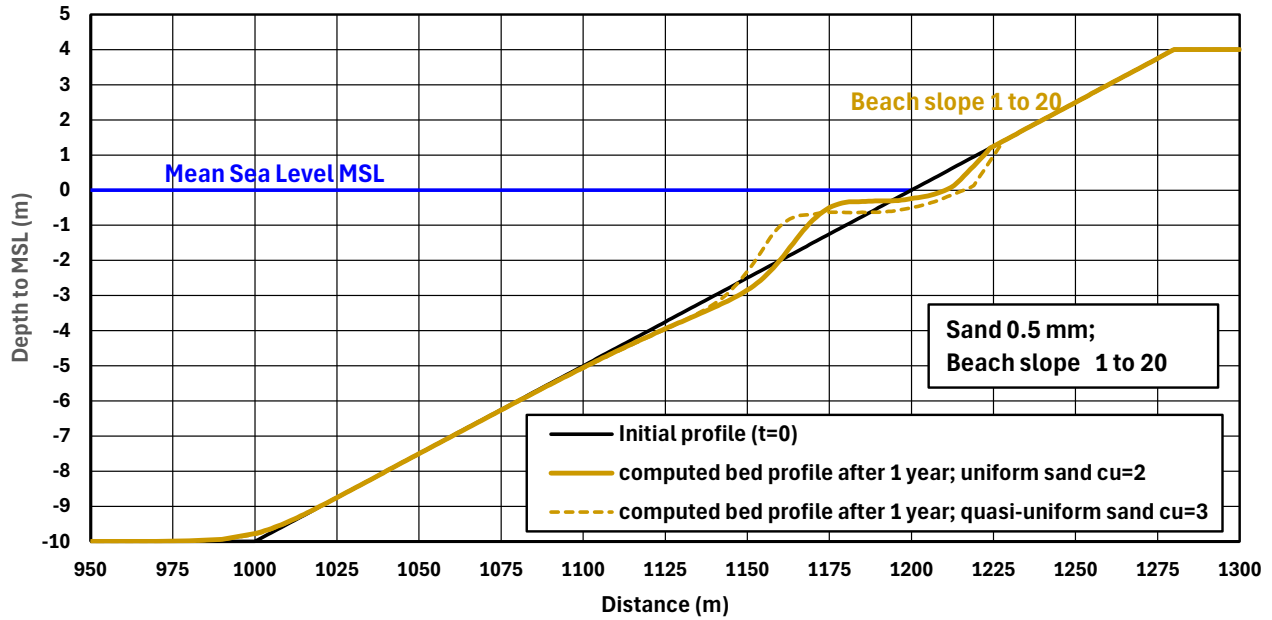


Figure 4.9.14 Computed beach erosion after 1 year annual waves (equation 3.2a); 0.5 mm sand; $c_u=2$ and 3.0.

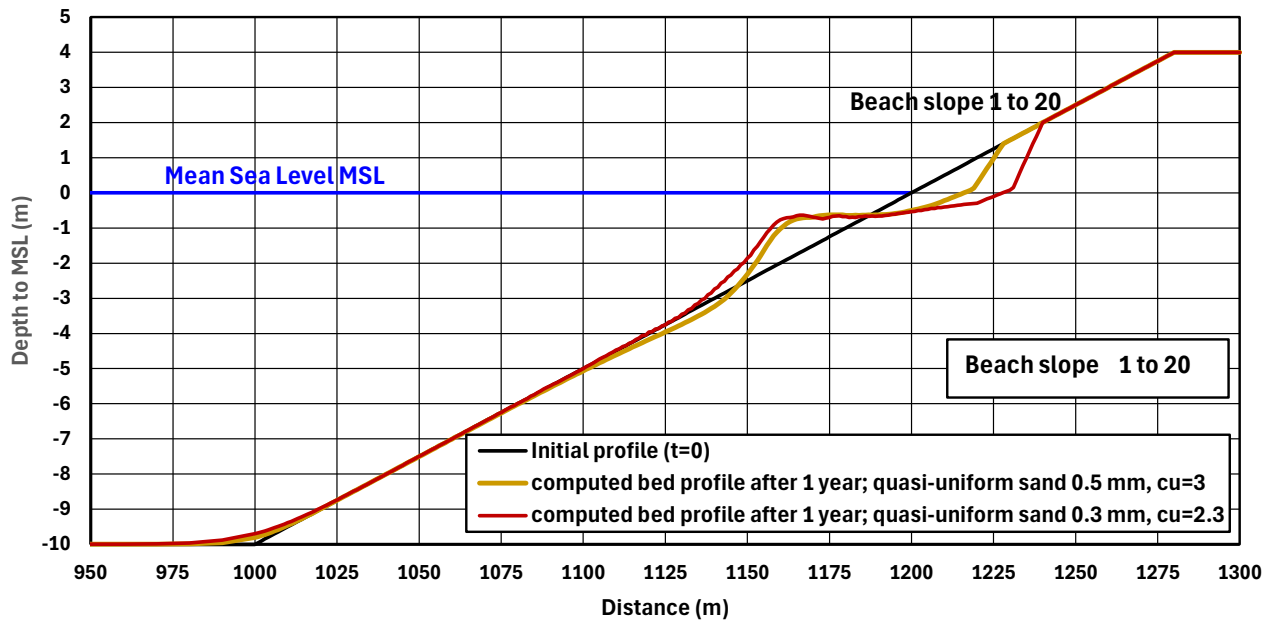


Figure 4.9.15 Computed beach erosion after 1 year annual waves (equation 3.2a); comparison of 0.5 mm sand with $c_u=2.6$ and 0.3 mm sand with $c_u=2.3$.



4.9.8 Effect of submerged sill on erosion along artificial beach

An artificial beach may consist of a sandy beach down to the original sea bed if sand is abundantly available. However, at many locations the availability of high-quality beach sand is problematic. The volume of high-quality beach sand required may be reduced by placing a submerged sill in the nearshore zone (zone between -3 m and -5 m below MSL). Various alternative designs have been studied and compared based on the computed bed profiles (CROSMOR-results), see Table 4.9.6.

Fairly mild annual wave conditions for 1 year and storm wave conditions for 1 day are considered, see **Table 4.9.7**.

The general model settings are:

- median sand diameter $d_{50}=0.4$ mm (± 0.1 mm);
- longshore current deep water=0.2 m/s
- maximum tidal levels 0.6 and -0.6 m to MSL; Storm surge level=1.15 m
- number wave classes NHW=10 (spectrum based on Rayleigh-distribution) per wave condition;
- sef=1; roller=0.5; coef5=coef6=3; facsmooth=10; faced=0.5; facsus=1; facsusw=0.

Case	Wave conditions	Computed erosion volume	Files
1. Sill at -3.1 m; slope 1 to 20	Annual A1	25 m ³ /year	UMM1a1.inp
	Annual A2	32 m ³ /year	UMM1a2.inp
	Storm S2	12 m ³ /day	UMM1s2.inp
2. Sill at -3.1 m; slope 1 to 15	Annual A2	55 m ³ /year	UMM2a2.inp
	Storm S2	15 m ³ /day	UMM2s2.inp
3. No sill; slope 1 to 20	Annual A2	12 m ³ /year	UMM3a2.inp
	Storm S2	12 m ³ /day	UMM3s2.inp
4. No sill; slope 1 to 15	Annual A2	13 m ³ /year	UMM4a2.inp
	Storm S2	15 m ³ /day	UMM4s2.inp
5. No sill; slope 1 to 20 down to -4 m and slope 1 to 15 between -4 and -10 m	Annual A2	12 m ³ /year	UMM5a2.inp
	Storm S2	25 m ³ /day	UMM5s2.inp

Table 4.9.6 Cases CROSMOR-model runs

Days	Annual wave climate A1			Annual wave climate A2			Days	Storm S1				Storm s2			
	H _{rms} (m)	T _p (s)	Dir (°)	H _{rms} (m)	T _p (s)	Dir (°)		H _{rms} (m)	T _p (s)	Dir (°)	surge (m)	H _{rms} (m)	T _p (s)	Dir (°)	Surge (m)
0.	0.3	3.5	10	0.5	4.0	10	0	1.0	6.0	10	1.15	1.3	6.5	10	1.15
200; 17.,280,000 s	0.3	3.5	10	0.5	4.0	10	1; 86400 s	1.0	6.0	10	1.15	1.3	6.5	10	1.15
201; 17,280,001 s	0.4	4.0	10	0.7	5.0	10									
300; 25,920,000 s	0.4	4.0	10	0.7	5.0	10									
301; 25,920,001 s	0.5	4.5	10	0.9	5.5	10									
360; 31,104,000 s	0.5	4.5	10	0.9	5.5	10									
361; 31,104,001 s	0.6	5.0	10	1.0	6.0	10									
365; 31,536,000 s	0.6	5.0	10	1.0	6.0	10									

Table 4.9.7 Wave climates (nearshore at -3 m MSL) of CROSMOR-model runs



The model results are shown in **Figure 4.9.16 to 4.9.20**. The computed erosion volumes are given in **Table 4.9.6**. The most striking features are:

- the annual beach erosion along a beach with slope of 1 to 20 terminated by a sill with crest at -3.1 m MSL (Case 1) amounts to about 30 m³/year; the storm-related erosion is up to 12 m³/day; the eroded sand is mainly deposited at the seaward toe of the submerged sill;
- the annual beach erosion in creases substantially to about 55 m³/year for a beach with slope of 1 to 15 terminated by a submerged sill (Case 2); the storm-related erosion increases to about 15 m³/day; the eroded sand is mainly deposited at the seaward toe of the submerged sill (this may be less if there is a larger difference between the crest level and the sand surface at end);
- the annual beach erosion along a straight beach slope of 1 to 20 (Case 3) without sill is much smaller at only 12 m³/year; the erosion increases slightly for a straight beach with slope of 1 to 15 (Case 4);
- the annual beach erosion along a beach with a break in slope (1 to 20 down to -4 m and 1 to 15 down to the original seabed) is similar to that along a straight beach with slope of 1 to 20; the storm erosion increases to 25 m³/day;
- the maximum erosion depth is about 1 m for beaches without a sill and about 1 to 1.5 m for beaches with a sill;
- the seabed activity along a straight beach without sill is minimum below -4 m MSL, which means the that high-quality upper beach layer can be terminated at -4 m MSL; the seabed below -4 m MSL can be made of coarse beach fill.

The beach erosion increases for cases with a submerged sill because the available distance where the bed can be eroded, is smaller (about 60 m; wave attack is concentrated on a relatively short distance) than for a straight beach (about 80 m), see **Figures 4.9.21 and 4.9.22**.

Conclusions

Given the mild wave climate, it may be considered to construct straight beaches without a submerged terminal sill. The slope of the upper beach can be safely designed as 1 to 15. An alternative is an upper beach at 1 to 20 in combination with a lower beach of 1 to 15. It is sufficient to extend the high-quality upper beach layer down to -4 m MSL, where the morphodynamic activity of the sea bed is minimum.

The construction of straight beaches requires more sand (most coarse beach fill material), but saves the construction of the submerged sills. It is noted that the placement of more fill material may lead to slightly increased turbidity levels.

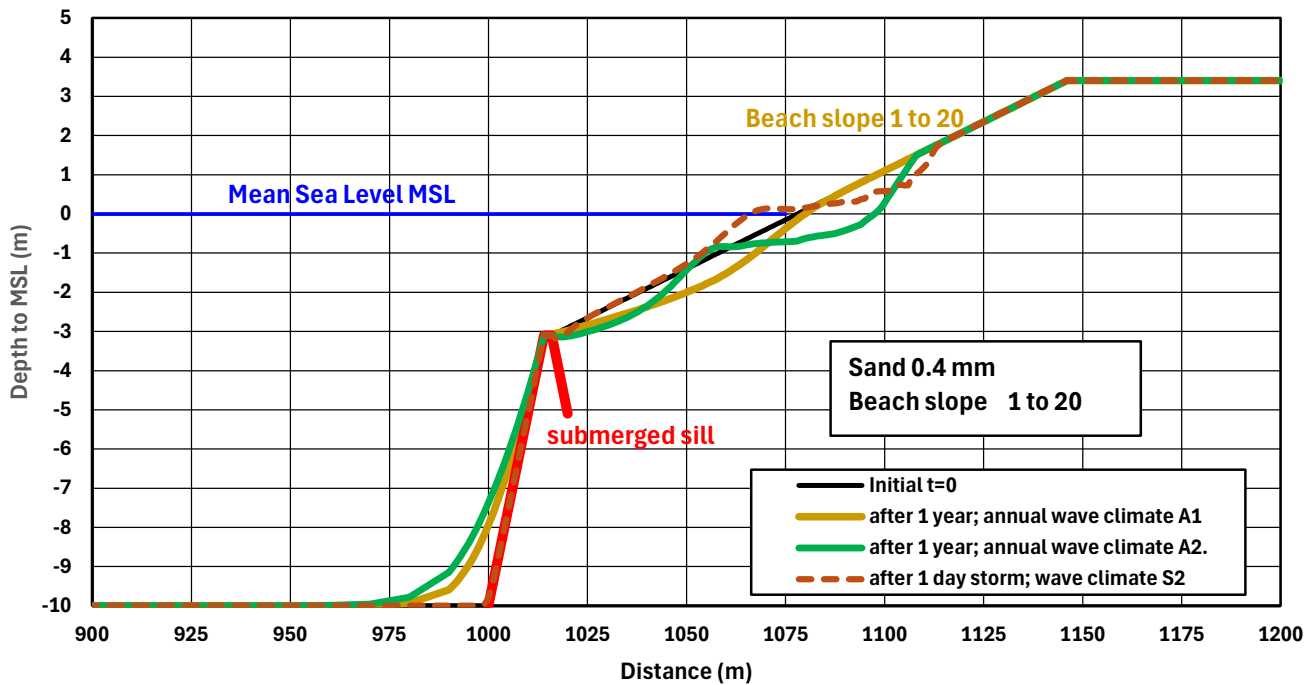


Figure 4.9.16 Beach erosion after 1 year for Case 1: Sill with crest at -3.1 MSL and beach slope 1 to 20.

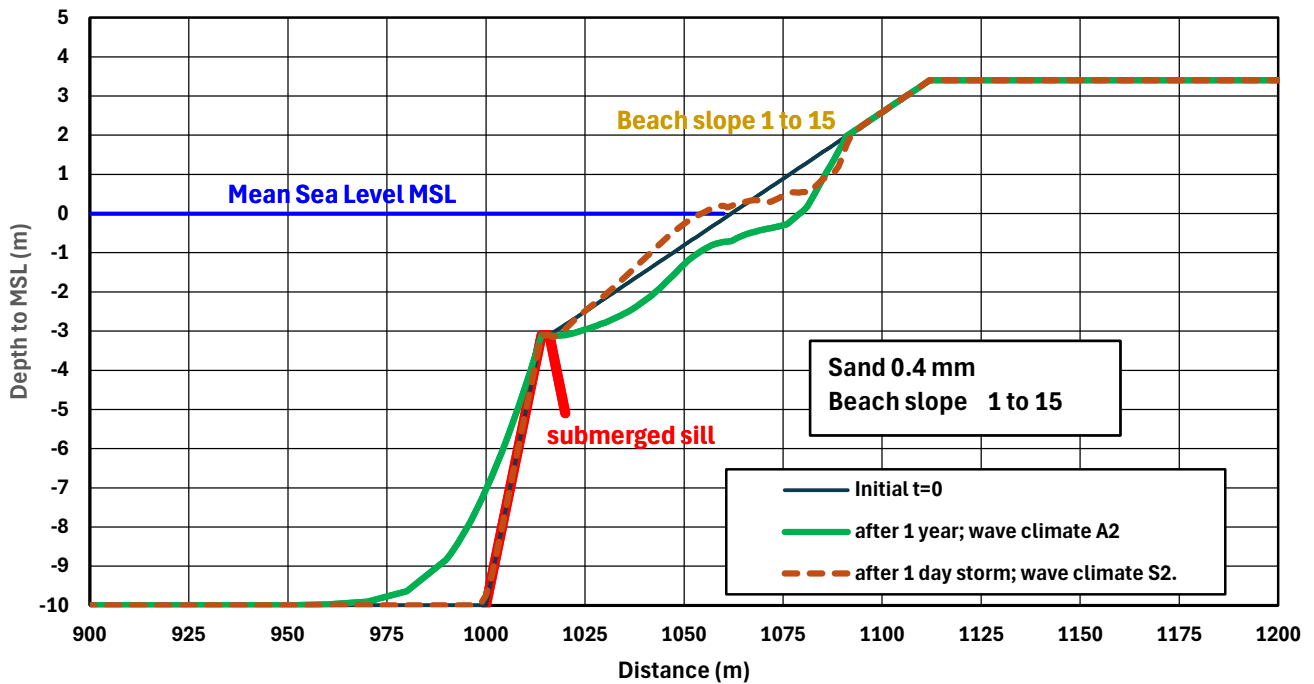


Figure 4.9.17 Beach erosion after 1 year for Case 2: Sill with crest at -3.1 MSL and beach slope 1 to 15.

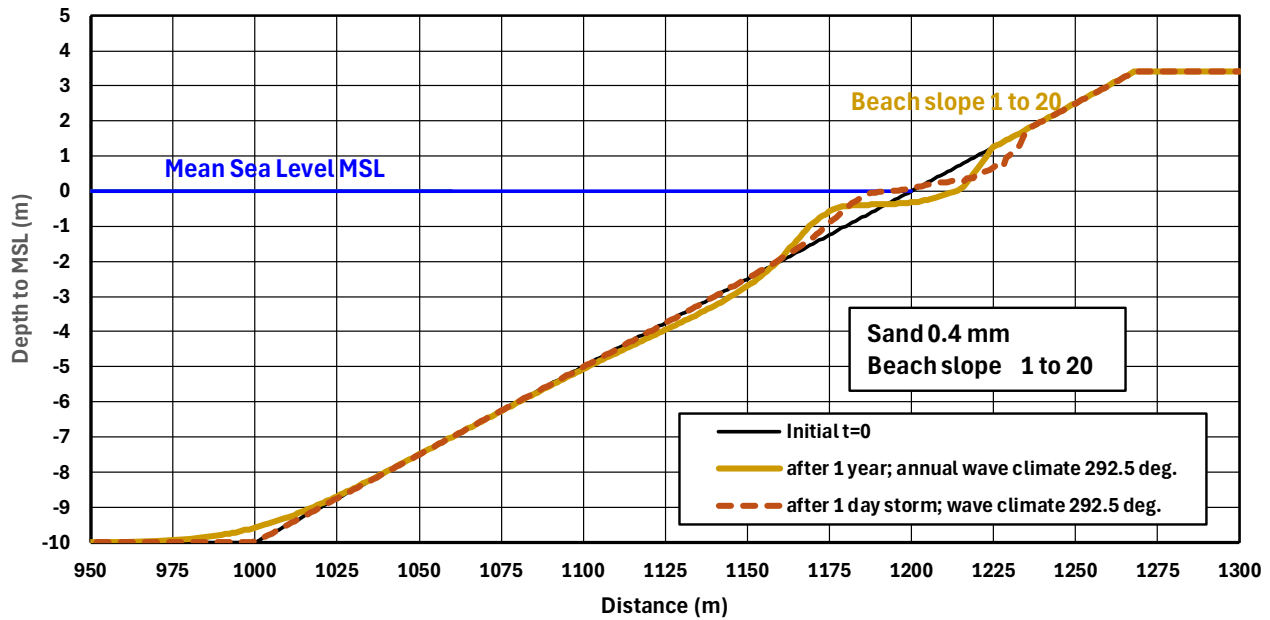


Figure 4.9.18 Beach erosion after 1 year for Case 2: No sill and beach slope 1 to 20.

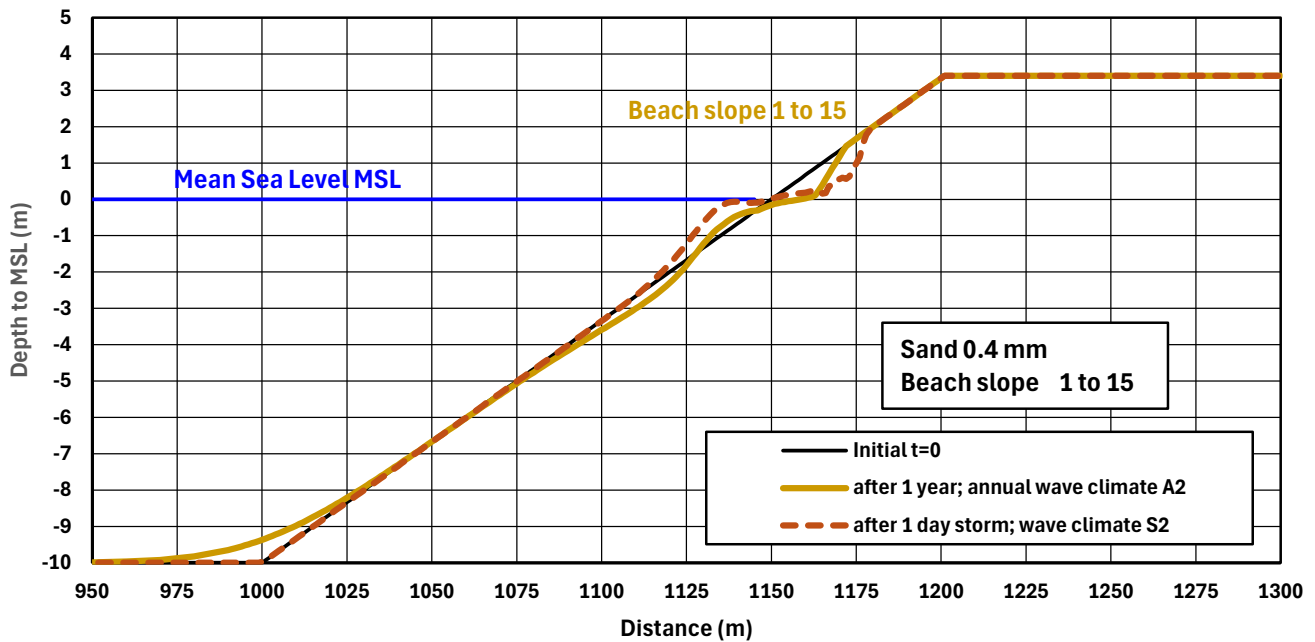


Figure 4.9.19 Beach erosion after 1 year for Case 2: No sill and beach slope 1 to 15.

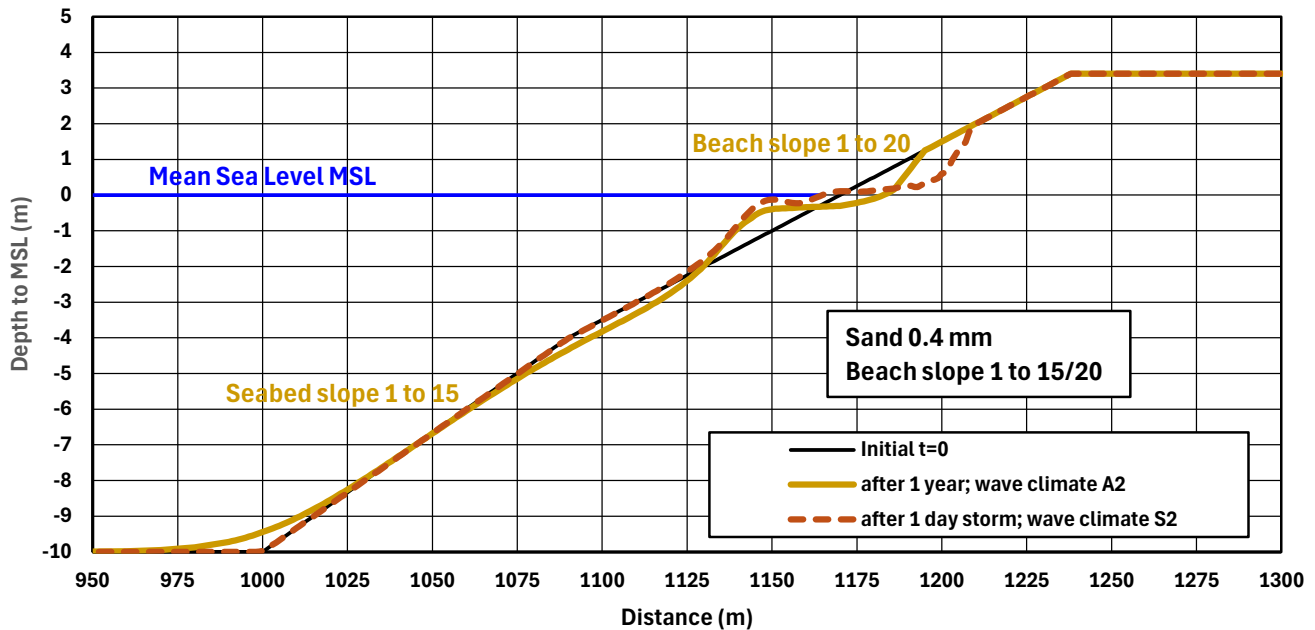


Figure 4.9.20 Beach erosion after 1 year for Case 2: No sill and beach slope 1 to 20 down to -4 m and 1 to 15 between -4 and -10 m.

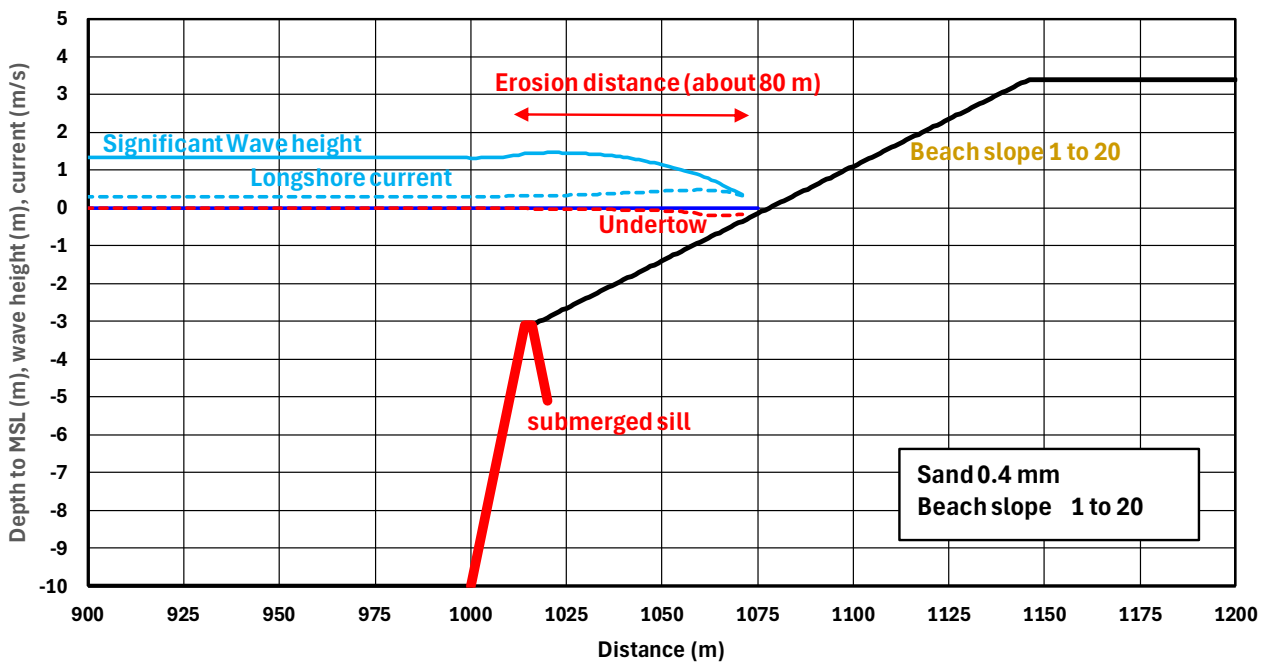


Figure 4.9.21 Wave height, longshore current, undertow at $t=0$ along beach with sill (slope 1 to 20); $H_s=1.4$ m at boundary $x=0$ m (depth of 10 m)

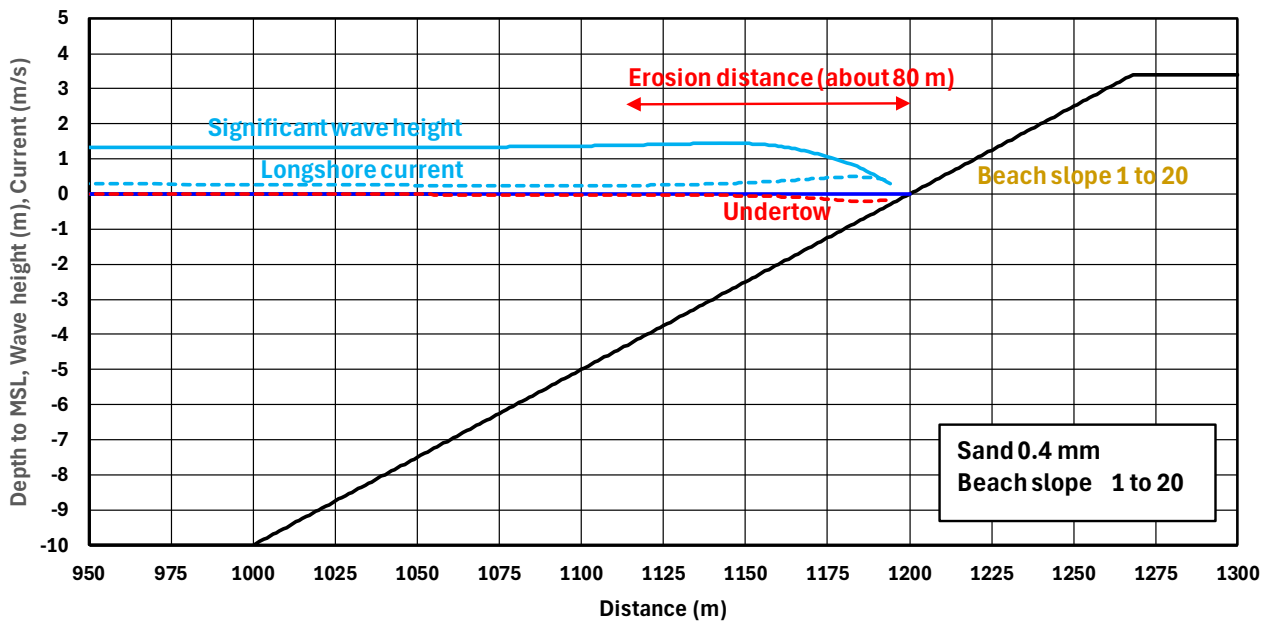
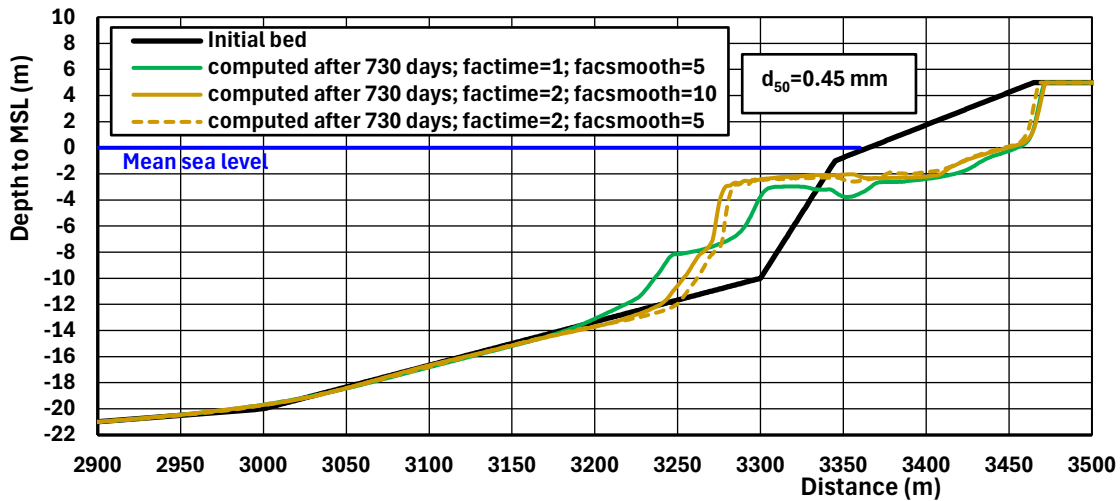
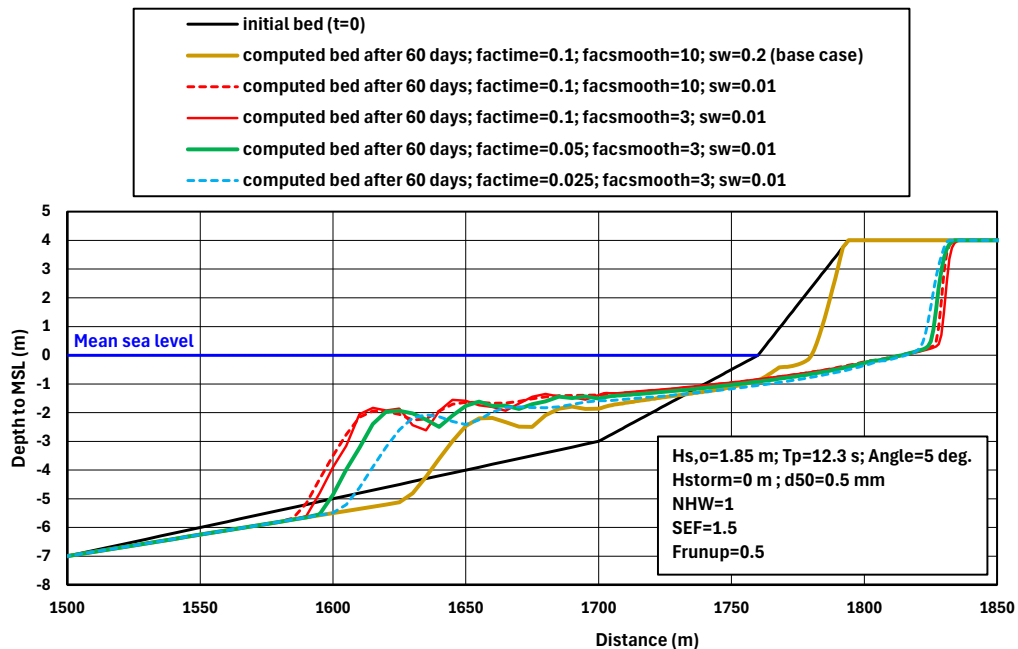
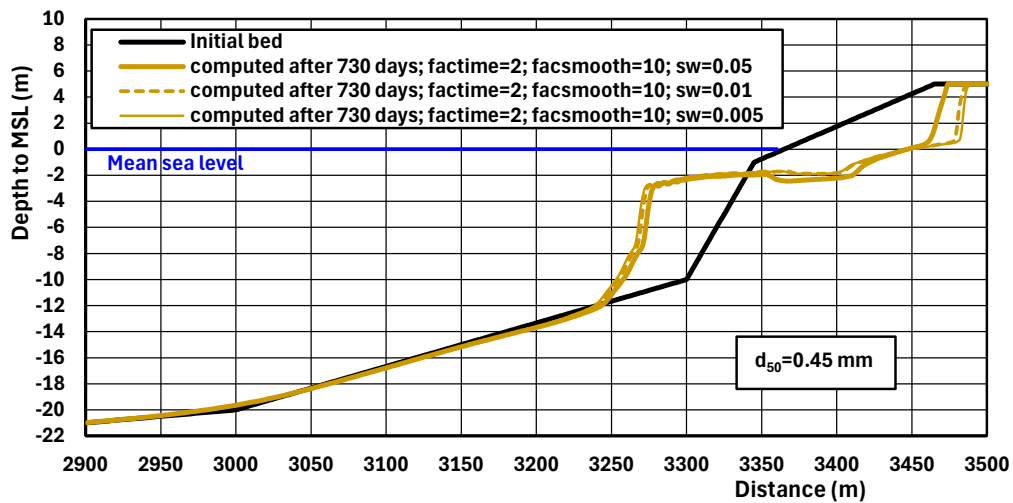
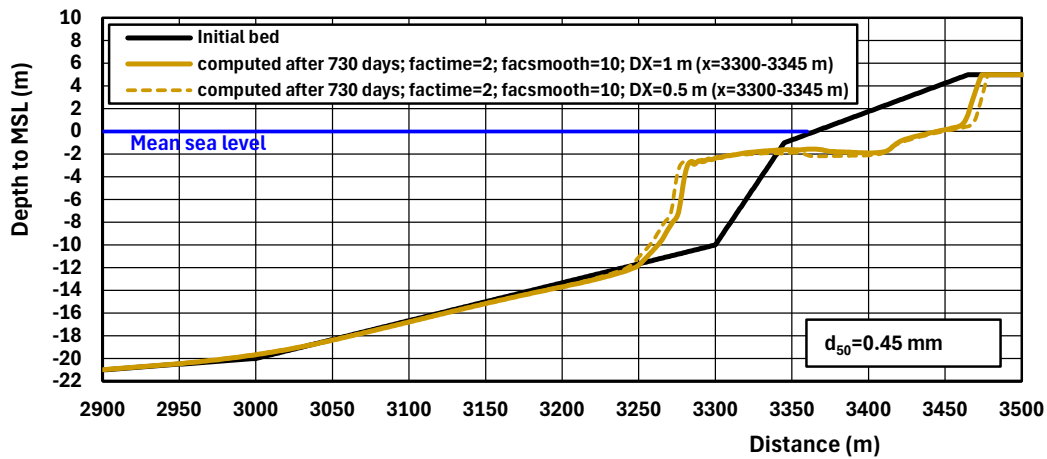


Figure 4.9.22 Wave height, longshore current, undertow at $t=0$ along straight beach without sill (slope 1 to 20); $H_{s,0}=1.4$ m at boundary $x=0$ m (depth of 10 m)

4.10 Results of sensitivity tests

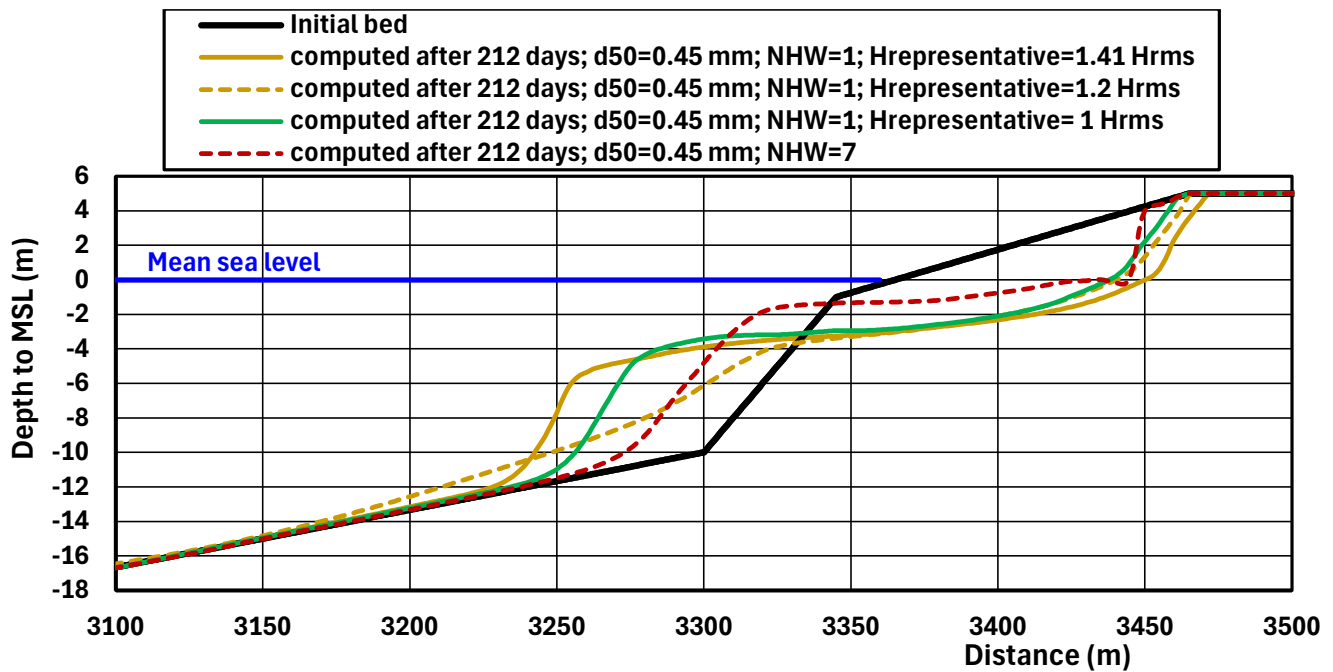
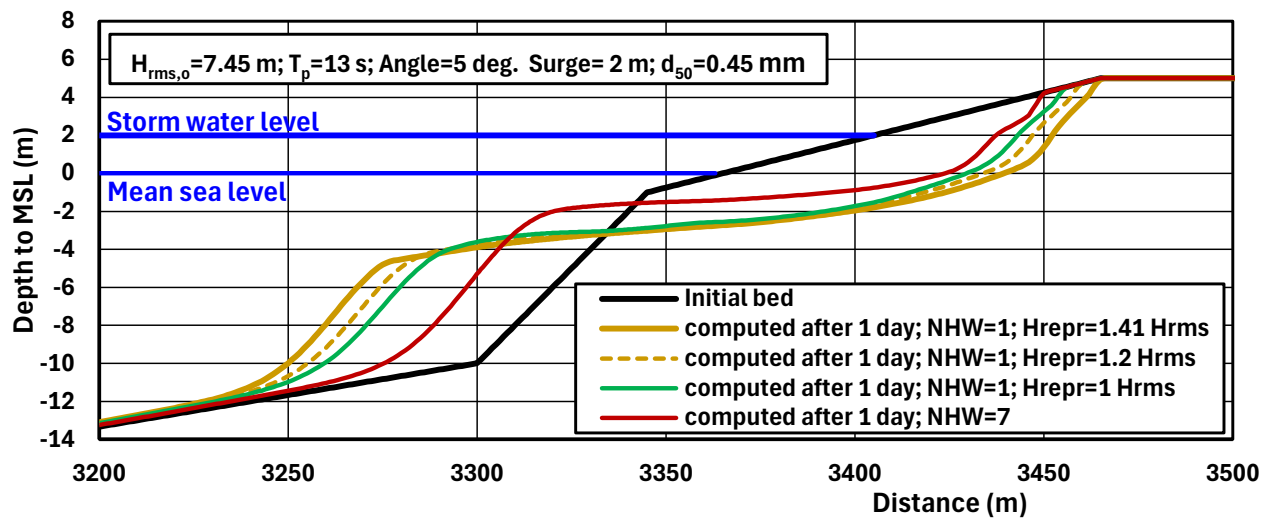
1. Effect of grid size, factime, facsmooth and SW

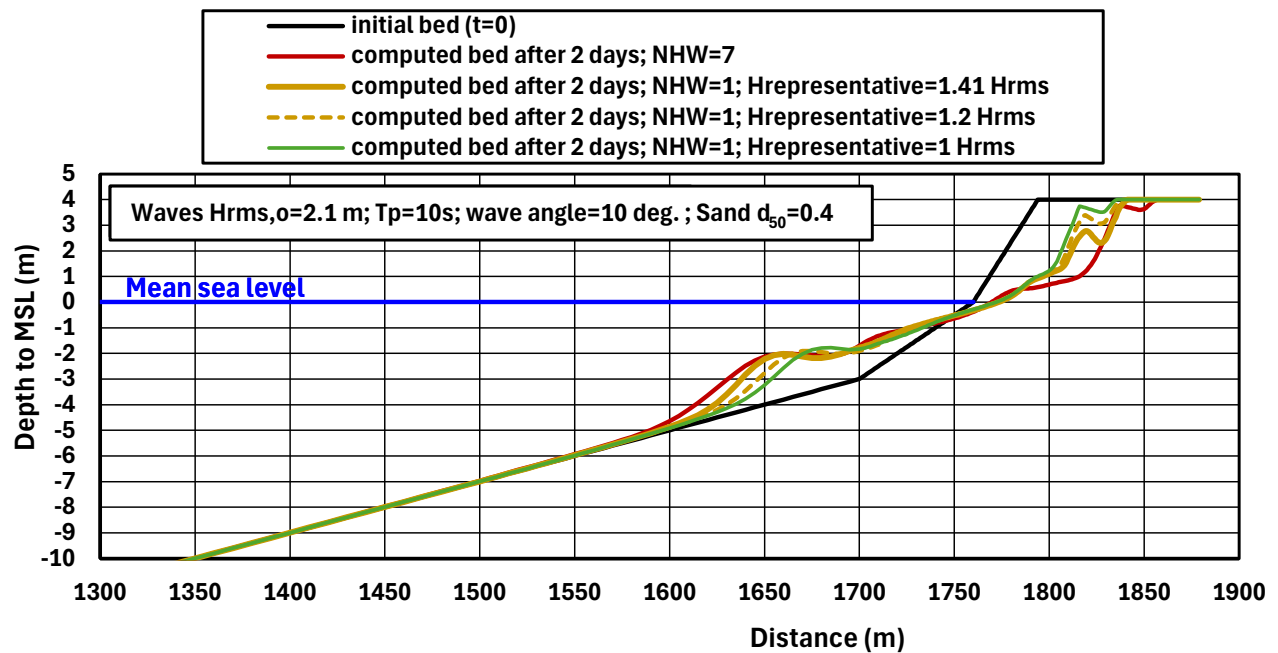
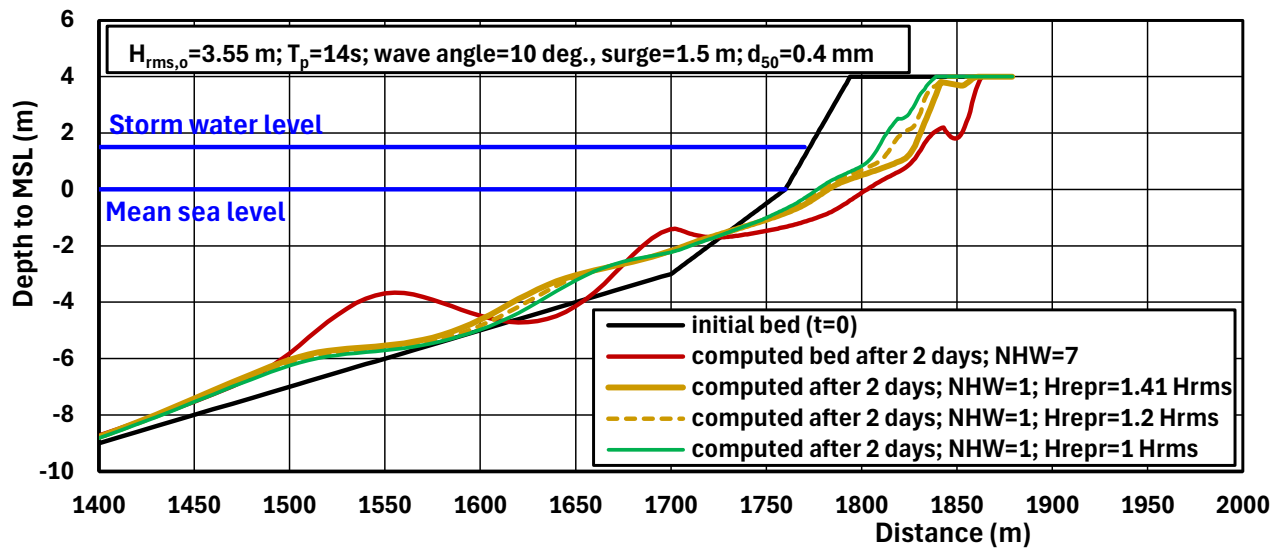






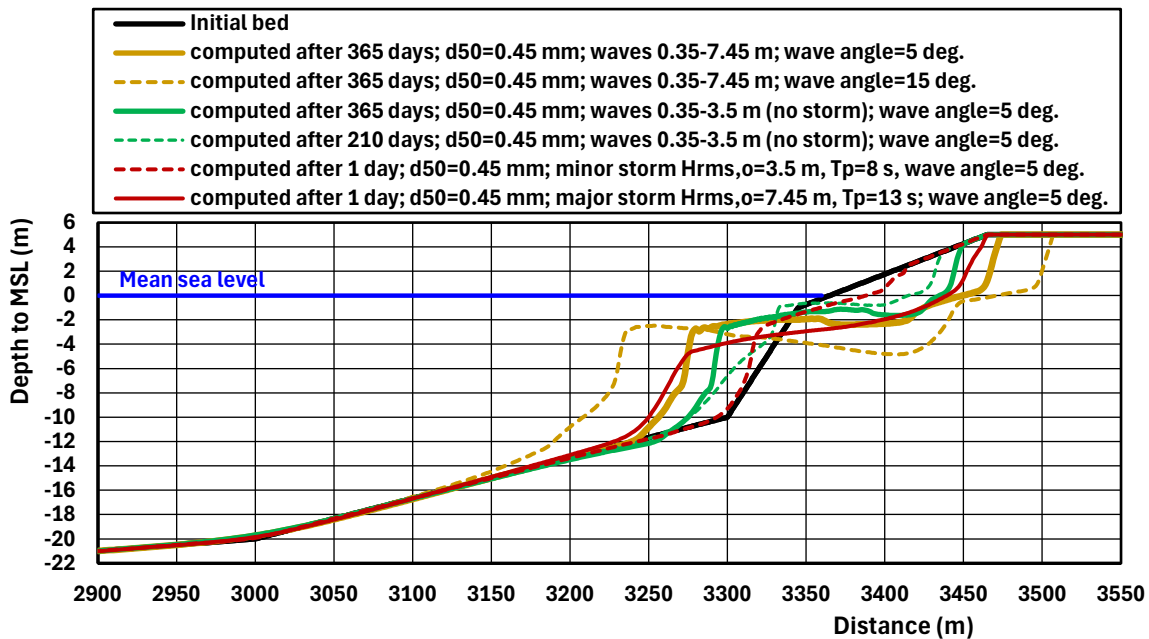
2. Representative wave height



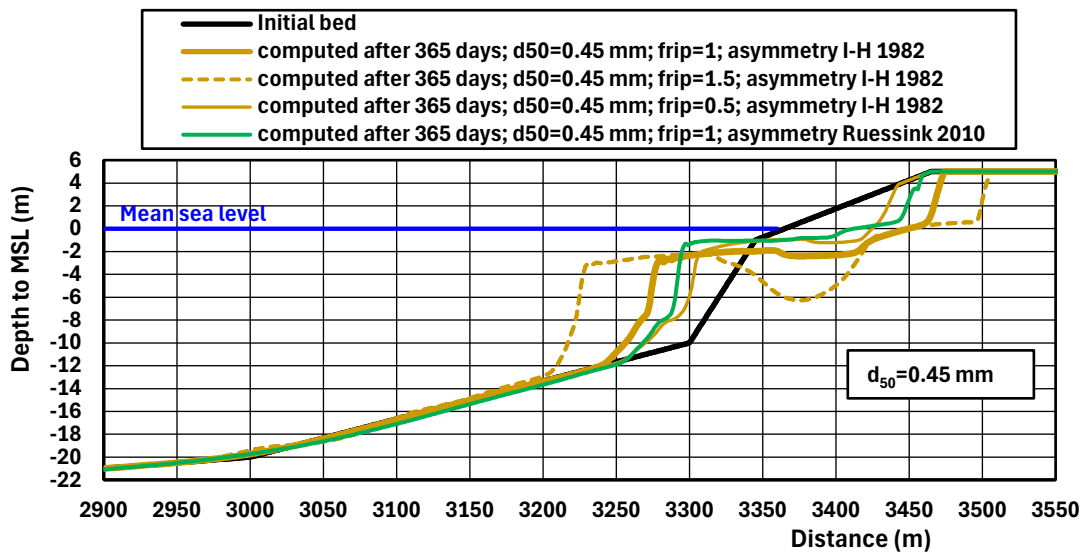




3. Effect of wave height and wave angle

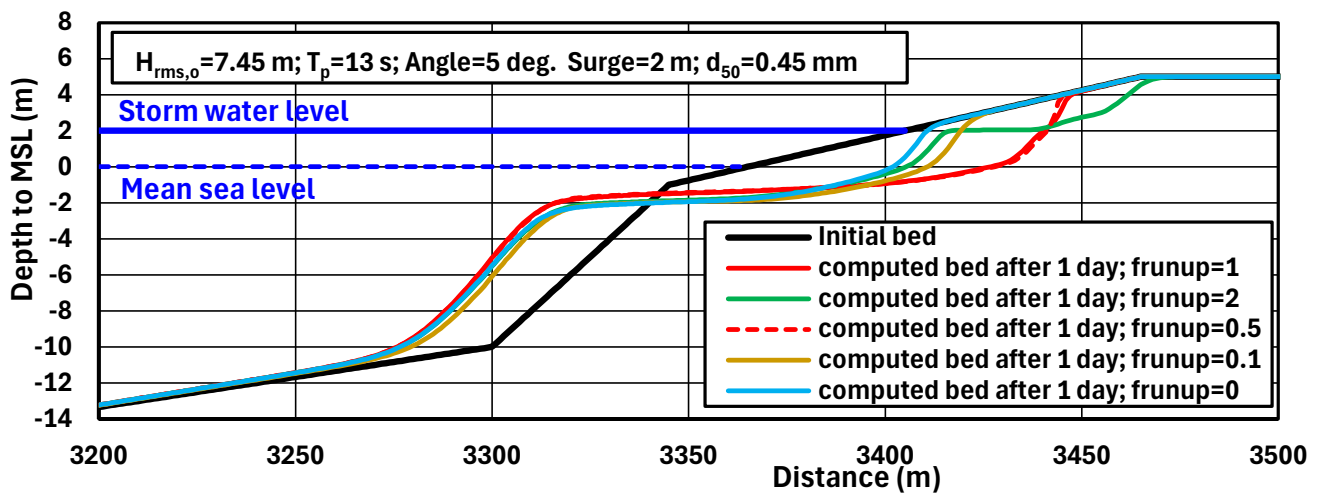
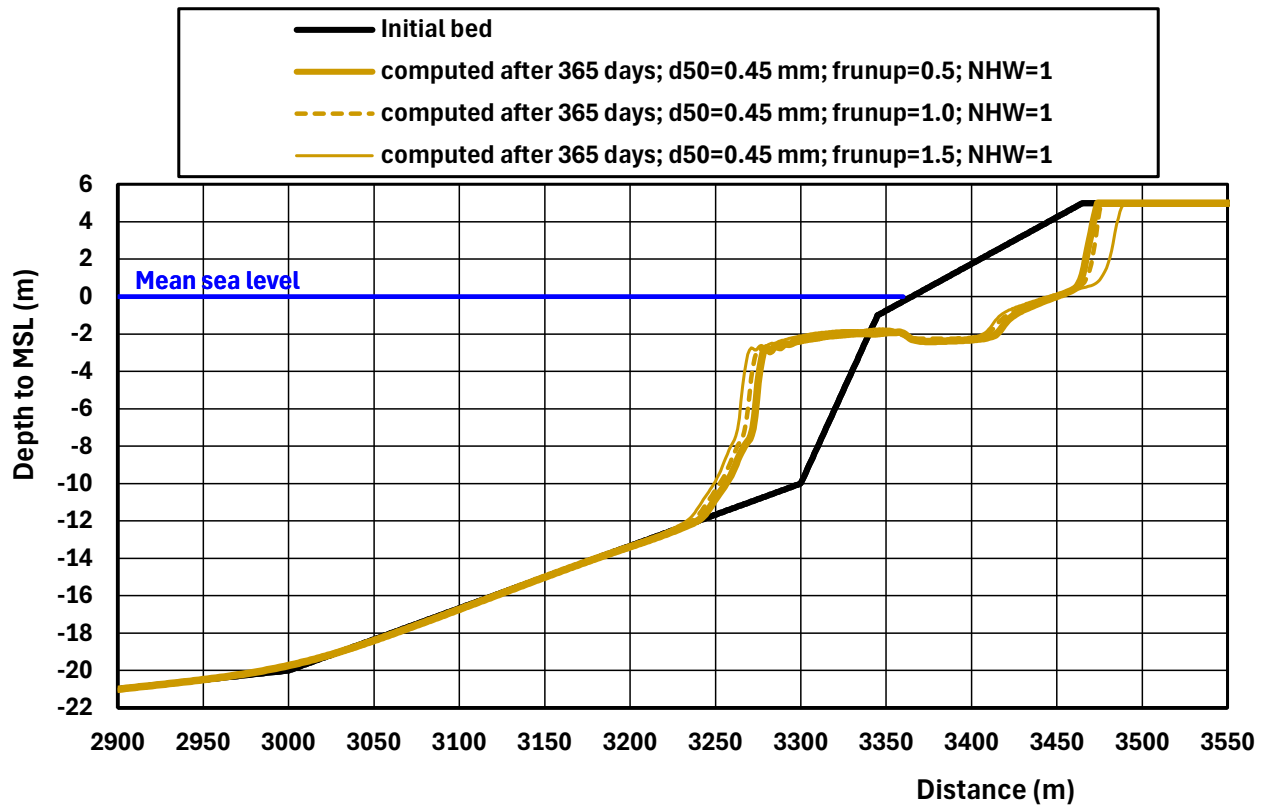


3. Effect of wave asymmetry and undertow



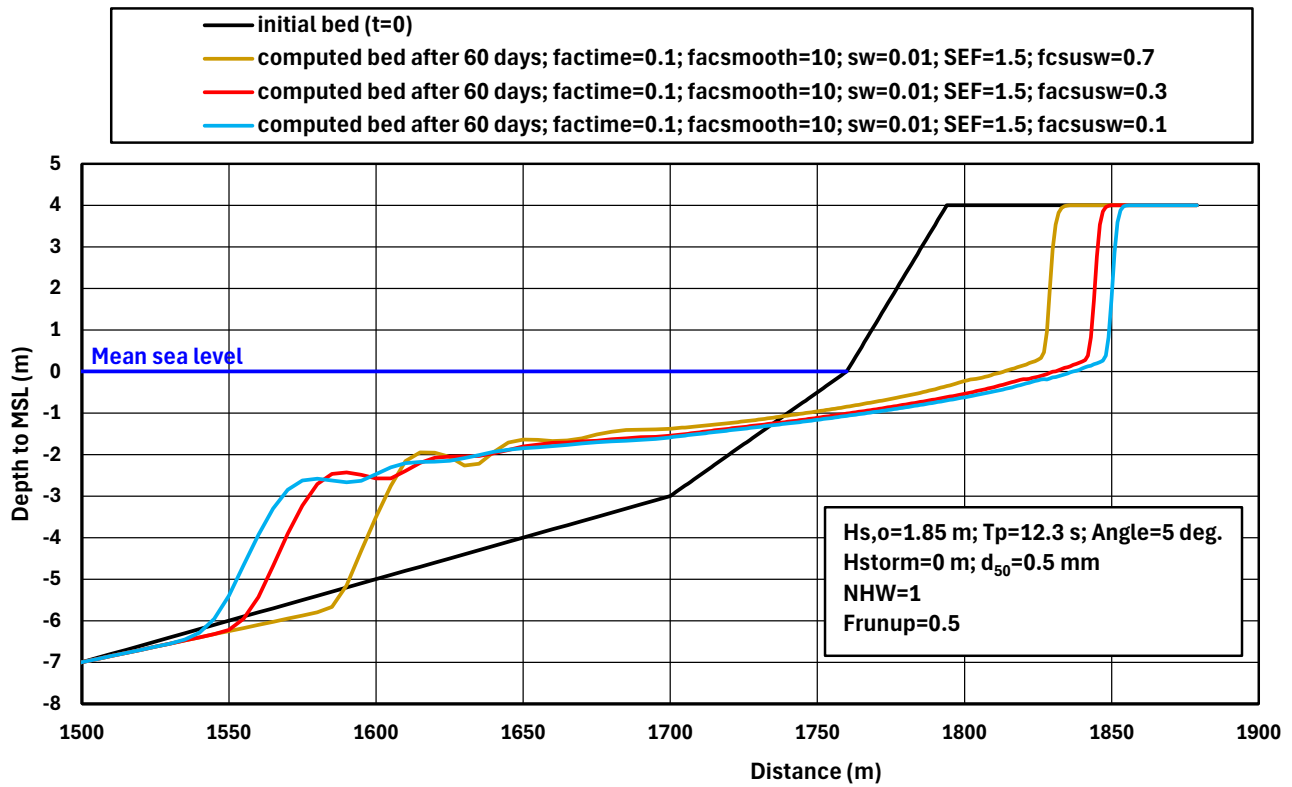
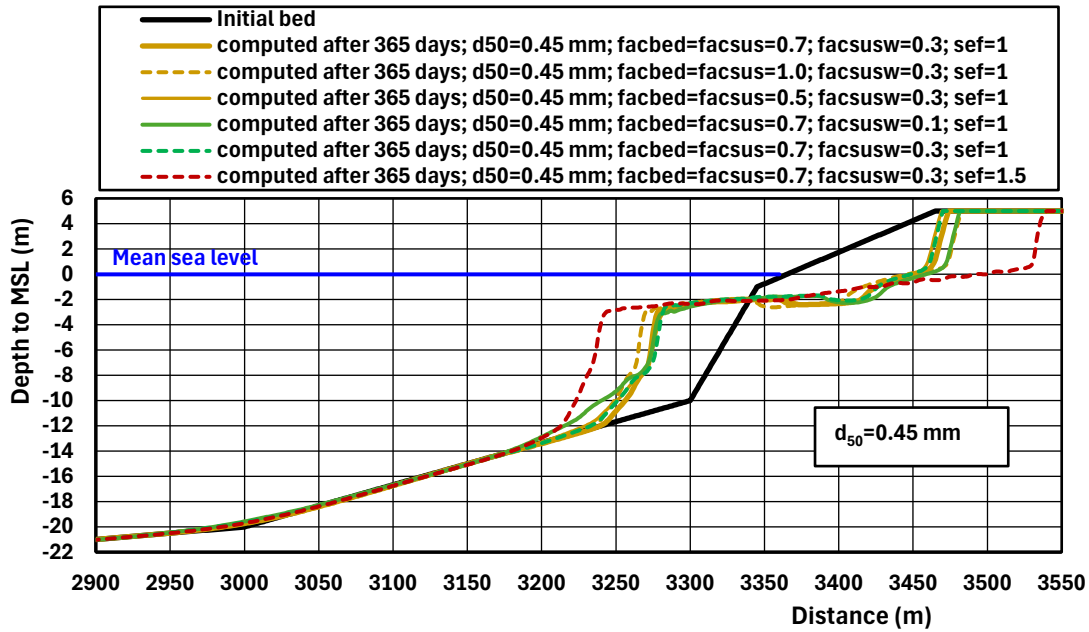


4. Effect of wave runup



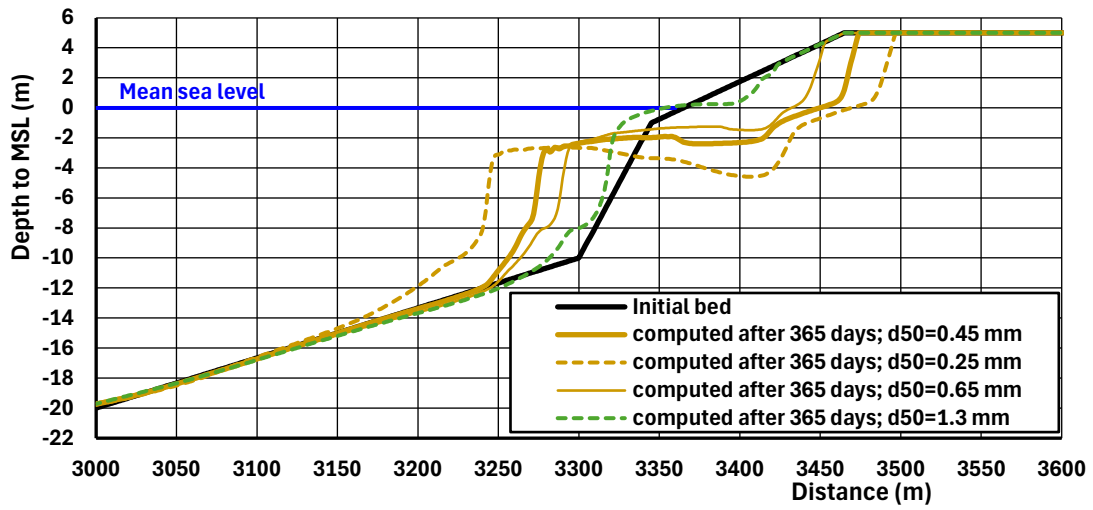


5. Effect of sand transport



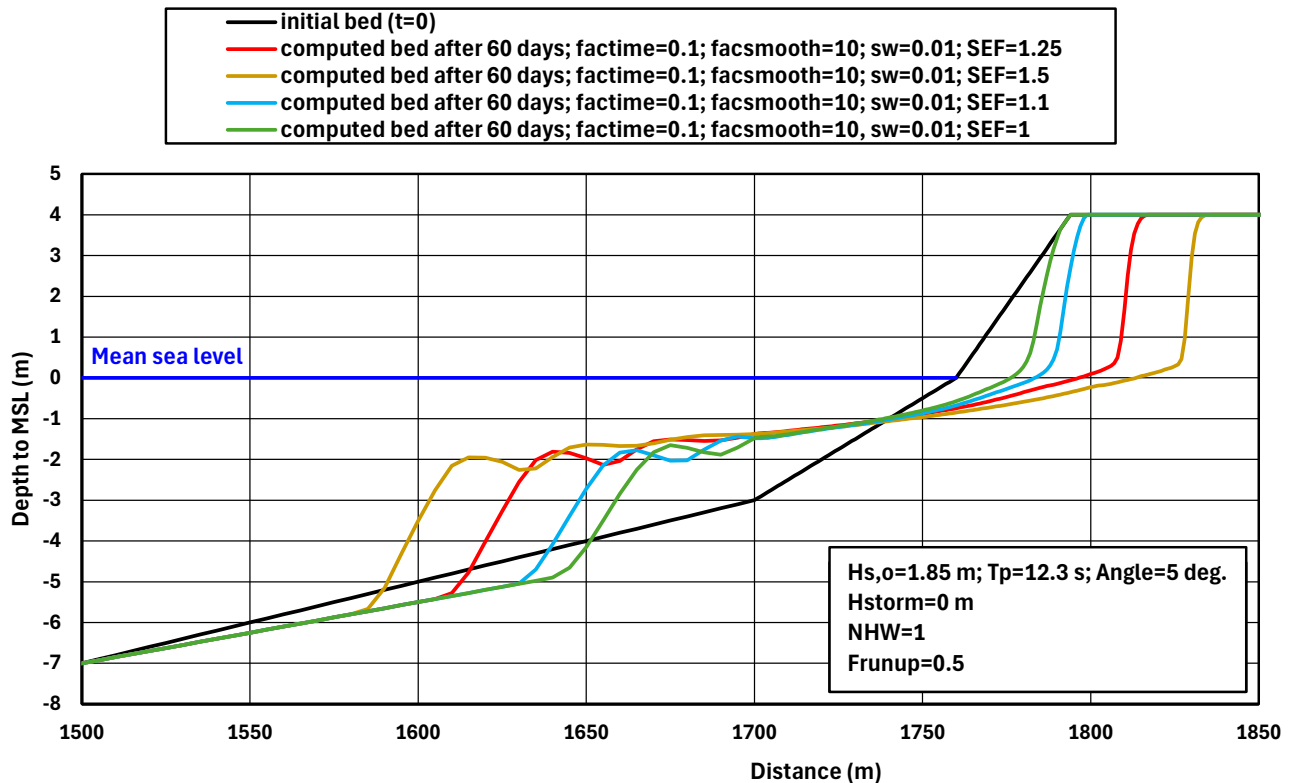


6. Effect of particle size





Effect of SEF-parameter



5. Offshore zone cases

5.1 Shoreface nourishment; Holland coast

The CROSMOR-model has been used to compute bed level changes along a shoreface nourishment, see **Figure 5.1.1**.

The tidal range is 1.1 m. The peak tidal velocity is 0.5 m/s at deep water.

The significant wave heights are between 1.7 and 2.7 m with periods in the range of 6.5 to 7.5 s over a period of 100 days. The wave incidence angle= 0 (perpendicular waves). The grain size is 0.3 mm.

Figure 5.1.1 shows the bed profile development after 100 days. Minor erosion occurs at the seaward end of the nourishment zone due to onshore transport.

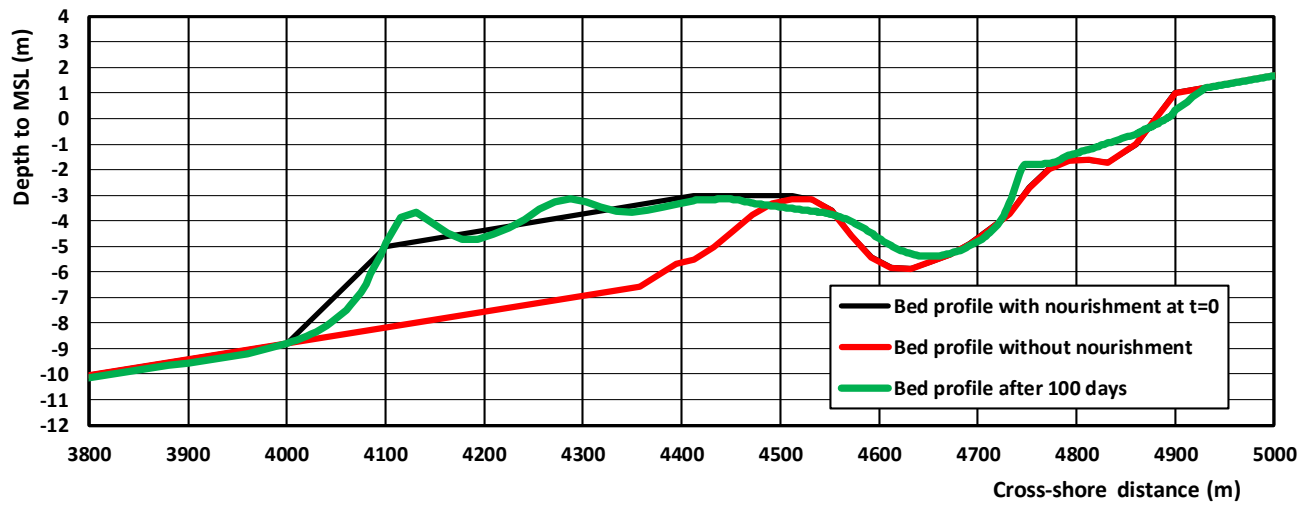


Figure 5.1.1 Erosion of shoreface nourishment at barred coastal profile



6. Hard structures at sea bed

6.1 General

Often, hard structures are present along the sea bed in the coastal zone. The CROSMOR-model was extended (in 2021) with functionality of sand transport across hard layers and bed level changes near the hard layers. Two tests cases have been defined, as follows:

- erosion downstream of submerged dam with a steady current;
- erosion at plane sloping beach with hard layer and a constant offshore wave height.

6.2 Model approach

Definition of hard layer

The hard layer is specified (input file; name.inp) in a similar way as the initial bottom by means of a table column with depth values of the hard layer (HRMSL) as function of the x-coordinate (cross-shore coordinate), see **Figure 6.2.1**. Furthermore, a coefficient (F_{sand}) can be specified to manipulate the sand transport around the hard layer, see **Figure 6.2.1**.

The bed is assumed to be hard if the hard bottom level is equal to the initial bed level (no sand on the hard level). If the hard bed level is lower than the initial bed level, then the sand layer thickness is the difference between both levels. The hard bed level can not be higher than the initial bed level.

In case of a fully mobile bed, the bed levels of the hard layer can be set a very low value (-100 m or -1000 m).

```

40 * table length of bottom schematization and hard layer
41 11
42 * X=cross=shore coordinate, HMSL=depth to MSL (neg below MSL),
43 * HRMSL= bed level of hard layer to MSL; NSTAP=number of space steps between table points
44 * X (m) HMSL (m) HRMSLm (m) NSTAP
45 0. -35. -100. 100
46 1000. -22. -100. 20
47 1160. -18. -18. 25
48 1185. -4. -4. 20
49 1205. -2. -2. 15
50 1220. -4. -4. 18
51 1238. -2. -2. 8
52 1242. -6. -6. 59
53 1360. -2. -100. 20
54 1400 4. -100. 50
55 1500. 4. -100.

164 * X = X-COORDINATE [ M ]
165 * RC = CURRENT-RELATED ROUGHNESS [ M ];if RC=0.; RC is computed by model
166 * RW = WAVE-RELATED ROUGHNESS [ M ]; if RW=0.; RW is computed by model
167 * PMUD = PERCENTAGE OF MUD IN BED [ % ]
168 * Frip= coefficient acting on undertow velocity (default=1)
169 * Fsand= coefficient acting on near-bed sand concentration (default=1)
170 * X (m) RC (m) RW (m) PMUD (%) Frip(-) Fsand(-)
171 0. .0 .0 0. 1. 1.
172 1140. .0 .0 0. 1. 1.
173 1180. .0 .0 0. 1. 1.
174 1200. .0 .0 0. 1. 1.
175 1500. .0 .0 0. 1. 1.

```

Figure 6.2.1 Input related to hard layer

Upper: bed level of hard layer; Lower: coefficient F_{sand} (manipulation of transport near hard bed)



Modification of cross-shore sand transport

At each time step, the thickness (δ_s) of the sand layer above the hard layer is computed as the difference of the actual bed level and the hard bed level.

In the case of sedimentation conditions with decreasing sand transport, the sand transport above the hard layer is not modified.

In the case of erosion conditions, the sand transport above the hard layer is modified (post-processing process) if the thickness of the sand layer on the hard layer is too small. The sand transport remains constant if there is no sand on the hard bed. The procedure is, as follows (see **Figure 6.2.2**):

- compute sand layer thickness ($\delta_{s,i}$) at each grid point;
- compute total sand transport ($q_{t,i}$) and sand transport gradient ($\Delta q_{t,i}$) at each grid point without presence of hard layer; total sand transport = bed load transport plus suspended load transport;
- compute potential sand transport gradient ($\Delta q_{t,*i}$) related to sand layer thickness on hard layer over 1 time step (Δt); $\Delta q_{t,*i} = \delta_{s,i} b_i \Delta x_i \rho_s (1-\varepsilon)$ with b_i =width, Δx_i =grid length, ρ_s =sand density, ε =bed porosity value;
- compute new sand transport in case of increasing sand transport without hard layer and not sufficient sand on hard layer ($\Delta q_{t,*i} < \Delta q_{t,i}$ or $\delta_s=0$): $q_{t,i} = q_{t,i-1} + \Delta q_{t,*i}$;
if $\delta_s=0$ then $\Delta q_{t,*i}=0$ and sand transport remains constant ($q_{t,i}=q_{t,i-1}$);
- no modification in case of sedimentation conditions (decreasing sand transport).

The computation method is demonstrated for 2 cases, as follows (see **Figure 6.2.3**):

A. Landward sand transport across hard layer

1. natural sand transport increases continuously in landward direction (curve a-b resulting in erosion):
if no sand is present on hard layer, the sand transport remains constant above hard layer (line d) from seaward end to landward end; after that the sand transport goes to point B on curve a-b;
2. natural sand transport increases in landward direction, but decrease at some point (curve a-c resulting in erosion and deposition):
if no sand is present on hard layer, the sand transport remains constant above hard layer (line d) from seaward end to landward end; after that the sand transport goes to point C on curve a-c;

B. Seaward sand transport across hard layer

1. natural sand transport increases continuously in seaward direction (curve e-f resulting in erosion):
if no sand is present on hard layer, the sand transport remains constant above hard layer (line h) from landward end to seaward end; after that the sand transport goes to point F on curve e-f;
2. natural sand transport increases in seaward direction, but decreases at some point (curve e-g resulting in erosion and deposition):
if no sand is present on hard layer, the sand transport remains constant above hard layer (line h) from landward end to seaward end; after that the sand transport goes to point G on curve e-g.

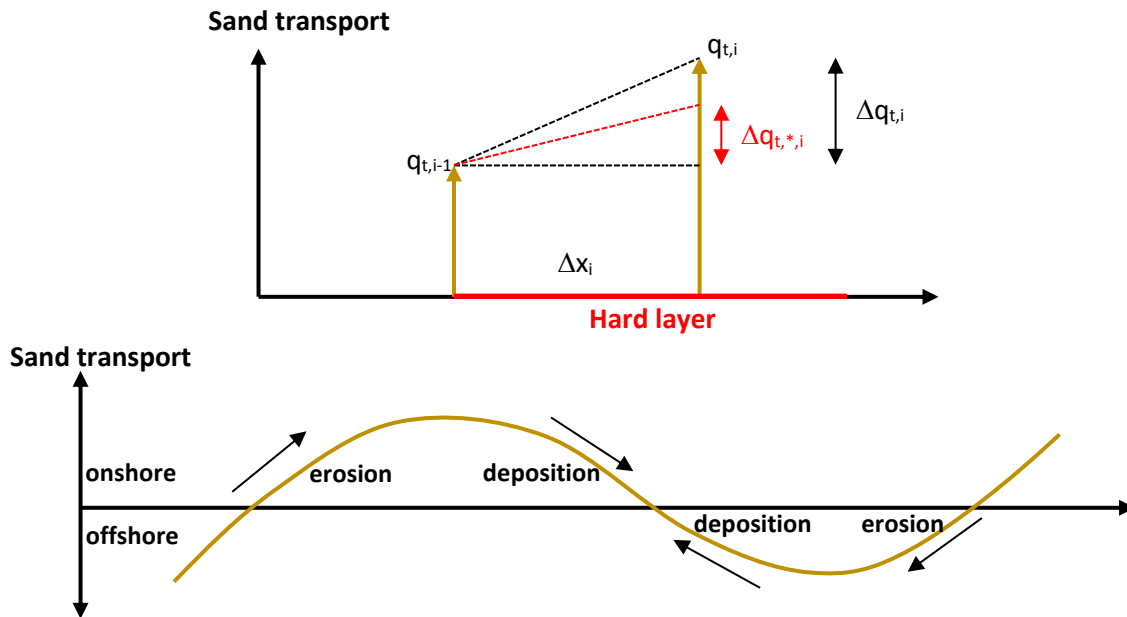


Figure 6.2.2 Cross-shore sand transport

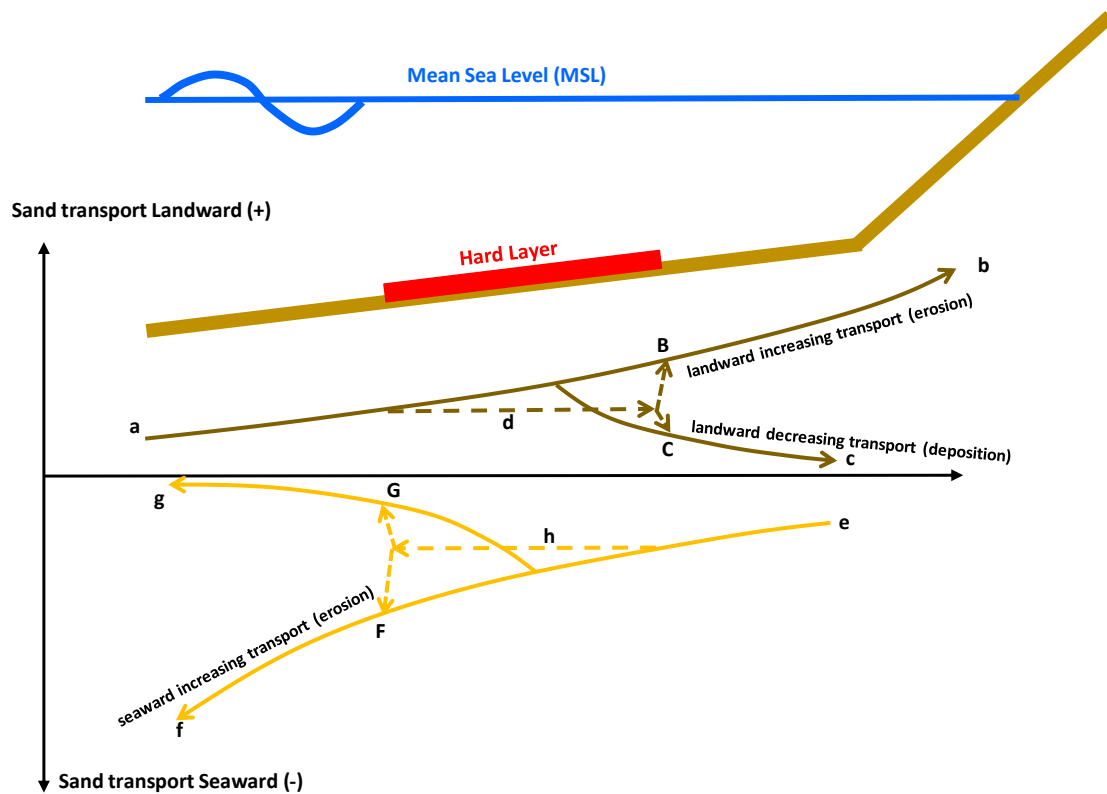


Figure 6.2.3 Schematization of sand transport across hard layer



6.3 Erosion downstream of submerged dam

The testcase consists of (see **Table 6.3.1**):

- water depth at inlet ($x=0$) = 10 m; water depth at end=3 m;
- water depth above dam=2 m;
- side slopes of dam: 1 to 10;
- steady current (no tide; no waves); velocity at inlet=0.2 m/s; velocity above dam=1 m/s;
- median sand diameter $d_{50}=0.25$ mm.

Figure 6.3.1 shows the bed levels (soft bed and hard bed), the sand transport rates with and without hard layer and the computed bed levels downstream of the submerged dam. The results are:

- sand transport above hard layer is much lower ($\cong 0.01$ kg/m/s; yellow line; **Figure 6.3.1upper**) than without hard layer ($\cong 0.6$ kg/m/s; yellow dashed line);
- sand transport downstream of dam ($x > 1140$ m) is about 0.13 kg/m/s; the increase of sand transport from 0.01 kg/m/s at end of hard layer to 0.13 kg/m/s (around $x=1150$ m) at the mobile sand bed causes erosion (maximum 0.1 m after 1 day);
- no erosion at hard layer region (1100 to 1140 m);
- erosion pit immediately downstream of hard layer (**Figure 6.3.1lower**); weak instabilities (saw-tooth pattern) for small grid size (1 m) and time steps; larger instabilities for large grid size (8 m) and time step; instabilities disappear if the suspended load transport downstream of the dam is enhanced (using $F_{sand}=1, 5, 1$ at $x=1140, 1160$ and 1180); bed instabilities are most likely related to the relatively small transport rates (current velocity=0.6 m/s) downstream of the dam.

Figure 6.3.2 shows the erosion of the dam without hard layer. Substantial erosion occurs which is partly deposited downstream of the dam and partly carried out of the domain (through downstream boundary).

PARAMETERS	Values
Water depth at entrance, exit; Water level	10 m and 3 m below Mean Sea Level (MSL); constant (no tide)
Cross-shore velocity at inlet; above dam	0.2 m/s; 1 m/s
Significant wave height, period	no waves
Crest submerged dam; side slopes	2 m below MSL; 1 to 10
Grid size	20 m upstream of dam; 2 m above and 1 m downstream of dam
Grain diameter sand d_{50}	0.25 mm
Coefficient bed concentration factor (F_{sand}) downstream of hard layer	1; maximum 5
Bed roughness	0.01 m
Bed smooth factor	70
Temperature and salinity	15° C and 30 promille
Files	ATEST2B.inp

Table 6.3.1 *Input data of CROSMOR-model*

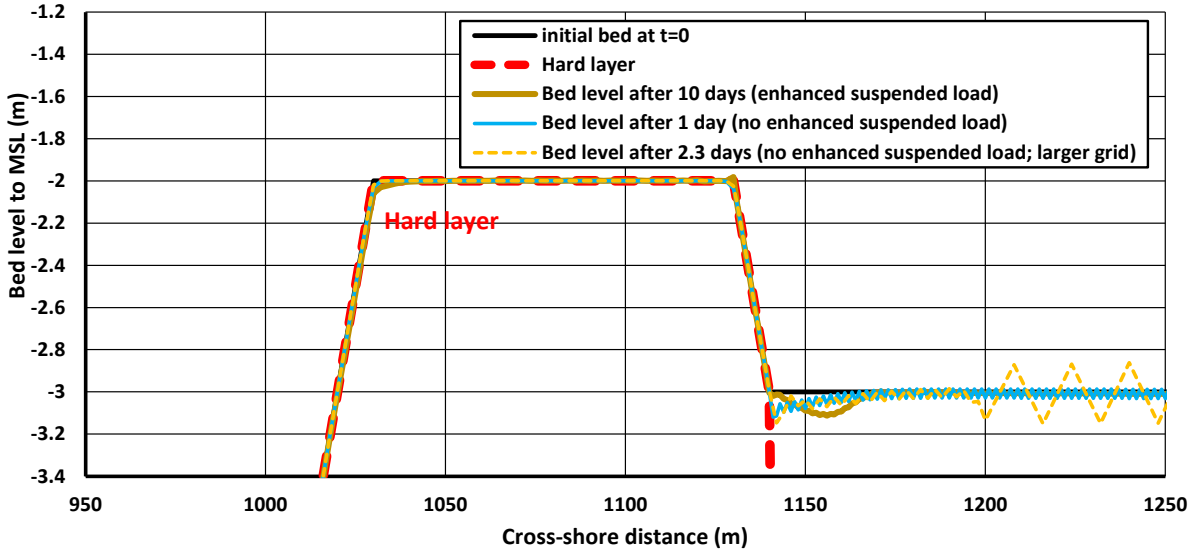
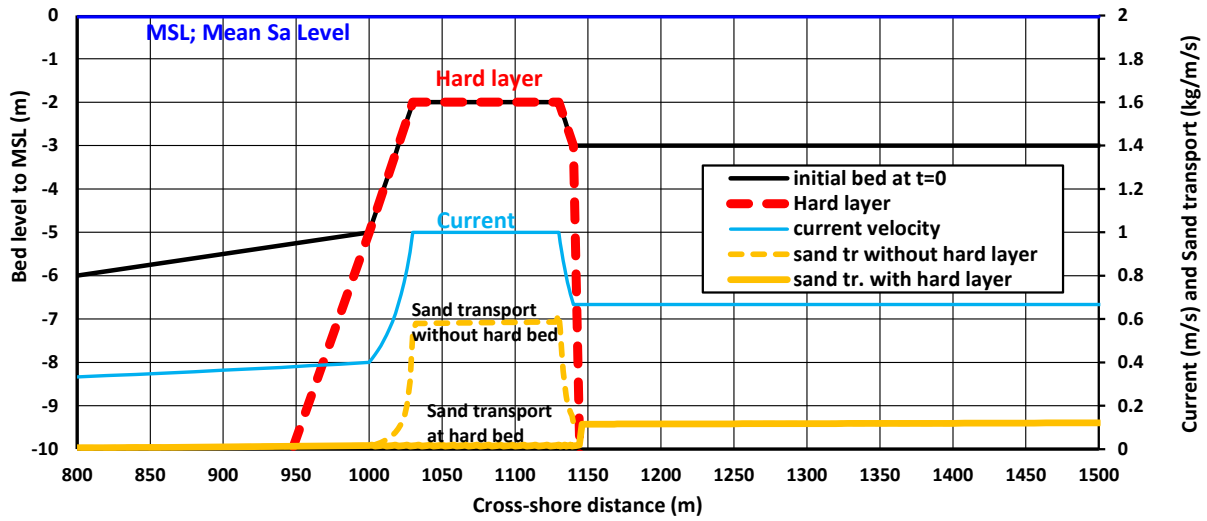


Figure 6.3.1 Erosion downstream of submerged dam with a steady current
Upper: bed levels and sand transport; Lower: computed bed level changes

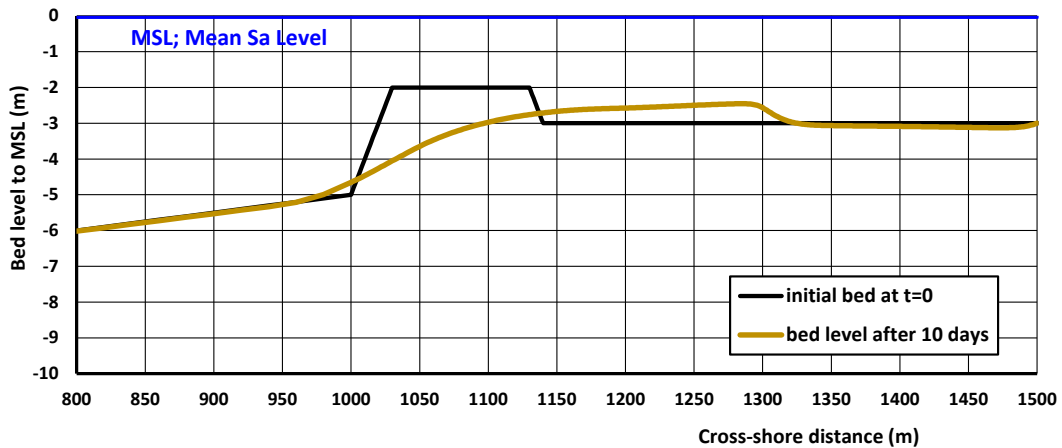


Figure 6.3.2 Erosion of submerged dam of sand (no hard layer)



6.4 Erosion at plane sloping beach with hard layer

The testcase consists of (see **Table 6.4.2**):

- horizontal bottom at 10 m below MSL;
- beach slope of 1 to 5;
- water depth at toe of beach=10 m below MSL
- water depth at beginning of hard layer= 2 m below MSL;
- constant water level (no tide);
- constant offshore wave height;
- longshore current velocity at offshore boundary (x=0)= 1 m/s;
- median sand diameter $d_{50}=0.25$ mm.

Figure 6.4.1 shows the bed levels (soft bed and hard bed), the sand transport rates with and without hard layer and the computed bed levels seaward of the hard layer. The results are:

- sand transport above hard layer is zero and remains zero (green solid curve);
- sand transport increases to about -2.5 kg/m/s in seaward direction at seaward end of the hard layer, where the sand bed is mobile which causes erosion (green solid curve);
- maximum erosion is about 1.5 m after 10 days and 5 m after 100 days; the total erosion volume is about 15 m³/m after 10 days and about 120 m³/m after 100 days.

Figure 6.4.2 shows the beach erosion after 10 days without hard layer. The total erosion is about 75 m³/m after 10 days or 7.5 m³/m per day. Hence, the bed protection by a hard layer reduces the erosion by a factor of about 5.

PARAMETERS	Values
Water depth at deep water; water level	10 m below MSL constant (no tide)
RMS-wave height, period and wave incidence angle at deep water	$H_{rms}=2$ m, $T_p=7$ s, angle= 10°
Beach slope	1 to 5; beach crest at 10 m above MSL
Boundary depth near beach	0.3 m
Grid size	10 m at horizontal bed; 1 m at beach
Number of wave classes per wave height	1
Wave asymmetry	Isobe-Horikawa
Coefficient Longuet-Higgins streaming; roller effect	0 (default=1); 0.5 (default=1)
Grain diameter sand d_{50}	0.25 mm
Coefficients sandtransportformulas	bed load=0; Suspended load=1.5 (default= 1)
Coefficient sandtransport wave asymmetry	0 (default= 1)
Coefficient sand entrainment beach zone	1 (default)
Coefficient bed concentration landward of hard layer	1; maximum 5
Coefficient undertow	1 (default)
Extra entrainment at dune front (sef)	1 (default)
Bed roughness	Automatic
Bed smooth factor	50 (default=10)
Time step factor	0.1 (default=1)
Temperature and salinity	15° C and 30 promille
Files	ATESH10.inp

Table 6.4.1 *Input data of CROSMOR-model*

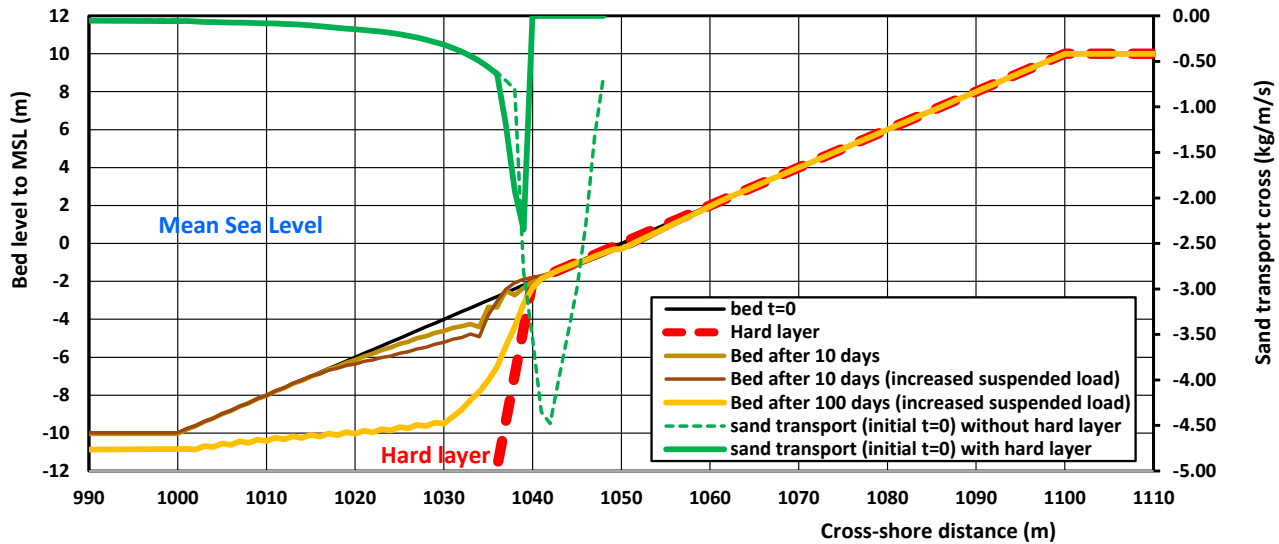


Figure 6.4.1 Erosion at toe of beach with hard layer (no bed load)

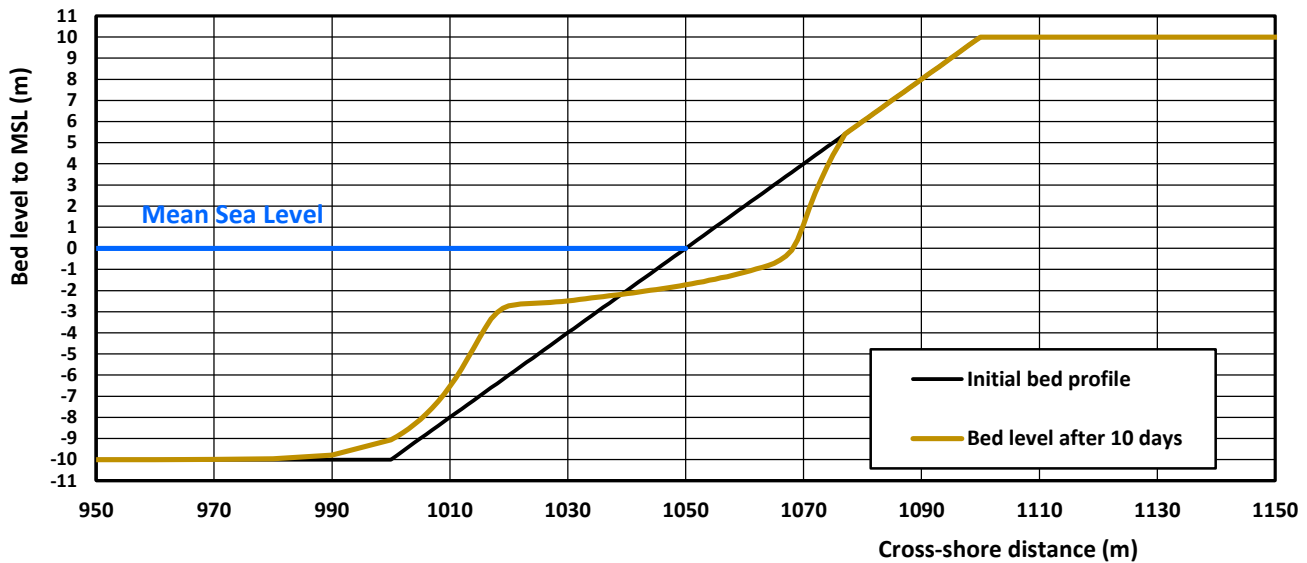


Figure 6.4.2 Beach erosion along slope after 10 days without hard layer (no bed load)

6.5 Erosion in lee of hard submerged shore-parallel breakwater

The testcase consists of (see Figure 6.5.1):

- sloping bed with hard structure;
- beach slope in lee of structure;
- water depth at toe of structure is -22 m below MSL
- constant water level (no tide);
- constant offshore wave height $H_{s,o}=7.3$ m; $T_p=12.5$ s, wave angle=20°;
- longshore current velocity at offshore boundary ($x=0$)= 0 m/s;
- median sand diameter $d_{50}=0.225$ mm.



Figure 6.5.1 shows:

- bed profile after 1 day in case of hard structure (Crosmor 2022);
- bed profile after 1 day in case of hard structure consisting of sand (Crosmor 2022 and Crosmor2013); results are slightly different as Crosmor 2013 does not use a 5 point-filter on cross-shore sand transport;
- sand transport (Crosmor2022) in case of hard layer consisting of sand; sand transport is shown with and without 5 point-filter (sand transport with filter is used for bed level changes).

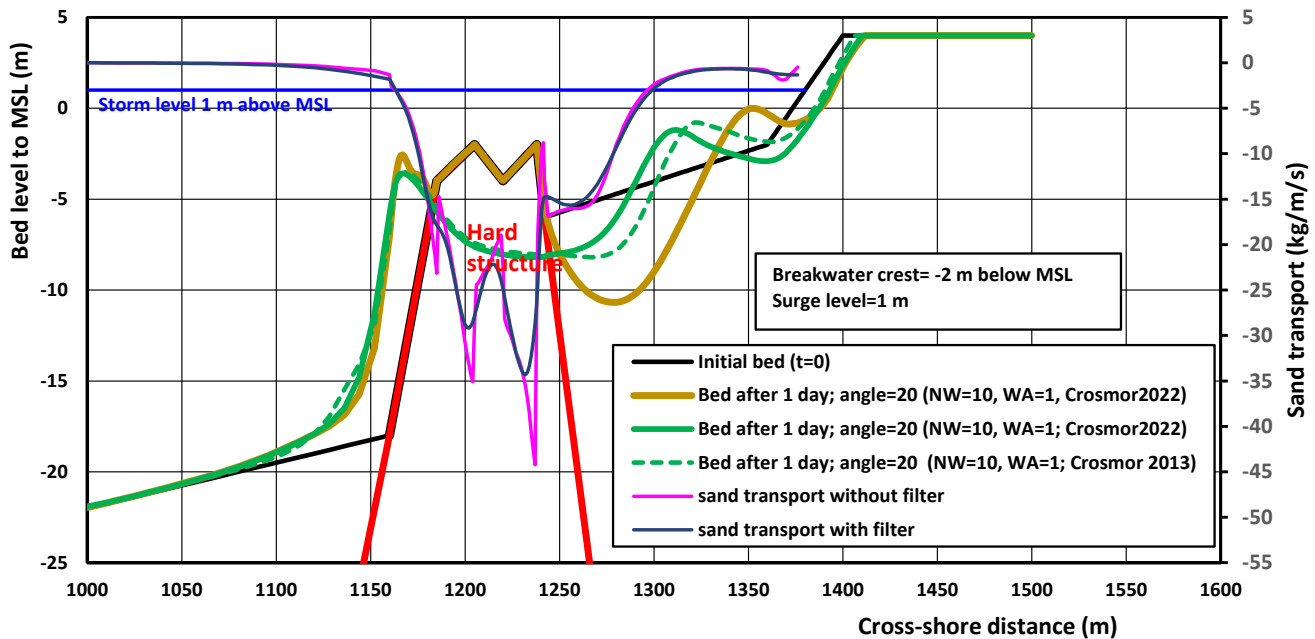


Figure 6.5.1 Bed profiles after 1 day; sand transport at $t=0$

6.6 Erosion of beach with emerged shore-parallel breakwater

The Jacksonville District of USACE is responsible for about 70% of the Florida coastlines (1800 miles). Currently, USACE is funding the entire cost of the beach renourishment works 2022-2023 at Miami Dade County (www.saj.usace.army.mil). Natural erosion and storm damage have eroded the Miami coastline, which is one of nation's best known vacation destinations. The beach renourishment works extends from Baker's Haulover Inlet in the north to Government Cut in the south. A total of about 0.7 million m^3 of beach sand along 3500 m ($200 m^3/m$) of coastline is now renourished in the Miami area. The beach width is extended locally to about 80 m, Figure 6.6.1.



Figure 6.6.1 Miami beach renourishment 2022-2023

A beach nourishment area with extended beach width is severely attacked by waves and eroded by longshore and cross-shore sand transport processes. This has been studied by using the Longmor-model and Crosmor-model for an example beach nourishment with alongshore length of 3000 m and cross-shore width of 80 m in the Miami Dade area (see below).

Longshore transport processes

The loss of sand from the nourishments area (see Figure 1) and the associated coastline changes due to alongshore sand transport processes can be computed by the 1D LONGMOR coastline model. The basic input data are: d_{50} of beach sand=0.3 mm, nearshore beach slope=1 to 20, wave breaking coefficient=0.6, height of active beach zone=6 m. The offshore wave climate is represented by two wave conditions: $H_s=1.3$ m ($T_p=6$ s), wave incidence angle= 10° to the shore normal during 200 days and $H_s=1.1$ m ($T_p=6$ s), wave incidence angle= -10° during 165 days. The model has been calibrated to give a net annual longshore sand transport of about 50,000 m³/year to south, which is the typical value for Miami Dade beaches.

Figure 6.6.2 shows the coastline changes after 3, 5, 10 and 20 years. The beach width reduces from 80 m to 30 m over a period of 20 years. The total beach erosion volume is about 0.7 million m³/year, which is deposited in the corner areas. The computed sand transport values (in m³/day) at initial time ($t=0$) for both wave conditions are also shown in Figure 1. The net longshore sand transport from north to south is $540 \times 200 - 340 \times 165 \approx 50,000$ m³/year. The sand transport values are highest along the flanks of the nourishment area where the wave incidence angles are highest.

Given these results, the lifetime of the nourishment is of the order of 15 to 20 years under the assumption that alongshore transport processes are dominant over cross-shore transport processes. This latter assumption may not be realistic given the relatively steep upper beach profiles (see below).

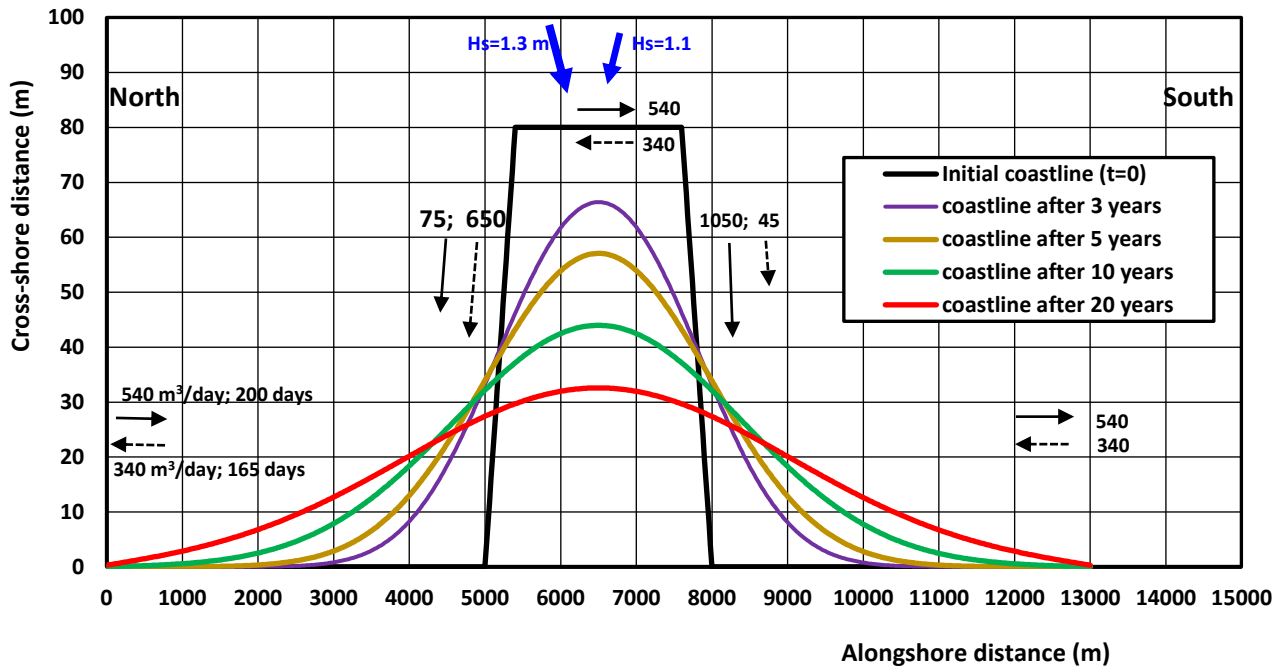


Figure 6.6.2 Coastline development due longshore transport processes; Longmor-model (miamiL1.inp)

Cross-shore transport processes

The engineering CROSMOR-model has been used to study the erosion of a beach nourishment of 0.3 mm sand ($d_{50}=0.3$ mm) due to cross-shore sand transport processes at a typical Miami Dade beach profile, see Figure The initial beach nourishment volume is about $250 \text{ m}^3/\text{m}$ with a horizontal beach width of 80 m at a level of $m+1$ m above MSL (Mean Sea Level), see **Figure 6.6.3**. The annual wave climate at a water depth of 50 m is: $H_s=0.4$ m ($T_p=4$ s) during 200 days, $H_s=1$ m ($T_p=5$ s) during 130 days, $H_s=1.5$ m ($T_p=6$ s) during 30 days and $H_s=2$ m ($T_p=7$ s) during 5 days. The wave incidence angle at 50 m depth is set to 10° for all conditions. The strength of the Florida Current at a depth of 50 m is set to 0.2 m/s to north. The slope of the original beach profile is 1 to 15 between -1 m and +1 m and 1 to 40 between -3.5 and -1 m. The outer beach profile of the beach nourishment is about 1 to 10, beach width of 80 m. The sand transport in the model is reduced (factor of 2) to account for the effect of coral materials.

The facsmooth-value should be as small as possible!!!

Figure 6.6.3 shows the computed beach profiles after 1, 2 and 3 years (file miami2.inp). The beach erosion volume after 1, 2 and 3 years is 50, 65 and $75 \text{ m}^3/\text{m}$. The erosion is highest in the first year. The eroded sediments are deposited at the toe of the beach profile (between -1 and -5 m). Onshore bed load transport occurs seaward of the -5 m depth contour resulting in a slowly growth of the deposition area. The coastal profile seaward of the -5 m depth contour is hardly affected. A steep erosion front is generated on the beach above the mean water line which is often seen in practice. A model run for a storm period of 72 hours (24 hours $H_s=2$ m, $T_p=7$ s + 24 hours $H_s=3$ m, $T_p=8$ s + 24 hours $H_s=2$ m, $T_p=7$ s; miami2s.inp) gives a storm erosion of about $15 \text{ m}^3/\text{m}$ in 3 days. A run with a storm of 45 hours with $H_s=3$ m ($T_p=9$ s) and a sand of 0.25 mm gives similar results.

The lifetime of the beach nourishment of $250 \text{ m}^3/\text{m}$ is estimated to be of the order of 5 to 10 years.

Nearshore hard structures may offer an efficient way to protect beach nourishments, particularly shore parallel breakwaters with length of 100 to 150 m interrupted by regular gaps (70 to 100 m) can be constructed in the beach zone.

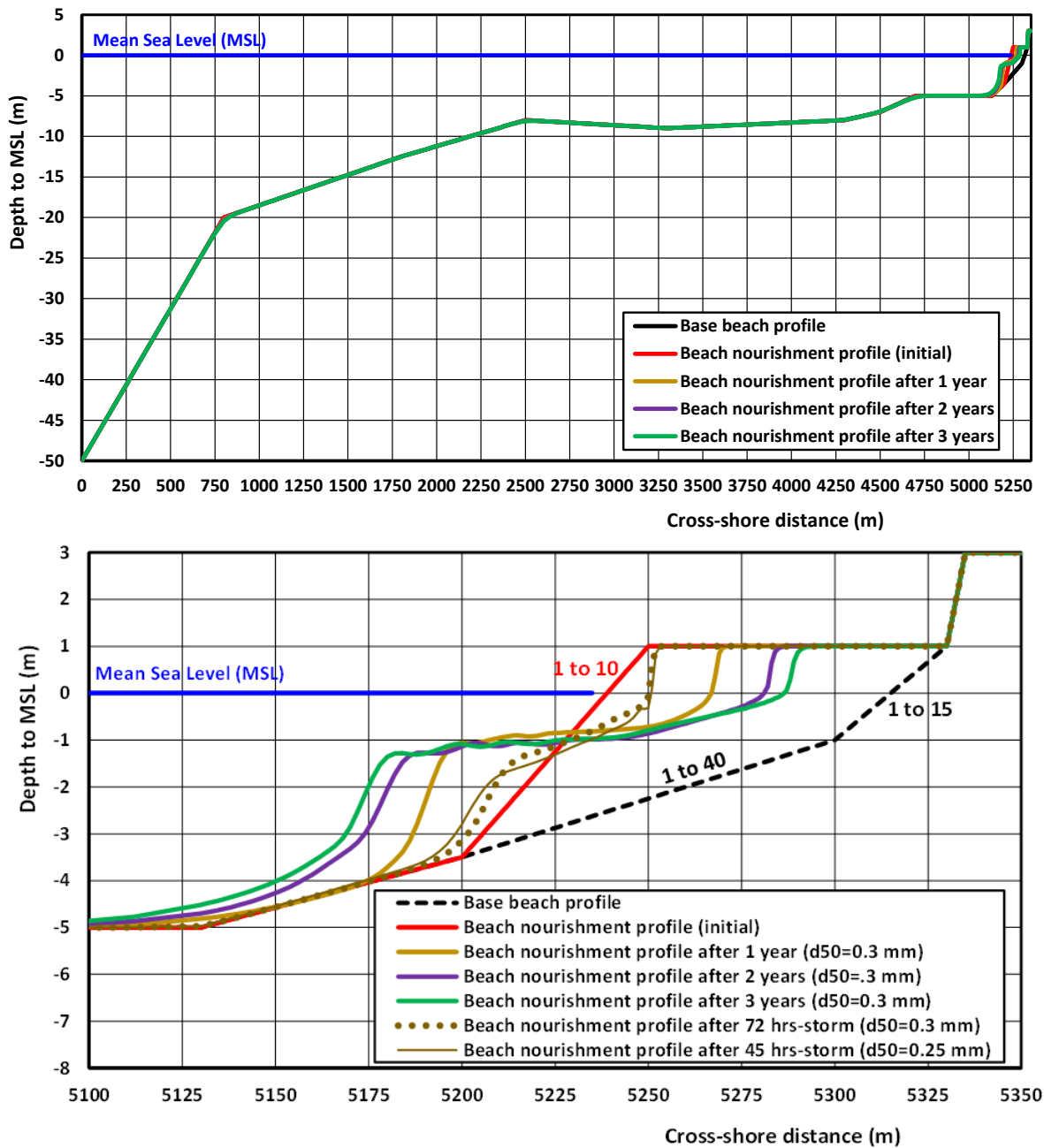


Figure 6.6.3 Beach nourishment development over 3 years; CROSMOR-model (miami2.inp; miami2s.inp)
Bed smoothfactor=15
faced=0.3; facsusw=0.1; facsusw=0; CLH=0.1.

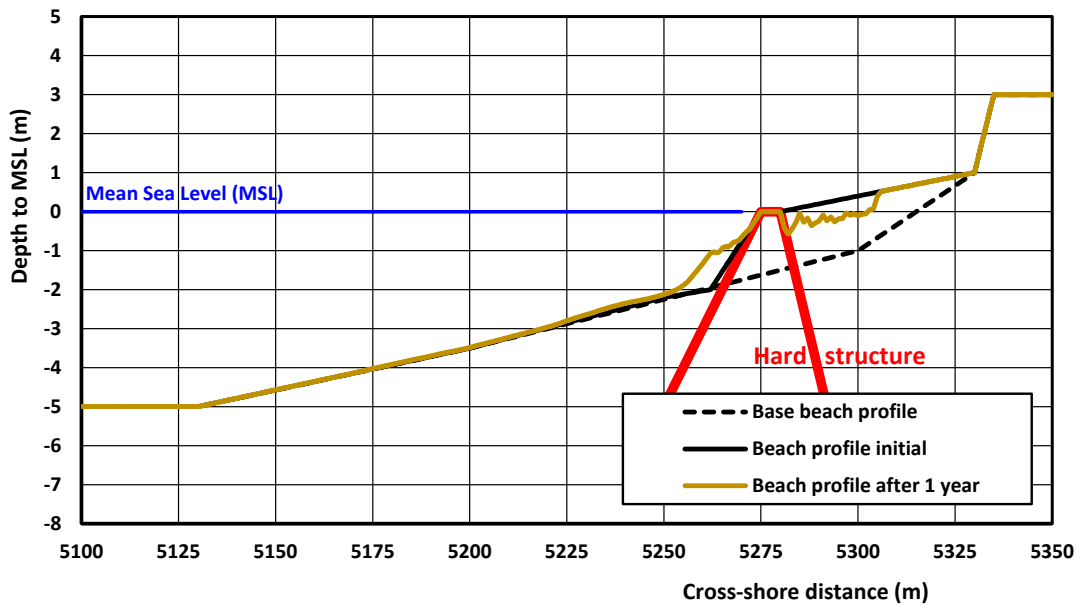


Figure 6.6.4 Beach protection by shore-parallel breakwater (Crest at MSL); CROSMOR-model (miami3h.inp)
Bed smooth factor=0.00001 (very small as transport rates are very small)
faceded=0.3; facsusw=0.1; facsusw=0; CLH=0.1.

Figure 6.6.4 shows a shore-parallel breakwater with crest at the mean sea level (MSL), which is about 50 m from the dune toe. The outer slope should be as mild as possible, say 1 to 4. The computed beach erosion after 1 year due to overwash processes is not more than about $10 \text{ m}^3/\text{m}$, which can be refilled regularly by sand using trucks from on-land borrow sites. The erosion is about nil, when the crest is situated at +1 m above MSL, see **Figure 6.6.5**. A scour pit is generated at the toe of the breakwater, but the model may underestimate the maximum scour depth. Substantial storm erosion damage due to hurricanes with high water levels is unavoidable, but is less than without breakwater protection. Further studies are required to assess the potential of this type of hard structures close to the shore.

Summarizing, it is concluded that cross-shore sand transport processes are of major importance due to the presence of steep beach profiles and most likely are dominant over along-shore sand transport processes resulting in severe beach erosion on a time scale of the order of 5 to 10 years (maximum lifetime). Shore-parallel breakwaters may offer an efficient method to protect the beach nourishment area.

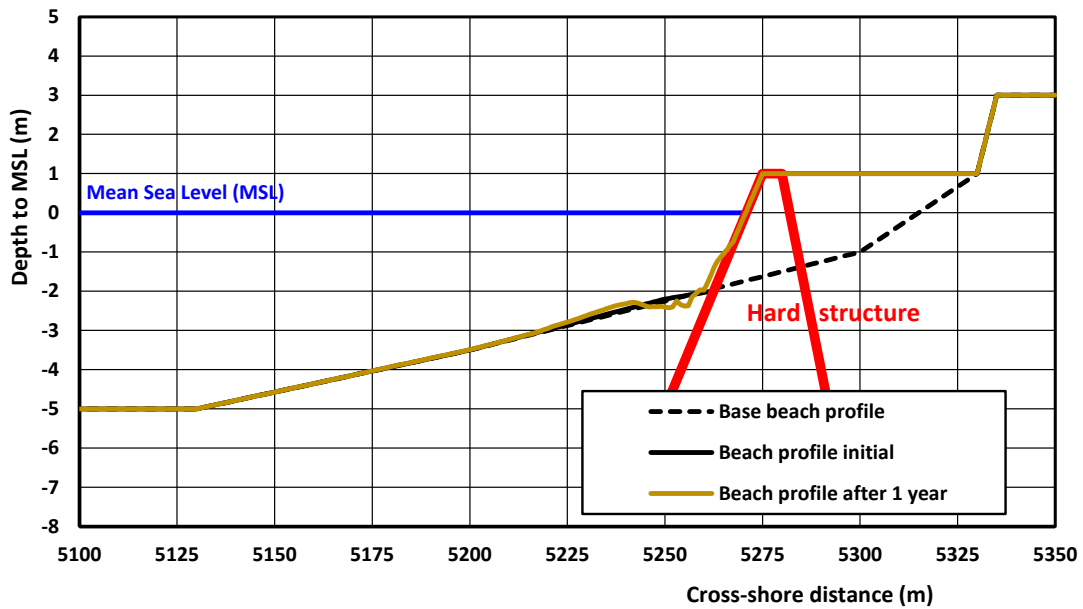
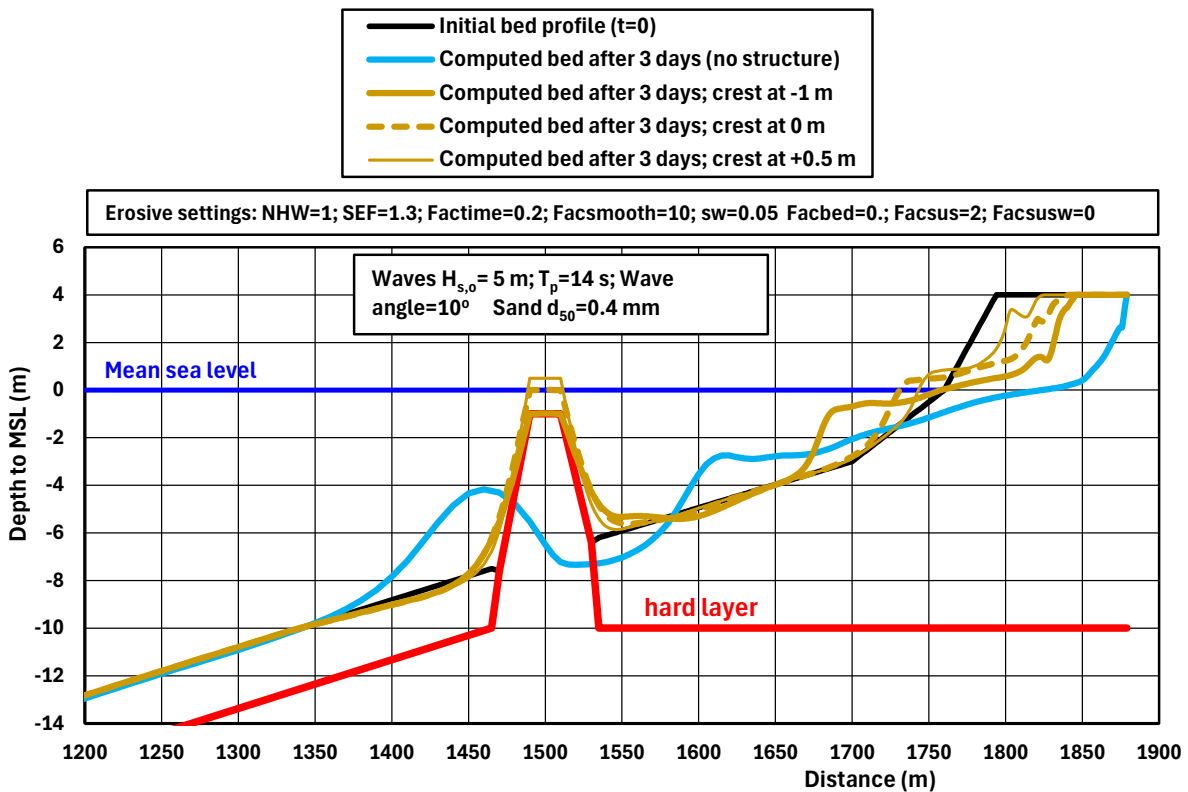


Figure 6.6.5 Beach protection by shore-parallel breakwater (Crest at +1 m MSL); CROSMOR-model (miami2h.inp)
Bed smooth factor=0.00001 (very small as transport rates are very small)
facbed=0.3; facsusw=0.1; facsusw=0; CLH=0.1.

6.8 Effect of structure





7. Gravel beach erosion

7.1 General

The CROSMOR-model can also be used for gravel beaches.

The model is validated in **Section 7.2.1**. Model runs are presented in **Section 7.2**. Model runs for the gravel beach at Pevensey Bay, Uk are given in **Section 7.3**.

7.2 Short and long term runs for beach of gravel ($d_{50}=40$ mm)

The new CROSMOR version 15 July 2025 has also been used to study the effect of a top layer of gravel ($d_{50}=40$ mm) to reduce the beach erosion. It is noted that the complete bed profile from deep water to the dune crest consists of gravel in the CROSMOR-model. In reality, there will be a gravel layer with thickness of the order of 1 m on top of the sand surface extending to the -3 m depth line. This composite situation cannot be modelled at present by the CROSMOR-model. The CROSMOR-model is validated for gravel beaches in **Section 7.2.1**.

Short term and long term runs for the beach of Benin/Togo are made presented in **Sections 7.2.2** and **7.2.3**.

7.2.1 Validation of CROSMOR-model for gravel beaches

To justify that the CROSMOR-model produces realistic results for steep gravel beaches, three approaches have been followed:

- the transport rates of gravel in unidirectional flow (river flow) computed by the CROSMOR-model are compared to the measured values of gravel flume experiments of Meyer-Peter and Mueller (1948);
- the longshore transport rates of gravel in coastal flow computed by the CROSMOR-model are compared to the measured values of longshore gravel transport at two field sites in the UK (Shoreham and Hurst Castle Spit);
- simulation results for a nourishment of coarse materials (40 mm) at a beach situated at Magdalen Island in St. Lawrence Bay, Canada).

Measured transport rates of gravel in unidirectional current (data of Meyer-Peter and Mueller, 1948)

Very relevant for coastal gravel transport are the flume experiments of Meyer-Peter and Mueller (1948) with relatively large water depths in the range of 0.5 to 1 m. Some of their data are shown in **Table 7.2.1**. Gravel of 28.7 mm was tested in a wide flume with width of 2 m. Gravel of 5.2 mm was tested in a small scale flume with a width of 0.35 m. Small-scale bed forms were present during most the experiments. The measured k_s -values (derived from the discharge, slope and water depth) were in the range of 0.15 to 0.045 m for the experiments with $d_{50}=5.2$ mm and in the range of 0.05 to 0.2 m for the experiments with $d_{50}=28.7$ mm. The transport of gravel with $d_{50}=28.7$ mm is relatively low (<0.03 kg/m/s) for a current velocity of about 2 m/s. Initiation of motion starts at a velocity of about 1.8 m/s, see also **Figure 7.2.1**. The transport rate of gravel increases to about 8 kg/m/s for a current velocity of 3 m/s. These results show that peak velocities in the range of 2 to 3 m/s are required to produce intensive transport of gravel in the coastal zone. Most likely, the gravel transport in field conditions is somewhat smaller than that in ideal flume conditions. Limiting factors in field conditions are wider size ranges and local armouring effects.

Figure 7.2.2 shows the measured bed load transport values (assumed error range of $\pm 50\%$) as function of the depth-averaged current velocity. Other measured values are also shown. To show that sediment transport of the CROSMOR-model can also be used to simulate gravel transport as measured in the flume experiments of Meyer-Peter and Mueller (MPM, 1948), the CROSMOR-model has been used in river mode (no waves; input file gravelr.inp) for a channel with a gravel bed. The water temperature is 15 °C and the salinity is 0 promille (fresh water). In the case of gravel of 5.2 mm, the water depth was increased to take the side wall roughness of the



small flume into account resulting in a lower bed-shear stress and lower bed load transport. The bed roughness was set to $k_s=0.03-0.06$ m to represent the bed form roughness. The computed bed load transport values are somewhat too small (factor2) for gravel of 28.7 mm, which can easily be calibrated. The effect of the sediment size decreases for increasing current velocity. Overall, the agreement between measured and computed values is quite reasonable.

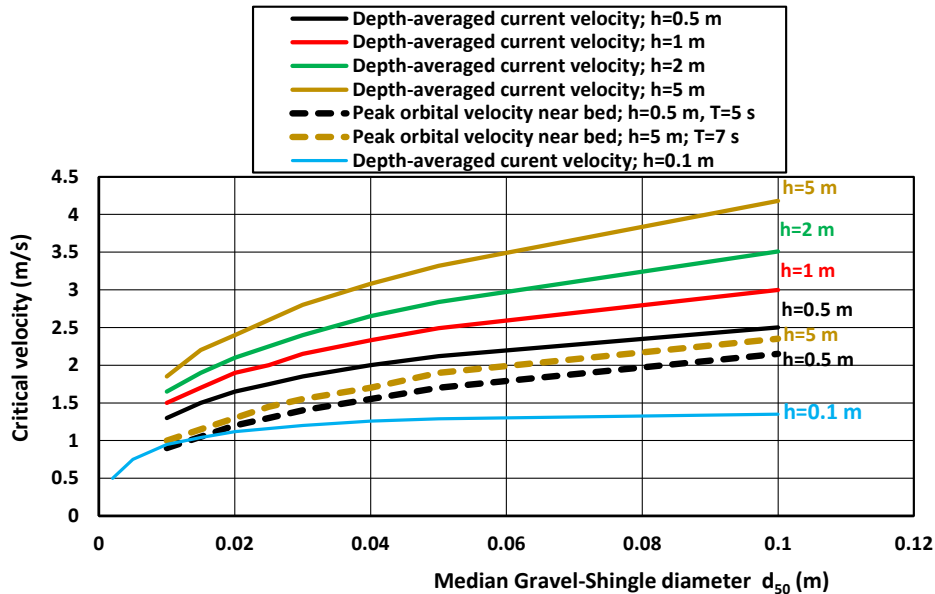


Figure 7.2.1 Initiation of motion of coarse (gravel) materials

Water depth (m)		Flume width (m)	Median gravel size (mm)	Depth-averaged current velocity (m/s)	Gravel transport (kg/m/s)
Range	Values				
0.6-0.75	0.6	2	28.7	2.73	8.46
	0.65	2	28.7	2.52	3.84
	0.7	2	28.7	2.34	1.91
	0.72	2	28.7	2.26	0.97
0.8-1.1	1.09	2	28.7	2.11	0.0294
	0.97	2	28.7	2.37	0.956
	0.96	2	28.7	2.40	0.952
	0.93	2	28.7	2.47	1.91
	0.91	2	28.7	2.52	1.93
	0.86	2	28.7	2.66	3.82
	0.85	2	28.7	2.68	3.79
	0.82	2	28.7	2.05	0.032
	0.8	2	28.7	2.88	8.43
	0.78	2	28.7	2.87	8.49
0.15-0.25	0.2	0.354	5.2	0.85	0.00082
	0.213	0.354	5.2	1.09	0.038
	0.182	0.354	5.2	1.26	0.154

Table 7.2.1 Gravel transport in flume experiments; $d_{50}=28.7$; 5.2 mm (Meyer-Peter and Mueller, 1948)

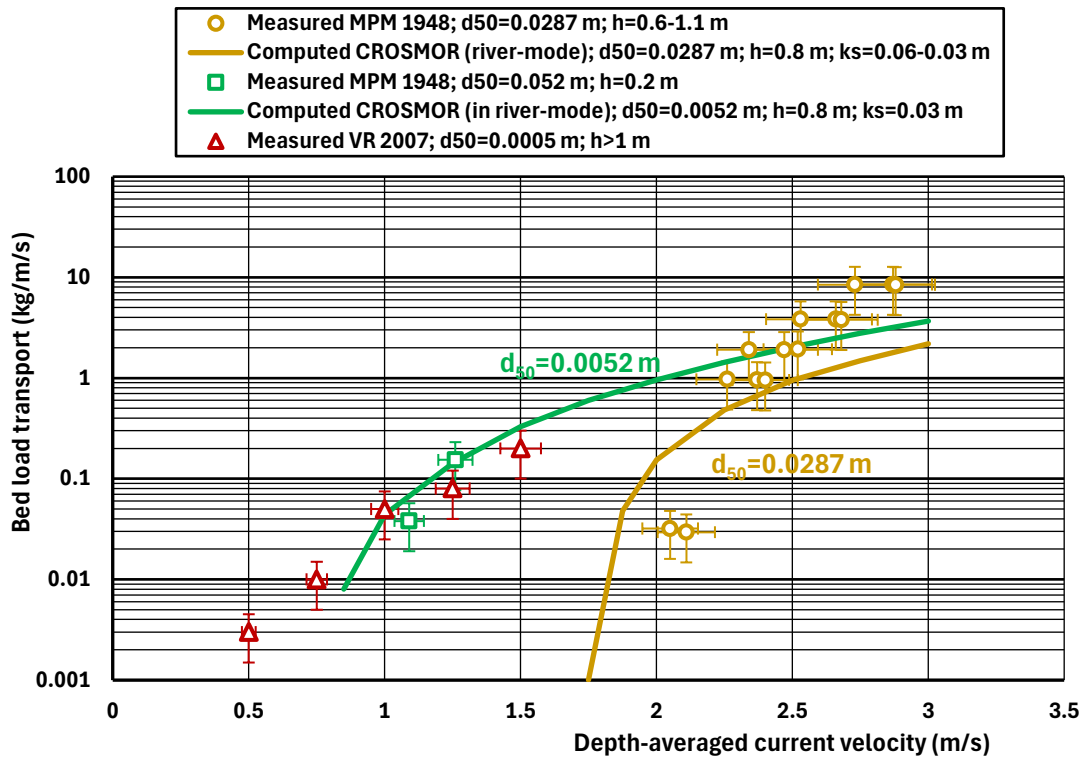


Figure 7.2.2 Measured and computed bed load transport rates for coarse sediments (gravelr.inp)

Measured longshore gravel transport data at Shoreham and Hurst Castle spit, UK

Measured longshore transport data of gravel/shingle are rather scarce. Herein, measured data from 2 sites in the UK are used for comparison to the computed values of the CROSMOR-model. These two sites are: Shoreham (Chadwick, 1989) and Hurst Castle Spit (Nicholls and Wright, 1991). The measured data are shown in **Table 7.2.2**. The offshore wave data are not known. It is assumed that the offshore wave height is about twice the value measured at the breaker line ($H_{s,o}=2H_{s,br}$).

Field sites UK	d_{50} (mm)	$\tan\beta$ (-)	$H_{s,br}$ (m)	θ_{br} (°)	T_p (s)	$Q_{t,mass}$ (kg/s)	Type of load
Shoreham UK 1989	20	0.1	0.3	15	3	0.05	bed load
	20	0.1	0.35	15	3	0.167	bed load
	20	0.1	0.4	15	3	0.3	bed load
	20	0.1	0.7	15	4	0.5	bed load
Hurst Castle Spit UK 1991	32	0.1	0.75	15	6	0.5	bed load
	32	0.1	1.0	15	6	1.5	bed load

d_{50} = particle size; $\tan\beta$ = beach slope, $H_{s,br}$ = significant wave height at breakerline, θ_{br} = wave angle to shore normal at breakerline, T_p = peak wave period,

Table 7.2.2 Measure longshore transport data of two field sites (shingle) in UK



A schematized cross-profile has been used, which is assumed to be valid for both sites. The beach with d_{50} of 20 mm used in the CROSMOR-model has a steep slope of 1 to 8. The crest level of the beach is at 10 m above MSL (mean sea level). The shoreface has a slope of 1 to 20. The tidal range is 4 m. The offshore significant wave height is varied in the range of 0.7 to 8 m. The bed roughness values are taken equal to the median grain sizes ($k_{s,c}=k_{s,w}=d_{50}$). The input data are given in **Table 7.2.3**.

Parameter	Values
Bed profile	slope of 1 to 20 between -30 m and -3 m slope of 1 to 8 between -3 m and +10 m
Sediment d_{50} ; d_{90}	0.02 m; 0.04 m
Bed roughness k_s	0.04 m
Horizontal mixing	0.1 m ² /s
Peak tidal water level	2 m (flood); -2 m (ebb)
Peak tidal velocity	0.6 m/s (flood); -0.6 m/s (ebb)
Offshore significant wave height $H_{s,o}$	2, 3, 4, 5, 6, 8 m (6 wave classes using Rayleigh distribution)
Peak wave period T_p	7, 8, 9, 10, 12, 15 s
Storm surge level above MSL	0, 0.5, 1, 2, 3, 4 m

Table 7.2.3 Data of field case of schematized shingle barrier

Figure 7.2.2 shows the computed values (in m³/day) of the longshore transport integrated over the cross-shore profile for a range of offshore wave heights between $H_{s,o}=0.7$ and 8 m. The computed values vary roughly between 5 m³/day and 9000 m³/day (including pores), see **Table 7.2.4**. About 80% of the longshore transport occurs in the surf zone landward of the -6 m depth contour and about 70% landward of the -4 m depth line. Measured longshore transport rates based on the work of Chadwick (1989) and Nicholls and Wright (1991) are also shown in **Figure 7.2.3** assuming that the offshore significant wave height is twice the observed nearshore breaking wave height. The computed longshore transport rates (in m³/day) for coarse gravel/shingle of 20 to 32 mm roughly are a factor of 2 to 3 too small for low wave conditions. This confirms that the CROSMOR-model may underpredict for coarse gravel conditions ($d_{50}>20$ mm).

It is noted that the measured values essentially represent the longshore transport of shingle/gravel in the swash zone (wave uprush and downrush zone). It should be realized that this zone is represented rather crudely using a sub-grid model approach.

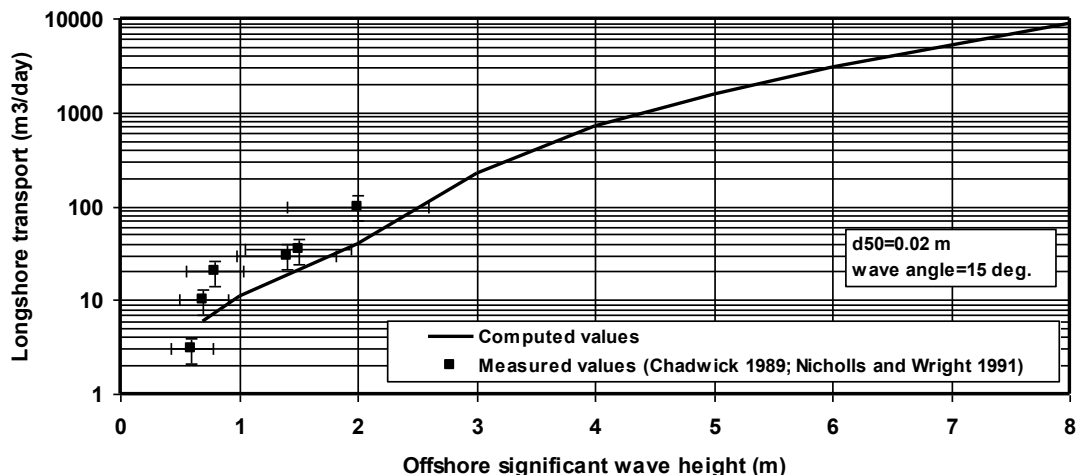


Figure 7.2.3 Longshore transport as function of offshore wave height



Offshore significant wave height $H_{s,o}$ (m)	Peak wave period T_p (s)	Storm surge level above Mean Sea Level (m)	Computed Longshore transport	
			(kg/s)	(m ³ incl. pores/day)
0.7	5	0	0.11	6
1	6	0	0.21	11
2	7	0	0.75	40
3	8	0.5	4.1	220
4	9	1	13	700
5	10	2	29	1565
6	12	3	56	3025
8	15	4	162	8750

Table 7.2.4 Integrated longshore transport of gravel ($d_{50}=20$ mm)

Nourishment of coarse materials at Magdalen Island, St Lawrence Bay, Canada

A gravel beach nourishment of coarse pebbles (40 mm) was constructed in 2022 and it is being eroded faster than expected. The observations suggest that the littoral transport of the gravel is happening in the swash zone. It seems that the waves are attacking at a marked angle and their runup is transporting the gravel/pebbles diagonally on the upper portion of the beach. The beach nourishment with an alongshore distance of about 900 m was built with the 40 mm pebbles in order for the material to stay in place for a longer time and to save material, see **Figure 7.2.4**. A terminal groin is present at the southwestern end of the nourishment site. The observations show that there is a zone where the gravel/pebbles and the sand below MSL mixes, but there is also cross-shore transport happening near the crest of the nourishment. The tidal range is about 1 m above and below MSL but the longshore transport is happening up to a height of 4 m above MSL.



Figure 7.2.4 Beach nourishment of coarse sediments ($d_{50}\geq 40$ mm) pebbles, Magdalen Island



The CROSMOR-model has been used to check whether offshore waves with heights in the range of 2 to 3.5 m (at depth of -6 m) are able to erode the coarse beach materials in the swash zone above the mean sea level. Wave simulations based on the SWAN-wave model show that the maximum significant wave height in the nearshore zone with depth of 6 m is of the order of 3.5 m.

Two wave conditions are considered:

- $H_{s,o}=2$ m, $T_p=7$ s, wave incidence angle $\theta_o=10^\circ$ to the shore normal; duration=30 days (representative for 5 years);
- $H_{s,o}=3.5$ m, $T_p=9$ s, wave incidence angle $\theta_o=10^\circ$ to the shore normal, storm setup=0.5 m; duration 5 days (representative for 5 years).

The wave conditions are applied at a depth of -6 m, which is about 700 m from the shore.

The schematized bed profile is shown in **Figure 7.2.5**, which is the mean profile of the measured bed profiles at +350, +550 and +850 (2023 and 2024). The beach front is very steep (1 to 3).

Given the uncertainty of CROSMOR-simulations for coarse materials, two types of model settings have been used, as follows:

- accretive setting promoting onshore bed load transports: CLH=1; CSW=0.5; Faced=0.3; Facsus=2; Frip=1;
- erosive settings promoting offshore-directed bed load transport: CLH=1; CSW=0.5; Faced=0.1; Facsus=2; Frip=2.

It is noted that the seabed and beach in the model simulations consist of coarse materials, whereas in reality the seabed consists of sand and the swash zone is made of coarse materials (40 mm). This composite bed with two types of sediment materials cannot be represented by the CROSMOR-model.

The model simulation results are shown in **Figure 7.2.5** and explained as follows:

- accretive settings: substantial accretion occurs between in the zone around the water line ($x=600$ to $x=620$ m); a submerged bar is formed for $H_{s,o}=2$ m from coarse materials eroded seaward of the bar, which is not present for a major storm event with $H_{s,o}=3.5$ m;
- erosive settings; accretion occurs in the zone around the water line; beach erosion does not occur.

These simulation runs show that waves with a maximum height of 3.5 m are not able to cause major beach erosion. The coarse materials in the swash zone are pushed onshore up to a level of +2 m. Bar formation of coarse materials is not realistic because the seabed consists of sand. These findings are in line with the field observations that the coarse materials are confined in the swash zone above MSL and that most of the erosion is related to longshore transport gradients.

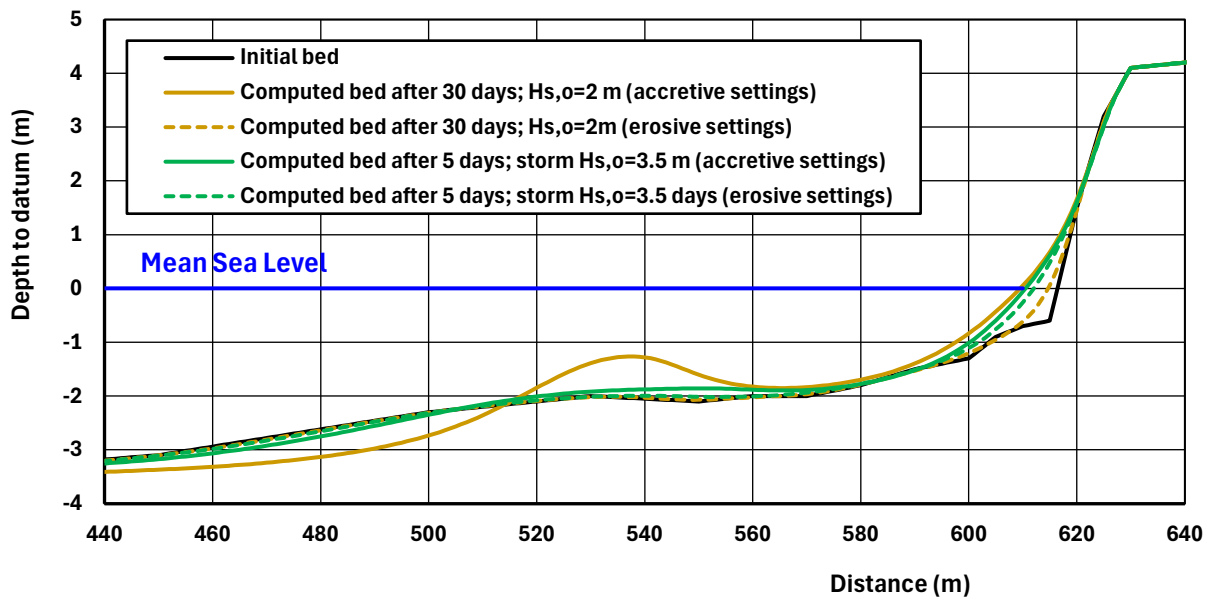


Figure 7.2.5 Computed bed profiles for accretive and erosive settings; CROSMOR-model

7.2.2 Results of CROSMOR-runs for gravel beach of Benin/Togo, Case4 ($d_{50}=40$ mm)

The evolution of a gravel beach is controlled by the (dominant) bed load transport, which is strongly influenced by the following five parameters (see Table 7.2.5):

- method (switch1) used to compute the wave asymmetry in the surf zone;
- strength of the undertow current in the surf zone (frip-coefficient);
- near-bed onshore-directed streaming velocity (CLH-coefficient);
- onshore-directed net swash velocity near the water line (csw-coefficient);
- calibration coefficient (faced) of the bed load transport.

Given the uncertainty of gravel bed runs, two types of settings have been used:

- erosive settings promoting more offshore-directed transport and
- accretive settings promoting more onshore directed transport, see Table 7.2.5.

Parameter	Erosive settings	Accretive settings for short term runs	Accretive settings for short term runs
Factime; time step	0.2	10	10
Facsmooth; bed smoothing factor	5	10; 0.05	10; 0.05
SW; bed smoothing near water line	0.05		
NHW; number of wave classes	7	7	7
Switich1; selection of method for wave asymmetry 0= method of Isobe-Horikawa 1=method of Ruessink 2008 2=method of Ruessink 2010	0,1,2		



Frip; coefficient to increase/decrease the undertow current	2	1.0	1.0
CLH; near-bed streaming velocity; CLH=0 means streaming=0 m/s	0		
CSW; coefficient to increase or decrease the onshore-directed net swash velocity; can only be used for NHW=1; CSW=0 means swash velocity=0 m/s	0		
SEF; sand entrainment at steep beach/dune front	1.3	1.3	1.3
Faced; calibration factor (increase or decrease) bed load transport	0.1	0.3	0.3
Facsus; calibration factor (increase or decrease) bed load transport	2.	2.	2.
Facsusw; calibration factor (increase or decrease) bed load transport	0.	0.	0.

Table 7.2.5 numerical and physical input data (settings)

The basic wave input data are given in **Table 7.2.6**.

It is noted that a larger offshore wave incidence angles lead to a stronger longshore current and thus to more beach-dune erosion.

Storm level to MSL Hstorm (m)	Offshore significant and rms-wave height H _{s,o} ; H _{rms,o} (m)	Peak wave period T _p (s)	Offshore wave incidence angle to shore normal θ _o (degrees)
0	1.85; 1.30	12.3	10
0	2.5; 1.77	12.5	10
0.5	3.0; 2.12	13.0	10; 30
1.0	4.0; 2.83	13.5	10
1.5	5.0; 3.55	14.0	10; 30
1.75	6.0; 4.25	14.5	10
2.0	7.0; 4.95	15.0	10; 30

Table 7.2.6 Offshore wave data

Erosive settings

The following effects on the gravel bed evolution have been studied:

- wave asymmetry method (switch1);
- strength of offshore-directed undertow velocity (frip);
- offshore wave incidence angle (θ_o);
- offshore wave height (H_{s,o});
- calibration-coefficients of bed load and suspended load transport (faced, facsus and facsusw); low values of faced and facsusw and a high value of facsus lead to erosive conditions).

The effect of the wave asymmetry method on the beach erosion of coarse gravel with d₅₀=0.04 m is shown in **Figure 7.2.6** for two offshore wave conditions: H_{s,o}=1.3 m and H_{s,o}=5 m. Three methods are available (Isobe-Horikawa 1982, Ruessink 2008 and Ruessink 2010). The maximum onshore and offshore-directed peak values of the near-bed orbital velocity are given in Table 6.2.7. The method of Ruessink 2010 produce the highest onshore



peak value, while the method of Isobe-Horikawa 1982 produces the lowest offshore peak value. The gravel beach erosion for the case with $H_{s,o}=5$ m is smallest for the method of Isobe-Horikawa 1982 and substantially larger (increase of factor of 1.5 to 2) for the method of Ruessink 2010, see **Figure 6.2.6**. The beach erosion is minor for $H_{s,o}=1.85$ m.

Wave asymmetry method	Offshore significant wave height $H_{s,o}=1.85$ m		Offshore significant wave height $H_{s,o}=5.0$ m	
	$U_{\max, \text{onshore-directed}}$ (m/s)	$U_{\max, \text{offshore-directed}}$ (m/s)	$U_{\max, \text{onshore-directed}}$ (m/s)	$U_{\max, \text{offshore-directed}}$ (m/s)
Isobe-Horikawa 1982	1.94 (x=1720 m)	0.77	2.59 (x=1540 m)	1.27
Ruessink 2008	1.80 (x=1735 m)	1.59	2.26 (x=1540 m)	1.67
Ruessink 2010	2.10 (x=1730 m)	1.58	2.90 (x=1500 m)	1.67

Table 7.2.7 Computed maximum wave asymmetry velocities near the bed

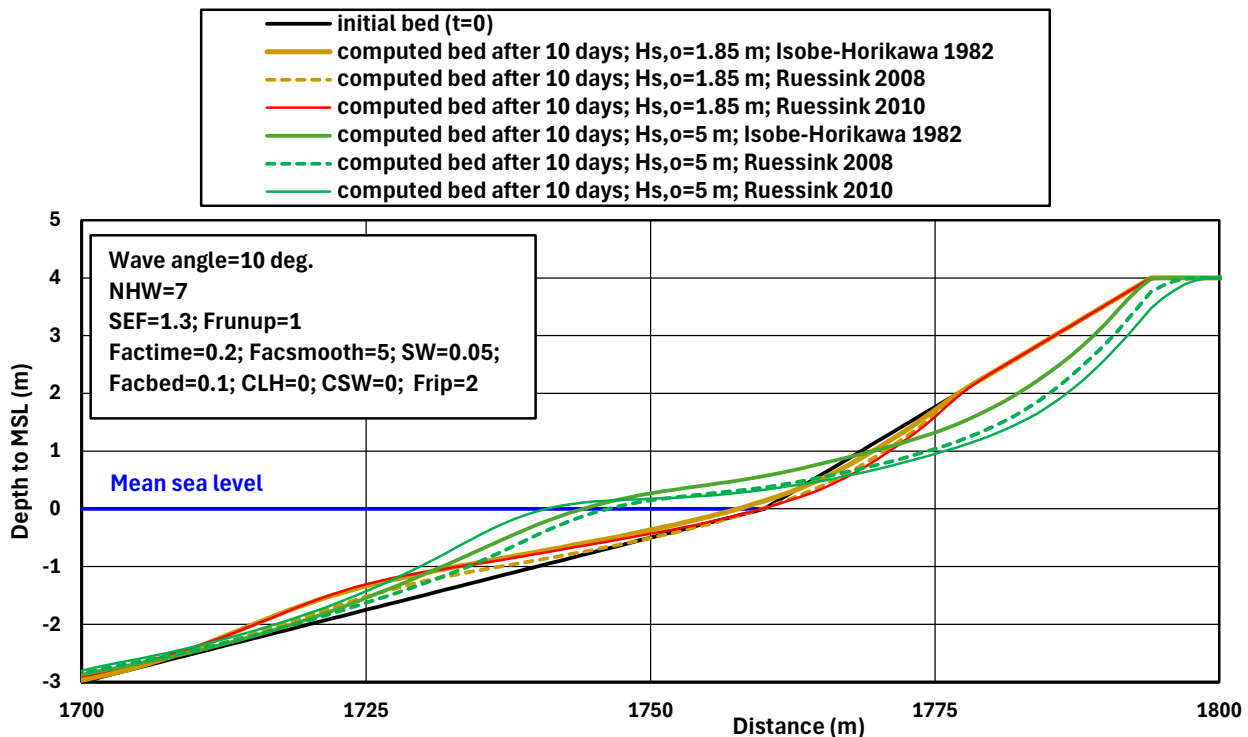


Figure 7.2.6 Effect of wave asymmetry method on gravel beach erosion after 10 days; erosive conditions

The effect of the offshore-directed undertow velocity on the gravel bed erosion is shown in **Figure 6.2.7** for two offshore wave conditions: $H_{s,o}=1.3$ m and $H_{s,o}=5$ m. The maximum undertow velocities are given in **Table 6.2.8**. The maximum undertow velocity in the surf zone is -0.74 m/s (Frip=1) for $H_{s,o}=5$ m, which increases to -1.48 m/s (Frip=2). The gravel beach erosion increases substantially for a higher offshore-directed undertow velocity. In the case of $H_{s,o}=5$ m, there is almost no erosion at the upper beach for Frip=1 in stead of Frip=2.



Offshore significant wave height $H_{s,o}$ (m)	Maximum offshore-directed undertow velocity u_{undertow} (m/s)	
	frip=2	frip=1
1.85	-1.15 (x=1763 m)	-0.583 (x=1763 m)
5.0	-1.48 (x=1763 m)	-0.743 (x=1763 m)

Table 7.2.8 Computed maximum offshore-directed undertow velocity

The effect of the offshore wave incidence angle on the gravel bed erosion is shown in **Figure 7.2.8** for three offshore wave conditions: $H_{s,o}=7$ m, 5 m and 3 m. The beach erosion increases substantially (factor 1.5 to 2) for an offshore wave incidence angle of 30° in stead of 10° , which is caused by the increase of the longshore current and the associated increase of the sand transport rate.

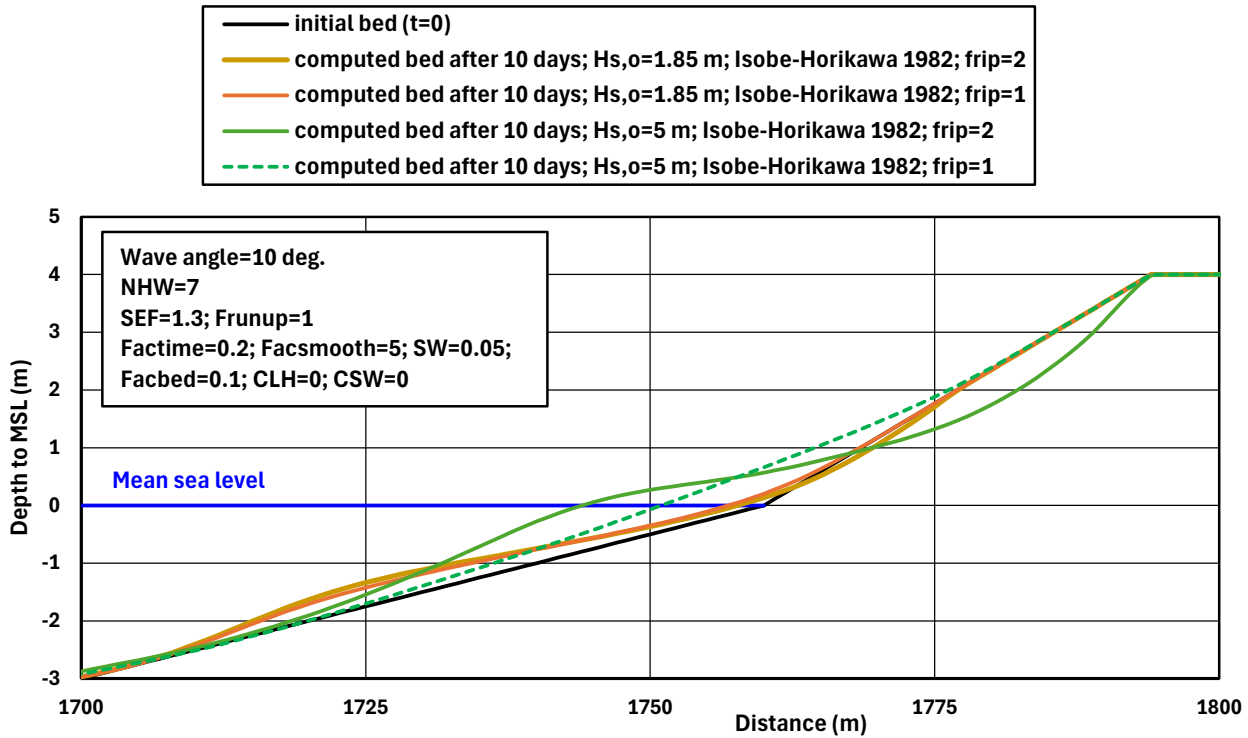


Figure 7.2.7 Effect of undertow velocity (Frip) on gravel bed erosion after 10 days; erosive conditions

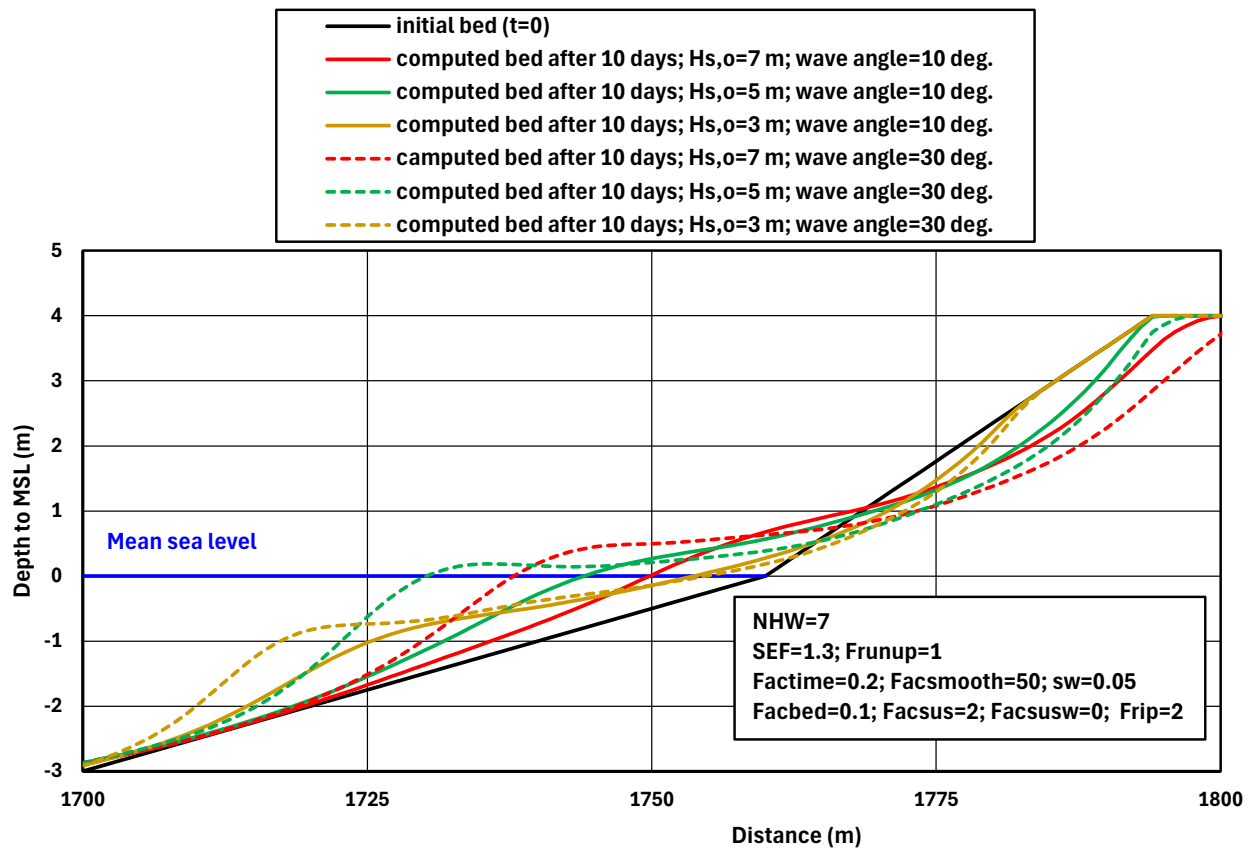


Figure 7.2.8 Effect of offshore wave angle on gravel bed erosion; erosive conditions

The effects of the offshore wave height ($H_{s,o}$) varied in the range of 1.85 to 7 m are shown in **Figure 7.2.9**. Beach erosion is very minor for $H_{s,o}=1.85$ m. Accretive conditions are present for all waves smaller than about 2 m. The beach erosion of gravel with $d_{50}=0.04$ m is largest (about $25 \text{ m}^3/\text{m}$ after 10 days) for $H_{s,o}=7$ m. Normally, the duration of an extreme storm is 12 to 24 hours, which means that the beach erosion of coarse materials (0.04 m) due an extreme storm of 1 day will be in the range of 2 to $3 \text{ m}^3/\text{m}$. This value of the CROSMOR-simulation is much smaller than the predicted erosion volume of about 65 m^3 after 12 hours produced by the XBEACH-gravel model (Report JDN) for an extreme storm ($R_p=100$ years).

The eroded materials are deposited around the MSL- at the toe of the beach above the -2 m depth line. More research is required to assess whether a sand beach can be adequately protected by a thick layer (1.5 to 2 m thick) of coarse materials ($d_{50}=0.04$ m) above the -3 m depth line.

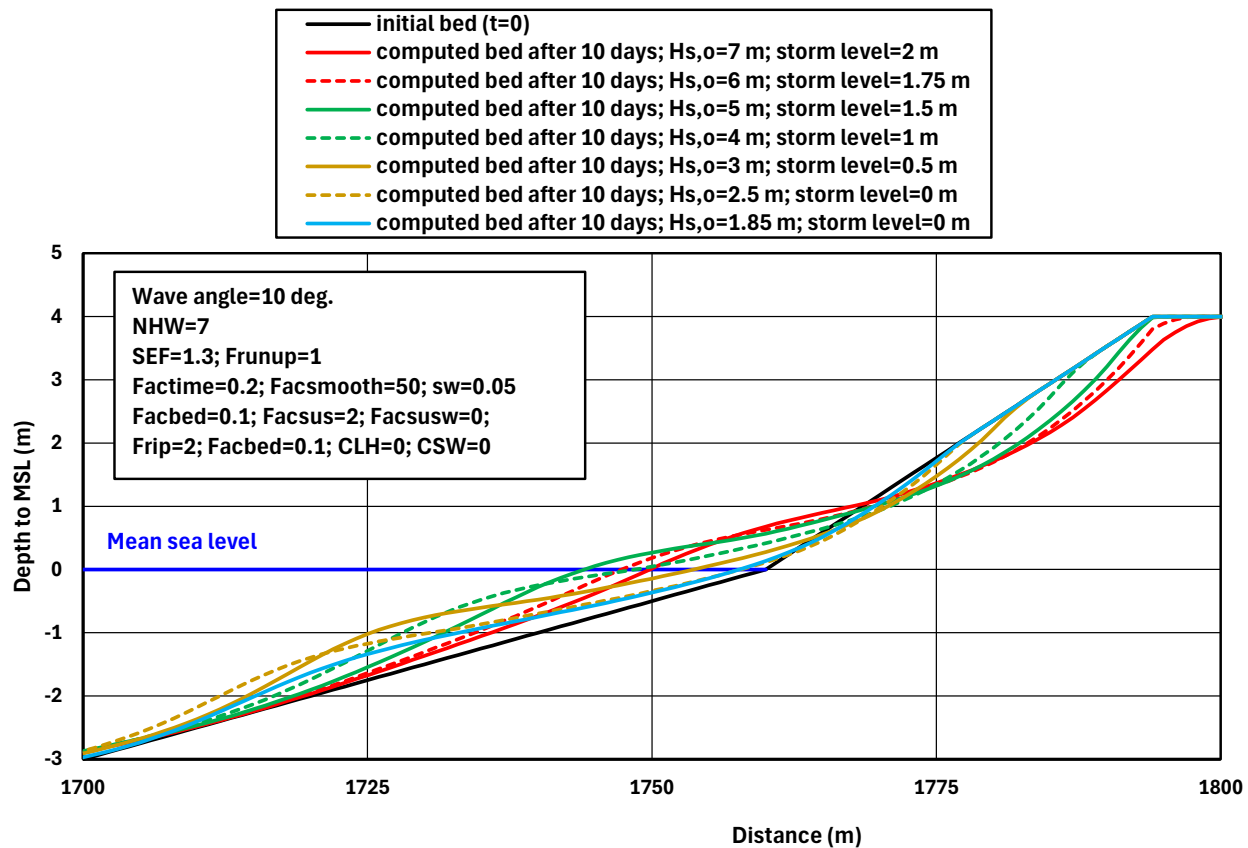


Figure 7.2.9 Effect of offshore wave height ($H_{s,o}$) on gravel beach evolution; erosive conditions

Accretive settings for short term runs

The main parameters controlling accretive conditions are:

- wave asymmetry method (switch1);
- onshore-directed streaming velocity (CLH-coefficient);
- onshore-directed net swash velocity near the water line (CSW-coefficient; NHW=1);
- calibration-coefficients of bed load and suspended load transport (facbed, facsus and facsusw); high values of facbed and facsusw and a low value of facsus lead to accretive conditions).

The effect of the onshore-directed near-bed streaming (CLH-coefficient) and the onshore-directed net swash velocity (CSW-coefficient) on the gravel bed evolution is shown in **Figure 7.2.10** for the mild wave condition with $H_{s,o}=1.85$ m.

Under accretive conditions, a submerged bar is generated from coarse materials gravel eroded from the seabed ($x < 1700$ m). The bar grows slightly for $CLH=1$. The bar is pushed onshore and grows vertically for $CSW=0.5$, 1, 1.5 and 2. Swash bar generation for $CSW=0.5$ and 1 is realistic, but the excessive growth for $CSW=1.5$ and 2 is unrealistic. Furthermore, it should be realized that the bed seaward of the bar consists of sand in the case of a local beach protection of coarse materials. In the latter case, the coarse materials landward of the -2/-3 m line will be pushed onshore forming a bar at the toe of the beach under accretive conditions.

Figure 7.2.11 shows the effect of wave height varied in the range of 1.85 to 5 m on the gravel bed evolution under accretive conditions. The submerged bar is gradually pushed onshore. These coarse materials are eroded from the seabed seaward of the bar. The bed becomes slightly unstable for the highest wave of 5 m.

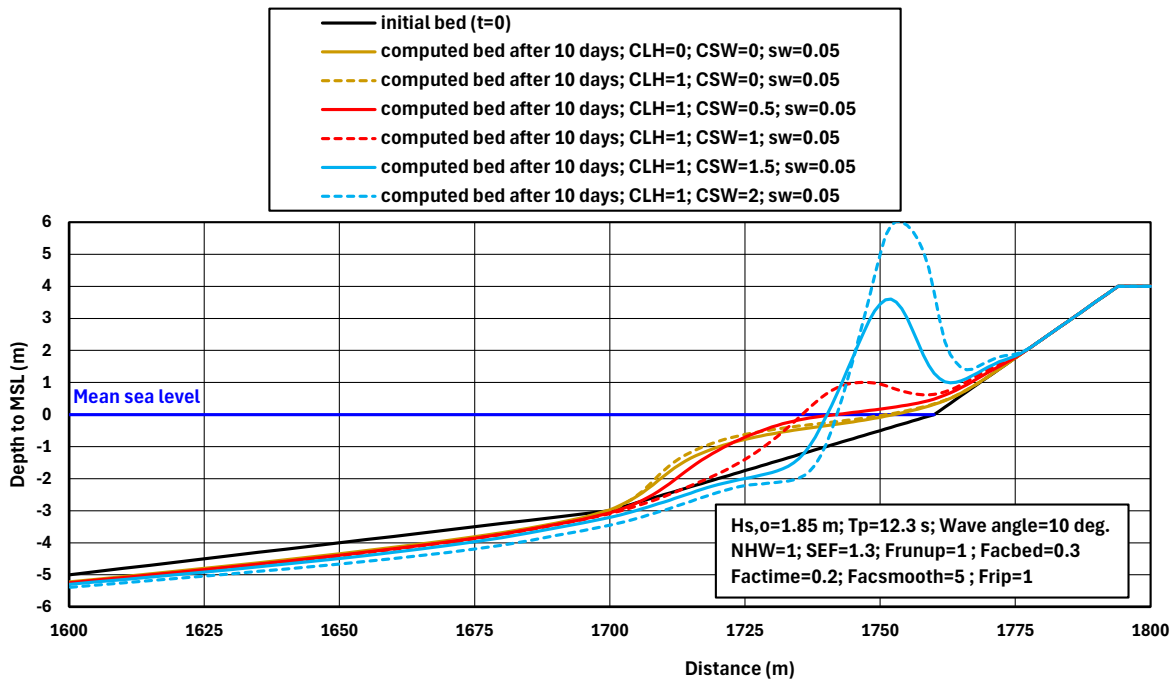


Figure 7.2.10 Effect of onshore-directed streaming (CLH) and net swash velocity (CSW) on gravel bed evolution; accretive conditions

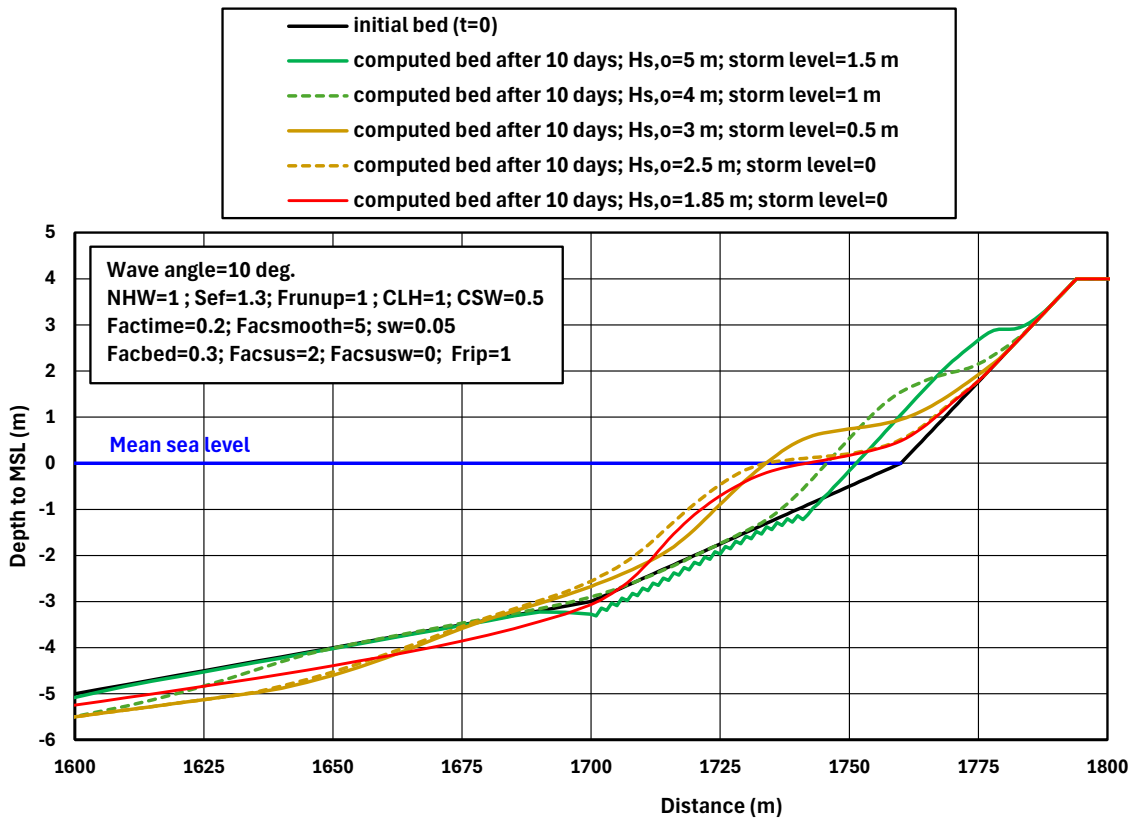


Figure 7.2.11 Effect of offshore wave height on gravel bed evolution; accretive conditions



Accretive settings long term runs

Figure 6.2.12 shows the effect of bed load transport on the long term evolution of a beach of coarse materials with $d_{50}=0.04$ m. The offshore wave height is a minor storm with $H_{s,o}=1.85$ m ($T_p=12.3$ s; offshore wave angle $\theta_o=10^\circ$). A period of 60 days with a constant wave height of 1.85 m is approximately representative for a real time period of 5 years (10 minor storm per year). A swash bar is generated from coarse material eroded from the seabed seaward of the bar ($x<1700$ m). The bar grows slightly for higher values of facbed and CSW.

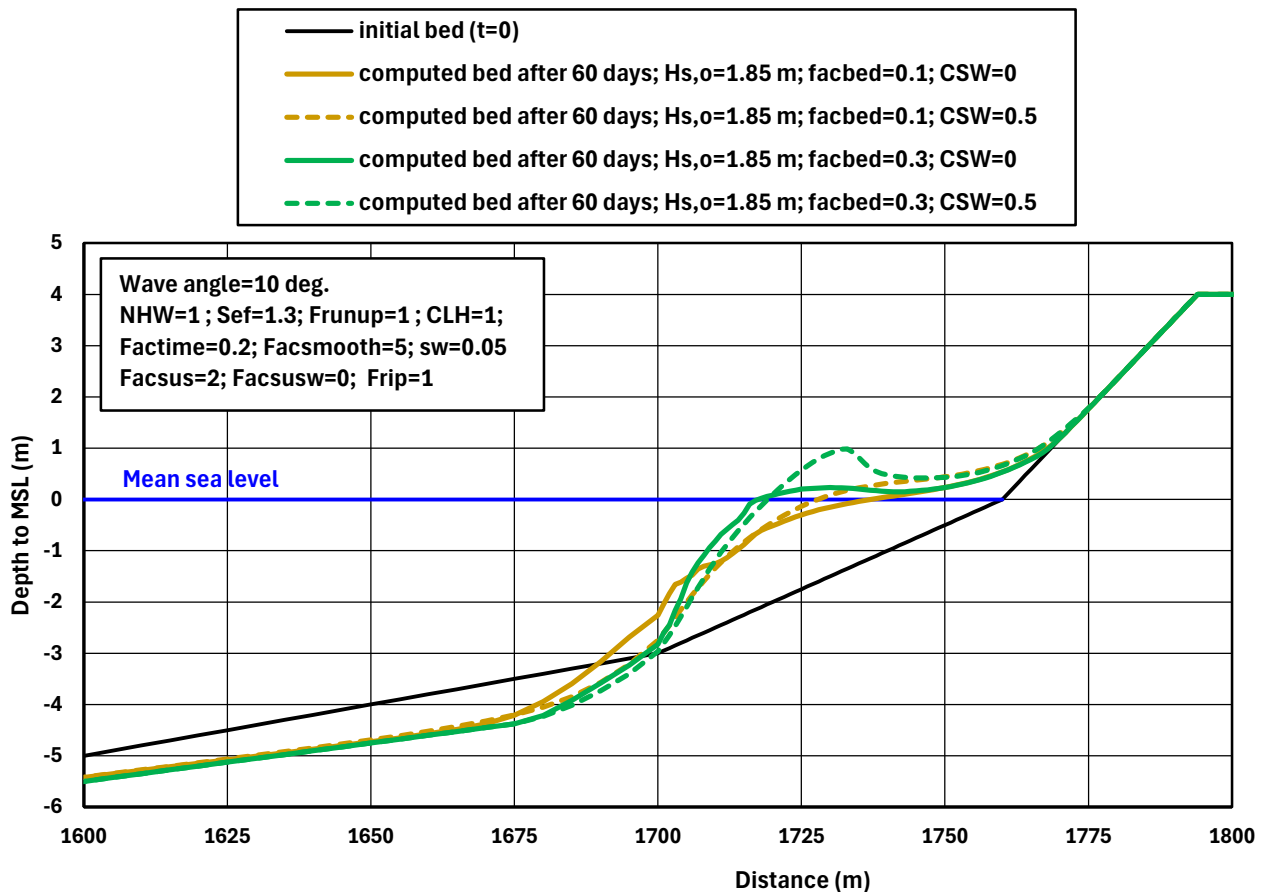


Figure 7.2.12 Effect of bed load transport (facbed; csw) on long term gravel bed evolution; accretive conditions

Overall conclusions for beaches of coarse materials

The CROSMOR-model can be used for computation of beach changes along a cross-shore profile of coarse materials (10 to 50 mm), provided that appropriate model settings are used. Given the uncertainty for gravel beach runs, it is recommended to use two types of settings: accretive settings and erosive settings. Beach erosion only occurs for relatively high offshore waves (> 3 m). The beach nourishment case with coarse materials (40 mm) shows that the coarse materials are mainly pushed up the beach and that the beach erosion is mainly caused by longshore transport gradients in the swash zone. The longshore transport of coarse materials in the swash zone is not (yet) included in the CROSMOR-model. The longshore transport model of Van Rijn (2014) has been recently extended to include the longshore transport in the swash zone above MSL.



7.3 Erosion of gravel barrier/dune due to extreme storms; exposed Pevensey Bay, UK

The CROSMOR-model has been applied to the 9 km long shingle barrier at Pevensey Bay, East Sussex, UK. The profile characteristics and boundary conditions are given in **Table 7.3.1**.

To obtain a very conservative estimate of the erosion volume along the profile, the seaward-directed undertow velocities have been increased by 50% and the erosion rate in the swash zone has been increased ($\text{sef} = 2$). Furthermore, the swash velocities near the water line and the streaming near the bed have been neglected ($c_{sw} = 0$, $c_{LH} = 0$).

Parameters	Values
Bed profile	slope of 1 to 62.5 between -30 m and -1.5 m (to MSL) slope of 1 to 8 between -1.5 m and +5 m slope of 1 to 4 between +5 m and +6 m crest width of 22.5 m
Sediment d_{50} d_{90}	0.01 to 0.1 m 0.04 m
Bed roughness k_s	0.01 to 0.1 m
Horizontal mixing	0.1 m ² /s
Peak tidal water level	Mean tidal range = 5.0 m OD (OD is approx. MSL) Spring tidal range = 6.7 m OD Neap tidal range = 3.7 m OD
Longshore peak tidal velocity (offshore)	0.5 m/s (flood); -0.5 m/s (ebb)
Offshore significant wave height $H_{s,o}$	1.5 to 6 m (6 wave classes using Rayleigh distribution for each case)
Peak wave period T_p	8 to 11 s
Wave incidence angle to coast normal	30°
Storm surge level above MSL	0 to 3 m

Table 7.3.1 Data of shingle barrier at Pevensey Bay, UK

Figure 7.3.1 shows the cross-shore distributions of the significant wave height and the longshore velocity during storm conditions with an offshore wave height of 6 and 3 m ($T_p = 11$ and 8 s), storm set-up value of 1 m and an offshore wave incidence angle of 30°. The tidal elevation is zero in this plot. During major storm conditions with $H_{s,o} = 6$ m, the wave height is almost constant up to the depth contour of -10 m. Landward of this depth the wave height gradually decreases to a value of about 2 m at the toe of the barrier (at $x = 1980$ m). During minor storm conditions with $H_{s,o} = 3$ m, the wave height remains constant to a depth of about 4 m. The wave height at the toe of the barrier is about 1.8 m. The longshore velocity increases strongly landward of the -10 m depth contour where wave breaking becomes important (larger than 5% wave breaking). The longshore current velocity has a maximum value of about 1.6 m/s for $H_{s,o} = 6$ m and about 1.7 m/s for $H_{s,o} = 3$ m (offshore wave angle of 30°) just landward of the toe of the beach slope. These relatively large longshore velocities in combination with the cross-shore velocities can easily erode and transport gravel/shingle particles of 0.02 m.

Figure 7.3.2 shows the barrier profile changes according to the CROSMOR-model for four storm cases at Pevensey Bay. The computed erosion area after 24 hours is largest (about 25 m³/m) for the largest offshore wave height of 6 m, which occurs for a storm setup of about 1 m. An offshore wave height of 3 m in combination with a setup of 2 m leads to an erosion area of about 20 m³/m. The maximum computed recession at the crest is of the order of 5 m. The 1 to 10000 year-storm event yields an erosion area of about 30 m³/m and a maximum crest



recession of about 15 m. In all cases the computed erosion profile is seaward of the envelope erosion profile (erosion area of about 100 m³/m) as used by the Pevensy Coastal Defence for the 1 to 400 year storm case.

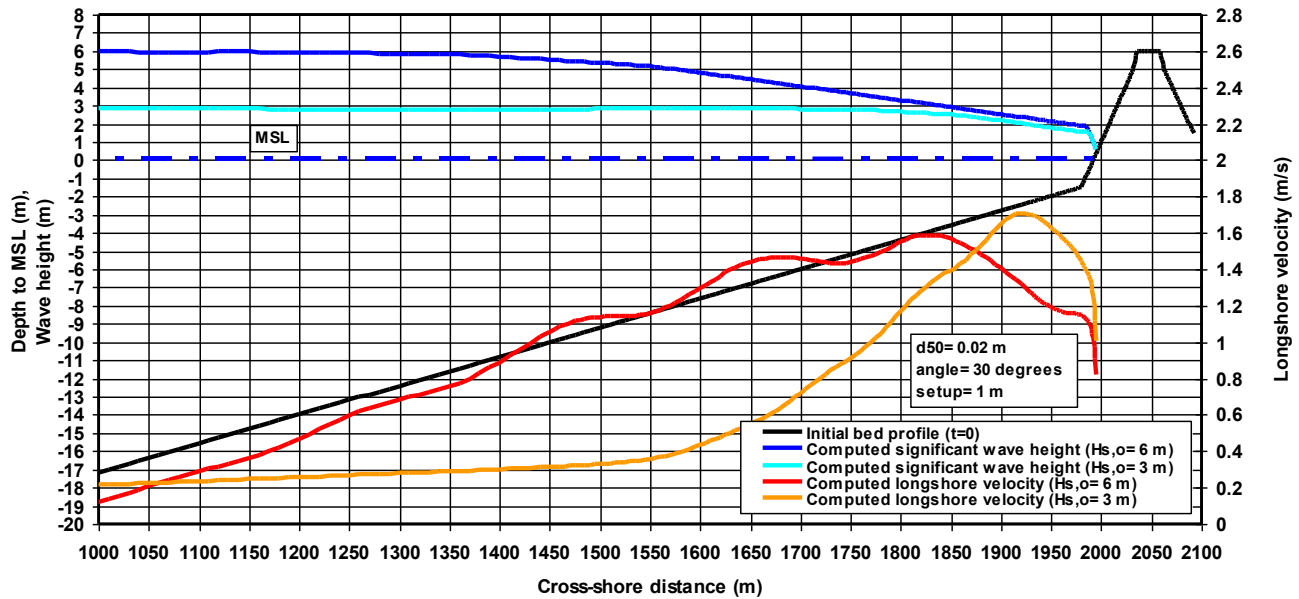


Figure 7.3.1 Bed profile, wave height, longshore velocity for offshore wave height of $H_{s,o} = 3$ and 6 m; setup=1 m; offshore wave incidence angle= 30° for Pevensy Bay shingle barrier, UK

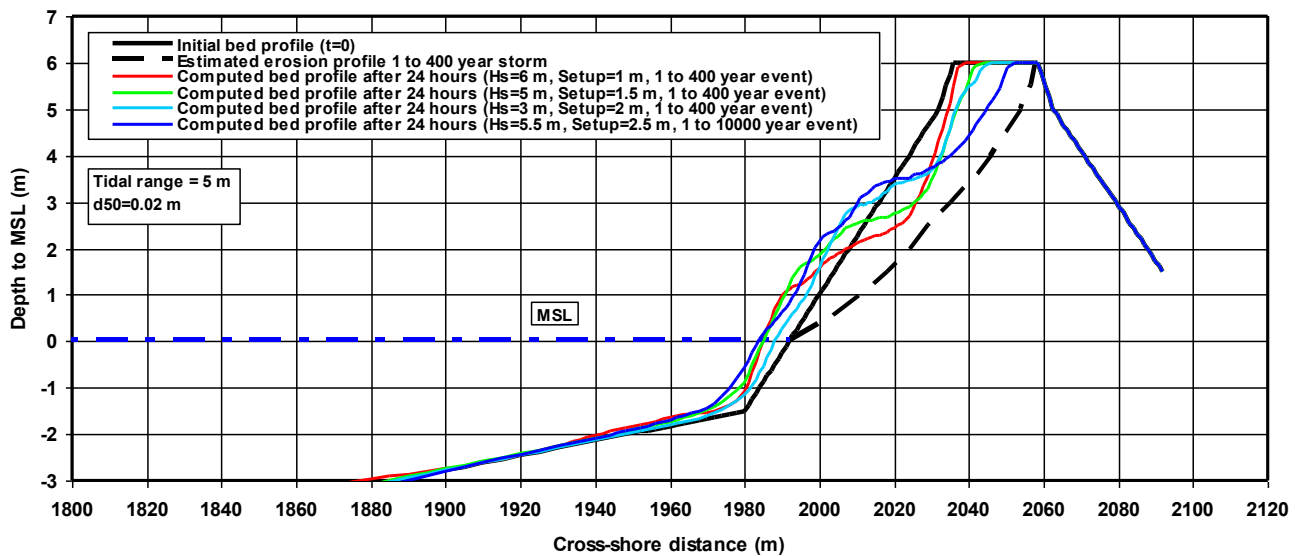


Figure 7.3.2 Effect of storm surge level and storm intensity on the erosion of Pevensy Bay shingle barrier



Figure 7.3.3 shows the effect of the shingle size (varied in the range of 0.01 to 0.10 m) on the erosion of the shingle barrier at Pevensey Bay, UK. The computed total erosion area after 24 hours based on the CROSMOR-model is about 30 m³/m for shingle size of 0.01 m and about 20 m³/m for shingle size of 0.03 m. The erosion area reduces greatly to about 3 m³/m when cobbles of 0.1 m are present. General cobble movement will occur at a (Shields) shear stress of about 85 N/m². Close to the shore the maximum orbital velocity is of the order of $U_{max} = 2$ m/s giving a bed-shear stress of about $\tau_{max} = 0.5 \rho f_w (U_{max})^2 \cong 100$ N/m² (using $f_w = 0.05$).

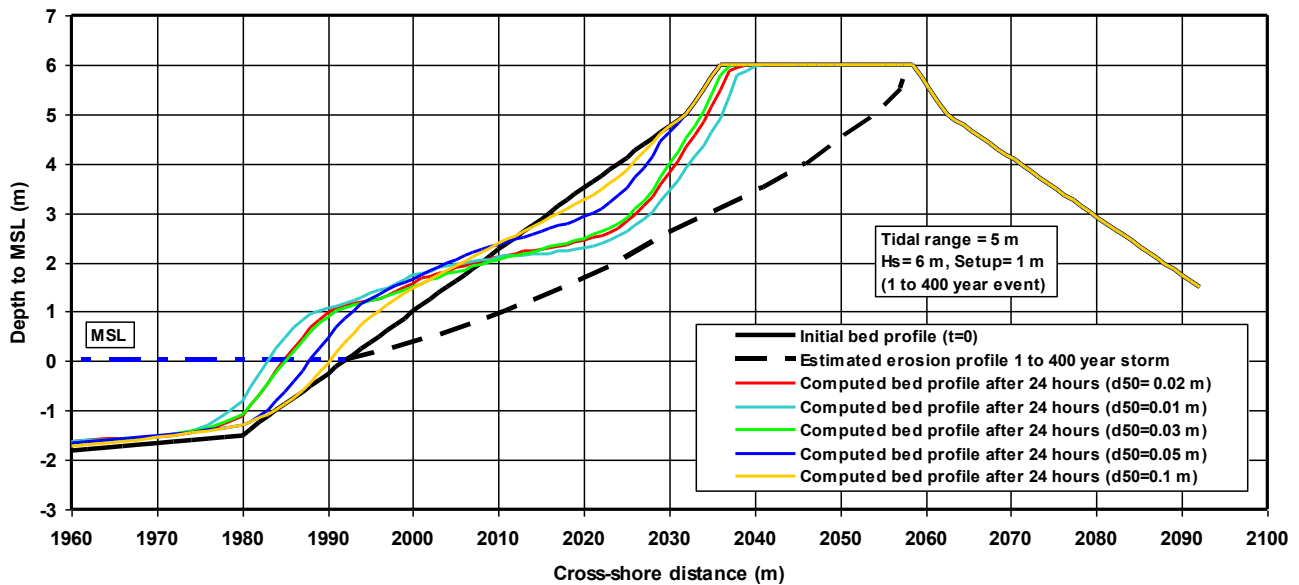
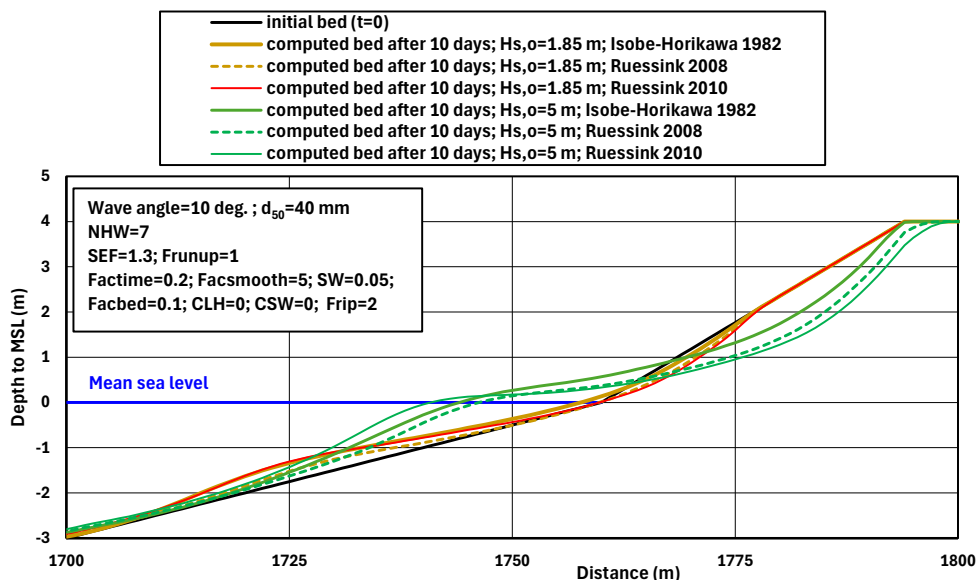
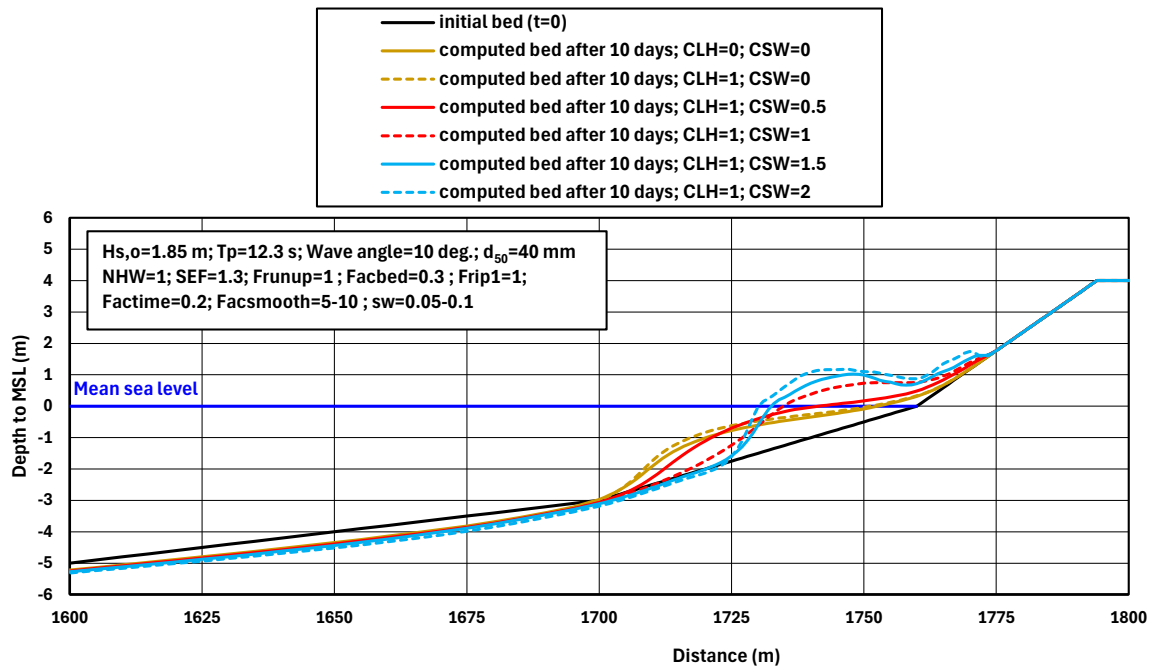
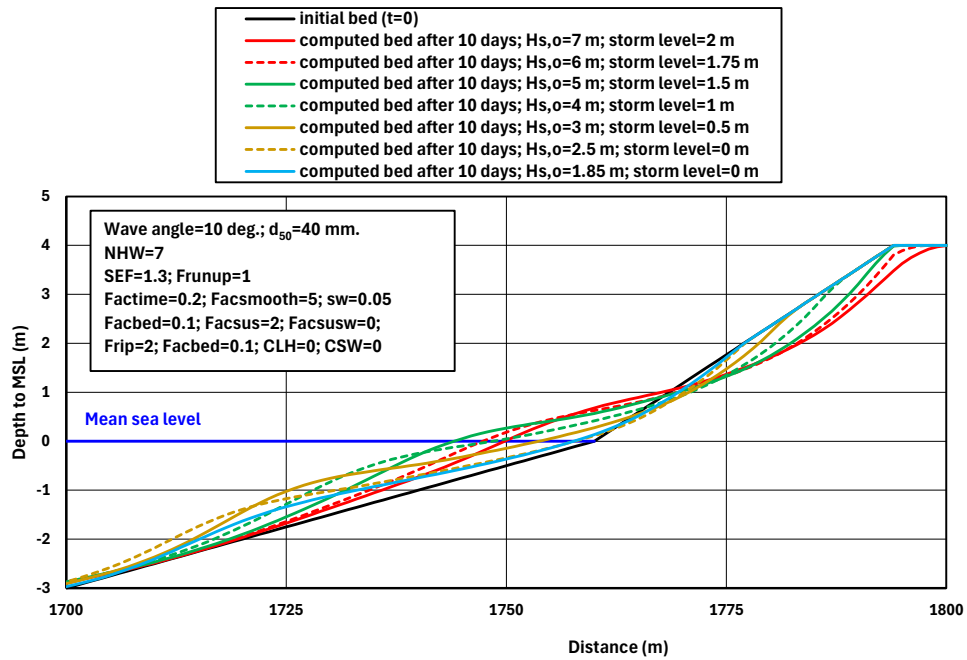


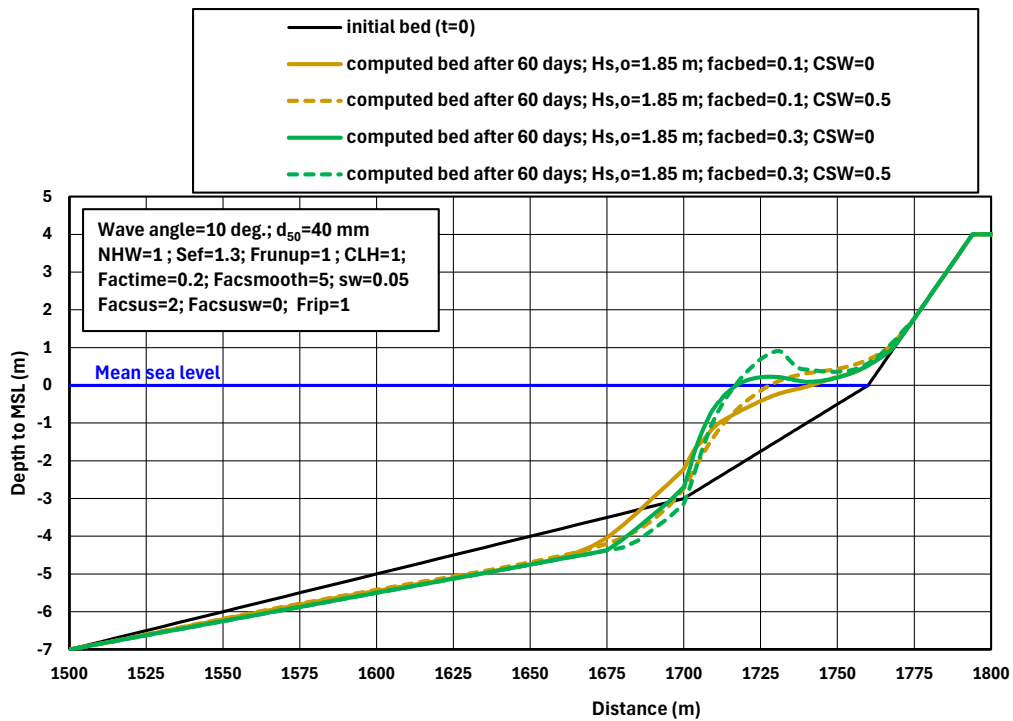
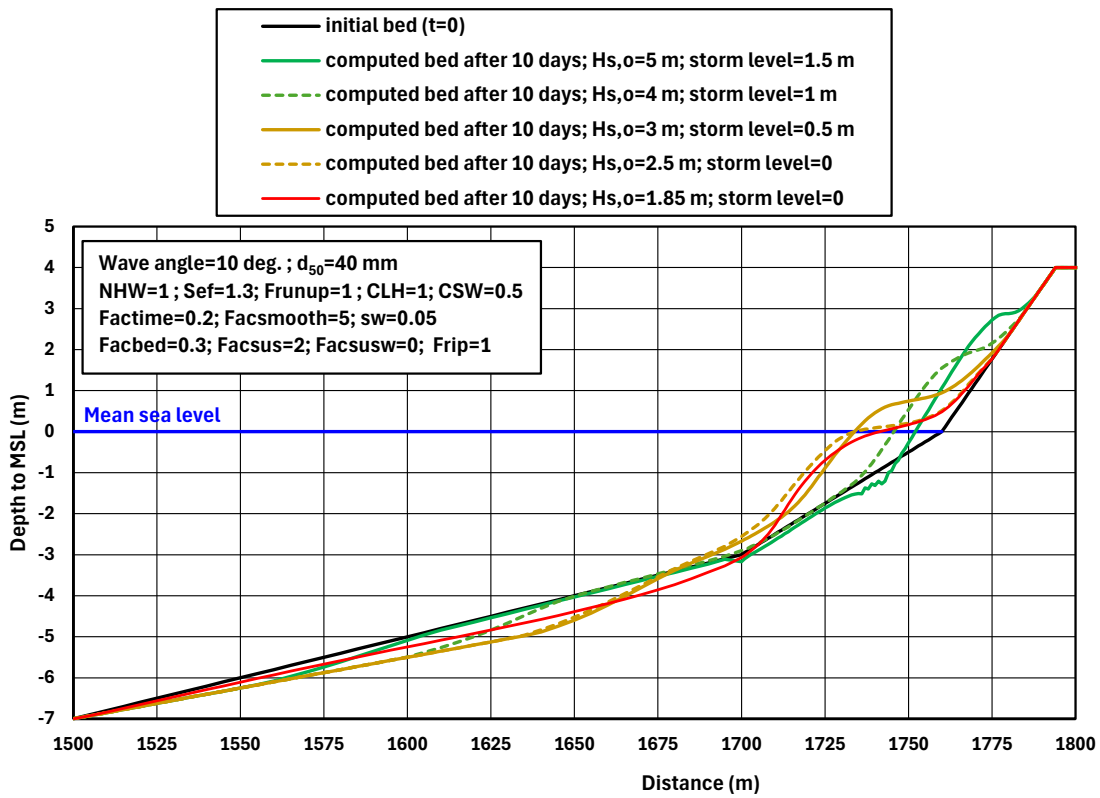
Figure 7.3.3 Effect of shingle size on the erosion of Pevensey Bay shingle barrier, UK

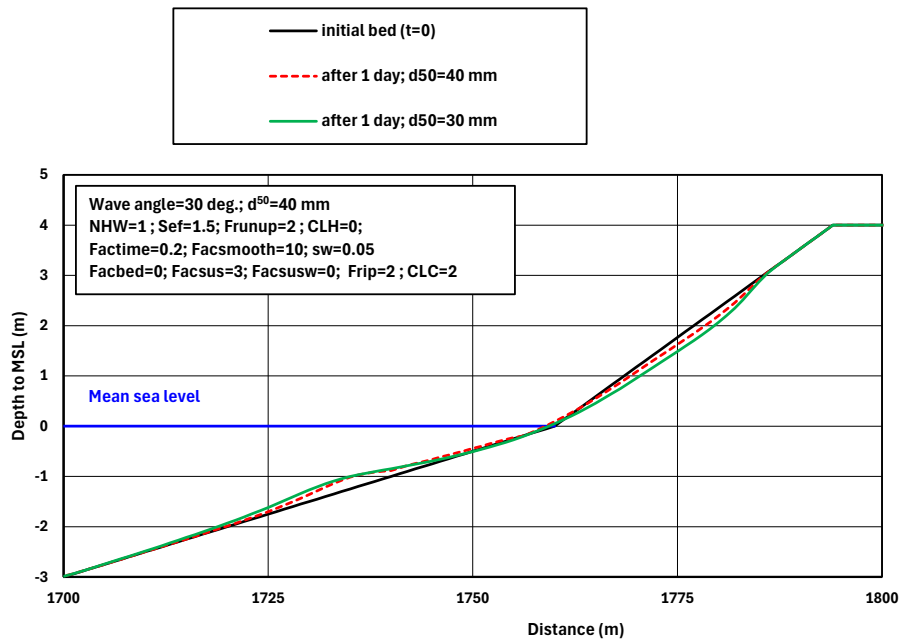
7.4 Results of sensitivity tests

1. Effect of various parameters

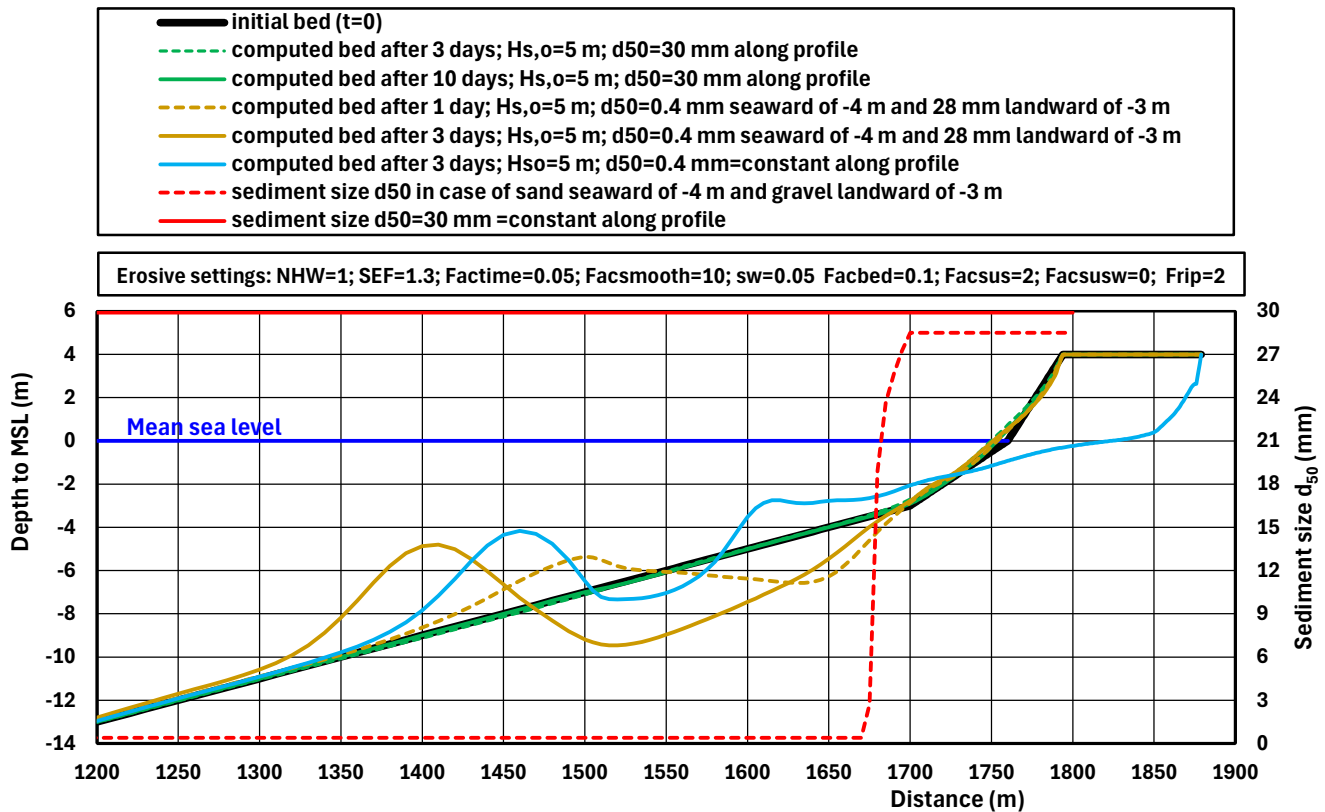


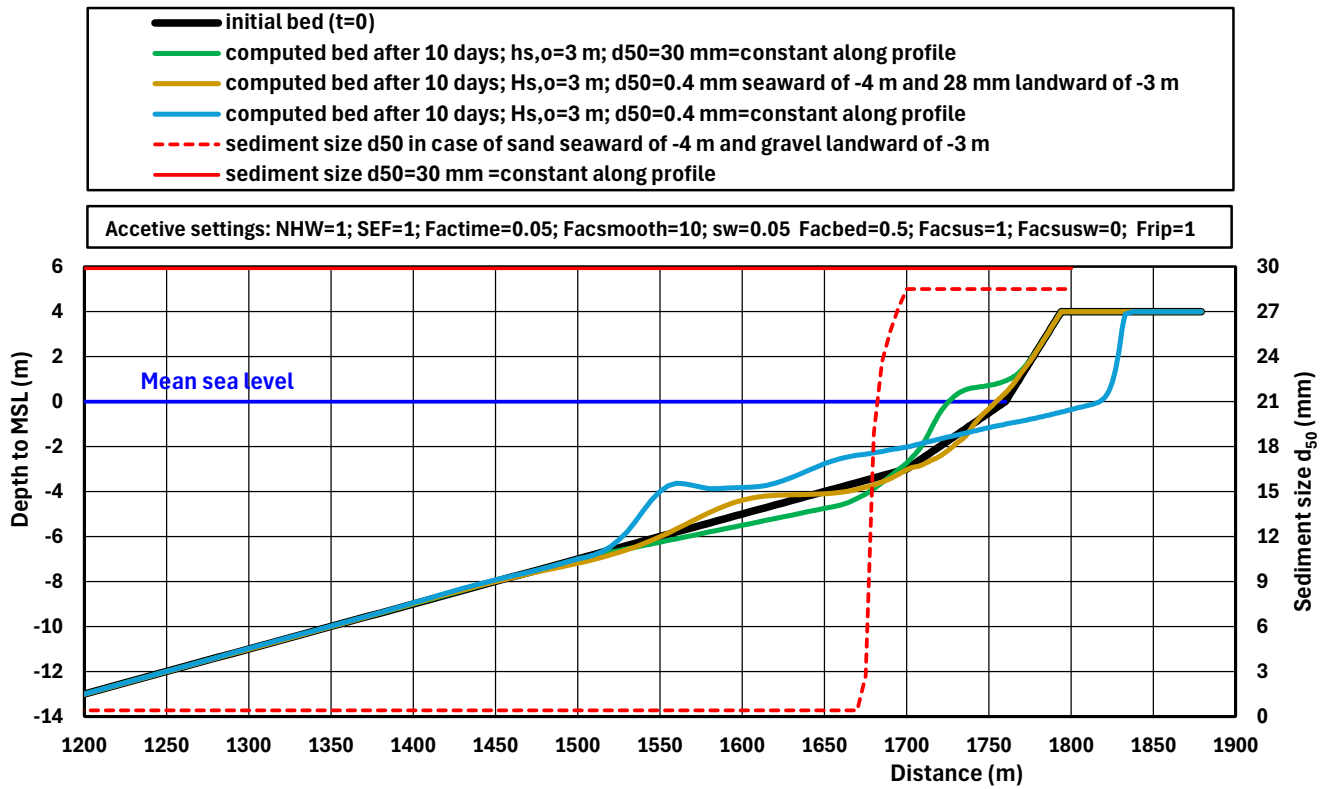






2. Effect of fractions







References

- Battjes, J.A., 1974.** Surf similarity. Proceedings of the 14th International Coastal Engineering Conference, vol. 1. American Society of Civil Engineers, pp. 466– 480.
- Chadwick, A.J., 1989.** Field measurements and numerical model verification of coastal shingle transport, p. 381-402. BHRA, Fluid Engineering Centre, Bedford, England
- Dally, W.R. and Osiecki, D.A., 1994.** The role of rollers in surf zone currents. 24th ICCE, Kobe, Japan
- Davies, A.G. and Villaret, C., 1997.** Oscillatory flow over rippled beds. In: J.N. Hunt (ed.), Gravity waves in water of finite depth: Chapter 6, p. 215-254. Advances in fluid mechanics, Computational Mechanics Publications
- Davies, A.G. and Villaret, C., 1998.** Wave-induced currents above rippled beds, p. 187-199. In: Physics of estuaries and coastal seas, edited by J. Dronkers and M. Scheffers, Balkema, Brookfield
- Davies, A.G. and Villaret, C., 1999.** Eulerian drift induced by progressive waves above rippled and very rough bed, p. 1465-1488. Journal of Geophysical Research, Vol. 104, No. C1
- Dodet, G., Leciker, F., Sous, D., Arduin, F., Filipet, J.F. and Suarez, S., 2018.** Wave runup over steep rocky cliffs. JGR Oceans, Vol. 123 (10), 7185-7205; Doi: 10.1029/2018jc013967
- Douglass, S.L., 1992.** Estimating extreme values of run-up on beaches. Journal of Waterway, Port, Coastal, and Ocean Engineering, vol. 118, no. 2. American Society of Civil Engineers, pp. 220–224.
- Elkersh, K., Atabay, S. and Yilmaz, A.G., 2022.** Extreme Wave Analysis for the Dubai Coast. Hydrology, Vol.9, 144. 2022. <https://doi.org/10.3390/hydrology9080144>
- Fordeyn, J. and Malherbe, B., 2012.** Coastal Defence of Lowlands with Sand: Morpho-Dynamic Concepts of Beach-Dune System Rehabilitation. 8th International Conference on Coastal and Port Engineering in Developing Countries, COPEDEC 2012, Madras, India.
- Gallagher, E.L., Elgar, S. and Guza, R.T., 1998.** Observations of sand bar evolution on a natural beach. Journal of Geophysical Research, Vol. 103, NO. C2, p. 3203-3215
- Grasmeijer, B.T., 2001.** Sand transport and morphology in the surf zone of Egmond, The Netherlands. Doc. Thesis, Dep. of Physical Geography, University of Utrecht, The Netherlands (in preparation)
- Grasmeijer, B.T. and Van Rijn, L.C., 1998.** Breaker bar formation and migration. Proc. ICCE., Copenhagen, Denmark
- Guza, R.T. and Thornton, E.B., 1982.** Swash oscillations on a natural beach. Journal of Geophysical Research, Vol. 87 (C5), 483-490
- Holman, R.A., 1986.** Extreme value statistics for wave runup on a natural beach. Coastal Engineering, vol. 9, no. 6. Elsevier, pp. 527–544.
- Houwman, K.T. and Ruessink, B.G., 1996.** Sediment transport in the vicinity of the shoreface nourishment of Terschelling. Dep. of Physical Geography. Univ. of Utrecht, The Netherlands
- Hughes, S.A., 2004.** Estimation of wave run-up on smooth, impermeable slopes using the wave momentum flux parameter. Coastal Engineering, Vol. 51, No 11-12, 1085-1104
- Hunt, I.A., 1959.** Design of seawalls and breakwaters. Journal of the Waterways and Harbors Division, vol. 85, no. WW3. American Society of Civil Engineers, pp. 123– 152.
- Isobe, M. and Horikawa, K., 1982.** Study on water particle velocities of shoaling and breaking waves. Coastal Engineering in Japan, Vol. 25.
- Larson, M., Erikson, C. and Hanson, H. 2004.** An analytical model to predict dune erosion due to wave impact. Coastal Engineering, Vol. 51, 675-696
- Malherbe, B. and Helewaut, M., 1993.** Design and execution of beach nourishments in Belgium. Coastal Zone 93, New Orleans, USA.
- Malherbe, B. and Fordeyn, J., 2013.** Smart Beach and Dune Nourishments to achieve Sustainable Coastal Protection. WODCON XX 2013 – World Dredging Congress, Brussels, Belgium
- Mase, H., 1989.** Random wave runup height on gentle slope. Journal of Waterway, Port, Coastal, and Ocean Engineering, vol. 115, no. 5. American Society of Civil Engineers, pp. 649– 661
- Meyer-Peter, E. and Mueller, R. 1948.** Formulas for bed load transport. IAHR 2nd meeting, Stockholm, 41-64



- Nicholls, R.J. and Wright, P., 1991.** Longshore transport of pebbles: experimental estimates of K-factor. Coastal Sediments, Seattle, USA, p. 920-933
- Nicholls, R.J. and Webber, N.B., 1988.** Characteristics of shingle beaches with reference to Christchurch Bay, South England, p. 1922-1936, Proc. 21st ICCE, Malaga, Spain
- Nielsen, P. and Hanslow, D.J., 1991.** Wave runup distributions on natural beaches. Journal of Coastal Research, 7(4), 1139–1152.
- Poate, T.G., McCall, R.T. and Masselink, G., 2016.** A new parameterisation for runup on gravel beaches. Coastal Engineering 117, 176–190; Doi: 10.1016/j.coastaleng.2016.08.003
- Roberts, T.M., Wang, P. and Kraus, N.C., 2010.** Limits of Wave Runup and Corresponding Beach-Profile Change from Large-Scale Laboratory Data. Journal of Coastal Research, Vol.26 (1), 184-198
- Senechal, N., Coco, G., Bryan, K.R. and Holman, R.A., 2011.** Wave runup during extreme storm conditions, J. Geophys. Res., 116, C07032, doi:10.1029/2010JC006819.
- Svendsen, I.A., 1984.** Mass flux and undertow in the surf zone. Coastal Engineering, Vol. 8, p. 347-365
- Stockdon, H.F., Holman, R.A., Howd, P.A. and Sallenger, A.H., 2006.** Empirical parameterization of setup, swash and runup. Coastal Engineering, Vol. 53, p. 73-588.
- Terwindt, J. J., 1962.** Study of grain size variations at the coast of Katwijk, The Netherlands, Note K-324, Rijkswaterstaat, Deltadienst, Den Haag
- Van Gent, M.R.A., 2001.** Wave runup on dikes with shallow foreshores. Journal of Waterways, Port, Coastal and Ocean Engineering, Vol. 127, No. 5, 254-262
- Van Lopik, J.H., Zazai, L., Hartog, N. and Schotting, R.J., 2019.** Nonlinear Flow Behavior in Packed Beds of Natural and Variably Graded Granular Materials. Transport in Porous Media. doi.org/10.1007/s11242-019-01373-0
- Van Rijn, L.C., 1984.** Sand transport Part II, Suspended load transport. Journal of Hydraulic Engineering, Vol. 110 (11), 1613-1641
- Van Rijn, L.C., 1990, 2011.** Principles of fluid flow and surface waves in rivers, estuaries and coastal seas. Aqua Publications, Nederland (www.aquapublications.nl)
- Van Rijn, L.C., 1993, 2006.** Principles of sediment transport in rivers, estuaries and coastal seas. Aqua Publications, Nederland (www.aquapublications.nl)
- Van Rijn, L.C., 1997.** Cross-shore sand transport and bed composition. Coastal Dynamics, Plymouth, England, p. 88-98
- Van Rijn, L.C., 1998.** The effect of sediment composition on cross-shore bed profiles. ICCE. Copenhagen, Denmark
- Van Rijn, L.C., 2005/2012.** Principles of sedimentation and erosion engineering in rivers, estuaries and coastal seas. www.aquapublications.nl
- Van Rijn, L.C., 2006, 2012.** Principles of sedimentation and erosion engineering in rivers, estuaries and coastal seas. Aqua Publications, The Netherlands (www.aquapublications.nl)
- Van Rijn, L.C., 2007a.** Unified view of sediment transport by currents and waves, I: Initiation of motion, bed roughness and bed-load transport. Journal of Hydraulic Engineering, ASCE, Vol. 133, No. 6, p. 649-667
- Van Rijn, L.C., 2007b.** Unified view of sediment transport by currents and waves, II: Suspended transport. Journal of Hydraulic Engineering, ASCE, Vol. 133, No. 6, p. 668-689
- Van Rijn, L.C., 2007c.** Unified view of sediment transport by currents and waves, III: Graded beds. Journal of Hydraulic Engineering, ASCE, Vol. 133, No. 7, p. 761-775
- Van Rijn, L.C., 2007d.** Unified view of sediment transport by currents and waves, IV: Application of morphodynamic model. Journal of Hydraulic Engineering, ASCE, Vol. 133, No. 7, p. 776-793
- Van Rijn, L.C., 2008.** Modelling of beach and dune erosion. Report Z4173/Z4230. Delft Hydraulics, Delft, The Netherlands
- Van Rijn, L.C., 2009.** Prediction of dune erosion due to storms. Coastal Engineering, 56, p. 441-457



- Van Rijn, L.C., 2010.** Coastal erosion control based on the concept of sediment cells. EU-Conscience project. Deltares, 2010, Delft, The Netherlands.
- Van Rijn, L.C. and Wijnberg, K.M., 1994.** One-dimensional modelling of individual waves and wave-induced longshore currents in the surf zone. Report R 94-09, Department of Physical Geography, University of Utrecht.
- Van Rijn, L.C. and Wijnberg, K.M., 1996.** One-dimensional modelling of individual waves and wave-induced longshore currents in the surf zone. Coastal Engineering, Vol. 28, p. 121-145
- Van Rijn, L.C., Walstra, D.J.R., Grasmeijer, B., Sutherland, J., Pan, S. and Sierra, J.P., 2003.** The predictability of cross-shore bed evolution of sandy beaches at the time scale of storms and seasons using process-based profile models, p. 295-327. Coastal Engineering, 47
- Van Wiechen, P., Rutten, J., Mieras, R., Anarde, K., Wrobel, M., Tissier, M., and De Vries, S. 2022.** The real dune/reflex experiment at the sand engine (pp 75-77). In: Strypsteen, G., Roest, B., Bonte, D. and Rauwoens, P. (Eds.), Book of abstracts Building Coastal Resilience 2022; Special Publication: Flemish Institute for nteh Sea (VLIZ), Vol. 89. Doi.org/10.48470/28



Memo: Crosmor modelling and applications
Date: 6 December 2025

